REPORT NO. OHIO-DOT-01-79

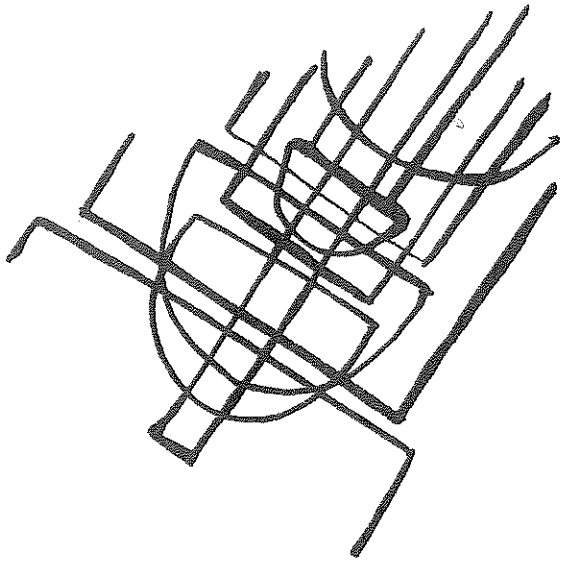

NOVEMBER 1977
FINAL REPORT

PILES & PILE DRIVING HAMMER PERFORMANCE FOR H-PILES DRIVEN TO BEDROCK

G.G. GOBLE
G.E. LIKINS, JR.
and
W. TEFERRA

Department of Civil Engineering
Case Western Reserve University
Cleveland, Ohio 44106

Prepared for:
Ohio Department of Transportation
and
Federal Highway Administration

Technical Report Documentation Page

1. Report No.	2. Government Accession No.	3. Recipient's Catalog No.
OHIO-DOT-01-79		

4. Title and Subtitle

PILES & PILE DRIVING HAMMER PERFORMANCE FOR H-PILES DRIVEN TO BEDROCK

5. Report Date: November 1977

6. Performing Organization Code

8. Performing Organization Report No.

7. Author(s)

G. G. Goble, Garland Likins, Wondemagegnehu Teferra

9. Performing Organization Name and Address

SCHOOL OF ENGINEERING
CASE WESTERN RESERVE UNIVERSITY
Cleveland, Ohio 44106

10. Work Unit No. (TRAIS)

11. Contract or Grant No.: State Job No. 14284(0)

12. Sponsoring Agency Name and Address

Ohio Department of Transportation
P. O. Box 899
Columbus, Ohio 43216

13. Type of Report and Period Covered: Final Report

14. Sponsoring Agency Code

15. Supplementary Notes

Prepared in cooperation with the U.S. Department of Transportation. Federal Highway Administration

16. Abstract

In recent years design stresses in piles have been increasing due to economic pressures and changes in pile driving specifications. Before unsatisfactory designs are executed where steel H piles are driven to bedrock, this research project was performed to study a current driving specification. Although a complete investigation of all bedrock/soil conditions, pile hammer and pile sizes was an impossible task, two bedrock/soil conditions were selected as the most critical cases. Several hammer types and sizes were used in order to determine safe pile design loads and proper driving specifications to avoid pile damage. Test piles were statically load tested and extracted. In addition, dynamic measurements were made to determine hammer performance and pile capacity for every blow. These measurement techniques are the result of previous research projects and make possible the determination of pile performance for the total length of driving.

17. Key Words

Damage, Dynamics, Foundation, Impact, Pile Driving, Specification, Stresses, Transducers, Wave Equation, Bearing Capacity

18. Distribution Statement

No restrictions. This document is available to the public through the National Technical Information Service Springfield Virginia 22161.

19. Security Classif. (of this report)	20. Security Classif. (of this page)	21. No. of Pages	22. Price
Unclassified	Unclassified	200	

Form DOT F 1700.7 (8-72) Reproduction of completed page authorized

F I N A L R E P O R T

PILES AND PILE DRIVING HAMMER PERFORMANCE FOR H-PILES DRIVEN TO BEDROCK

November 1977

by

G.G. Goble

Garland Likins, Jr.

Wondemagegnehu Teferra

This research was sponsored in cooperation with the Ohio Department of Transportation and the U. S. Department of Transportation, Federal Highway Administration. The opinions, findings and conclusions expressed in this publication are those of the authors and not necessarily those of the State or the Federal Highway Administration. This report does not constitute a standard, specification or regulation.

Case Western Reserve University
Department of Civil Engineering
University Circle
Cleveland, Ohio 44106

ACKNOWLEDGEMENTS

The cooperation and advice on technical matters of Raymond Grover and Richard Engel of the Bridge Bureau of the Ohio Department of Transportation were appreciated. In administrative matters, the assistance of L.O. Talbert of the Research and Development Office of the Ohio Department of Transportation was most helpful.

The following also provided support and their cooperation is gratefully acknowledged:

Associated Pile and Fitting Corp. who provided pile points and the piles to which they were attached.

L.B. Foster Co. for donating the use of all Kobe hammers at both sites.

National Engineering and Contracting for providing pile driving services to obtain data from sites on production driving which proved invaluable in final soil-bedrock and hammer selection.

The American Iron and Steel Institute for donating all of the piles that were driven without points.

The Great Lakes Construction Company for supplying dead weight for reacting the static load test.

The Day Equipment Company, the A. L. Bentley Company, the Foundation Equipment Company and the National Engineering and Contracting Company for their careful performance of subcontract work on the project.

TABLE OF CONTENTS

CHAPTER I

Introduction

In 1972, the Ohio Department of Transportation changed their pile driving specification to read, H-piles shall be driven to refusal on bedrock or to 20 blows per inch for the last few inches of penetration independent of hammer size (at least within the limits of generally acceptable hammers). The previous driving criteria was based on hammer size, pile length, soil strength and design load. At the same time, the general trend in the United States has been to use higher allowable stresses in steel piles.

The project reported here had as its goal to examine the consequences of the new driving specification on the safety of pile installation. At the same time data might be obtained to provide data about hammer performance, the behavior of H-piles driven to bedrock on a batter through soft soil, the performance of pile tip reinforcement and the effect of a batter on hammer operation.

Originally, it was intended to drive and test piles at three different sites. The cost of the operation made it necessary to limit testing to two sites with substantially different conditions. The Sandusky site was selected for the soft, shallow overburden and the level surfaced hard bedrock. It to be an almost ideal site. The second site, on the west side of Cleveland, was selected for the firm shallow overburden soil over the soft, weathered shale.

Pile driving was done at the Sandusky site in July, 1975, by the A.L. Bentley and Sons Co. of Toledo, Ohio. The operation was quite trouble free. Attempts to perform load tests on these piles resulted in pull-out of the anchor system. A great deal of time was lost during the late summer and fall of 1975 in unsuccessfully attempting to complete the tests. During the winter of 1975-76, the load testing system was substantially modified and load testing was completed during the summer of 1976.

At the second site, the piles were driven in August, 1976, by National Engineering and Contracting Co. Driving took longer than was estimated but static load testing went very well and was quickly completed.

The details of the test results are presented in the Appendix. Chapter II describes the test planning in detail while Chapter III presents the test methods and data analysis. The results are summarized in Chapter IV. In

Chapter V, conclusions and recommendations responsive to the original proposal are presented.

A great volume of data is available from these tests and much can be learned by further analysis. However, this is beyond the scope of the report.

CHAPTER II

Design of Tests

2.1 Ohio Pile Driving Specifications

During the past twenty years, the State of Ohio has used three specifications to govern the driving of H-piles to bedrock. From 1957 to 1972, the specification set maximum design loads as a function of both quality of overlying soil and depth of penetration as shown in Table 2.1. According to the 1957 specifications, this load is based on the premise that the shallower the depth and poorer the quality of the overlying soil, the greater the portion of each pile's load that must be borne by point contact with bedrock and vice versa. It is based also on the premise that the adequacy of the point contact cannot be seen, that penetrations through poor soil causes column action to be of concern, that the shorter the penetration and poorer the soil the greater the possibility that the driven piles will not maintain their contact with the rock, and that where piles are of relatively short penetration a greater number can be used at modest cost.

Table 2.2 indicates minimum capacities from the Engineering News formula to be specified on the construction plans to assure adequate contact with bedrock for the design load. It relates load, depth and quality of soil, and hammer size. If a value is not given the hammer is considered inadequate. Values with the asterisk (*) are for formula use only and are not intended to reduce the required design capacity. If the desired capacity is not achievable with the smallest hammer having 7000 ft-lb. energy, then a larger hammer must be specified.

Interpolation aids, such as Figure 2.1, were available to obtain the required formula capacities for intermediate cases. These formula capacities were obtained from a comprehensive pile capacity formula to obtain the rate of penetration for the design load. Using this rate of penetration in the simpler ENR formula the corresponding required capacity was obtained.

In 1972 the requirement was changed to read, "Piles shall be driven to refusal on bedrock or to 20 blows per inch for the last few inches of penetration. The design load is __ tons per pile for the abutment piles and __ tons per pile for the pier piles." The loads were dependent on pile size and corresponded to 9 ksi working stress in the steel. For the HP10 x 42 piles used

in this research project, the design load would be 55 tons. With the common safety factor of two, the Ohio Specification would require a minimum "yield" load of 220 kips or an ultimate failure load of 245 kips. Yield load is approximately 90% of the ultimate load. This provision ignores important variables such as hammer size, pile penetration, quality of overburden and type of bedrock. In addition, it may not allow for the most economical structure. To require a capacity based on pile size and not on applied loads might result in fewer piles being required but could also increase the cost of the structure in the design of the pile cap system.

The 1972 code was the governing specification at the time of the research project. Piles were driven in most cases to comply as nearly as possible with this code.

In 1977, the 1972 specification was revised to read, "Piles shall be driven to bedrock. The bearing capacity shall be considered obtained by refusal on hard bedrock or by penetrating soft bedrock for several inches with a minimum resistance of 20 blows per inch. The design load is __ tons per pile for the abutment piles and __ tons per pile for the pier piles."

The 1977 specification attempts to take into consideration the bedrock type but still retains all other shortcomings of the 1972 code.

2.2 Test Site Selection

In the original planning for the tests a larger number of test sites were planned. The important parameters were judged to be the hardness (or soundness) of the bedrock and the depth and strength of the overburden soil. A complete study of all of these parameters would have been prohibitively expensive. Therefore, two of the most interesting combinations were selected: (1) a soft overburden soil and a hard bedrock, and (2) a firm overburden soil and a soft bedrock. In both cases, it was desirable that the depth to bedrock be about uniform on the site.

Several other features were considered in the selection of the test sites.
(1) the location must be easily accessible to all construction equipment and be of sufficient size for the test program. The location was to be on State property.
(2) The ground surface should be reasonably level.
(3) The depth to bedrock was to be reasonably shallow. Originally rock anchors were to be used to provide the reaction force. The piles were to be

recovered by extraction or excavation. Thick soil strata before bedrock would then be prohibitive in price for static load testing and extraction. (After contract approval, the price of rock anchors was greatly increased and the reaction system was changed to include anchor piles.) The depth to bedrock should be roughly 15 to 20 feet to meet the above criteria.

After visual inspection of possible sites and a review of nearby soil borings, two sites were particularly attractive. The first location was near Sandusky, Ohio, at the junction of State Routes 2 and 4. Route 2 is a dual lane divided expressway with a diamond interchange with Route 4. The northeast triangle (between the exit ramp and Routes 2 and 4) was selected as the site with the best access. Previous borings indicated soft overburden with a hard limestone at a depth of approximately 20 feet. The entire ground surface was level. This location will be referred to as Sandusky in the remainder of this report.

The second location was in Cleveland, Ohio, near Lorain Road and West 92nd Street. Construction in the area for Interstate 90 was in progress. Soil borings for a nearby pedestrian bridge indicated a weathered shale at a depth of about 16 feet which gradually graded into a firm shale. Access was satisfactory and the ground surface reasonably level. This site will be referred to as W92 in the remainder of this report.

2.3 Soil Investigation

Two soil borings were obtained for each site by personnel of the Ohio Department of Transportation. Borings were taken as close to the test site as possible and are intended to show soil profiles, and bedrock depth and properties. Sampling techniques included standard penetration tests (140 pound weight with drop height of 30 inches), Shelby tubes for obtaining undisturbed soil samples, and rock cores for at least the first ten feet of bedrock. Analysis and testing of the samples were performed at the Soil Mechanics Laboratory at CWRU.

The soil borings for the Sandusky site are presented in Tables 2.3 and 2.4. The soil is basically 20 feet of weak silt overlaying a one foot layer of firm silt. The bedrock is a hard limestone located at a depth of 21 feet. Borings for an existing bridge about 200 feet away from the site confirmed the uniformity of soil conditions and bedrock depth over the entire area.

The soil borings for the W92 site (Tables 2.5 and 2.6) show different conditions.

The overlaying soil has a higher standard penetration resistance of about 20 blows per foot and is silt and clay. At about 16 feet penetration, weathered shale is first encountered. The shale became less weathered with increasing depth. The shale samples were tested the following day to avoid expected deterioration of the specimens.

2.4 Hammer Information

A total of eight different hammers were used on the two test sites. They were selected by size, type and availability considerations to represent the range of hammer sizes and types typically seen by the Ohio Department of Transportation. Table 2.7 lists the hammers used. their ram weights, manufacturer's maximum rated energy, hammer type and at which site the hammer was used.

The MKT 9B3 is a small double acting air/steam hammer. The Vulcan 08 represents large single acting air/steam hammers. The Kobe and Delmag hammers are single action, or open end diesel hammers, while the Linkbelts are closed end or double acting diesels.

It was desired to use the same hammers at the W92 site as had been used at Sandusky. However, the K13 was not available, therefore, a D15 was used as the substitute. The smaller D5 was added to the hammers so that very small diesels would be represented. After the load tests at the W92 site failed at very low loads. it was desirable to restrike some of the piles to verify that relaxation had occurred. A LB520 would have been desirable since it was one of the hammers used in the original driving. However. the only hammer that the contractor could supply was the LB440.

2.5 Pile Details

All piles tested were HP 10x42 steel sections. Pile lengths during driving were generally 30 feet at Sandusky and 25 feet at W92, although there were some exceptions. The steel was of the A36 type and was confirmed by laboratory testing to have a yield strength between 36 and 37 ksi. For the entire HP 10x42 cross section of 12.4 square inches, a force of about 450 kips before yield was expected if the loads were applied concentrically.

A total of 15 piles were driven in a line on five foot centers at Sandusky. Four of these piles were fitted with pile points. The four piles with points and six without points were driven vertically. The remaining five piles were driven at 1:4 batter. Each of the piles was designated with the hammer's name and suffixes V, P or B to indicate if the pile was vertical without point, vertical with a point or battered without a point, respectively

For example, Pile K13P is a vertical pile driven by a Kobe K13 hammer and fitted with a pile point. Relative pile locations are shown in Figure 2.2.

A total of 22 piles were driven at W92 and relative locations are shown in Figure 2.3. The same pile designation system was used as in Sandusky. Four of the piles were driven at W92 as Special Piles and are labeled SP1, SP2, SP3 and SP4. These piles were driven to test the effect of different batters on the hammer performance.

CHAPTER III

Test Methods and Data Analysis

3.1 Static Load Test Procedure

Static load tests were performed on twelve piles at the Sandusky site. Seven vertical piles were tested with a vertically applied load while a horizontal load was applied simultaneously with the vertical load on all five batter piles. At the W92 site, static load tests were run on ten piles (nine vertical and one batter).

The load test system was designed and constructed at CWRU. In Sandusky, the reaction for the load test was provided by means of anchor piles driven into the ground in two parallel rows on each side of the test pile. They were driven at an angle of 60° from a horizontal reference in order to provide a larger reaction force. A box beam was inserted between each row of anchor piles and connected by pins at three locations. Another beam (W36 x 150) was placed across the top of the two box beams and held to them by four heavy bolts in order to provide a reaction when jacking.

Twelve anchor piles were driven for a single load test. Unfortunately, the anchor piles did not provide sufficient reaction due to the weak soil conditions. This problem necessitated the use of dead weights made of concrete blocks to be combined with the reaction developed by the anchor piles in order to counteract the jacking force. The Sandusky test setup is shown in Figure 3.1. After one load test was completed, four of the anchor piles were pulled and redriven at the next location for the next load test by the Case crew. This operation was continued for all of the twelve piles load tested.

At the W92 site, the load test system in Figure 3.1 was modified as follows. Instead of the twelve anchor piles, driven at 60°, the contractor was requested, after completing the driving of the test piles, to drive the anchor piles vertically into the shale to refusal or until the anchors were damaged. Only one anchor was driven at each pin location. Thus, six anchors were used instead of the twelve at Sandusky. The concrete dead weights were available but were not needed as the test piles failed before the reaction system pulled out. Except for driving the anchors, the Case crew performed the entire load testing sequence at W92.

A 200 ton jack was used to apply the vertical load using a Constant Rate of Penetration (CRP) test for all vertically driven piles. In this test, the load was applied gradually so that the top of the pile experienced a constant rate of displacement into the ground. The displacement rate was controlled at 0.02 inches per minute for loads less than 100 kips. The rate was then reduced to 0.01 inches per minute and continued until the pile began to fail. The rate was then further reduced to only 0.005 inches per minute. This was done so that the ultimate failure load contained as little rate dependent effects as possible.

The magnitude of the jacking force at any instant was measured by a load cell placed between the jack and the reaction beam. The load cell was a 10" O.D., 1-1/4 inch wall thickness pipe of 7 inches length. Eight strain gages were mounted on the inside wall of the load cell and wired in a full bridge arrangement. The load cell was calibrated in the laboratory so that the measured magnitude of the strain during field testing could be converted into load by using the determined calibration factor. Corresponding pile top displacements were read from dial indicators. All readings were taken at one minute intervals. The jacking system is shown in Figure 3.1.

For the batter piles, the vertical and horizontal loads were applied simultaneously in the ratio of 4:1. Corresponding displacements were read at the same time. Loads were calculated in advance for five kip vertical increments. Both horizontal and vertical loads were then applied manually so that the ratio was held as nearly as possible to 1:4 so that the effective load was axial. At five kip intervals the loads were brought to the 1:4 ratio exactly and the pile displacements in both the horizontal and vertical directions were read.

A load test curve was plotted for each of the piles and an ultimate load was determined by the Davisson Method. In this method a line is constructed having a slope proportional to the pile stiffness.

$$K = \frac{EA}{L}$$

and a displacement offset calculated from

$$\delta = 0.15 + 0.1D/12$$

where δ is in inches and D is the tie diameter in inches. (In this case a ten inch dimension is used.) The point of intersection of this line with the load test curve is defined as the ultimate load. These lines have been constructed on load test curves shown in the Appendix.

Other failure criteria might be used. It is the strong opinion of the authors that the Davisson failure criteria, together with some form of rapid load test is the best method of pile capacity determination.

3.2 Dynamic Testing

The primary purpose of these tests was to evaluate the performance of piles driven to bedrock using different driving systems. In order to evaluate and understand hammer and driving system operation it was necessary to measure as many dynamic parameters as possible during driving. Strain and acceleration measurements were made at the pile top during driving in order to assess pile bearing capacity, transferred energy to the pile and other dynamic quantities. Two accelerometers and two strain transducers were attached diametrically opposite in order to cancel any bending effects that may arise in the pile while driving. These measurements were made on all the piles for the full length of driving and were recorded on analog magnetic tape for further analysis. The following additional measurements were also obtained during the driving of the test piles:

1) Set-rebound was measured on a paper attached to the pile by moving a felt pen across a straight edge supported at a convenient level.

2) For the Kobe and DELMAG hammers, ram stroke was measured and recorded on a cassette recorder for every hammer blow by visually observing the rise of the ram top against a measuring rod attached to the hammer cylinder.

3) Bounce chamber pressure was recorded on a cassette recorder for each blow of the Link Belt hammer.

Data of ram stroke and bounce chamber pressure for the W92 site were later lost before the information could be processed when the cassettes were stolen.

Methods for measuring acceleration at the pile top have been developed over the last decade by the Case Piling Research Project and they have now become routine procedures. Acceleration of the pile is measured by accelerometers

mounted on aluminum blocks which are then bolted to the pile. Commercially available high frequency piezoelectric accelerometers are used.

A Pile Driving Analyzer was used to provide the necessary power supply and signal conditioning for the accelerometers and strain transducers. A previous research project developed a small portable computer to obtain pile capacity by processing the measurements in the field, and the Analyzer is an expanded version of the research device. The Pile Driving Analyzer was used on this project to obtain pile capacities, measured force maximums and transferred energies. It verified when the pile contacted bedrock and was used as a preliminary tool to investigate pile damage in addition to its primary function as signal conditioner. As the pile approached and contacted rock, the capacities would increase rapidly. When pile damage occurred at the tip, the capacities would then decrease substantially.

3.3 Dynamic Data Processing

The field records on the analog magnetic tape were automatically converted to a digital form using an analog-to-digital converter controlled by a minicomputer. All field information containing the hammer blows was stored on a digital magnetic tape for further analysis. Using the Case Processing system the acceleration record was integrated to obtain velocity and integrated a second time to produce displacement. The strain obtained from the strain transducer was converted to force using pile cross sectional area and material modulus. The force and velocity records were used to predict the capacity of the pile from the Case Method as in Equation 3.3.

Maximum pile top velocities, displacements, forces and Case Method capacities were printed for each blow analyzed. The hammer energy transferred to the pile was calculated from the expression

$$E(t) = \int_0^t F(t)\, v(t)\, dt \qquad (3.1)$$

where the energy, E(t), force F(t) and velocity v(t) are all functions of time. The energy obtained from Equation 3.1 which was also printed, is the energy available in the pile to do work. It excludes the impact losses due to heat, friction and sound, it also eliminates the uncertainty of combustion efficiencies, ram impact velocity, and inelastic collisions in the driving cap

assembly. In addition, plots of velocity, force and energy as a function of time were made on a CALCOMP drum plotter.

Typical blows were selected for each of the piles for wave equation analysis using the Case Pile Wave Analysis Program (CAPWAP). The essence of the CAPWAP is briefly described in Section 3.5. Maximum force in each of the pile elements (spring forces), measured force, velocity, and displacement at the top, mid-length and toe of the pile were printed. The resistance distribution along the length of the pile and soil damping constants and quakes were determined. Plots of computed and measured force matches were obtained. The set rebound, stroke and blow count data were processed manually.

3.4 Case Method

In 1964, a research project began at Case Western Reserve University to develop a method of predicting pile bearing capacity from dynamic measurements. Electronic measurements during pile driving were proposed to predict pile bearing capacity. Pile top acceleration, a, and pile top force, F, were measured. The pile was originally assumed to be a rigid body of mass, m, and the soil resistance force calculated using Newton's law as

$$R = F - (m)a \tag{3.2}$$

where F and a are functions of time. In order to eliminate resistance force components dependent on pile velocity, F and a were chosen when the pile top velocity, v, found by integration of acceleration, became zero.

Further studies including longer piles (more than 60 feet) showed that the pile elasticity cannot be neglected. Assuming uniform piles and ideal plastic soil behavior, the following equation was derived from a closed form solution to the one-dimensional wave equation

$$R = \tfrac{1}{2}[F(t_1) + F(t_2)] + \frac{mc}{2L}[v(t_1) - v(t_2)] \tag{3.3}$$

where $t_2 = t_1 + 2L/c$ and t_1 is a selected time during the blow. The pile length is L, the velocity of the pile top is v and c is the wave transmission speed in the pile material.

The Case Method models the soil resistance R, called the Phase IV or P4 method in some previous publications, as the sum of a static component, S and

a dynamic component, D:

$$R = S + D \tag{3.4}$$

The damping resistance, D, is obtained approximately as

$$D = J \frac{mc}{L} v_{toe} \tag{3.5}$$

where J is a dimensionless damping constant and v_{toe}, the pile toe velocity. J is dependent on the soil type and is generally larger as the soil contains more fines. The wave theory shows that the pile toe velocity can be calculated as

$$v_{toe} = 2v_{top} - \frac{L}{mc} R \tag{3.6}$$

where v_{top} is the pile top velocity at time t_1. It should be noted that t_1 is chosen at the time of the maximum velocity of the pile top (time of impact).

Equation 3.6 is approximately correct for the first 2L/c time after the initial arrival of the stress wave at the toe.

The pile top force is proportional to the pile top velocity until soil resistance (or non-uniform pile cross section) reflections are felt at the pile top. The proportionality constant EA/c, can be shown to be equivalent to mc/L since

$$E = \rho c^2 \tag{3.7}$$

is a relationship for all materials. In the above, E is the pile material modulus of elasticity, ρ is the mass density, c is the material wavespeed and A is the pile cross sectional area.

The damping resistance, D, then becomes

$$D = J[2\ F(t_1) - R] \tag{3.8}$$

The static soil resistance, S, is obtained by subtracting the calculated damping resistance, D, from the total driving resistance

$$S = R - J[2\ F(t_1) - R] \qquad (3.9)$$

All the values on the right hand side of this equation are available from the dynamic measurements except for the soil damping constant, J. A large effort was made to correlate the value J with the soil type. This study confirmed that for most cases the soil at the pile tip was the dominant factor.

The developments summarized above were reported in a series of reports to the Ohio Department of Transportation and the Federal Highway Administration. A more detailed presentation of these developments can be obtained from the previous research (1,2,3,4).

Further research and consulting experiences have confirmed the basic values of damping constants as given in Reference 4. For completeness, the expanded data correlation of all piles tested both statically and dynamically is presented in Table 3.1 and Figure 3.3. Experimental work in correlating with piles that were driven to bedrock shows that the J should not be less than 0.10 in any case. The weathered shale encountered at W92 gave best results with a J of 0.15 and work in mica schist gave a J of 0.25.

It must be realized that the total driving resistance (Equation 3.3) and the static capacity (Equation 3.9) from the Case Method are valid for the time of testing. If measurements are taken during initial driving of a pile into soil strata which exhibits substantial setup or relaxation effects, then comparisons with static load tests which are usually run several days later are no longer compatible. The pile should be tested by the Case Method after a suitable waiting period and then compared with the static test. Often the static test can be used to calibrate the J in Equation 3.9 to a specific soil condition when both static and dynamic tests are available as J can be computed. Setup/relaxation effects can be further investigated by testing during initial driving and again after a waiting period and observing the difference. In case of further uncertainty regarding the proper damping constant, it should be noted that the selection of higher J values will tend to give a conservative static capacity prediction.

3.5 The CAPWAP Method (CAse Pile Wave Analysis Program)

The CAPWAP analysis procedure was developed during the Case Piling Research Project and is described in detail in Reference 3. The program seeks to determine

the resistance forces acting on the pile during driving and their distribution. The pile is divided into a series of discrete masses and springs. Soil resistance forces are allowed to act on each mass element and are assumed to be characterized as elastic-plastic springs and linear dashpots. Thus the spring elements produce a displacement dependent resistance force that is described by two constants, the ultimate resistance force and the displacement where the resistance law becomes plastic. The dashpot assumes a linear relationship between velocity and resistance force.

The analysis proceeds by introducing the pile top motion as an input together with an assumed resistance system (the top pile element is required to move as specified by the measured acceleration). The dynamic analysis is made using a method similar to that suggested by Smith (5) and pile top force is obtained. This force is compared with the measured force.

The computed and the measured pile top force, in general, will not agree with each other. It is necessary to improve this match iteratively by changing the assumed soil resistance parameters. Finally, a computed pile top force will be obtained that will agree with the measured top force. The corresponding parameters of the soil model are then the correct values. The results of the CAPWAP analysis are the magnitude and location along the pile of both static and dynamic resistance forces. Static computations can be used to predict the static load test curve of the pile.

In 1970, a program was written that performed the necessary computations and decisions automatically. This program resulted in satisfactory solutions for piles which were less than 75 feet in length (3). For longer piles, computation times became excessive. In 1975, the program was changed and now performs the computations "interactively." In the interactive mode, one analysis is obtained using a minicomputer and the engineer determines necessary changes of soil parameters for the next analysis.

3.6 Wave Equation

For many years a computer solution known as "The Wave Equation" has enjoyed increasingly widespread usage. The Wave Equation is actually an analysis which models the hammer pile system by springs and masses. Soil resistances are assumed parameters modelled as an elastic plastic spring and a linear dashpot. (This is the same model as that used in CAPWAP.) First made popular by E.A.L. Smith around 1960 (5), many have since improved and refined the

analysis although the basic concept remains unchanged. Two recent programs sponsored by the FHWA are the WEAP and TTI analyses (6,7). Both programs do an adequate job of modelling air steam hammers. The WEAP program does a more realistic analysis in modelling the thermodynamic processes of diesel hammers.

The Wave Equation analysis makes assumptions in the hammer-cushion system but also requires the user to input a total static resistance as well as its distribution. Important output information is the penetration resistance or blow count for a particular static capacity as well as the maximum pile stress. Often inaccurate input information regarding helmet weight, cushion and cap-block stiffness, hammer efficiency, static resistance distribution and damping parameters adversely affects results. Also, sensitivity to high blow counts has led to criticism. However, the Wave Equation is still the best tool to study pile behavior before actual construction begins.

After construction begins, Case Method testing can be used to verify that the hammer system is performing as the model assumed. Unusual hammer efficiency or cushion properties are then observable. Although the Case Method can be used to determine the total static capacity, the CAPWAP procedure is in many ways even more valuable.

There are essentially three unknowns in the normal pile driving problem; the pile forces, the pile motion, and the soil resistance forces (both magnitude and location of static and dynamic resistance). If any two are known the third can be obtained. The usual Wave Equation approach is to assume the soil forces and model the hammer impact to produce the pile forces and permanent set. CAPWAP is a wave equation type analysis in that it models the pile by elastic springs and lumped masses and uses standard wave equation soil models (elastic plastic springs and dashpots). CAPWAP uses the measurements of force and velocity of the pile top to obtain the soil resistance distribution. The hammer system is eliminated as a variable in both the Case Method and CAPWAP procedures.

CHAPTER IV

Results

4.1 General

The following sections are given as an overall description of the results obtained during this project. It is not an attempt to present in detail the results of each pile tested. These individual descriptions are given in the Appendix for the interested reader. Further information may be extracted by vigorous examination of the data presented in the Tables and Figures of the Appendix. Instead the comparisons of different driving conditions and hammer types, and evaluation of pile damage and capacities will be given in this section.

4.2 Comparison of Tests in Sandusky

All piles exhibited similar behavior up to and including the first blows on bedrock. Capacities were small in the overburden. Capacities increased somewhat in the thin layer immediately above bedrock. When bedrock was encountered the capacity of all piles (except K13V) increased to at least 90% of the pile structural capacity.

All piles showed high Case Method and CAPWAP capacities when the pile first hit the hard limestone. The attempt was made to drive the piles to the 1972 specification of "20 blows per inch for the last few inches of penetration."

The Linkbelt 520 was the first hammer used. Pile 520V had only one inch in excess of 20 BPI while 520B had two inches and 520P had three inches. Pile 520P (reinforced point) failed in a gross buckling mode above the ground but several feet below the pile top. This was a characteristic of all piles driven with points. Driving was then terminated and it was considered that the pile had met the criteria. Final dynamic capacities and static load test confirmed this pile to have high load capacity as shown in Table 4.1.

Continued driving on the piles without point protection caused the blow count to decrease. Additional driving for several feet failed to produce blow counts much higher than 10 BPI. The driving record indicated a succession of peaks and valleys. Extraction of the piles revealed the pile tip to be damaged. Figure 4.1 shows the tips of these piles to have failed in a fan fold mechanism. These fan folds are the apparent reason that the blow counts and pile capacities

both show trends which alternately increased and decreased. Final capacities for these two piles with damaged tips shown in Table 4.1, were lower than that of the 520P pile with no tip damage. Pile 520V had an exceptionally weak capacity of 120 kips.

None of the 520 piles exhibited significant penetration into bedrock. Attempts to drive the piles into bedrock several inches only has the effect of damaging the piles and weakening the static capacity.

All of the piles driven by the 08 hammer were damaged before a blow count of 20 BPI was reached. Summary data in Table 4.1 shows that only 08P pile exceeded 7 BPI before it failed in gross column buckling similar to the 520P at about 16 BPI. Pile 08V was damaged at the pile top probably due to poor hammer pile alignment. Figure 4.2 shows that damage to the 08V tip was minimal. Final dynamic capacities confirm that both 08V and 08P had high bearing capacities (430 + kips) even though the 1972 driving specification had not been met. Examination of tip damage in Figure 4.2 and capacities in Table 4.1 for 08B reveals that while the capacity was satisfactory (max P4) at the time bedrock was first encountered continued driving for three extra feet with the heavy ram hammer only caused the tip to fail in the same fan fold shape as did the 520 piles and the final capacity of the 08B pile was significantly reduced (151 kips) due to this damage. Real bedrock penetration was not achieved in this hard material.

All piles driven by the K13 achieved at least 20 BPI for at least one inch. Pile K13Pbuckled in column action above ground similar to all other piles with points but only after extremely high penetration resistance (about 20 blows for 1/8 inch) were encountered. Further attempts at attaining several inches penetration were abandoned and the pile was considered to be at refusal. The penetration requirement was relaxed for pile K13B after only two inches in excess of 20 BPI. The second inch had 70 BPI. For both of these piles capacities by either load testing or dynamic testing proved to be in excess of 350 kips. The K13P showed no tip damage. Pile K13B had major flange distortion as seen in Figure 4.3 but the web was still straight and the fan fold behavior which had so reduced capacities on the other piles was not present.

Pile K13V displayed peculiar behavior. A relative maximum in blow count and capacity was observed at 22 feet. However the pile weakened again before obtaining 20 BPI and its maximum capacity at 23 feet penetration. Continued driving obviously damaged the pile as capacities and blow counts continued to fall. Pile K13V had the lowest final dynamic capacity and static test load

(106 kips) of any pile at Sandusky as seen in Table 4.1. The pile tip damage seen in Figure 4.3 is not of the fan fold type It is not known whether the unusual driving record was caused by boulders or fissures in the limestone or by the pile being deflected horizontally along bedrock. Since pile removal was aided by an extractor it is also not known if the pile shape is as it was in the ground or if the large kink on the left flange in Figure 4.3 represents where the pile had possibly deflected horizontally.

None of the piles driven by the K25 achieved 20 BPI before structural damage. Pile K25P did make 16 BPI before gross column buckling. Pile capacity in Table 4.1 was adequate. Figure 4.4 shows the pile tip for K25P. Although the general shape shows no major damage it is noticed that the flanges are no longer perfectly straight. This was probably caused by the high forces in the pile which were slightly above yield.

A blow count of 7 BPI was the highest achievable penetration resistance for both pile K25B and K25V. Damage to the pile tip was then observed in the electronic measurements. Driving was continued for several additional feet before stopping. Although maximum capacities when the pile first reached the limestone were in excess of 400 kips in Table 4.1, continued driving reduced the pile strength. Final static capacities were reduced to 150 and 318 kips as in Table 4.1 for K25V and K25B respectively. As with all other piles which sustained tip damage, no particular criteria was used to determine when to stop driving since the blow counts did not meet the specification requirement. Thus, pile capacities varied substantially depending upon the tip condition at the time driving was stopped. However, in every case significant damage dramatically reduced the bearing capacity of the pile. Pile K25V was the only pile which could not be extracted. Tip damage to K25B is observed in Figure 4.4. While the section was not fully recovered, it appears that the left flange may half been torn from the web during driving and deflected along the bedrock surface. The remaining section probably also deflected along bedrock but in a different direction.

It was noticed that several piles had sections which were not recovered as with the K25B for example. Many of the extracted fan folded tips had larger visible "tears" in the steel. Evidence from the tear locations and the larger plastic deformations occurring during driving indicates that the tear occurred during driving rather than during extraction.

Pile K25VE was a pile driven without a point but in a controlled manner.

This was intended to show that even the largest hammer could drive a pile to a larger capacity without damaging the pile. Driving was carefully monitored and as soon as the pile first touched bedrock, driving was immediately stopped. Case Method capacity was used in the field to varify that bedrock had indeed been reached and the capacity was sufficiently large. Figure 4.5 shows the pile tip damage to be negligible. Capacities in Table 4.1 are higher than for any other pile tested at Sandusky.

The last hammer used at Sandusky was the 9B3. Both piles showed similar behavior. Driving was stopped after the blow count had exceeded 20 BPI for "several inches" as required by the 1972 specification. Examination of pile load test data in Table 4.1 indicates that performance was satisfactory. Examination of Figure 4.6 of the pile tip after extraction shows local damage to the tip flanges. The web, however, remained straight. Due to questions regarding the calibration of the analog tape recorded data, all dynamic electronic records were discarded. The results were plotted to show waveform shapes only. A more thorough examination of each pile is given in the Appendix.

The soil resistance distribution and damping outputs from CAPWAP can be used as input into Wave Equation programs. This eliminates the soil as a variable and leaves only the hammer system as an unknown. This was done for piles 08P and K25P at Sandusky. As this was a well controlled test, helmet weights and cushion descriptions were accurately known. In both cases the hammers were in excellent operating condition as the WEAP program (which contains the best model for the K25 diesel hammer) assumes. Therefore, with a well defined hammer system and the correct soil resistance distribution, it is not surprising that the WEAP Wave Equation did an excellent job of predicting dynamic pile behavior. Predicted blow counts agreed well with measured values (13 blows per inch predicted versus 16 measured). The WEAP program also predicts the stroke of diesel hammers. Excellent correlation (8.0 ft. predicted, 8.0 $\pm$ 0.3 ft. measured) was observed between the calculated and measured stroke. Predicted pile top forces and velocities agreed well with measured force and velocity curves as seen in Figures 4.7 and 4.8. In both cases the most serious discrepancy is the apparent underprediction of maximum force. However, in both cases the predicted and measured maximum force exceeded the yield strength of the steel.

4.4 Comparison of Tests at W92

Six hammers were used at W92 at the time of initial driving and were of

comparable size to those used at Sandusky. The piles behaved in a consistant manner. The larger hammers produced deeper pile penetrations. Greater embedment in the shale produced higher capacities. The extra strength was due to theshale being gradually more firm with depth causing increased top bearing and also added skin friction in the shale layer.

It was intended to drive all piles to 20 blows per inch for a minimum of one inch. This would provide a uniform driving criteria yet would cause different pile penetrations into the shale depending upon the hammer size. However, large hammers often caused pile top damage before the 20 BPI criteria was reached. Extraction of the piles proved that tip damage which structurally weakened the pile performance under static loads at Sandusky was not present at the W92 site. Some flange spreading at the tip (See Figures 4.9 to 4.11) was noticed as the hammer size increased but the spreading did not appear to affect the static pile performance. Table 4.2 contains much of the summary information obtained at the W92 site. As with the Sandusky site, the Appendix also contains a more detailed description of the W92 pile driving and test performance.

Piles driven by the 9B3 reached a resistance of 20 BPI within one foot after first reaching the weathered shale. The ultimate capacities at the time of driving and also during static testing were less than design load for this pile section as shown in Table 4.2.

Piles driven by the D5 achieved the blow count criteria at the shallowest penetrations of all piles at the W92 site. Since the tip penetrated only the upper portion of the weathered shale zone it was not surprising that dynamic capacity predictions in Table 4.2 were again smaller than twice the design load. Capacities for these piles were the smallest encountered in this site. No tip distortions were observed after extraction.

The results of these two small hammers indicate that driving piles into weathered shales leads to insufficient embedment in the shale to develop the required static capacity.

The piles driven by the 520 penetrated the shale about one foot further than the D5 or 9B3. Since the shale becomes more firm with depth and with an additional foot of skin friction in the shale. the dynamic capacities (Table 4 2) at the end of driving were over 100 kips (282-170) higher than the piles driven by the D5 and 9B3. The load test for pile 520V (Table 4.2) approximately two weeks later showed a reduction in pile bearing capacity of about 100 kips (282-184). This pile which originally had sufficient capacity with a safety factor of 2.3 now only

had a safety factor of 1.5. The capacity loss is due to two probably causes. First, as the pile is driven into the shale, some shale is displaced laterally. This side pressure causes skin friction to be substantial. However, with time this side pressure reduces as the shale "flows plastically," thus causing a reduction of skin friction. The second cause is a reduction in tip capacity due to additional weathering of the shale. Due to the pile driving, the shale at the tip has a new channel for additional exposure to water, thus leading to further weathering. Also pressures at the tip at the end of driving could allow for relaxation with time due to shale flow.

Although the authors had confidence in their dynamic capacity predictions at the end of driving, it was believed that the lower static test results would lead to suspicion of inaccuracy in the dynamic tests. Since this same trend of results was observed with all piles driven by the larger hammers, a restrike of some piles was suggested and accepted. The dynamic methods were to be used again to verify that the capacities at the time of testing were accurate and that the apparent strength loss was due to relaxation. The contractor proposed the substitution of a Linkbelt 440 since the 520 was not currently available. Restrike of pile 520V with the 440 (labeled 520V/440R in Table 4.2) gave dynamic capacities consistant with the static test. The CAPWAP results show that the loss of capacity was due to a reduction of support on the tip element. Both tip resistance and skin friction for the bottom element of the CAPWAP wave analysis are combined and listed as R_{toe} in Table 4.3. It is not possible to determine whether the resistance loss is from the tip or from the skin friction on the last element. It can be stated only that the reduced capacity resulted from a change in strength of the shale.

All piles driven by the 08 hammer were driven in excess of 20 BPI. Penetration was again increased and is attributed to the increased hammer size. Dynamic capacities at the end of driving are also larger. Table 4.2 shows the dynamic capacities to be between 372 kips for 08B and 405 for 08P. The dynamic data with depth did not show a sudden increase in capacity near the end of driving as indicated by the driving record. Measured average stresses of 34 ksi caused pile top damage due to local stress concentrations. This damage consumed a portion of the energy transmitted and resulted in the apparent increase in driving resistance. Further data and descriptions are contained in the Appendix.

Static testing of pile 08V gave an ultimate load of 240 kips, again a significant load loss compared with capacity at the time of driving. Restrike of this pile with the 440 (listed as pile 08V/440R in Table 4.2) showed good

correlation of dynamic capacities with the load test. The CAPWAP results again demonstrated that the soil strength loss occurred on the tip element, probably due to changes in the shale with time.

Extraction of these piles showed some distortion of the flanges at the pile tip as shown in Figure 4.9. This is probably caused by a larger soil pressure between the flanges than on the outside of the flange. The soil pressure is due to the horizontal soil displacement due to pile penetration. It is unlikely that this distortion contributed to a reduction in pile capacity.

The piles driven by the D15 had similar results to those driven by the 08; both hammer have similar energy ratings. Only the D15V reached the 20 BPI criteria without sustaining pile top damage. Dynamic capacity predictions were in the mid 300 kip range at the end of driving (Table 4.2). The time lapse between driving and static load testing again showed a larger capacity decrease attributed to strength changes in the shale. As in the case of the 520 piles, the piles driven with the D15 no longer met the 1972 specification for capacity with a safety factor of 2. They would, however, satisfy the 1957 specification. No restrike was made for those piles as it was felt that the dynamic capacities had been shown to be accurate at the time of dynamic testing and the static tests confirmed a time depended strength loss. Tip deformation of D15B is shown in Figure 4.10. The top damage experienced with the D15 was probably due to the fact that the available helmet was designed for 12-inch piles. It was impossible to hold the pile accurately aligned with the hammer and an eccentic hammer blow resulted. This problem again illustrates the importance of hammer alignment.

The piles driven by the K25 could not be driven to the 1972 criteria of 20 BPI due to pile top damage. However, they were driven to the deepest penetration of any of the piles driven at the W92 site. Due to this extra penetration, dynamic capacity predictions in Table 4.2 were also the largest on the site. The larger capacities, approximately equal to the pile structural strength, are due to extra skin friction in the shale and to increased tip resistance since the shale is more firm with depth. Static load testing again indicates a substantial loss in capacity due to changes in the shale layer with time. However, the piles still had adequate capacity for the 1972 specification. Flange distortion at the pile tip was largest in the W92 piles for K25V, shown in Figure 4:11. It was not felt that pile capacity was affected due to this type of cross section change.

The soil strength of the overburden is also important in determining the likelihood of damage. Larger skin resistance forces tend to reduce the downward traveling compression wave with the result that the maximum force at the pile tip is reduced. This smaller tip force is less likely to cause tip damage. This was the situation of W92. Inspection of the maximum spring forces in CAPWAP shows a reduction in maximum forces with depth due to the relatively large skin friction. For the piles at Sandusky with little skin resistance, the input compression wave travels unchanged to the pile tip. If tip resistance is small, the wave reflects as tension and the net force is small at the tip. If tip resistance is larger, however, the compression wave reflects in compression. The two waves superimposed are then likely to cause damage.

Four additional piles were driven at the W92 site to study effects of pile batter. Special Pile 1 (SP1) was driven vertically. SP2 and SP3 were measured at approximately 1:6 batter, while SP4 was near 1:2. All four piles were driven initially with the D5 and then tested for several inches of penetration with each of the other hammers. Summary results of this testing are included in Table 4.4.

A combination of events reduced the effectiveness of these special tests. First, it was not intended that SP2 and SP3 have such similar batters. Electronic problems made results for the D15 test of no value. In the case of SP4, the larger batter was more than the contractor felt was safe for the operation of the heavier 08 and K25 hammers. Actual pile penetrations were not recorded making capacity predictions less valuable since the original purpose of these tests was not to check capacity but rather to monitor hammer performance. Although results of these special tests on pile batter are inconclusive, some valuable information was obtained. For example, it was noticed that some soil setup effect was present in the overburdened soil layers. In the time between testing for SP1 the total capacity increased from 95 at the end of the D5 test to 114 kips at the beginning of the 520 test. An increase from 236 to 276 kips between the 520 and 08 tests was also noted. Similar increases can be found in the other tests also given in Table 4.4. This setup effect is often noted in the blow count records. For example, pile SP4 shows a larger capacity increase between the D5 and 520 testing. However, while the first inch of 520 testing showed 8 BPI the penetration resistance quickly diminished to only 3 BPI, demonstrating a rapid loss of setup capacity. Thus, in general, it can be observed that the setup in the silt for one day is larger than the relaxa-

tion or deterioration in the shale. This effect was noticed in both restrike piles 520V/440 and 08V/440 in Table 4.2. Pile 08V for example,showed a loss in the ultimate resistance in RU of 175 kips. However, the capacity loss R_{toe} on the tip element was 197 kips. The difference must be setup on the rest of the pile.

Information regarding hammer efficiencies at different pile batters was studied. Although much of the information for SP4 with the larger batter was not obtained, it does appear that efficiency for the 520 was less at this batter than at any other test on the W92 site. The transferred energy (EMAX) was only 6.3 kips feet maximum compared with 7.3 for SP1, SP2 and SP3. The results on piles SP2 and SP3 with a 1:6 batter are not significantly different than results on the vertical SP1. Inspection data in the Appendix on all batter piles driven at 1:4 also show no significant differences in hammer efficiency from similar piles driven vertically. Thus, it appears that hammers are unaffected at batters less than 1:4 but are less efficient at 1:2.

CHAPTER V

Conclusions and Recommendations

5.1 General Dynamic Testing and Analysis Techniques

1. The dynamic testing instrumentation provides a reliable, accurate means of measuring strain and acceleration at the pile top during hammer blows. The measurements are easily made and require only a short interruption of the contractor's operation.

2. The Case Method capacity shows good agreement with the pile's static capacity at the time of dynamic tests. If soil strengths do not change after pile driving, dynamic predictions at the time of initial driving agree well with the static load tests. If changes in soil strengths do occur after pile driving, comparisons of static test results should be made with dynamic testing by restriking the pile after a sufficient waiting period.

3. Setup or relaxation effects can be observed by dynamic testing during initial driving and then after various waiting times in a restrike operation.

4. Measurements of force and velocity can be used to detect and determine the location of structural pile damage. This can be most useful when H piles are driven to bedrock or for other pile types when visual inspection is not possible. The damage detection is accomplished by examining the measured force and velocity record (obtained by integration of the acceleration). If the velocity increases sharply relative to the force at any point earlier than the 2L/c time it indicates damage has weakened the pile.

5. Using a processing system controlled by a minicomputer, a large number of data records can be analyzed. Useful parameters such as pile top energy, velocity, force and capacity are easily calculated and printed. Computer controlled plots of the dynamic record can be made from the digital record.

6. The CAPWAP procedure uses dynamic pile top measurements to obtain the locations of resistance forces, to separate the static and dynamic resistances, and to investigate driving stresses at locations other than the pile top.

7. Wave Equation analysis programs such as WEAP which contain realistic hammer models can be used effectively to investigate pile driving problems. The Wave Equation analysis is more accurate when the correct soil parameters as determined by CAPWAP are available. Comparisons of Wave Equation results with dynamic force-velocity measurements will certify that the hammer-capblock-helmet-cushion system

is modelled correctly in the analysis. Incorrect input concerning hammer performance, cushion or capblock properties, and soil parameters are the main reasons why errors are caused in Wave Equation results.

5.2 Field Testing Results at Sandusky

1. All piles driven to the hard limestone were at one time capable of supporting loads approximately equal to the pile yield load. These maximum pile capacities were observed by either Case Method testing or by static load tests.
2. Continued driving in the attempt to obtain 20 BPI for the last few inches of penetration into bedrock caused pile structural damage, confirmed by electronic measurements and pile extraction. This structrual damage was responsible for large reductions in static load test capacity.
3. Larger hammers (08, K25) clearly damaged the piles before the 1972 driving specification was satisfied. If piles were not excessively driven (08V)where driving was stopped early due to local top damage or K25Ve which was stopped intentionally after only one blow on rock, good static load test performance was achieved.
4. Pile tip protection prevented tip damage at this hard bedrock site. Piles then failed structurally above ground in gross column buckling during driving but this portion of the pile was removed before static test loading. This mode of pile failure did not therefore, adversely affect the compressive static load test capacity.
5. Best results for driving piles at the Sandusky site would not use a blow count criteria. Blows per inch is meaningless since real bedrock penetration was not achieved. The blows per inch gave only an indication of how effective the hammer was in damaging the pile structurally. Driving beyond 30 BPI for the 520 and K13, and beyond 6 BPI for the 08 and K25 after contacting bedrock was an invitation for structural pile damage.
6. The dynamic field instrumentation did an excellent job of determining when the pile first had sufficient capacity or when the pile was being damaged.
7. There was no indication that the undamaged batter piles exhibited any tendency to slip horizontally on the rock during static load testing since they carried loads nearly equal to their yield stress.

5.3 Field Testing Results at W92

1. For the bedrock consition of weathered shale gradually becoming more firm with depth, it was found that the largest pile capacities were obtained from the

deepest pile penetrations. Similarly, the lowest capacities corresponded to the shallowest penetrations.

2. Large hammers produced greater pile penetrations than the small hammers when complying with the 1972 specification. Piles driven by larger hammers has higher capacities.

3. The largest hammers (K25 and 08) damaged the pile tops before the 1972 driving criteria was achieved.

4. Although no pile tip sustained severe structural damage which would reduce load test capacity, the flange tips of several of the piles were spread apart. The greatest flange distortion was caused by the larger hammers.

5. The capacities of the piles driven by the 520, D15, 08 and K25 at the end of driving were adequate for a 9 ksi design and safety factor of 2.0 but the static tests two weeks later revealed a significant loss in ultimate capacity. At this time only the piles driven by the 08 and K25 still had sufficient capacity but the piles driven by the 520 and D15 had an insufficient capacity for a 55 ton design load with a safety factor of 2.0.

6. The piles driven by the D5 and 9B3 had ultimate capacities at the end of driving and during the static tests that were insufficient for a 9KSI design with a safety factor of two.

7. Dynamic testing, by restriking the 520V and 08V piles after the static tests, also showed a loss of capacity after initial driving. Comparison of the CAPWAP analyses for these piles reveals that the loss of capacity was due to resistance losses in the shale. A small set up resistance was observed in the soil overburden.

8. Pile tip protection had little, if any, effect on static pile load performance at the W92 site. The soft bedrock prevented tip damage. It is hypothesized that the resistance developed gradually as the pile penetrated the shale and the lateral restraint was sufficient to prevent buckling of the pile tip.

5.4 General Conclusions and Comments

1. These two sites represent limiting conditions for the range of bedrock strengths of interest.

2. The pile stresses were substantially influenced by the bedrock stiffness and soil overburden. Gross buckling of the pile occurred on all tip reinforced piles at the Sandusky site.

3. Major pile tip damage can occur when the bedrock is hard and the pile will not penetrate. Penetration into soft bedrock prevents this structural damage.

4. There was no evidence of lateral motion of the tips of the batter piles during load testing. At the Sandusky site, the soil above the bedrock was soft and the bedrock was nearly level. Therefore, this problem does not appear to be a serious one for pile design.
5. Due to limited data, we cannot define the line between hard and soft bedrock. Until more data is available, a definition remains subjective.
6. Perhaps a displacement pile type would perform better than H piles for the soft bedrock condition. A closed end pipe pile might have sufficient tip bearing after relaxation of the shale to provide an adequate factor of safety. A thicker wall than used for friction piles would be necessary to prevent damage when seating the pile in the soft bedrock.

5.5 Recommendations

In the past 10 to 20 years the trend in pile foundation design specifications has been for the allowable design stresses to move upware. For H-piles allowable stresses of 12 ksi have become common. The American Iron and Steel Institute has recommended allowable stresses as high as 18 ksi. Considerable controversy has developed with both sides of the question citing specific examples as proof of their point of view. It is frequently forgotten that an allowable stress represents an upper limit that may not always be fully used due to specific site conditions or the economics of a particular structural design. It is obvious that the bearing capacity of a pile is usually unrelated to the pile material properties but rather is determined by the soil characteristics.

Considering the above comments and the results of the tests the following recommendations are appropriate:
1. For piles driven to hard bedrock, tips similar to the type tested in this program should always be used. It is possible to drive H-piles in conditions like the Sandusky Site without tips (even with larger hammers) as demonstrated by pile K-25VE. However, the construction control becomes extremely sensitive and not practical for routine use.
2. If a blow count criteria is used for hard bedrock it must be related to hammer size. Furthermore, it must not be applied for more than one inch penetration. The criteria might be stated "Piles shall be driven to a blow count of ____ blows per inch for not more than one inch." It is recommended that a dynamic formula be used to select the required blow count.
3. In spite of the fact that piles were successfully driven at the hard bedrock site by all of the hammers it seems unwise to use very large hammers under such

conditions. The important variables are numerous and include hammer energy, ram weight and pile weight. Recommendations on hammer size can be made that should be treated as guidelines rather than rigid rules. For piles of the sizes typically encountered in highway structures diesel hammers rated in excess of 35,000 foot-pounds and air/stream hammers larger than 20,000 foot-pounds should be used with care.

4. For soft bedrock the driving criteria should be selected in the same manner as is used for piles founded in soils.

5. If the soft bedrock is of shale similar to that encountered at the W92 site then the presence of relaxation can be checked by restriking the pile after an appropriate wait time. Since the pile will immediately tighten up the penetration for the very first blows should be measured. The decision must then be made regarding restriking all of the piles or accepting the capacity available after relaxation.

6. The relaxation observed in the shale is considered to be critical. This problem is common in weathered shale. It could lead to foundation failures if not controlled by restrike testing. If control procedures are implemented larger design stresses are justified.

7. The use of pile tips for soft rock offers no observable advantages. Therefore, they should not be used.

8. Unfortunately, a line between hard and soft bedrock cannot be defined. It is recommended that, in future construction work involving piles driven to bedrock having strengths between the two cases here, one or two piles with unprotected tips should be deliberately overdriven and performance monitored with the Pile Driving Analyzer. If possible the pile should be extracted. If performance is correlated with bedrock strength it may be possible to gradually develop a defined line between hard and soft bedrock.

9. The fact that a pile tip is extensively damaged does not mean that it cannot carry load effectively. Consider piles 520-B and K25-B. Both support a 55 ton design load with a safety factor greater than two. Only one of the piles (K13-V) would have had a safety factor of less than one (0.96) using the conservative failure criteria by Davisson. Certainly tip damage is undersirable but with the Pile Analyzer the capacity of a damaged pile can be measured and the pile can be used.

APPENDIX

A.1 General Data Presentation

The collection of field data for these tests was only a small portion of the total effort on this project. The major time spent on the project was in the laboratory in the analysis of the data. It is difficult to present such a large volume of data so that the reader gets a general overview of the results. In this Appendix the data will be reviewed in a rather detailed manner. Driving records and load test curves were drawn to standard scales for ease of comparison. Soil samples were analyzed and important information summarized on the boring logs. Case Method processing was applied to every blow recorded. Since in a driving sequence many blows are similar, only sample results will be presented to show the major trends of the data. The blow counts, penetrations and the bounce chamber pressures or strokes, are listed with these data so that the representative blow can be referenced to its location in the entire driving sequence.

Several dynamic parameters are presented with the Case Method results (Table A1, for example). VMAX is the maximum velocity at the pile top and is in ft/sec units. The maximum pile top displacement in inches is DMAX. EMAX is the maximum energy transferred to the measurement location near the pile top. This energy is often called ENTHRU and is only a percentage of the manufacturer's rated value due to inelastic collision, friction, heat, cushions, and helmet masses above the pile. It can be accentuated by poor hammer performance due to improper maintenance, inadequate air pressure, or incorrect fuel. The transferred energy is probably the most important measure of the driving system performance. The maximum measured force at the pile top is FMAX. The last two columns are the capacity predictions. P4 is the total driving resistance, i.e., the sum of both static and dynamic resistance, and is the reaction force which the hammer must overcome in order to drive the pile. After making an estimate of the damping constant, J, for the soil, the dynamic resistance is calculated. The static resistance (pile capacity), labeled CD, is found by subtracting the dynamic component from the P4 resistance. The damping constants used in processing were 0.1, 0.2,...0.6. The pile capacities printed were determined from J = 0.1 for Sandusky and J = 0.2 for W92.

The summarized data in Tables 4.1 and 4.2 are capacities from the original, more complete, data lists and are averaged over several blows in many cases. F1, Tables 4.1 and 4.2, is the force at the time of the first relative maximum of velocity. This time is the definition of impact which is used in this report. The value is truncated to two significant digits in the computer output so a value reported as 320 is between 320 and 329 kips. Damping constants of 0.1 for Sandusky and 0.15 for W92 were used for this summary. The 0.15 value for W92 is the most realistic one for those soil conditions. Due to averaging and a slight difference in damping constant for W92, the CD capacities in the summary table may differ slightly from those in the Case Method of Processing tables in this Appendix. For the Sandusky site, the maximum P4 capacity before the pile was damaged is also given. When pile tip damage occurred at Sandusky, the capacity often was changing so rapidly that the last blow alone was used. When only pile top damage occurred, the pile capacity is given for blows before the damage since such changes only represent the structural properties of the pile above ground and not necessarily of the pile section below ground. The gross buckling of the pile section above ground for the Sandusky point piles reduced the dynamic capacity but did not reduce the static load capacity of the undamaged pile section below ground. Since the pile was cut off at ground level for the static tests, the maximum observed capacities before damage are appropriate for the capacity prediction.

CAPWAP analyses were performed for several piles. For Sandusky, data were analyzed for blows giving the maximum Case Method capacity (before pile tip damage). CAPWAP analyses were not made for any battered piles at Sandusky. The CAPWAP capacity for Sandusky cannot be compared with the static tests on piles that had tip damage. The analysis was performed for the maximum capacity blows to determine where the maximum capacity was derived and to investigate the forces which were maximum at this time and were causing the pile damage. For W92, only piles which were load tested had CAPWAP analyses.

For the CAPWAP analysis (Table A6, for example) the pile was split into seven elements with springs between each element. The eighth element is for the pile tip resistance and damping. Program output is the element number and depth from instrumentation location to the bottom of the element. The soil

quake is the displacement where the static soil resistance changes from elastic to plastic behavior. CAPWAP allows the skin and toe quakes to be different. RES is the static soil resistance on a particular element or at the tip, and SUM RES is a sum of all of the resistance forces. (It is also the force at that location when the ultimate capacity is reached during the static load test.) J is the dimensional damping constant assigned to the element. [The tip J is EA/c times the tip dimensionless damping constant (JT) as given in Table 4.3. The sum of all element J's is EA/c times the skin damping constant (JS) in Table 4.3.] The skin J's are distributed proportionately according to the static soil resistance (RES) on that element. The weight of the pile segment and the stiffness of the interconnecting springs are given. The Max Spring Force is the largest computed force observed for that spring for the entire duration of the blow. Listed are the Maximum Measured Pile Top values of force, velocity and displacement as well as the Maximum Computed Pile Toe velocity and displacement. The Maximum Sum of Damping Forces Occurring Simultaneously indicates the dynamic portion of the total resistance. Table 4.3 is a convenient summary of the CAPWAP results.

A.2 Narrative Descriptions for Sandusky

A.2.1 MKT9B3 Hammer

Two piles were driven with the MKT9B3, a double acting, air/steam hammer. One pile was driven vertically while the second was battered at 1:4 and neither had a protective pile point at the tip. This was the smallest hammer used at the Sandusky site. The hammer characteristics are given in Table 2.7.

The driving records are shown in Figure A1. In both cases, blow counts exceeded 10 blows per foot before reaching 10 feet and 20 blows per foot before reaching 20 feet. Both driving records have sudden increases of about five blows per inch to greater than 20 for several consecutive inches, probably upon encountering bedrock. Blow counts of at least 70 blows per inch were achieved for each pile. The damage shown in Figure 4.6 probably was due to excessive driving.

The load test curves in Figure A2 show that pile 9B3V did not fail under the maximum attainable load of 386 kips. Pile 9B3B failed at 400 kips as seen in Figure A3. The load test curve for 9B3B was essentially elastic until near the failure load where it became plastic. Both of these piles could have been

loaded to a design load of over 90 tons using a factor of safety of two. The rather limited damage at the tips of these piles apparently had only a modest effect on their load carrying capacity.

Sample plots of force and velocity for 9B3V are given in Figure A4. Blow number 40 shows behavior that is typical of easy driving. The velocity, given in the first plot on the page, shows a steep rise from zero to a relative maximum designated as impact and marked by the first tick mark on the horizontal axis. Impact is completely defined by the hammer input. Since force is proportional to velocity for uniform piles until resistance effects are noticed, the force in the second plot has a similar shape at impact. This similarity continues until approximately 2L/c after impact as designated by the second tick on the horizontal axis. The value 2L/c is the time necessary for the stress wave to travel from the pile top along the pile length, L, reflect off of the pile tip, travel up the pile and return to the pile top. For easy driving at 2L/c, the velocity increases and the force decreases. The pile had encountered little resistance so displacement was large at the tip, the downward compressive wave reflected as tension, and pulled the pile top down (velocity increase) and away from the hammer so that the force between hammer and pile decreases. In very easy driving, as in blow 40, this phenomenon is observed for several 2L/c cycles in the velocity although the force is essentially zero after the first 2L/c.

After encountering bedrock, blow 238 shows a different behavior. At 2L/c, the velocity decreases and the force begins increasing. This is caused by the tip experiencing little movement after encountering bedrock, the downward compression wave then reflects as a compression wave superimposed on the downward travelling wave causing the top force to increase. This hammer is so small that the full soil resistance effect did not occur by 2L/c after impact but only later when the force had increased to the next relative maximum. Several causes contributed to this behavior. The 9B3 had little cushioning causing a rather sharp rise from zero to initial impact. Integration of the velocity gives a small displacement of less than 0.05 inches (the maximum displacement was less than 1/4 inch). This small displacement is less than the soil quake (displacement where model soil spring becomes plastic in a wave analysis), therefore, the full resistance does not occur upon arrival of the impact wave at the tip. The full resistance effect is delayed until the

displacement exceeds the quake

Further driving was similar except for one small change. Blow 309 shows a small increase in velocity and decrease in force at 2L/c. The soil resistance did not decrease because of the reflected increase in force after 2L/c. Something caused an apparent decrease in stiffness (increase in displacement) near the pile tip at precisely 2L/c when the stress wave travelled the pile's full length. This stiffness reduction is due to local damage at the pile tip. This was verified by inspection after extracting the pile as shown in Figure 4.6.

Table A1 contains the manual field observations of pile 9B3V. There were questions later raised concerning the calibrations of the recorded analog signals. Therefore dynamic Case Method results are not presented.

Figure A5 shows similar results for Pile 9B3B. For this test there were questions regarding the gain settings on the recording instruments and there fore, the Case Method processing results are not presented.

Due to the high accelerations associated with the small amount of cushioning present in this hammer the CAPWAP analysis became unstable. Therefore, results from CAPWAP are unavailable for these piles.

A vast wealth of information is obtainable in the Case Method processing results and especially in the plots. The concepts described for pile 9B3V can be studied and applied to each pile in this report.

A.2.2 Linkbelt 520 Hammer

Three piles were driven by the 520, a closed end or double acting diesel hammer. The piles were driven vertically without a point, vertically with point, and on a 1:4 batter without a point and are designated 520V, 520P (or 520VP) and 520B, respectively.

The driving records are shown in Figure A6. In all cases the blow counts are relatively small until rock is reached. Blow counts then exceed 20 blows per inch (BPI). Driving for 520V and 520B was continued in order to obtain several inches of driving at greater than 20 BPI. Pile 520V showed one inch of penetration greater than 20 blows per inch while Pile 520B had two inches greater than the 20 blows per inch requirement. In both cases, driving resistance decreased and fluctuated between 5 and 10 BPI. Driving on 520P

continued to exceed 20 BPI until the pile buckled in column action above ground, a few feet below the pile top. Approximately 10 feet of pile extended above ground.

The load test curves are given in Figures A7, A8 and A9. In the first and last cases, the initial slope is the same as the theoretical elastic compression slope for the failure definition indicating negligible skin friction. For 520V, at a very low load, a slope change occurred indicating a stiffness change in the pile (damage). Definition of ultimate failure occurred at 120 kips although the pile continued to carry additional load. A load of 235 kips was eventually recorded at a displacement of almost one inch. Pile 520P showed an ultimate load of 410 kips. This represents a stress that is near the yield stress in the pile material. The pile was damaged by gross buckling of the top portion above the ground line. However, there was probably some permanent bending deformation below the ground since it is not reasonable to expect that the pile would be fully restrained. The resulting lack of straightness produced the load test curve shown. The pile 520B's ultimate load was 354 kips with a maximum of 373 kips. The results of the load test on Pile 520B require some explanation. The data indicates a very flexible behavior at the beginning of the test up to about 200 kips. At that point the load deflection curve begins to exhibit a much stiffer behavior. The most logical explanation for this impossible physical performance is that errors were made in the measurement of vertical displacement. For example, it is possible that, due to the horizontally applied load, lateral motion of the pile top may have induced apparent vertical displacements due to the arrangements of the dial gage mount. This behavior is supported by the fact that the unloading curve followed the same path in the lower part of the curve as the loading path. The stiffness of the upper part of the curve is similar to that measured on the other piles. Therefore, the load test was analyzed by extending the upper part of the curve back to zero load and then starting the usual analysis with that point. The resulting capacity is 354 kips in spite of the damage shown in Figure 4.1.

Sample Case Method plots of force and velocity are given in Figure A10. Piles 520V and 520B show comparable results. Blow 72 for 520B shows a high force returned at 2L/c. By blow 257, the high force return at 2L/c has

disappeared. A force valley occurs at a time slightly less than 2L/c. This indicates that the initial downward wave was reflected by a pile section of reduced stiffness caused by pile damage near the pile tip. Continued driving with this large hammer caused the local pile tip damage to propagate up the pile similar to a fan fold shape. This accounts for the increases and decreases in blow counts as well as the capacities given in Tables A2 and A4. The bounce chamber pressure (B.C.P.) is given for 520V in Table A3.

The force and velocity plots for 520P in Figure A9 show continually increasing resistance at 2L/c. Table A3 contains the sample printed results. Contact with bedrock is readily observed by the increased capacities while forces in the pile are near the yield point. A characteristic of all diesel hammers is observable in this Table. Namely, when driving resistance is low, bounce chamber pressure (or stroke) is also low. As driving resistance increases, the BCP (or stroke) increases causing a greater ram impact velocity, thus increasing the pile top velocity. Since pile impact force and velocity are proportional by EA/c, force also increases and if the pile is short and the ram pile weight ratio large, the reflection from the pile tip arrives back at the pile top prior to a large decline in the incoming force causing a further increase, in this case, to the level of damaging the pile. Maximum energy also increases.

This hammer is equipped with a variable fuel throttle. If the bounce chamber pressure becomes too high, the hammer will lift off the pile. This "racking" can be damaging to the pile and hammer unless the fuel throttle is reduced. The 520P was driven full throttle and racking occurred when the pile contacted bedrock. The throttle was reduced between 21'-8" and 21'-9" (see Table A3) and velocities, energies, forces and capacities showed a corresponding decrease. The throttle was again increased slowly and the Case Method results returned. Throttling back caused the blow count to increase artifically. If the reason for the lower velocities and forces had been damage or weaker soil, the blow count would have decreased and the force-velocity records would have shown either signs of damage or reduced force at 2L/c, neither of which occurred.

The Case Method is supposed to give capacity results that are independent of hammer energy. However, in hard driving (high blow counts) experience shows that it underpredicts. This problem is accentuated when the input

forces are small and the failure conditions are not mobilized. The piles driven by the 9B3 hammer are an extreme example of this phenomenon.

Use of Case Method measurements is an effective tool for analyzing pile driving. Effects of throttle reductions are readily apparent. Questions regarding blow count increases can be properly assigned to poor hammer performance or soil resistance increases. Pile types which could not previously be inspected (steel H, timber, solid concrete sections) for damage visually except by excavation or extraction can be easily verified for damage using only force and acceleration measurements at the pile top (8). This quality control technique is sufficiently developed for use in the field by an experienced engineer. In general, quality control can be improved.

The force matches from CAPWAP for 520V and 520P are shown in Figure 11 and results are listed in Table A5 and in summary form in Table 4.3. For all CAPWAPs on the Sandusky site, the blows selected for analysis were those just after contacting bedrock and before damage had occurred. The measured and computed forces match well for 520V. Of the 369 kips predicted capacity, 353 kips occurred at the pile tip. Damping was small, due in large part to the small damping constant (J) at the pile tip. The maximum force occurring in the pile was 443 kips near the pile top. The maximum force near the pile tip was 382 kips. These results would be anticipated with a pile driven through weak overburden to a hard bedrock. Since a pile tip rarely has perfect contact with a bedrock surface, local stress concentrations could easily damage a pile tip with such a high average stress. This is especially true for all piles that are driven on a batter.

The force match for 520P is not as good for several reasons. First, a large offset of the measured force at the beginning of the record due to an unbalanced bridge circuit should be subtracted from the remainder of the record. This adjustment alone would significantly improve the match. However, the skin and toe quakes are very small due to the rock stiffness. This was required since the maximum computed toe displacement was also very small. It is probable that the actual pile quakes are more like those for the other piles at this site and of a reasonable value; but in order to activate all the resistance forces, they had to be less than the toe displacement. This also contributed to a poor force match. Of the 399 kips predicted capacity, 384 kips came from the pile tip. The maximum computed force in the pile was

377 kips at the pile tip.

Figure 4.1 shows the damage at the pile tips for 520V and 520B. In both cases the effective pile length was shorter than the initial pile length due to fan folding, as predicted by Case Method measurements. Pile 520V was longer than the photograph indicates as the pile broke during extraction and only the upper portion was recovered.

A.2.3 Vulcan 08 Hammer

Three piles were driven by the 08, a single acting air/steam hammer. The piles were 08V driven vertically without a point, 08P driven vertically with a point, and 08B driven without a point on a 1:4 batter. This hammer had the heaviest ram of any at the site.

The driving records for all these piles are given in Figure A12. In no case did the blow count exceed 20 BPI before damage occurred. Pile 08B was "driven" (damaged) over three feet after contacting bedrock. The blow count was the highest when bedrock was first encountered and declined after damage. At no time did it exceed 7 BPI. Pile 08V was driven to bedrock and driving was quickly stopped when the pile top was locally damaged probably due to the high resistance force reflection and poor hammer alignment. Further driving was not attempted. Pile 08P failed in gross column buckling above ground after the blow count reached more than 15 BPI on bedrock.

The load test curve for 08V in Figure A13 shows no sign of failure at 362 kips when the anchor system failed. The load test curve for 08B in Figure A14 begins at the elastic slope but quickly shows signs of damage with a reduced slope which is relatively linear. The defined ultimate failure load is 151 kips although the pile was accepting additional loads at 300 kips with large displacements.

Sample plots of force and velocity are shown in Figure A15. The first blows are for easy driving where velocity increases and force goes to zero at 2L/c after impact. Blow 43 for 08V and blow 37 for 08P show excellent load bearing capabilities with their high force curve reflections at 2L/c. Note the difference in the force curve immediately after impact for blows 47 of both 08V and 08P compared to the previous curves. This smoothing of the curve is due to pile damage located near the top.

Pile 08B never shows as strong a behavior in the plots like blow 43 of 08V, for example. The best blow for 08B is number 29. Even on this blow, the relative force minimum near 2L/c is present indicating pile tip damage starting to occur. Subsequent blows show this force valley to not only increase in magnitude but to also occur sooner and before 2L/c. This indicates that the damage is increasing in severity and is progressing up the pile as driving is continued.

The Case Method results are given in Tables A6 through A8. In all cases a sudden distinct increase in Case Method capacity was observed when bedrock was encountered. Early blows gave a maximum force at impact proportional to velocity by EA/c. With the higher resistance offered by bedrock, the force increased at 2L/c to levels high enough to cause top structural damage. Piles 08V and 08P sustained this top damage and maintained the high capacities at the end of driving. However, 08B showed a capacity trend of increases and decreases after the pile became damaged, corresponding to the pile being crumpled at the tip. Final capacities from the Case Method matched the load test results well.

The CAPWAP force matches for pile 08V and 08P are shown in Figure A16 and are both of good quality. Results are listed in Table A9 and are summarized in Table 4.3. Predicted capacity of 08V is 450 kips and 438 kips being tip bearing from the hard limestone. Tip damping was small and the quakes were of normal magnitude. The maximum force of 512 kips occurred near the pile top. However, if the pile had not failed locally at the top, forces near the pile toe were sufficiently high to cause local damage and would have led to pile 08V sustaining a crumpled tip. Pile 08P had 501 kips predicted capacity with 494 kips at the tip. The maximum force was 549 kips near the pile top with high forces along the entire length.

Figure 4.2 shows the pile tips for 08V and 08B. The flange tip of 08V shows the beginning of pile tip failure. Had the top not failed, the tip damage would have been greater. Pile 08B shows the results of continued driving crumpling the tip.

A.2.4 Kobe K13 Hammer

Three piles were driven by the K13, an open end, or single acting, diesel hammer. The piles were K13V driven vertically without a point, K13P driven vertically with a point, and K13B driven without a point on a 1:4 batter.

The driving records for all piles are shown in Figure A17. Pile K13V displayed behavior different from all other piles at the site. It is possible that local soil conditions were slightly different. Relative maxima at 20 feet and 22 feet penetrations were encountered. Blow counts of 20 BPI were achieved after 23 feet penetration but pile damage may have already occurred. Piles K13P and K13B both reached very high blow counts upon contact with bedrock and driving was stopped.

The static load test curves are given in Figures A18 and A19. Pile K13V began loading along the elastic compression slope but soon deviated and finally leveled off at 154 kips maximum at 0.7 inches displacement. The ultimate load was 106 kips. Pile K13B had not reached the ultimate load at 350 kips when the load reaction system failed.

The sample plots of force and velocity are given in Figure A20. The first blows of each pile are easy driving. Pile K13P shows strong resistance with little change in the record from blow 128 on. Pile K13B shows little change from blow 59 to the end. One item of interest on these blows is that the force record shows a larger relative minimum after impact and before 2L/c as compared with pile K13P. This indicates that something at the pile tip is not quite as good. Pile K13V never does show strong tip reflection. Blow 364 shows damage near the pile tip as the velocity increases and the force valley occurs slightly before the 2L/c time.

Case Method processing results are given in Tables A10 through A12. The capacity of K13V varies before obtaining the 20 BPI at 23'-3" and maximum capacity. Further driving produced additional damage which reduced blow counts, strokes, pile forces and capacities. Pile K13P shows behavior typical of all piles driven with points. Capacities are low until bedrock is encountered, then, the pile's structural yield strength is exceeded. High force levels are measured, and the pile fails in gross buckling above the ground surface. Pile K13B shows trends similar to the K13P except that forces and capacities are somewhat lower due to the smaller velocities measured at the top of the pile.

The CAPWAP force matches for K13V and K13P are given in Figure A21. The match for K13P is of very good quality. Results are presented in Table A13 and are summarized in Table 4.3. Pile K13V had 241 of the total 255 kips concentrated at the pile tip. The maximum force in the pile was 326 kips about halfway down the pile. With local stress concentrations, tip forces were high enough to cause pile tip damage. Pile K13P has 418 of its 429 kips predicted capacity at the tip. The maximum force of 424 kips occurred near the pile top. The maximum computed toe displacement is equal to the quake and this accounts for the force match quality in Figure A20.

Figure 4.3 shows the pile tips for K13V and K13B. Damage for the K13B was confined to the tip area while pile K13V shows damage over a longer length with part of the pile not recovered. It is possible that during retrieval the pile extractor also straightened out some of the kinks.

A.2.5 Kobe K25 Hammer

Four piles were driven with the K25, an open end, single acting, diesel hammer. Pile K25V and K25V-E were driven vertically without a point. K25P driven vertically with a point, and K25B without a point but on a 1:4 batter. This hammer had the largest rated energy of any hammer used during the tests.

The driving records are given in Figures A22 and A23. Only pile K25P was able to exceed 7 BPI before damage. Piles K25V and K25B were driven in a normal manner and reached as high as 7 BPI. In both cases driving was continued for several feet after reaching bedrock. Blow counts were decreasing and never recovered indicating probable damage. Pile K25V-E was not driven according to the specification in that pile driving was stopped immediately after the pile definitely contacted bedrock. It was intended to show that the K25 hammer could drive this pile to a satisfactory capacity, without damage, provided proper care was taken during the driving.

The static load tests are given in Figures A24 through A26. Pile K25V was loaded to 231 kips although ultimate failure was at 150 kips. Pile K25B was loaded to 350 kips with an ultimate failure of 318 kips. Pile K25V-E was loaded to the maximum of the hydraulic jack system at 414 kips with linear elastic response.

The sample plots of force and velocity are shown in Figures A27 and A28.

Pile K25V shows pile tip damage which is progressing up the pile in blows 177 and 228. The velocity increase and force valley come sooner after impact (and before 2L/c) as the undamaged pile length becomes shorter. Pile K25B shows a strong behavior for blow 37. However, by blow 140, the force return at 2L/c is not as large and a force before 2L/c indicates a moderate structural weakening. Pile K25P shows a return at 2L/c which continues to grow as driving continues. Note that the residual force at the end of the record indicates that at some time during the blow the pile top reached the yield of the steel and some plastic deformation occurred. The energy curve becomes negative due to the large permanent set when the velocity is negative.

Figure A28 shows the records for each blow on pile K25V-E. The first five blows show easy driving where the velocity increases and force decreases at 2L/c. Blows 6 through 9 show a steady gain in resistance as evidenced by the increasing trend in the force return at 2L/c. Blow 9 was considered as bedrock and driving was terminated.

Results of the Case Method Processing are listed in Tables A14 through A17. Pile K25V shows several cycles of capacity increase and reduction. Stroke, blow count and maximum forces show similar trends. Pile K25B has similar features but the differences between peaks and valleys is less. At the end of driving, pile K25B had a higher Case Method capacity than K25V, probably due to less structural damage. Pile K25P has increasing trends, however, the forces (capacities indirectly) have values which are too high due to the pile top yielding. The strain transducers used to measure force assume a linear stress strain curve. However, the plastic strains converted to force by this linear curve are unrealistically high. Therefore, forces and capacities for blows where the forces are over 500 kips ignore the Case Method predictions except to note that the yielding occurred. Pile K25V-E shows a definite higher resistance after bedrock contact with the increasing capacity/force trend culminating at the last blow where driving was stopped.

CAPWAP force matches as shown in Figures A29 and A30 are of reasonable quality except for K25P where the pile yielding affected the measured force. The computed force curve is parallel to the measured curve in this later region. CAPWAP results are listed in Tables A19 and A20.

A capacity of 400 kips was found for pile K25V with 374 kips at the tip

and a maximum force in the pile of 451 kips. Of the 550 kips capacity predicted for K25P, 538 kips were at the pile tip and the maximum force was 597 kips but these values are too large due to the inability to match the measured strain caused by yielding of steel. Pile K25V-E showed 450 kips of its 464 kips capacity at the tip and a maximum force in the pile of 500 kips.

Figure 4.4 shows the actual damage observed to the tip of pile K25B. Much of the pile was not recovered during extraction. The extractor was not capable of extracting the K25V. Pile K25P shows no local damage at the tip indicating effectiveness of the point even on such a larger hammer. Pile K25V-E showed almost no signs of damage, Figure 4.5.

A.3 Narrative Descriptions for W92

A.3.1 MKT 9B3 Hammer

The driving records for these piles are given in Figure A31. In all cases blow counts are comparatively high beyond a 15 feet penetration. Since the weathered shale begins at about 16 feet, the piles penetrated a small distance into bedrock before 20 BPI was reached and driving was terminated. All pile tips were in weathered shale.

The load test curves for piles 9B3V and 9B3P, vertical piles driven without and with points, respectively, are shown in Figures A32 and A33. The ultimate load for pile 9B3V was 160 kips with a maximum of 202 kips while the 9B3P ultimate load was 168 kips with a maximum of 227 kips. Maximum loads were achieved at large displacements.

Sample plots of force and velocity are given in Figure A34. Data from Pile 9B3B could not be processed due to electronic malfunctions. Both piles fail to show significant resistance effects at or after 2L/c as at Sandusky. Printed Case Method results are listed in Tables A20 and A21. Since the maximum force occures at impact which is controlled by hammer input it is relatively constant. The capacity predictions show a continuously increasing trend. Final capacities matched well with the static tests.

CAPWAP plots of the computed and measured forces are given in Figures A35 and A36. Force matches are of reasonable quality. Printed results are listed in Table A22 and summarized in Table 4.3. Of the 151 kips total resistance for 9B3V, only 62 kips occurs at the last element. Almost all resistance is located in the lower ten feet of the pile. The maximum pile force was only 238 kips near the pile middle. Damping, especially at the pile tip, was higher than at Sandusky, as was generally the case for the W92 site. Pile 9B3P

showed 60 kips of its 170 kips capacity on the last element. Maximum force of 250 kips was near the pile middle. Tip forces were small.

All piles were later extracted and none had sustained even the slightest amount of tip damage. Pile 9B3B had slight damage at the top due to improper alignment.

A. 3.2 Delmag D5 Hammer

Three piles were driven by the D5, a single acting diesel hammer. Two piles were driven vertically, one each with and without a point. The third pile was driven on a 1:4 batter.

The driving records are given in Figure A37. All three piles reached 20 BPI shortly after reaching the weathered shale and driving was stopped.

The static load tests are given in Figures A38 and A39. Pile D5V had a maximum capacity of 151 kips and an ultimate load of 141 kips. The ultimate load for pile D5P was 124 kips with a maximum of 131 kips.

Sample plots of force and velocity are given in Figure A40. Early blows again show weak resistance with velocity increase and force decrease at 2L/c. Later blows still show a force valley at 2L/c and no strong resistance reflection effects. Force in every case is a maximum at impact.

Case Method results are given in Table A23 through A25. In all cases maximum measured force was small such that stresses were at most 12 ksi. Driving stresses are usually much larger to be efficient, but the D5 was too small to induce anything larger. Capacities showed a generally increasing trend. Final capacities compared well with the static load tests for the vertical piles. The batter pile with a smaller Case Method capacity was not tested statically.

CAPWAP plots of the force matches given in Figures A41 and A42 are both of very good quality. Results listed in Table A26 are summarized in Table 4.3. For D5V, CAPWAP predicted a capacity of 130 kips with 40 kips at the last element. Maximum force in the pile was 164 kips at about the pile mid-length. For D5P the capacity was only 117 kips with 42 kips at the last element and a maximum force of 162 kips in the pile. Forces at the pile tip were small.

Extraction of these piles showed no signs of damage.

A.3.3 Linkbelt 520 Hammer

Three piles were driven with the LB520. Pile 520V was driven vertically without a point, 520P was driven vertically with a point, and 520B was driven on a 1:4 batter without a point.

The driving records for all three piles are given in Figure A43. All three piles achieved a blow count in excess of 20 BPI. Final penetrations for the 520 piles averaged 17'6" while the 9B3 averaged only 16'10" and the D5 only 16'2".

Sample plots of force and velocity are given in Figure A44. The last blows of each pile appear remarkably similar (velocity for 520V is plotted at a different scale). Note that the maximum force no longer occurs at impact as was the case for 9B3 and D5. This is due to a combination of the hammer characteristics and higher resistance effects.

Results of Case Method processing are given in Table A27 through A29. Resistance showed an increasing trend with capacities at the end of driving slightly less than 300 kips on the average. Maximum measured forces ranged from 323 kips for 520V to 366 kips for 520B giving stresses of about 27 ksi.

The CAPWAP force match for pile 520V is given in Figure A45 and is judged satisfactory. Results are listed in Table A30 and summarized in Table 4.3. The predicted capacity for 520V was 280 kips with 235 on the last element. This pile had significantly more capacity than any of the 9B3 or D5 piles with the increase due to the pile tip being imbedded further into the shale. As the depth increases, the shale becomes less weathered and hence stronger. The maximum force in the pile was 327 kips near the pile top.

The static load test was performed almost two weeks later. The load test curve for 520V is given in Figure A46. The ultimate load was 184 kips while the maximum was 187 kips. These values are about 100 kips less than the capacities as predicted by dynamic testing at the time of driving. It was theorized that the reason of the capacity reduction was a change in the shale conditions after driving the pile. Apparently, the shale strength had "deteriorated" around the pile tip.

The pile was retested dynamically to prove the hypothesis. The 520 hammer was to be used for this restrike but was unavailable and the contractor supplied a Linkbelt 440. This hammer is the same type but of a smaller size than the 520. The size is adequate to obtain comparable readings and the hammer is commonly used throughout Ohio to drive piles on similar jobs. In restriking the pile, the reference for set measurements shifted but the pile had an estimated blow count of 20 BPI.

Figure A47 shows the sample plots of force and velocity for three blows early in the restrike and three plots after about 40 blows. Results of Case Method Processing are given in Table A31. Capacities begin at 218 kips and gradually increase to about 240-250 kips. Further increases would be expected had driving continued.

In order to further confirm the dynamic tests two CAPWAP analyses were run. The first was from an early blow and labeled 520V/440E since it was an early blow for the 440 hammer on pile 520V. The CAPWAP force match in Figure A48 is of good quality. Results are listed in Table A32 and are summarized in Table 4.3. The CAPWAP predicted capacity was 190 kips, a value in very good agreement with the static load test results (184 kips). The toe capacity was found to be 27 kips at this time versus 145 kips after initial driving. Thus, the capacity reduction was due to a deterioration of pile tip capacity from the shale exhibiting weakened load bearing properties.

The later CAPWAP analysis for a blow late in the restrike is designated 520V/440L. The CAPWAP force match in Figure A49 is again of good quality. Results in Table A32 and 4.3 show that the continued driving had increased the capacity to 239 kips from 190 kips with 120 kips versus 75 kips at the last element. This blow demonstrates that the capacity increase observed with continued driving is due to strength gains near the tip as the pile is being redriven into shale with no deterioration.

Since the Case Method and CAPWAP results for the beginning of restrike matched the static test load, it can be concluded that the dynamic tests were correct at the time of initial driving. However, due to changing conditions in the shale, most of the pile tip capacity was lost before the static tests, two weeks later. Restrike showed that the dynamic methods correlated well with load tests. Continued restrike demonstrated that capacity increases are possible when the pile is redriven into firm shale.

The piles were later extracted. Pile 520V and 520P showed no sign of damage at the pile tip. Pile 520B showed the beginning signs of flange distortions which became more apparent with the larger hammers. A photograph of this deformation is shown in Figure 4.10. "Damage" of this type should not reduce the structural performance of the pile as indicated by dynamic testing procedures.

A.3.4 Vulcan 08 Hammer

Three piles were driven by the 08 hammer. The 08V pile was vertical with no point, the 08P pile was vertical with a point, and the 08B was without a point and on a 1:4 batter.

The driving records for all three piles are shown in Figure A50. All piles achieved a minimum blow count of 20 BPI. The average penetration was 18 feet. This larger hammer was able to achieve larger penetrations than those previously mentioned.

Sample plots of force and velocity for these piles are shown in Figure A51. Blows 42 for 08V, 19 for 08P and 22 for 08B are typical of structurally undamaged pile of good bearing resistance. Note that in these cases a relative maximum of force can be clearly noted at the time of impact. For the last blows on these piles this relative maximum is missing which is a clear indication of the pile top damage that did occur on the piles. The damage acts as a mechanical filter for the high shocks.

Results of the Case Method Processing are listed in Tables A33 through A35. In every case the capacities generally showed an increasing trend with maximums near the end. Pile 08B shows a downward trend at the end of driving. This was assumed to be caused by the pile top damage and not to an actual decrease in shale strengths. The next interesting observation is the maximum measured energy (Emax). After the pile became damaged, the maximum energy transferred to the pile dropped. Pile 08P, for example, showed a drop from 15 kip feet at 18'1" penetration to only 11 kip feet two inches later. Since the rise in blows per inch is equally rapid, it can be postulated that the reason 20 BPI was achieved is because of the decrease in hammer performance. No sudden increase in bearing capacity of the pile from the Case Method was observed which could account for the larger blow count. Final capacities reached into the high 300 kip region. Maximum forces for the piles reached 420 kips or a stress of 34 ksi. With high average stresses, local eccentricities can cause damage to the pile.

The CAPWAP force match for pile 08V in Figure A52 is for a blow where the pile damage was relatively insignificant. The match is of good quality. Results are listed in Tables A36 and 4.3. Of the total predicted capacity of 405 kips, 260 kips occurred as resistance of last element, undoubtedly due to increased penetration in the shale. The maximum force in the pile of 453 kips occurred near the pile mid-length.

The dynamic capacity for the 08V was 386 kips at the time of driving. Again, two weeks elaspsed before the static test load. The load test curve for 08V, Figure A53, has an ultimate load of 240 kips (54 ton design) with a maximum, at very large displacements, of 333 kips. Again, it was decided to dynamically restrike the pile to be sure that the capacity loss of 146 kips before performing the static load test was due to changes in the shale with time.

Force and velocity plots of the restrike on 08V using the Linkbelt 440 hammer are given in Figure A47. Results of Case Method processing in Table A37 show capacity predictions of 219 kips at the beginning increasing to 260 kips. The CAPWAP force match for an early restrike blow is given in Figure A54 and is

satisfactory. Results are listed in Tables A38 and 4.3. The CAPWAP capacity for this restrike blow was 230 kips, a difference of less than 5% from the static test. At this time the toe capacity was determined as 63 kips versus 260 kips toe capacity (Table A36) during the original driving, therefore, the entire capacity loss can be attributed to strength losses in the shale.

Proof is presented, again, that the dynamic testing techniques accurately reflect the true pile capacities at the time of testing. Results from initial driving indicated substantially higher capacities than measured during the static test two weeks later. Restrike confirmed the shale strength loss.

Figure 4.9 shows the flange distortion at the pile tip for piles 08V and 08P caused by this comparatively larger hammer. No tip distortion was observed for 08B. All three piles sustained local top damage during driving.

A.3.5 Delmag D15 Hammer

Three piles were driven by the D15 hammer. Pile D15V was driven vertically without a point, D15P was driven vertically with a point, and D15B was driven without a point on a 1:4 batter. This hammer was close in size and type to the K13 used at the Sandusky site. It was the only open end diesel hammer available at the time in this size range.

The driving records are shown in Figure A55. Pile K15V and K15B attained a driving resistance of 20 BPI. Pile D15P was badly damaged at the pile top and driving was terminated at only 14 BPI. Pile D15B was also damaged at the top at the end of driving. Average penetration was 18 feet. This damage was primarily due to misalignment. The only helmet available was 12 inch squares causing a misalignment between the driving system and the pile.

Sample plots of force and velocity for D15V and D15B are given in Figure A56. Electronic malfunctions prevented recording accurate data for pile D15B. Sample blows from the entire driving sequence are given for D15V, while those for D15P are from near the end of driving. Results from Case Method processing are listed in Table A39. Final capacities are in the mid-300 kips range.

The CAPWAP force matches are given in Figures A57 and A58. The match is better for pile D15P than for D15V. Results are listed in Tables A40 and 4.3. Pile D15V had 290 kips total capacity with 182 kips at the last element. Pile D15P had CAPWAP results of 201 kips at the last element of the 351 kips total capacity.

All of the above predictions are for the pile at the time of driving. Eleven days later the static load tests were run. Load test curves are given

in Figures A59 and A60. The ultimate load for pile D15V was 194 kips with a maximum of 230 kips at 1.2 inches displacement. The ultimate load for pile D15P was 197 kips with a maximum load of 204 kips at 0.8 inches displacement. These lower failure loads indicate that the shale at the pile tip had deteriorated after driving the pile.

Excavation of the piles showed that no major pile tip damage had occurred. Figure 4.10 shows minor tip distortion of the flanges for pile D15B.

A.3.6 Kobe K25 Hammer

Three piles were driven with the K25, the hammer with the largest rated energy. Pile K25V was driven vertically, Pile K25P was driven vertically with a pile point and Pile K25B was driven without a point at a 1:4 batter.

Driving records are given in Figure A61. A driving resistance of 20BPI was never achieved. Pile K25V did get as high as 15 BPI, but final driving resistance was 13BPI. Piles K25P and K25B had a final resistance of 9 BPI and 8 BPI, respectively. In each case, pile driving was stopped due to pile top damage. The average penetration was slightly more than 18' 11", or almost one foot deeper than piles driven by other hammers.

Sample plots of force and velocity are shown in Figure A62. Pile K25B was not processed because of electronic malfunctions. All sample blows were taken before pile top damage occurred. Both K25V and K25P show good bearing characteristics as evidenced by the lack of significant force valleys and the appearance of a resistance reflection at 2L/c.

Case Method results are given in Table A41. Capacities show an increasing trend with increasing penetration into the shale. Final capacities were around 500 kips for K25V and 480 kips for K25P. Maximum measured forces were about 490 kips for both piles. This is a stress of 39.5 ksi. It is easy to see why these piles incurred damage with a specified yield of 36 ksi. Even though the actual yield stress is slightly higher, any slight misalignment will cause local stress concentrations and produce local damage.

The CAPWAP force match for K25V in Figure A63 is of excellent quality. The results are listed in Tables A42 and 4.3. The capacity for this blow was 450 kips with 270 kips from the last element. The maximum force in the pile was 480 kips near the midlength. Forces at the pile tip were larger for this pile than any other pile at the W92 site. Since average forces at the top were approximately equal to the midlength forces and a higher potential for local stress concentrations exist at the top, it is not surprising that the damage occurred at the top.

The above capacities are for the time of initial driving. After nine days, the K25V pile was statically load tested with an ultimate and maximum load of 264 kips (Figure A63). This demonstrates the shale deterioration causing a capacity reduction of 236 kips. Pile K25B was tested statically, yielding at 317 kips. Restriking of these piles was not attempted for correlation with the dynamic tests.

Figure 4.11 shows the K25V flange distortion at the pile tip. This was the most deformation observed for any pile at this site. The extractor was unable to pull the K25B because of site conditions.

A.4 Special Test Piles at W92

Four additional piles were driven at the W92 site. The piles are labeled special pile one, SP1, special pile two, SP2, and so on. SP1 was driven vertically, SP2 was started at a 1:6 batter, SP3 at 3½:24 and SP4 at 9½:24. The measured batter at the pile tops at the end of driving are given in Table 4.4.

Driving records for all piles are shown in Figures A65 and A66. The piles were driven to initial elevations. The penetration depth in the figures is referenced, in inches, from this initial elevation. Blow counts are in blows per inch. Along the right hand edge of each record is a label indicating the portion of the record corresponding to the hammer being used.

Table 4.4 presents a summary of the data for these piles including driving resistance, Case Method capacities, measured energies, forces and batters. There was no significant difference in the delivered energy (Emax) between the vertical SP1 pile and piles SP2 and SP3 at 1:6 nominal batters. Pile SP1 at 1:2.4 batter shows some loss of efficiency for the 520 hammer. The heavier weight hammers were not used on pile SP4 since the contractor felt it unsafe for the crane at such larger batters.

Effects of soil set up can be observed in the pile capacity before penetrating into the firm shale. The beginning capacity of piles driven by 520 was more than the final capacity of piles driven by D5 due to the time period between testing although data not shown, pile SP1 had a driving interruption while using the 520 hammer and the restart showed a higher blow count. Occasionally, at the beginning of driving for hammers D5, 520 and 08, the blow counts would decrease from the beginning resistances in the first few inches of penetration before increasing again as further penetration was achieved. Blow counts were kept low so that the pile could be driven to further penetrations by the next hammer. It was intended to drive the pile to 20 BPI with only the K25, however, the K25 damaged the pile top in each case at approximately 10 BPI and driving was discontinued.

REFERENCES

1. Goble, G.G., Scanlan, R.H. and Tomko, J.J., "Dynamic Studies on the Bearing Capacity of Piles," Vol. I and II, Case Institute of Technology, 1967.

2. Goble, G.G., Tomko, J.J., Rausche, F. and Green, P.M., "Dynamic Studies on the Bearing Capacity of Piles, Phase II," Vol. I and II, Report No. 31, Division of Solid Mechanics, Structures and Mechanical Design, Case Western Reserve University, July, 1968.

3. Goble, G.G., Rausche, F. and Moses, F., "Dynamic Studies on the Bearing Capacity of Piles, Phase III," Report No. 48, Division of Solid Mechanics, Structures and Mechanical Design, Case Western Reserve University, 1970.

4. Goble, G.G., Likins, G.E., Jr. and Rausche, F., "Bearing Capacity of Piles from Dynamic Measurements," Final Report," Department of Civil Engineering, Case Western Reserve University, March 1975.

5. Smith, E.A.L., "Pile Driving Analysis by the Wave Equation," Journal of the Soil Mechanics and Foundations Division, Proceedings of the ASCE, Paper 2574, SM4, August 1960, pp. 35-61.

6. Goble, G.G. and Rausche, F., "Wave Equation Analysis of Pile Driving, WEAP Program," Vols. 1-4, Report No. FHWA-IP-76-14.1, National Technical Information Service, Springfield, Virginia 22161, July 1976.

7. Hirsch, T.J., Carr, L. and Lowery, L.L., Jr., "Pile Driving Analysis-Wave Equation Users Manual-TTI Program," Vols. 1-4, Report No. FHWA-IP-76-13.3, National Technical Information Service, Springfield, Virginia 22161, April 1976.

8. Rausche, F., "Criteria for the Determination of Pile Damage from Pile Top Force and Velocity," Notes prepared by Goble & Associates, Cleveland Heights, Ohio, August 1977.

9. Eiber, R.J., "A Preliminary Laboratory Investigation of the Prediction of Static Pile Resistances in Sand," Master's Thesis, Dept. of Civil Engineering, Case Institute of Technology, 1958.

10. Goble, G.G., Scanlan, R.H. and Tomko, J.J., "Dynamic Studies on the Bearing Capacity of Piles," Highway Research Record, Number 167, Highway Research Board, Washington, D.C., 1967.

11. Goble, G.G. and Rausche, F., "Pile Load Test by Impact Driving," paper presented to the Highway Research Board Annual Meeting, Washington, D.C., January 1970.

12. Rausche, F., Goble, G.G., and Moses, F. "A New Testing Procedure for Axial Pile Strength," Third Annual Offshore Technology Conference, Paper No. OTC 1481, Houston, Texas, 1971.

13. Goble, G.G., Fricke, K. and Likins, G.E., Jr., "Driving Stresses in Concrete Piles," Journal of the Prestressed Concrete Institute, Vol. 21, No. 1, Chicago, Illinois, Jan.-Feb. 1976.

14. Goble, G.G. and Rausche, F., "Dynamic Measurements of Pile Behavior," Proceedings of the Conference on Design and Installation of Pile Foundations and Cellular Structures, Lehigh University, April 1970.

15. Goble, G.G., Moses, F. and Rausche, F. "Prediction of Pile Behavior from Dynamic Measurements," Proceedings of the Conference on Design and Installation of Pile Foundations and Cellular Structures, Lehigh University, April 1970.

16. Goble, G.G., Walker, R. and Rausche, F., "Pile Bearing Capacity-Prediction vs. Performance," Proceedings of the Specialty Conference on Performance of Earth and Earth-Supported Structures, Vol. I, Part 2, Purdue University, Lafayette, Indiana, June 1972.

17. Goble, G.G., Kovacs, W.E. and Rausche, F., "Field Demonstration: Response of Instrumented Piles to Driving and Load Testing," Proceedings of the Specialty Conference on Performance of Earth and Earth-Supported Structures, Volume III, Purdue University, Lafayette, Indiana, June 1972.

18. Goble, G.G., and Rausche, F., "A Static and Dynamic Pile Test in Pocatello, Idaho," Division of Solid Mechanics, Structures and Mechanical Design, Case Western Reserve University, Cleveland, Ohio June 1971.

19. Goble, G.G. and Rausche, F., "A Static and Dynamic Timber Test Pile Test in Monticello, Minnesota," Division of Solid Mechanics, Structures and Mechanical Design, Case Western Reserve University, Cleveland, Ohio, December 1971.

20. Goble, G.G. and Rausche, F., "Static and Dynamic Tests on Two Pipe Piles in Philadelphia, Pennsylvania," Division of Solid Mechanics, Structures and Mechanical Design, Case Western Reserve University, Cleveland, Ohio, January 1972.

21. Goble, G.G. and Rausche, F., "A Static and Dynamic Pile Test in Oneonta, New York, Division of Solid Mechanics, Structures and Mechanical Design, Case Western Reserve University, Cleveland, Ohio, April, 1972.

22. Goble, G.G. and Likins, G.E., Jr., "A Static and Dynamic Pile Test in Whitehall, New York," Department of Solid Mechanics, Structures and Mechanical Design, Case Western Reserve University, Cleveland, Ohio, August 1973.

23. Goble, G.G. and Likins, G.E., Jr., "A Static and Dynamic Pile Test in West Palm Beach, Florida," Department of Solid Mechanics, Structures and Mechanical Design, Case Western Reserve University, Cleveland, Ohio August, 1973.

24. Goble, G.G. and Likins, G.E., Jr., "Predicting the Bearing Capacity of a Pile from Dynamic Measurements in Tarver, Georgia," Department of Solid Mechanics, Structures and Mechanical Design, Case Western Reserve University, Cleveland, Ohio, February 1974.

25. Goble, G.G., Fricke, K.E. and Likins, G.E., Jr.,"A Static and Dynamic Pile Test in Dade County, Florida," Department of Solid Mechanics, Structures and Mechanical Design, Case Western Reserve University, Cleveland, Ohio, March 1974.

26. Goble, G.G. and Fricke, K.E., "A Static and Dynamic Pile Test in Tallahassee, Florida, Department of Solid Mechanics, Structures and Mechanical Design, Case Western Reserve University, Cleveland, Ohio, December 1973.

27. Goble, G.G. and Likins, G.E., Jr., "A Static and Dynamic Pile Test in Fairmount, Minnesota," Department of Solid Mechanics, Structures and Mechanical Design, Case Western Reserve University, Cleveland, Ohio July 1974.

28. Goble, G.G. and Likins, G.E., Jr., "A Static and Dynamic Pile Test in Stow, New York," Department of Civil Engineering, Case Western Reserve University, Cleveland, Ohio, February 1976.

Quality of Overlying Soil	Depth of Penetration	Preferable Maximum Design Load
Poor	10 feet	20 tons
Poor	20 feet	25 tons
Poor	35 feet	30 tons
Poor	50 feet	35 tons
Fair	10 feet	30 tons
Fair	20 feet	35 tons
Fair	35 feet	40 tons
Fair	50 feet	45 tons
Very Good	7 feet	30 tons
Very Good	10 feet	35 tons
Very Good	20 feet	40 tons
Very Good	35 feet	50 tons
Very Good	50 feet	60 tons

Table 2.1: 1957 Ohio DOT H-Pile to Rock Driving Specifications

Depth of Penetration	Energy Rating of Hammer, in ft. lbs., Design Load, in tons, and Required Formula Capacity in tons								
	7,000 ft. lbs.			11,000 ft. lbs.			15,000 ft. lbs.		
	25T	35T	45T	25T	35T	45T	25T	35T	45T
	Poor Overlying Soil (Such as soft clay and silt)								
10'	--	--	--	80	--	--	65	--	--
20'	--	--	--	60	--	--	50	--	--
35'	--	--	--	52	--	--	42	100	--
50'	--	--	--	52	--	--	39	95	--
	Fair Overlying Soil (Such as medium clay and silt)								
10'	44	--	--	37	64	--	35	56	95
20'	38	--	--	29	50	--	27	43	70
35'	34	--	--	25	43	--	23*	36	60
50'	34	--	--	25	43	--	22*	35	55
	Very Good Overlying Soil (Such as compact sand & gravel)								
10'	28	47	--	25	39	58	25	37	52
20'	24*	39	--	20*	31*	45	20*	29*	40*
35'	21*	35	--	17*	27*	39*	17*	24*	34*
50'	21*	35	--	17*	26*	38*	15*	23*	31*

*For those required capacity values identified by an asterisk in the above tabulation it will be expedient (in order to avoid concern on the part of persons reading the plans) to specify the design load as the required capacity, rather than the smaller value shown (which is correct for the pertinent conditions and is shown in order to facilitate interpolation and extrapolation.)

Table 2.2: 1957 Ohio DOT H Pile to Rock Driving Specification

Depth in Feet	Description of Soil	Blows per 6" Standard Penetration	Moisture Content %	Wet Density lb./cu. ft.	Dry Density lb./cu. ft.	Liquid Limit %	Plastic Limit %	Uncons. Shear Strength (ksf)	Compress Stress (ksi)
0	Top Brown Soil								
5	Clayey Silt	2,2,3	27.1	126.5	99.6	29.9	17.3	1.71	
10			27.3	128.3	100.9	26.9	21.3	2.53	
15	Gray clayey silt with few rock fragments	1,2,2	21.0	122.1	100.9	29.1	19.1	0.87	
20	Clayey silt with gravel	2,2,4	13.0	149.1	132.0			13.10	6.8 9.5
25	Hard Lime Stone								6.9 5.5
30									3.8 6.9
35									7.3

Table 2.3: Soil Profile of Bore Hole No. 1, Sandusky

Depth in Feet	Description of Soil	Blows per 6" Standard Penetration	Moist. Content%	Wet Density lb./cu. ft.	Dry Density lb./cu. ft.	Liquid Limit %	Plastic Limit %	Unconf. Shear Strength (ksf)	Compression Stress (ksi)
0	Top Brown Soil								
		2,3,6							
5	Clayey Silt								
			26.4	128.4	101.6	30.8	20.5	2.75	
10									
		2,2,3	26.8	128.0	101.0	31.1	20.2	2.59	
15	Clayey silt with few rock fragments		27.5	130.0	102.0	30.8	18.4	0.68	
	Clayey silt with gravel	2,5,7	13.0	146.9	130.0			8.4	
20									7.4
		16,24, 40							7.6
25	Hard Lime Stone								4.1
									5.2
									5.3
30									5.7
35									

Table 2.4 Soil Porfile of Bore Hole No. 2, Sandusky

Depth in feet	Description of Soil	Blows per 6" Stand. Pen.	Moist. Content %	Wet Density lb./cu. ft.	Dry Density lb./cu. ft.	Liquid Limit %	Plastic Limit %	Uncnf. Shear Strength (ksf)	Compress. Stress (ksi)	Silt %	Clay %
0	Br.&Gray Clay (some silt)		18			30.4	23.2	8.64		42	58
5		5,9,12	18			30.0	23.9				
	Clay/Rock Fragments Silt Clay		19	122.7	105.8	34.0	22.8	10.02		36	64
10		6,10,15	18			26.8	19.4				
	Silt Clay		18			32.0	20.2			90	10
15 Clay	Gray Clay	3,5,10	15			25.0	18.2				
	Hard Clay to Clay Shale	50 .4'	7	132.5	115.8	27.5	20.3			95	5
Shale	Weathered Clay Shale		7						1.2	Grain sizes mostly med. to fine silts & coarse clay	
20	Clay Shale								2.2		
									1.3		
									1.1		
25	Clay Shale								1.1		

Table 2.5 Soil Profile of Bore Hole No. 1 W92

Depth in Feet	Description of Soil	Blows per 6" Stand. Pen.	Moist. Content %	Wet Density lb./cu. ft.	Dry Density lb./cu. ft.	Liquid Limit %	Plastic Limit %	Unconf. Shear Strength (ksf)	Compress. Stress (ksi)	Silt %	Clay %
0	Clay		12			25.8	18.2	2.30		55	45
5	Clay	5,9, 11	14	122.7	105.8	24.8	19.3	7.20			
	Clay		14	132.6	115.0	32.5	21.0	8.86		70	30
10	Clay	4,6,9	20	126.5	107.8	29.5	19.2				
Clay	Clay		20			29.8	19.5			40	60
15	Gray Clay (damp)	3,7,8	20								
	Gray Clay Till		10			19.0	13.7			72	28
Shale	Weathered Clay Shale	9,50 for 4'	10								
20	Clay Shale								1.1		
									1.5		
									1.2		
									1.0		
25	Clay Shale								2.0		

Table 2.6: Soil Profile for Bore Hole No. 2 W92

Hammer	Rated Energy Foot-pounds	Ram Weight pounds	Type	Sandusky	W92
Delmag D5	9100	1100	Open end diesel	No	Yes
Delmag D15	27,100	3300	Open end diesel	No	Yes
Kobe K13	24,400	2870	Open end diesel	Yes	No
Kobe K25	50,700	5510	Open end diesel	Yes	Yes
Link Belt LB440	18,200	4000	Closed end diesel	No	Yes
Link Belt LB520	30,000	5070	Closed end diesel	Yes	Yes
Mck Terry 9B3	8750	1600	Double Acting Air/Steam	Yes	Yes
Vulcan 08	26,000	8000	Single Acting Air/Steam	Yes	Yes

Table 2.7: Hammer Information

COMPARISON OF CASE METHOD WITH STATIC LOAD TEST RESULTS

No.	Name	Date	Hammer	Pile Description			Blows	Capacity - kips		Tip Soil
				Type	Area in^2	Length ft	Foot	Static Test	Case Method	
1	91A	6-66	V1	12" CIP	7.8	76.5	25	264	261	si cl
2	692	8-66	LB520	18" CIP	14.5	76	67	300	351	si cl
3	C1	1-67	D12	12" mono	5.8	59	44	184	201	sa gr
4	F30	6-67	LB440	12" CIP	9.8	33	30	87	101	sa si
5	F50	6-67	LB440	12" CIP	9.8	51.5	60	194	170	si
6	F50A	7-67	LB440	12" CIP	9.8	51.5	480	218	233	si
7	F60	7-67	LB440	12" CIP	9.8	60.5	96	180	217	si
8	F60A	7-67	LB440	12" CIP	9.8	60.5	144	218	208	si
9	CIN 68	1-68	D12	12" CIP	6.7	66	46	160	176	gr sa
10	272	4-68	LB440	12" CIP	6.7	57.5	R	194	218	sa si
11	T050	9-68	D12	12" CIP	9.8	48	16	47	40	si cl
12	T050A	9-68	D12	12" CIP	9.8	48	NA	92	153	si cl
13	T060	9-68	D12	12" CIP	9.8	60	57	39	43	si cl
14	T060A	9-68	D12	12" CIP	9.8	60	NA	81	145	si cl
15	Logan	11-68	D12	12" CIP	6.7	58	46	210	206	si gr sa
16	W56	6-69	D12	12" CIP	6.7	56.3	52	94	113	cl

Table 3.1: Case Method vs. Static Load Test Correlation

No.	Name	Date	Hammer	Pile Description			Blows	Capacity - kips		Tip Soil
				Type	Area in^2	Length ft	Foot	Static Test	Case Method	
17	W76	6-69	D12	12" CIP	6.7	78.2	100	163	163	cl
18	CH41	8-69	D12	12" CIP	6.7	41	50	180	200	gr sa
19	RI50	1-70	D12	12" CIP	9.3	50	NA	37	32	si cl
20	RI50A	1-70	D12	12" CIP	9.3	50	NA	60	54	si cl
21	CR7-74	1-71	LB520	14" CIP	9.5	75	57	390	391	si
22	CR5-72	1-71	LB520	14" CIP	8.8	80	47	279	263	cl si
23	CR6-52	2-71	LB520	14" CIP	8.8	90	400	262	251	cl si
24	T073	3-71	LB440	12" CIP	6.7	47	134	192	192	gr si cl
25	Idaho	3-71	LB312	16" CIP	18.6	46	52	390	389	sa
26	CP1	5-71	LB520	12" CIP	6.7	46	R	280	238	sa
27	CR1-63	8-71	LB520	14" CIP	9.5	103	156	286	286	si cl
28	Monticello	9-71	LB440	Timber	98.0	30	27	130	122	F sa si
29	PHIL77	11-71	V-1	12" CIP	7.1	45	72	230	195	gr sa
30	PHIL78	11-71	V-1	12" CIP	7.1	43	48	155	148	F sa
31	CIN 14.5	1-72	LB440	12" CIP	6.7	42	41	182	159	si cl
32	CIN 170	1-72	LB440	12" CIP	6.7	52	70	147	162	si cl
33	Oneonta	2-72	V1	12" CIP	9.6	86.5	10	221	248	si

Table 3.1 (con't.)

No.	Name	Date	Hammer	Pile Description			Blows	Capacity - kips		Tip Soil
				Type	Area in^2	Length ft	Foot	Static Test	Case Method	
34	Purdue	6-72	D12	10HBP57	19.2	50	40	166	164	gr si
35	CP2	7-72	C5	Timber	144.0	49	38	164	158	M F sa
36	CP3	7-72	V1	Timber	111.0	49	20	196	161	F sa tr si
37	CP4	7-72	C5	Timber	160.0	49	30	105	95	F-VF sa tr si
38	TP 4-5	9-72	D30	12" CIP	19.2	61	20	282	238	F-C si sa & gr (SM)
39	TP 5-5	9-72	D30	10HP57	16.8	75	11	210	196	F-C si sa, s.gr (SM)
40	TP 1-5	9-72	D30	Timber	161.0	45	19	280	263	M-C sa, s. gr (SW)
41	CP5	10-72	D22	12" CIP	6.7	59	27	136	125	cl till
42	GA	10-72	DE30	16" CIP	12.8	39.7	96	260	288	cl sa si (SC)
43	TP 6-1A	11-72	D30	12" PSC	143.0	66	23	260	266	si cl & F-M sa (CL-SM)
44	TP 1-1A	11-72	D30	Timber	177.5	50	24	350	377	F-C sa (SW)
45	TP 4-1A	11-72	D30	12" CIP	12.2	104	6	380	280	O. cl (CH)
46	TP 4-5A	11-72	D30	12" CIP	16.9	70	20	282	220	F-C si sa & gr (SM)
47	TP 5-5A	11-72	D30	10HP57	16.8	79	11	210	181	F-C si sa, s. gr (SM)
48	TP 1-5A	11-72	D30	Timber	161.0	45	19	280	335	M-C sa, s. gr (SW)
49	Whitehall	1-73	V06	14" PSC	196.0	140	127	150	118	si cl
50	CP6	3-73	H39	11" PSC	130.0	49.2	89	252	256	C sa & shell

Table 3.1 (con't.)

No.	Name	Date	Hammer	Pile Description Type	Area in^2	Length ft	Blows Foot	Capacity - Kips Static Test	Case Method	Tip Soil
67	CP14	2-74	K25	12" CIP	9.8	99	42	310	326	F sa, si (SP)
68	CP15	2-74	K25	14" PSC^{oct}	162.0	100	56	470	535	M sa (SP)
69	CP16	2-74	K25	14" PSC^{oct}	162.0	100	82	440	545	F sa & si (SP)
70	CP17	2-74	K25	16" CIP	18.4	104	32	440	392	(SP)
71	Maine 1	2-74	DE20	10" CIP	10.0	45	12	32	41	F si sa, s. mica
72	Maine 2	3-74	DE20	10" CIP	10.0	45	14	42	64	F si sa, s. mica
73	CP18	3-74	D22	16" mono	10.8	128	132	512	469	F sa, gr (SP-SM)
74	CP19	5-74	D30	18" PSC	314.0	24.8	152	550	578	sa
75	CP20	10-73		14" PSC^{oct}	162.0	48.5	NA	194	186	sa
76	Chat8	12-73	K60	360D5"PSC	487.0	150.0	36	516	554	si
77	Chat12	6-74	K60	360D5"PSC	487.0	153.0	23	650	646	si & cl
78	CP21	10-74	D30	18"PSC	324.0	65.0	60	354	321	limestone
79	CP22	11-74	D30	18"PSC	324.0	65.0	72	210	210	limestone
80	CP23	1-75	D30	14"PSC	196.0	57.0	90	416	352	limestone
81	CP24	2-75	D30	14"PSC	196.0	67.0	120	420	426	limestone
82	S-520V	7-75	LB520	10HP42	12.4	28.5	48	120*	122*	hard limestone
83	S-520P	7-75	LB520	10HP42	12.4	28.5	240	410	413	hard limestone
84	S-520B	7-75	LB520	10HP42	12.4	28.5	60	354*	297*	hard limestone

Table 3.1 (con't.)

No.	Name	Date	Hammer	Pile Description			Blows	Capacity - kips		Tip Soil
				Type	Area in^2	Length ft	Foot	Static Test	Case Method	
51	CP7	3-73	H39	11" PSC	190.0	49.2	224	450	439	C sa & shell
52	CP8	3-73	H39	11" PSC	190.0	49.2	238	480	521	C sa & shell
53	CP9	3-73	LB660	12" CIP	19.2	75	110	578	525	cl sa, till (SC)
54	WPB1	4-73	F20	18" PSC	324.0	45	114	234	197	sa & shell
55	WPB2	4-73	F20	18" PSC	324.0	35	59	170	148	sa & shell
56	CP10	4-73	65C	14" PSC	196.0	74	76	320	278	si F sa
57	CP11	5-73	65C	Timber	144.0	63	57	233	231	sa, cl si layers
58	CP12	5-73	65C	10" PSC	100.0	73	58	176	195	sa cl si layers
59	Tallahassee	5-73	F20	18" PSC	324.0	40	276	328	317	sa cl
60	Miami 1	7-73	D30	18" PSC	324.0	25	12	437	484	Oolitic limerock
61	Miami 2	7-73	D30	18" PSC	324.0	35	18	358	376	sa limerock & shell
62	Fair A	8-73	D15	Timber	132.8	29	60	169	184	cl, till
63	Fair D	8-73	D15	Timber	151.7	33	24	146	125	cl, till
64	CIN 1471	10-73	LB440	12" CIP	7.0	48	150	180	173	si cl
65	CR10E	1-74	LB520	12" CIP	8.1	53	42	140	146	cl si
66	CP13	1-74	K13	12" mono	7.0	50	50	382	374	sa, till

Table 3.1 (con't.)

No.	Name	Date	Hammer	Pile Description Type	Area in^2	Length ft	Blows Foot	Capacity - kips Static Test	Case Method	Tip Soil
85	S-08B	7-75	V08	10HP42	12.4	28.5	32	151*	163*	hard limestone
86	S-K13V	7-75	K13	10HP42	12.4	28.5	36	106*	129*	hard limestone
87	S-K25V	7-75	K25	10HP42	12.4	28.5	18	150*	138*	hard limestone
88	S-K25B	7-75	K25	10HP42	12.4	28.5	36	318*	311*	hard limestone
89	CP25	7-76	DA35B	12"PSC	144.0	27.0	156	366	378	si sa
90	W92-9B3V	8-76	9B3	10HP42	12.4	23.5	480	160	152	weathered shale
91	W92-9B3P	8-76	9B3	10HP42	12.4	23.5	240	168	170	weathered shale
92	W92-D5V	8-76	D5	10HP42	12.4	23.5	240	141	146	weathered shale
93	W92-D5P	8-76	D5	10HP42	12.4	23.5	240	124	123	weathered shale
94	W92-520V	8-76	LB440	10HP42	12.4	23.5	240	184	213	weathered shale
95	W92-08V	8-76	LB440	10HP42	12.4	23.5	240	240	224	weathered shale
96	CP26	8-76	K25	14HP89	26.1	90.0	216	470	405	mica schist
97	CP27	9-76	LB520	18"PIPE O.E.	27.5	81.0	250	472	577	mica schist
98	CP28	9-76	LB520	18"PIPE O.E.	27.5	70.0	260	580	577	mica schist
99	CP29	10-76	DA35B	12HP53	15.7	85.0	156	380	340	si
100	CP30	11-76	DA35B	12"PSC	144.0	35.0	76	344	354	si sa
101	CP31	4-77	LB440	12"CIP	6.6	43.5	17	108	118	sa cl
102	CP32	4-77	LB440	12"CIP	6.6	48.5	52	143	133	cl

Table 3.1 (con't.)

Table 4.1: Summary of Sandusky Test Data

Pile	Testing		Final	Blows/Inch		*Dynamic Data (Kips)					CAPWAP[6]			Static Tests	
	Dynamic	Static	Penetration	Max	Final	**Max P4	FMax Force	FI	P4	Case Method	RU	R_{toe}	FMax	Davisson kips	Max kips
9B3-V	7/24/75	7/14/76	22'-4"	75	75									--	386
9B3-B	7/24/75	7/8/76	22'-11"	70	70									400	400
520-V	7/21/75	10/7/75	26'-2"	32	4	367	195	165	141[5]	122	369	353	443	120	235
520-P	7/21/75	7/16/76	22'-1"	30	10+[1]	423	464	260	423	413	399	384	377	410	410
520-B	7/21/75	6/23/76	24'-11"	50	5	435	407	252	316[5]	297				354	373
08-V	7/22/75	11/1/75	22'-2"	13/2[2]	13/2	455	496	226	443	424	450	438	512	--	362
08-P	7/22/75		22'-0"	23/1½	23/1½[1]	460	524	210	450	439	501	494	549		
08-B	7/22/75	6/27/76	26'-4"	6	4/1/½	389	297	210	205	173				151	300
K13-V	7/23/75	7/15/76	24'-6"	20	3	315	215	215	157[5]	129	255	241	326	106	154
K13-P	7/23/75		21'-10"	20/⅛	20⅛[1]	426	444	250	416	407	429	418	424		
K13-B	7/23/75	7/2/76	22'-10"	70	70	346	368	225	346	336				--	350[3]
K25-V	7/22/75	7/15/76	25'-10"	7	3/2	414	235	190	160[5]	138	400	374	451	150	231
K25-P	7/22/75		22'-2"	12/¾	12/¾[1]	435	474	300	435	419	550	538	597		
K25-B	7/22/75	6/30/76	25'-10"	7	3	431	370	295	336[5]	311				318	350
K25-VE	7/23/75	7/16/76	19'-6"	3/6"	3/6"	462	485	298	462	449	464	450	500	--	414

SANDUSKY DATA

1. Pile buckled in column action above ground
2. Pile top damaged locally
3. Load test curve close to failure
4. Quake sensitivity
5. Pile tip damage observed from dynamic measurements
6. All CAPWAPS for blow with Max P4 (just after pile hit rock and before pile damage)

Case Method = Total static capacity

P_4 = Total driving resistance

*At end of driving except where pile top damage occurred

**Before pile damage

Pile	Dynamic Test	Static Test	Final Penetration	Final Blows/Inch		Final Dynamic Data** FMax	FIMP	P4	CD=.15*	CAPWAP[2] RU	R3	FMax	Static Load Davission	Max
						Force		Resistances-kips-ultimate				kips	kips- ultimate	
9B3-V	8/3/76	8/19/76	16'-5½	20/½		213	213	198	152	151	62	238	160	202
9B3-P	8/3	8/19	16'-6"	20		225	225	217	170	170	60	250	168	227
9B3-B	8/3		17'-5"	20		--								
D5V	8/4	8/18	16'-5"	20		153	153	173	146	130	40	164	141	151
D5P	8/4	8/18	16'-2"	20		151	151	153	123	117	42	162	124	133
D5B	8/5		15'-10"	20		115	115	106	81					
520V	8/5	8/18	17'-4"	20		317	233	313	282	280	235	327	184	187
520P	8/5		17'-3"	20/3/4		362	285	347	315					
520B	8/5		17'-10"	20/7/8		363	263	334	305					
08V	8/6	8/20	17'-7"	20[1]		427	298	416	390	405	260	453	240	333
08P	8/6		18'-3"	19/3/4[1]		453	295	428	405					
08B	8/6		18'-1"	24/½[1]		415	283	397	372					
D15V	8/9	8/20	17'-3"	25		311	295	375	340	290	182	307	194	230
D15B	8/9		18'-3"	20[1]		--								
D15P	8/9	8/20	18'-5"	14[1]		335	307	412	382	351	201	357	197	204
K25V	8/11	8/21	18'-9"	13[1]		485	364	539	509	450	270	480	264	264
K25B	8/11	8/21	19'-1"	9[1]		--							317	317
K25P	8/11		19'-0"	4/½[1]		484	375	526	490					
520V/440R	9/22	8/18			***	213	169	234	213	190	75	207	184	187
08V/440R	9/22	8/20			***	224	178	246	224	230	63	237	240	333

W92 & I90 Data

* CD values as listed on table A21 etc. are computed using J = .20.

** At end of Driving Except When Pile Top Damage Occurs

*** These Values are for Beginning of Restrike

1. Pile Top Buckled
2. All CAPWAPS for Last Blows When P4 Was Maximum
3. Last Element

Table 4.2: Summary of W92 Test Data

Pile	Resistance (Kips) R	R_{Toe}	Damping	CAPWAP SUMMARY Force (Kips) FMax	Damping Constant JS Skin	JT Toe	Quake QS Skin	QT Toe	Displacement DTMX Pile Top
Sandusky									
520V	369	358	47	443	.25	.05	.1	.12	.25
520P	399	388	47	377	.4	.05	.01	.04	.04
08V	450	442	70	512	.4	.05	.1	.15	.24
08P	501	496	46	549	.2	.05	.15	.15	.25
K13V	255	245	53	326	.25	.05	.1	.15	.31
K13P	429	421	51	424	.3	.05	.1	.1	.1
K25V	400	382	148	451	.45	.1	.1	.4	.44
K25P	550	542	58	597	.3	.05	.1	.1	.17
K25VE	464	454	76	500	.35	.05	.1	.15	.17
W92									
9B3-V	151	62	96	238	.3	.15	.1	.15	.16
9B3-P	170	60	98	250	.4	.15	.07	.12	.12
D5-V	130	40	63	164	.32	.18	.06	.12	.12
D5-P	117	42	74	162	.3	.2	.1	.1	.16
520V	280	235	55	327	.25	.1	.1	.16	.27
08V	405	260	75	453	.3	.15	.1	.3	.37
D15V	290	182	74	307	.2	.1	.1	.12	.18
D15P	351	201	98	357	.2	.2	.1	.2	.22
K25V	450	270	115	480	.4	.2	.12	.17	.34
520V/440E	190	75	68	207	.45	.2	.06	.11	.13
520V/440L	239	120	58	235	.37	.22	.04	.12	.12
08V/440	230	63	52	237	.35	.1	.06	.1	.14

Table 4.3: Summary of CAPWAP Analysis

Hammer	Pile	Date	Blows/Inch Initial	Interm	Final	Inches Driven	Capacity (Kips) Initial	Final	EMax Transfer energy (Kip-Ft)	Force Max Initial	Final	Batter
D5	SP1	8/4/76	15		13	2	77	95	2.	112	135	Plumb
520		8/5	5	3	10	14	114	236	7.3	153	312	
08		8/6	2		5	7	276	319	15.0	357	412	
D15		8/9	11		11	2						
K25		8/11	5		10	3						
D5	SP2	8/4	7		4	13	44	40	2.	113	132	4"/2'
520			4	3	6	6	77	240	7.2	108	330	(1:6)
08		8/6	4	3	6	5	263	313	15.1	345	397	
D15		8/9	8		11	3						
K25		8/11	5		10	3	380		14.6	430		
D5	SP3	8/4	5	4	5	16	45	46	2.	107	117	3-5/16/2
520		8/5	17		20	2	130	220	7.3	156	291	(1:6)
08		8/6	5	3	5	5	272	289	15.0	366	377	
D15		8/9	9		8	3						
K25		8/11	4		9	4	340	370	14.3	375	395	
	SP4											10-5/16"
D5		8/4	10	6	8	9	46	44	2.	105	107	10-5/16"/2' (1:2 .4)
520		8/5	8	3	12	18	141	225	6.3	175	313	
D15		8/9	10		11	2						

Table 4.4: Summary of W92 Special Pile Test Data

Figure 2.1
Interpolation Aid
for
Piling Table
1957 Specification

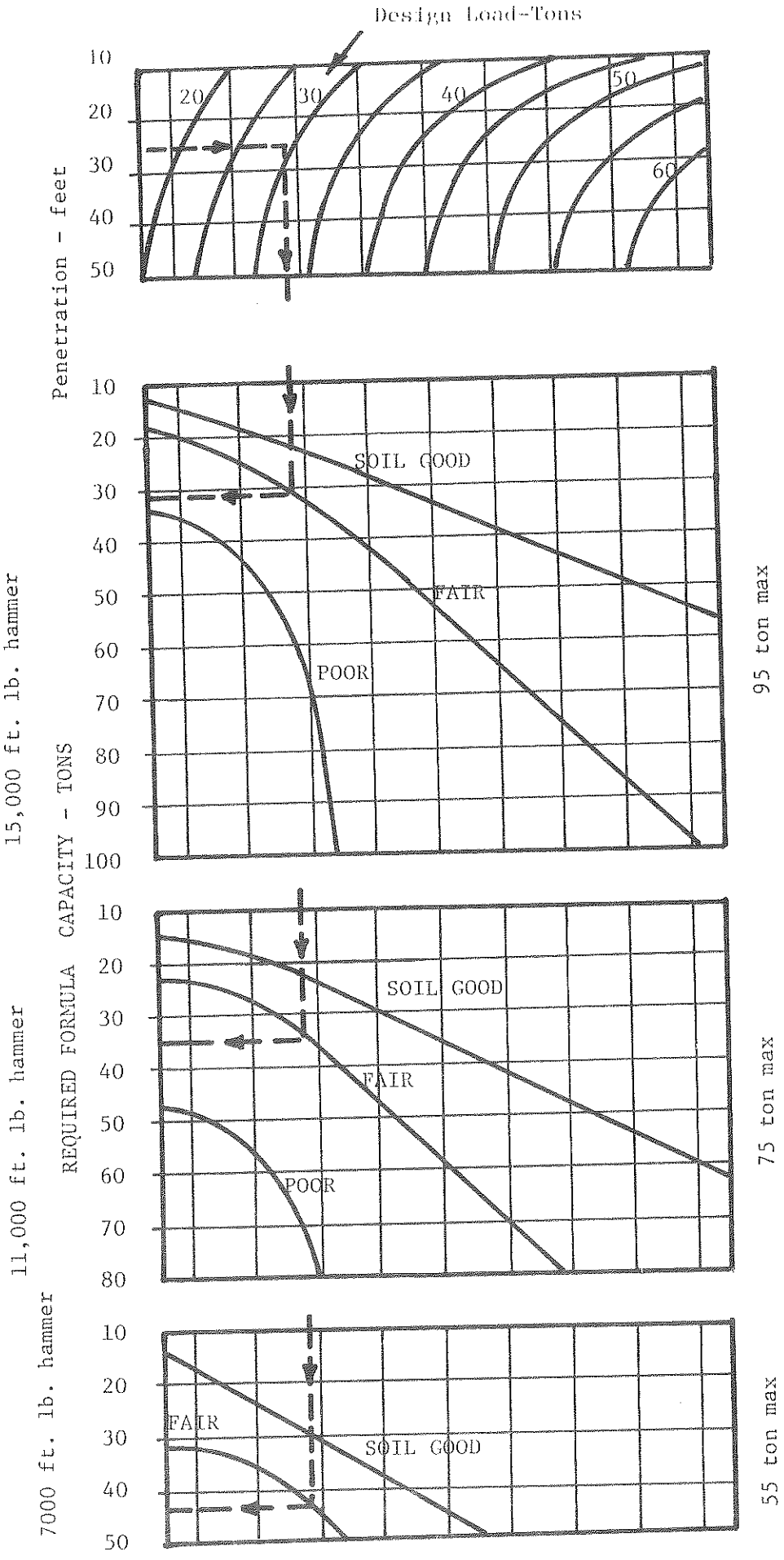

EXAMPLE

Select Penetration in upper left corner (25 ft.)

Move right to DESIGN LOAD (29T)

Move down to type of SOIL (Fair) observing the Energy Rating of Hammer

Move left and read REQUIRED FORMULA CAPACITY

for Hammer

15,000 - (31T)

11,000 - (35T)

7000 - (43T)

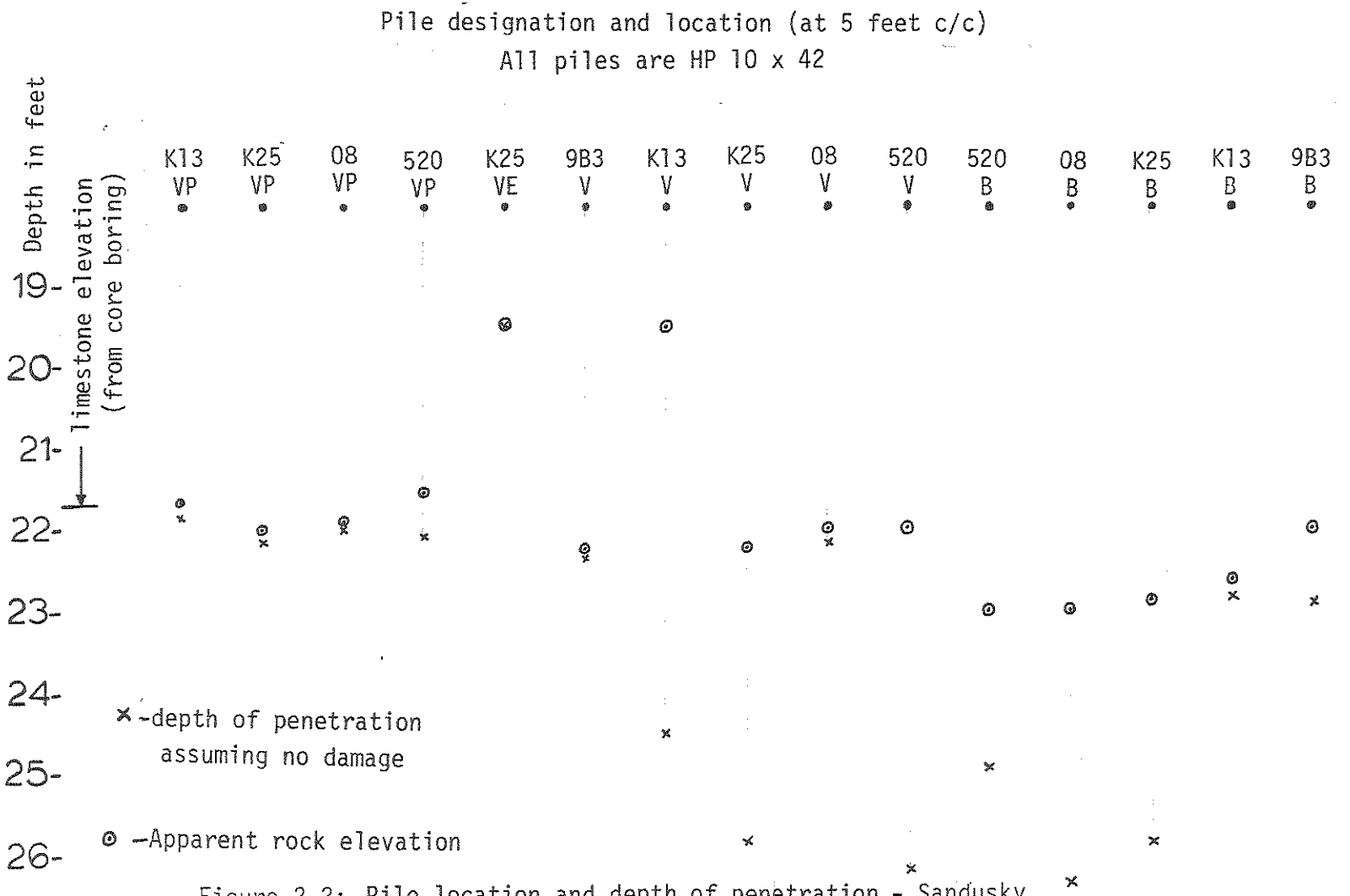

Figure 2.2: Pile location and depth of penetration - Sandusky

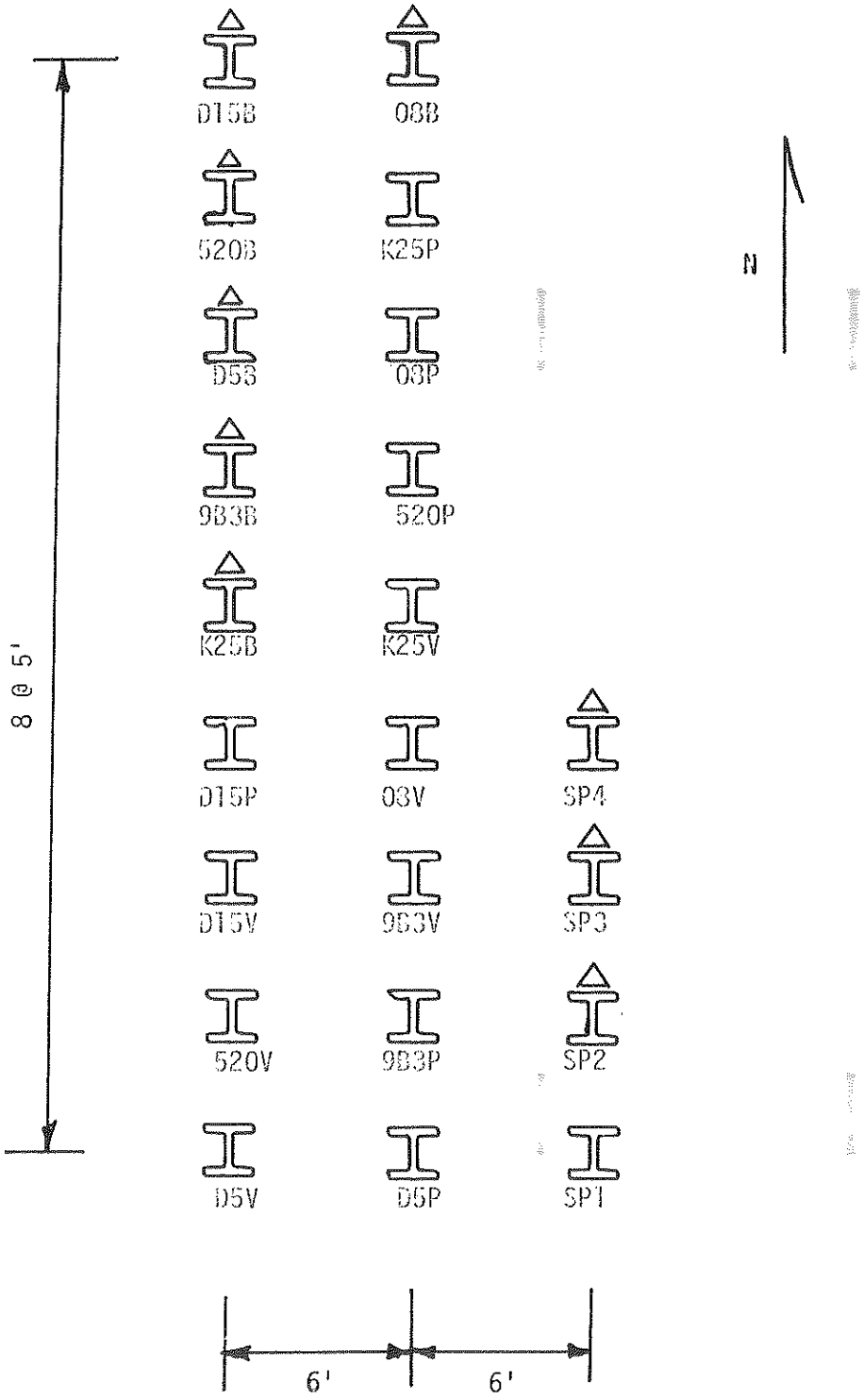

Figure 2.3: W92 Pile Locations

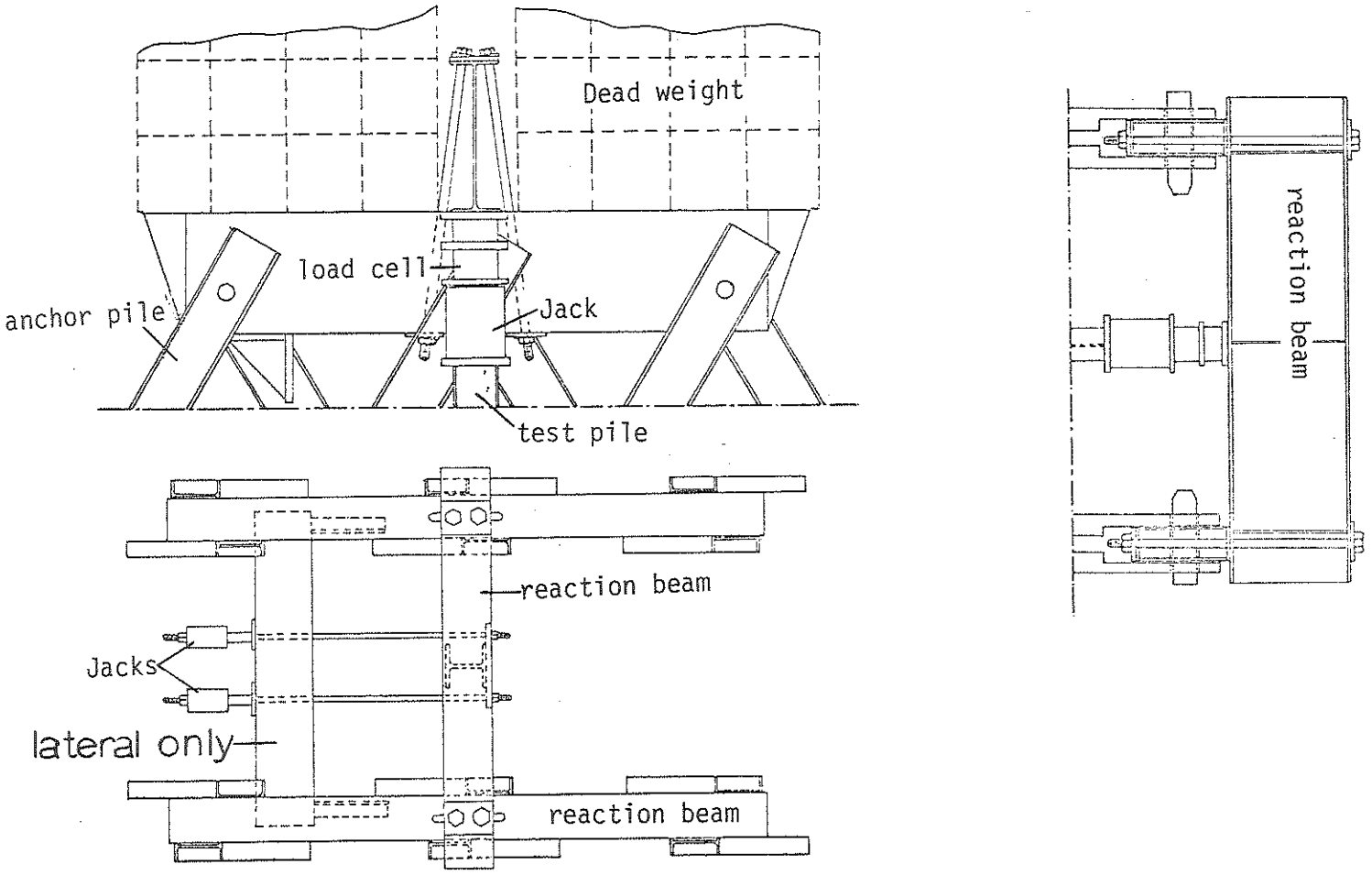

Figure 3.1: Static load test system

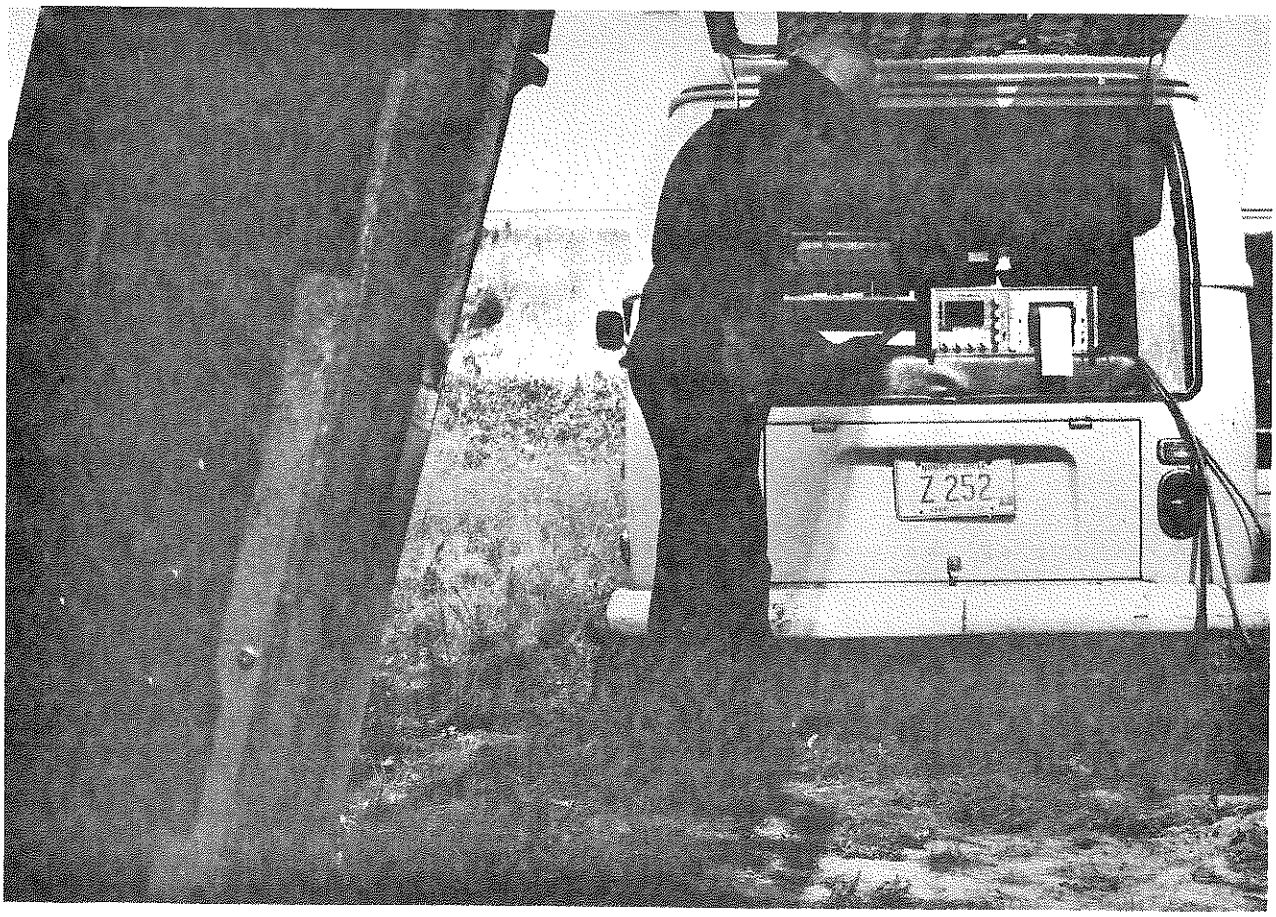

Figure 3.2: Strain Transducer and Accelerometer on Pile

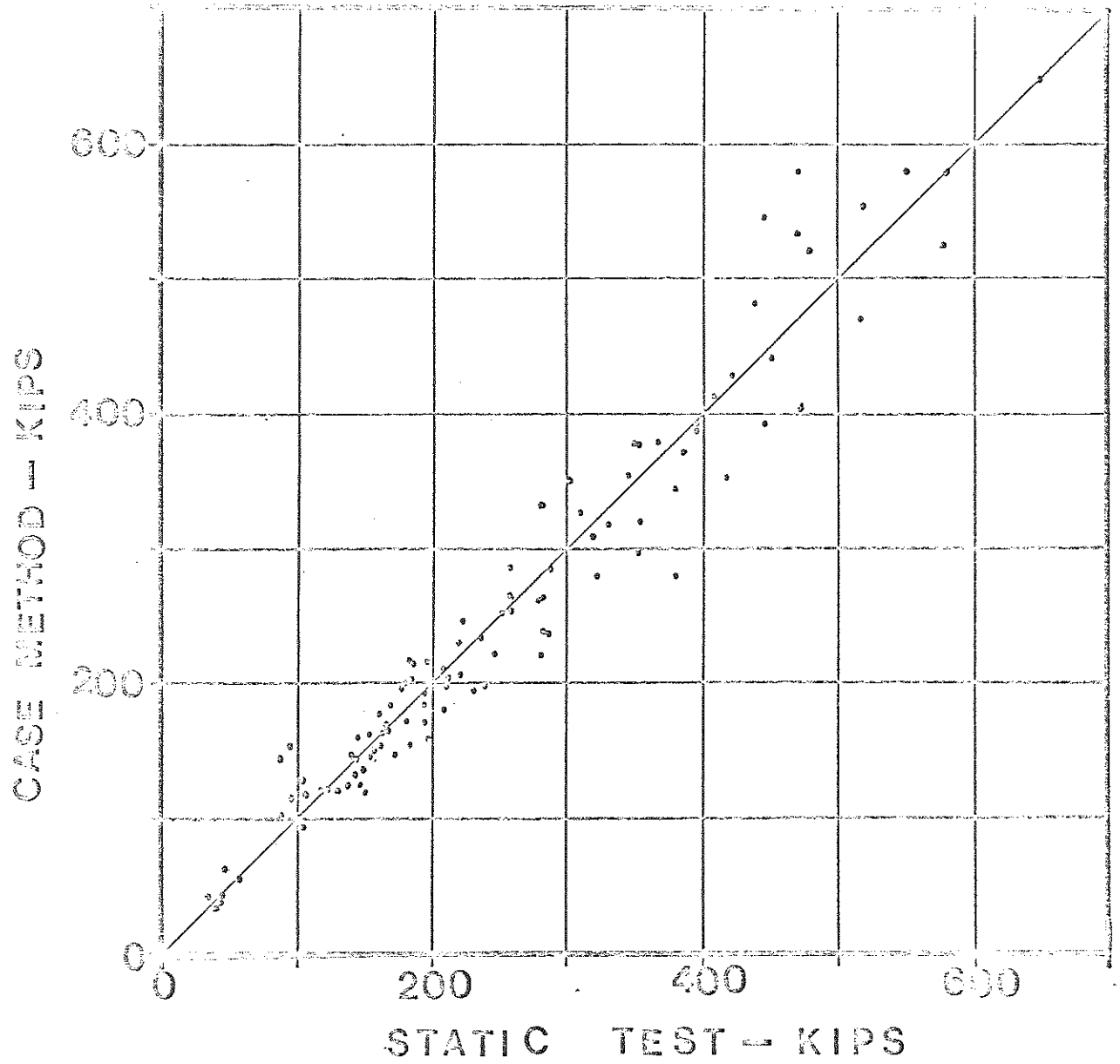

Figure 3.3: Case Method vs. Static Load Test Correlation

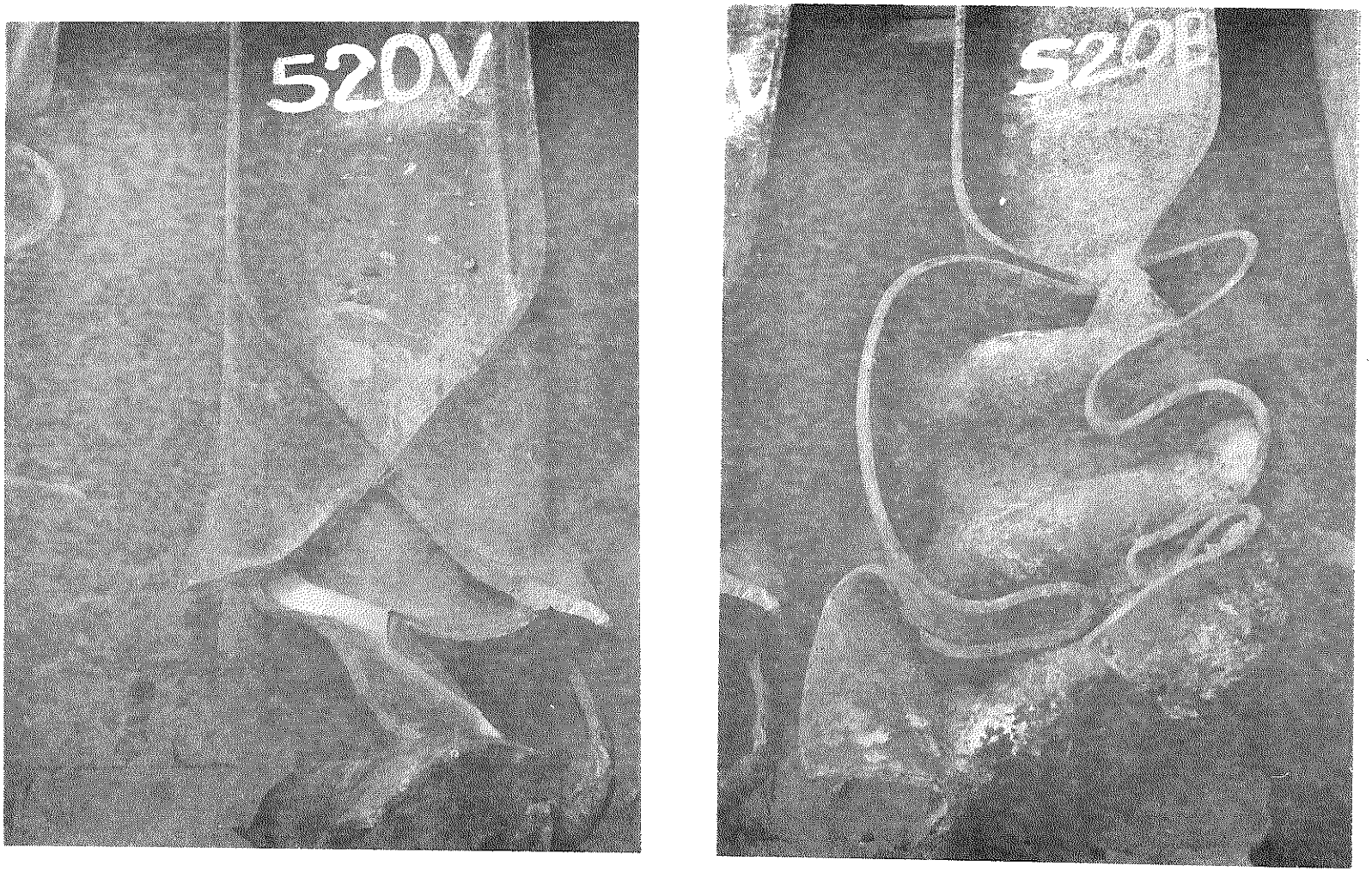

Figure 4.1: Tips for Piles Driven at Sandusky by the 520 Hammer

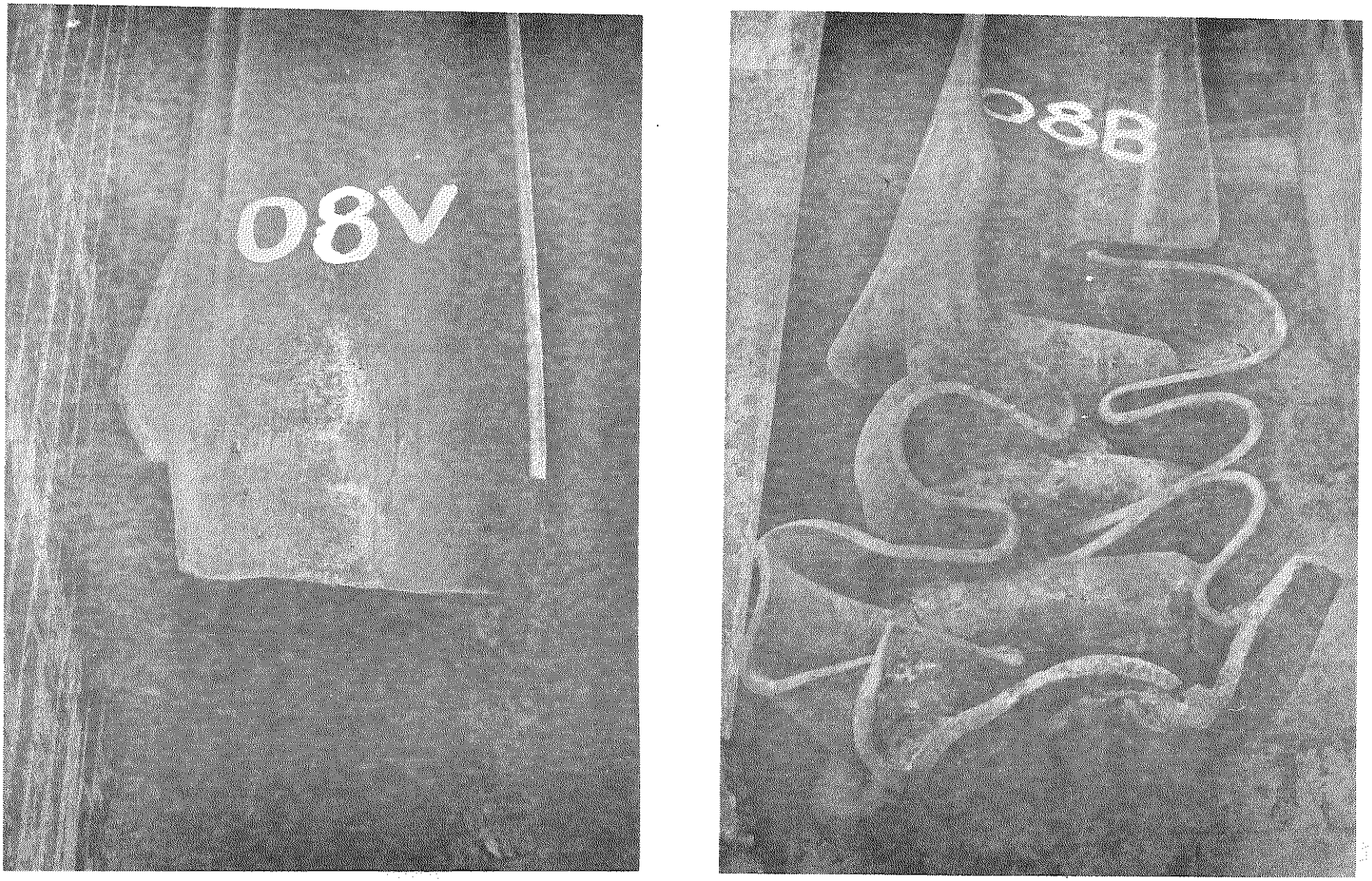

Figure 4.2: Tips for Piles Driven at Sandusky by the 08 Hammer

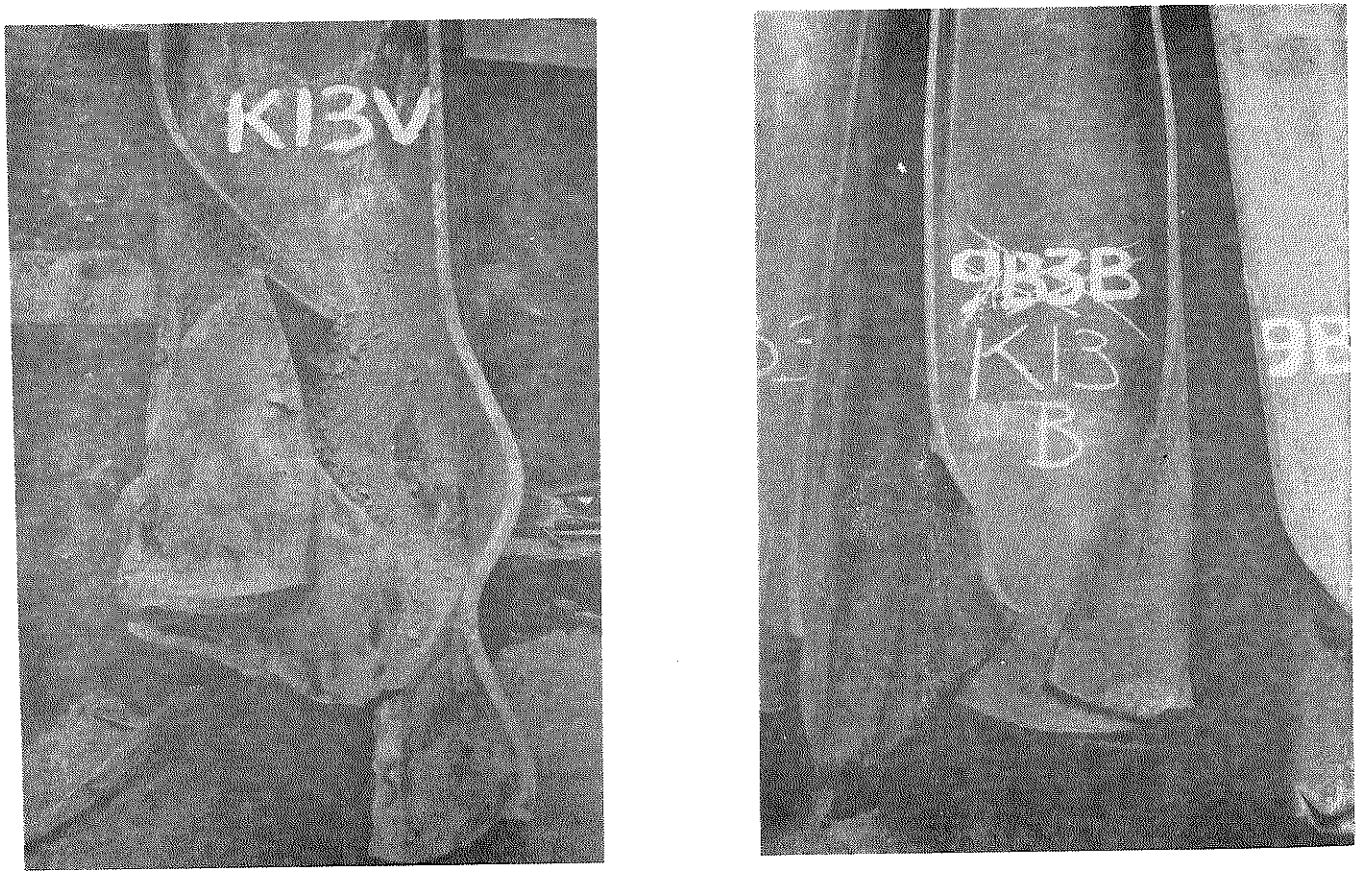

Figure 4.3: Tips for Piles Driven at Sandusky by the K13 Hammer

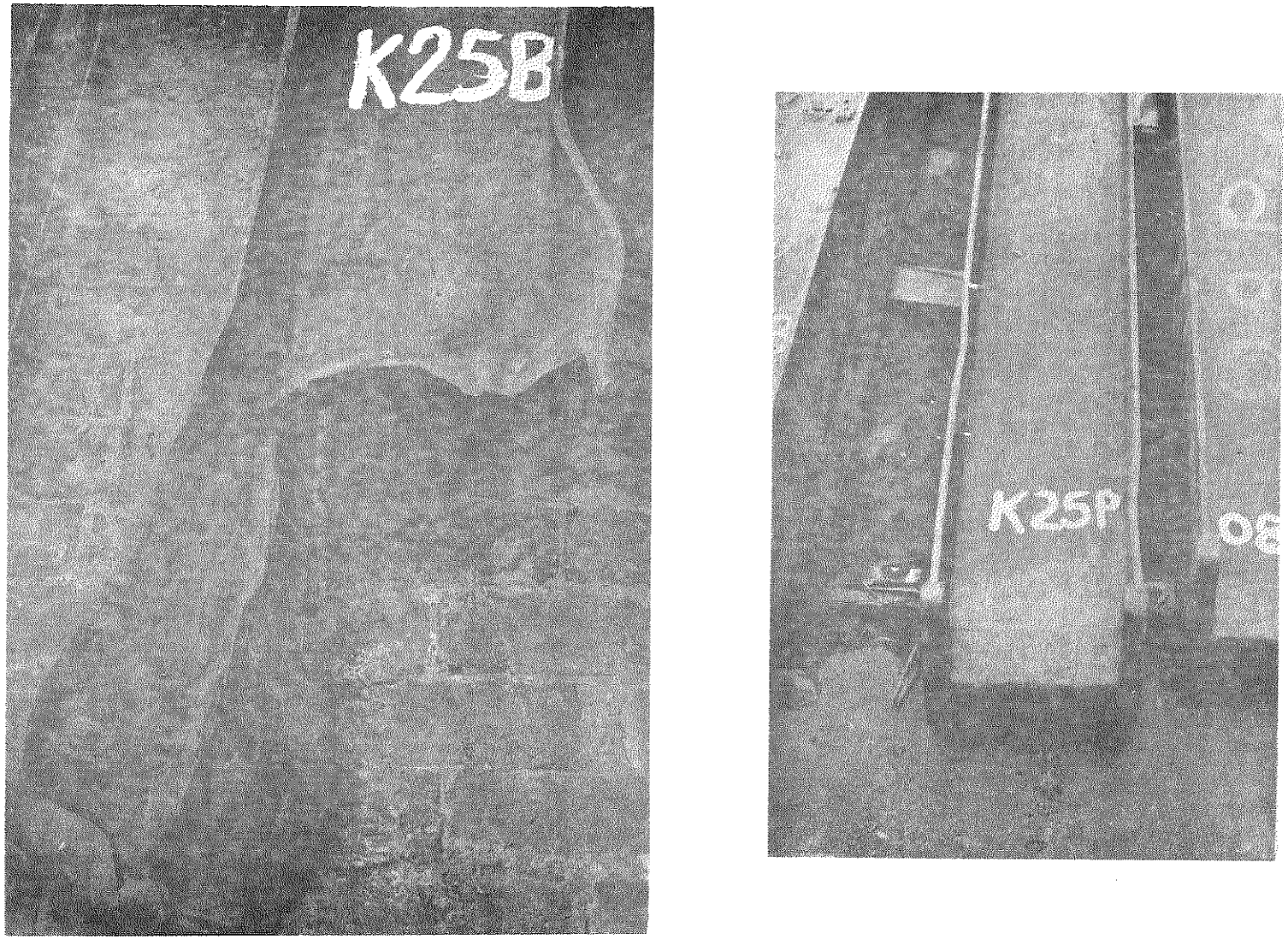

Figure 4.4: Tips for Piles Driven at Sandusky by the K25 Hammer (K25B, K25P)

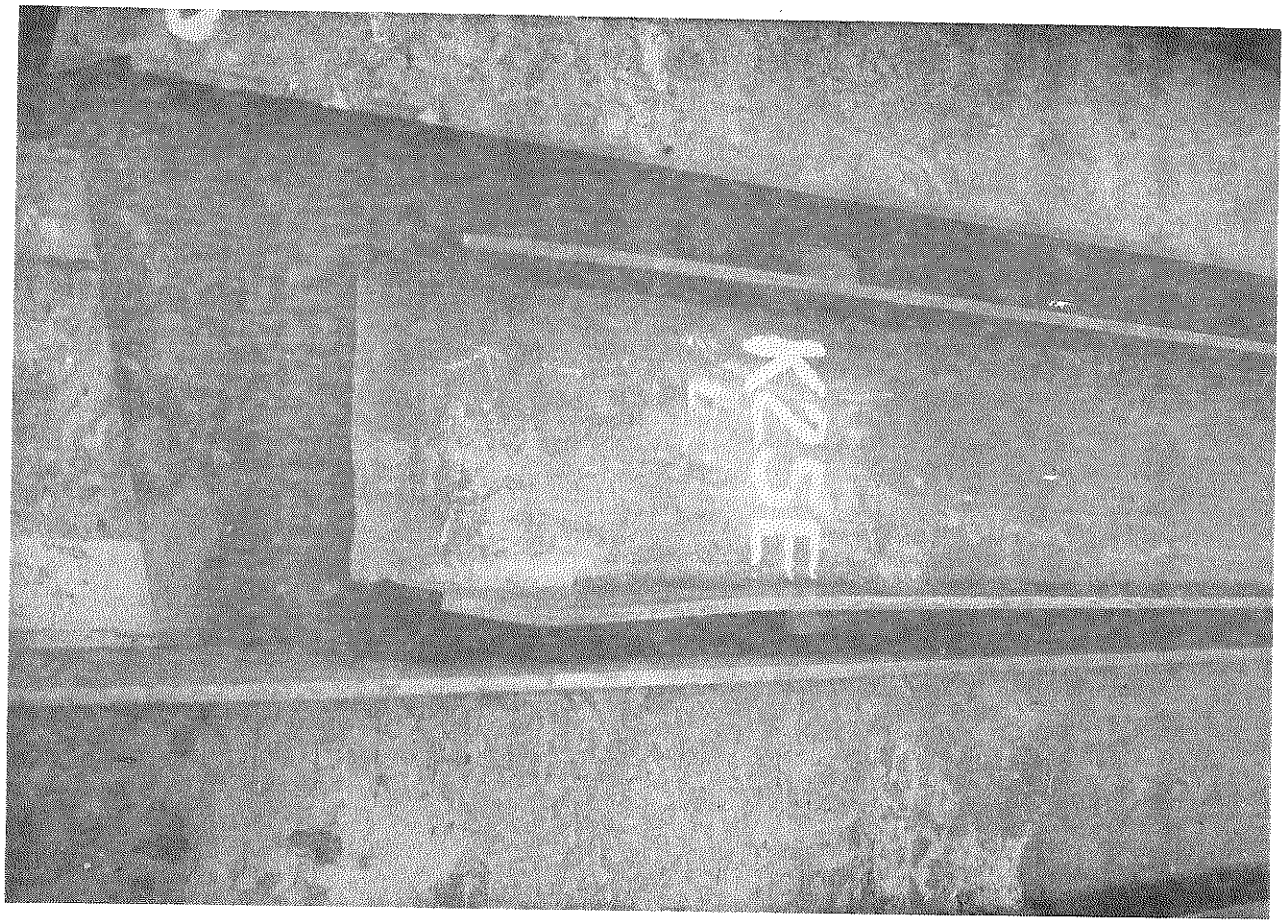

Figure 4.5: Tips for Piles Driven at Sandusky for the K25VE

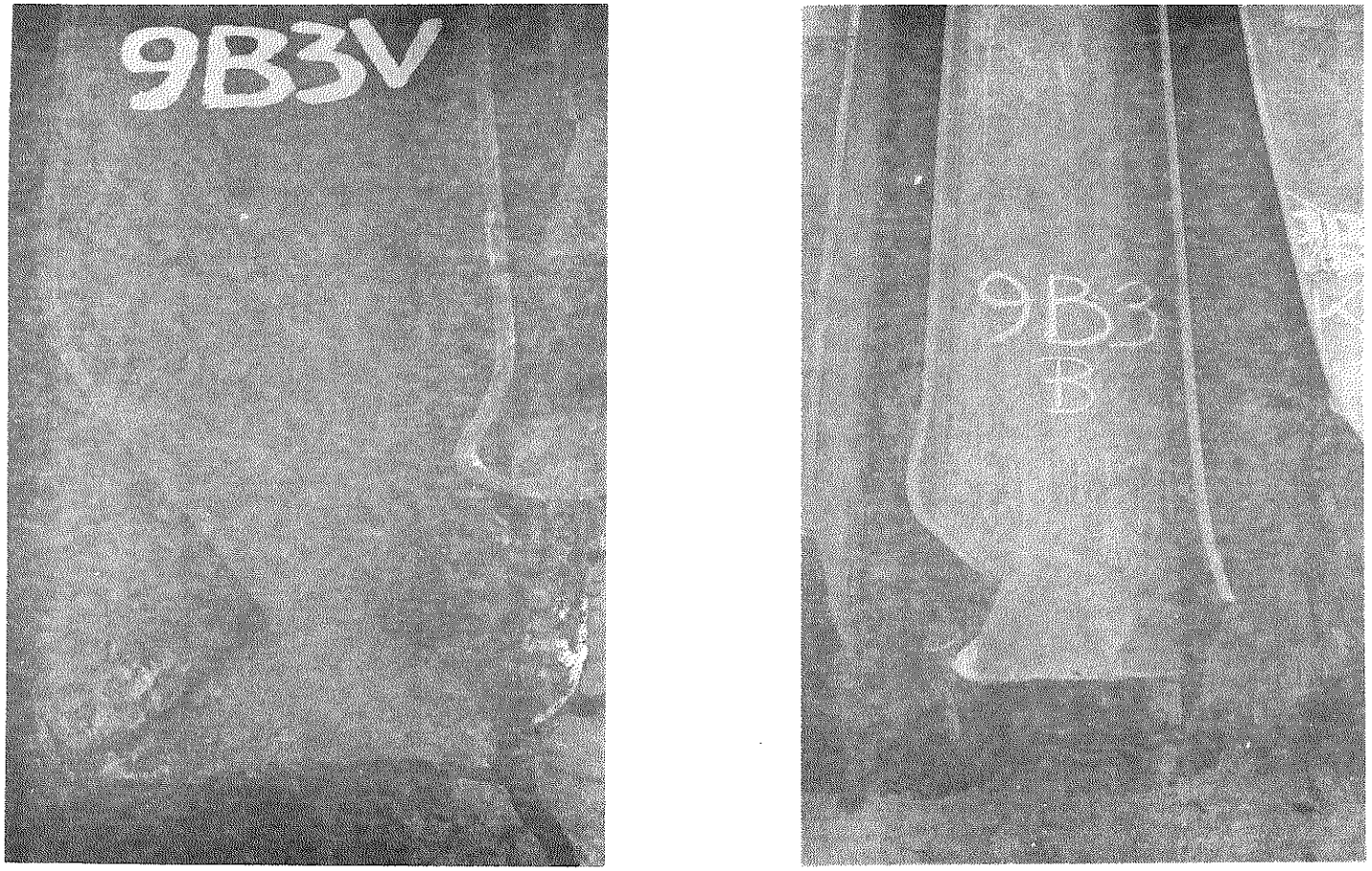

Figure 4.6: Tips for Piles Driven at Sandusky for the 9B3 Hammer

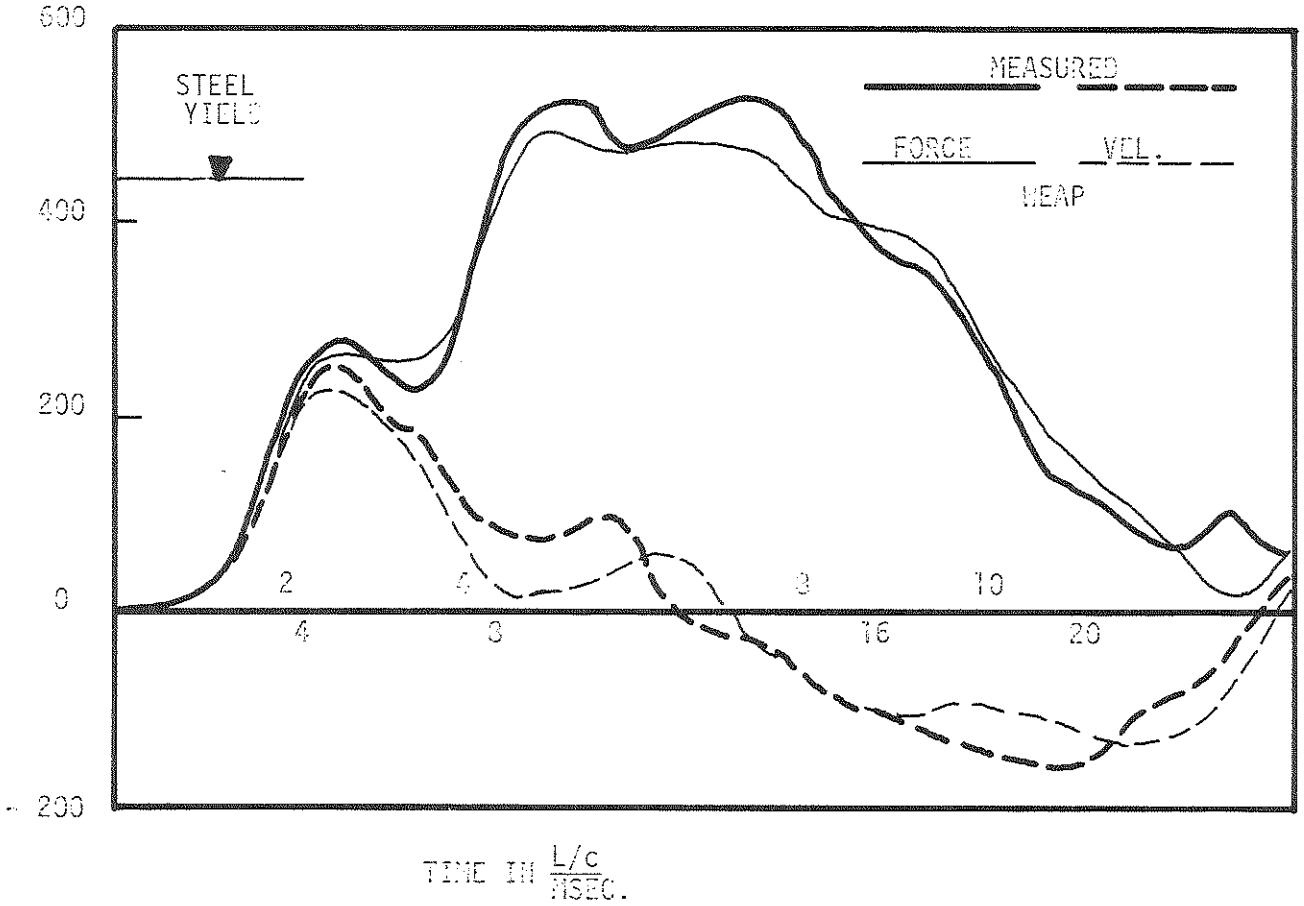

Figure 4.7: Force and Velocity Match of Measured Data with MEAP Predictions for Pile OSP at Sandusky

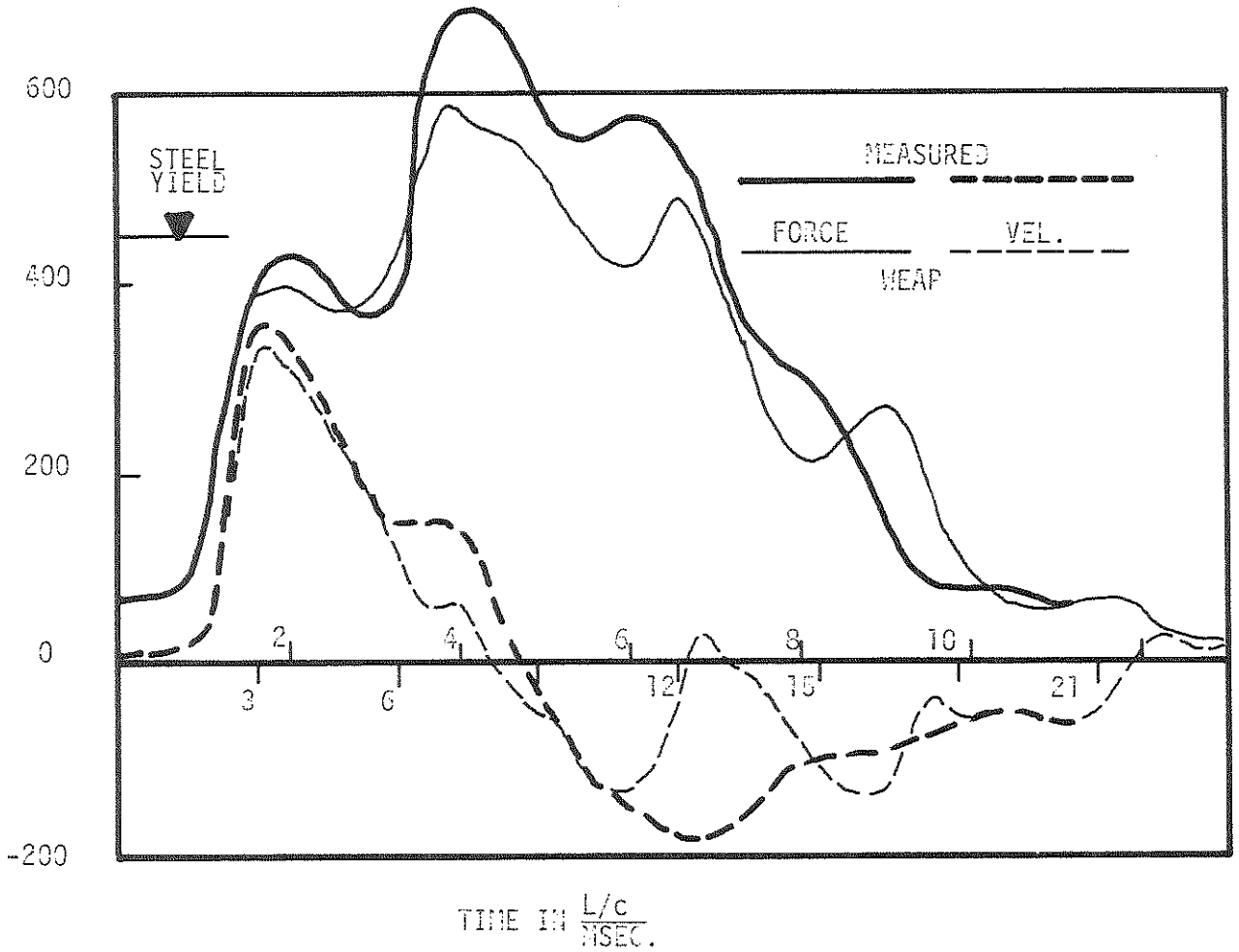

Figure 4.8: Force and Velocity Match of Measured Data with WEAP Predictions for Pile K23P at Sandusky

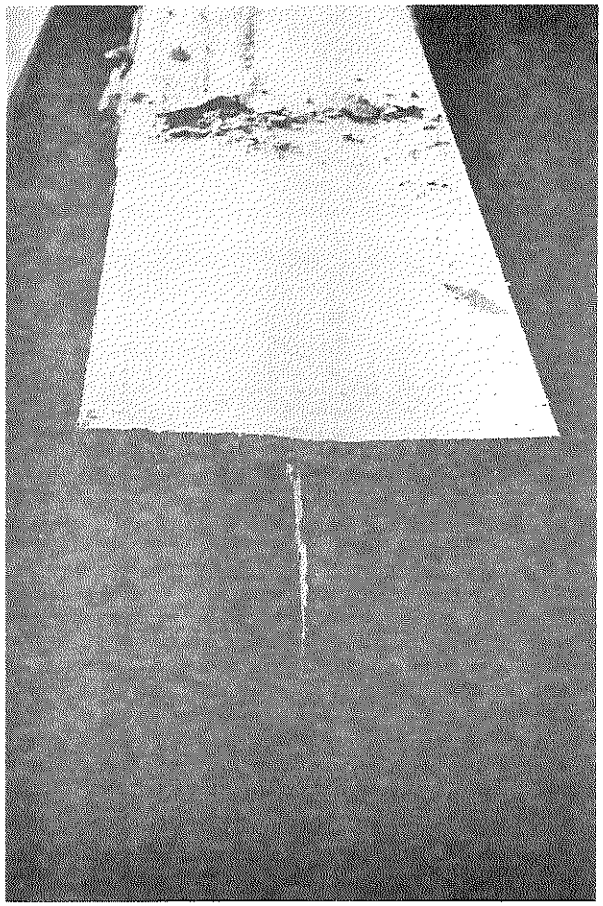

08V

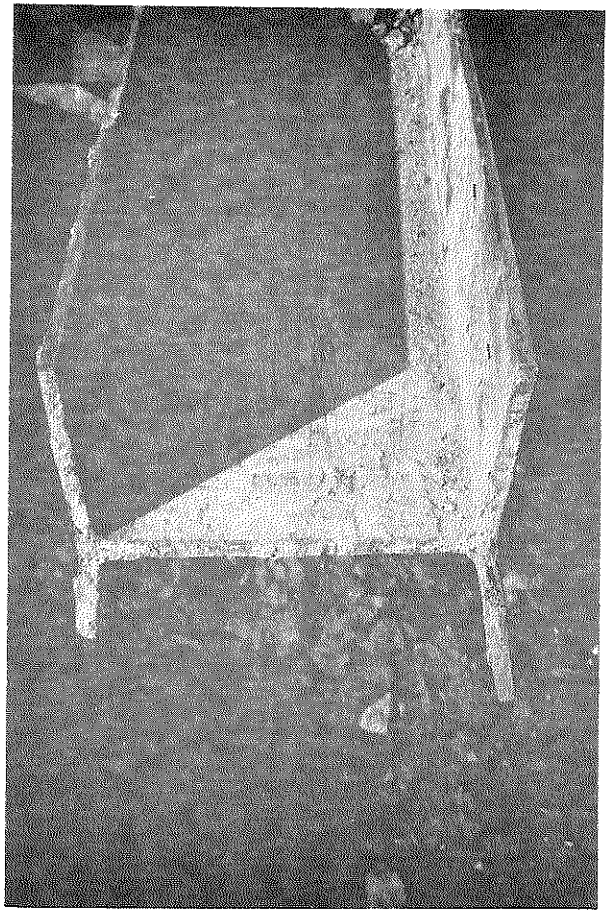

08B

Figure 4.9: Tips for Pies Driven at W92 by the 08 Hammer

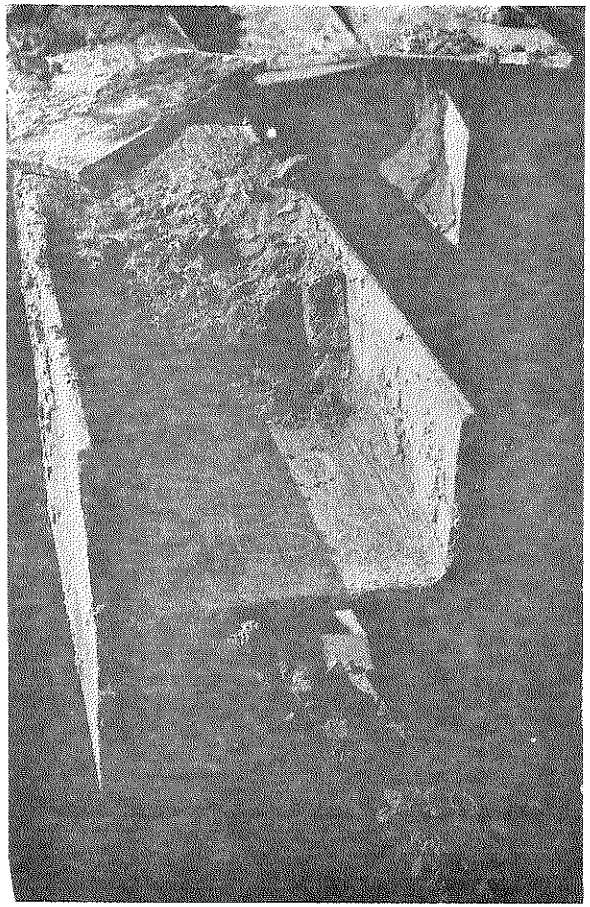

520

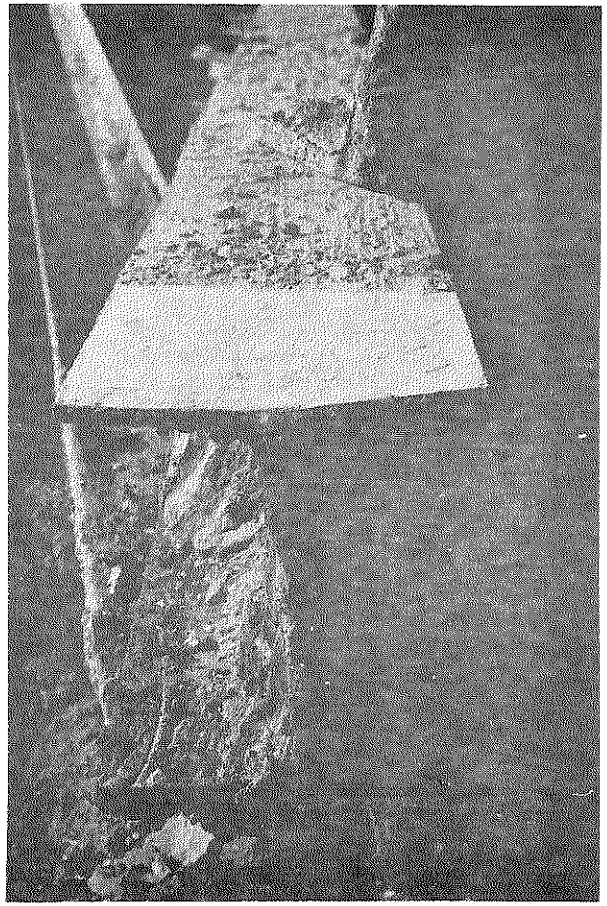

D15B

Figure 4.10: Tips for Piles Driven at W92 by the 520 and D15B Hammers

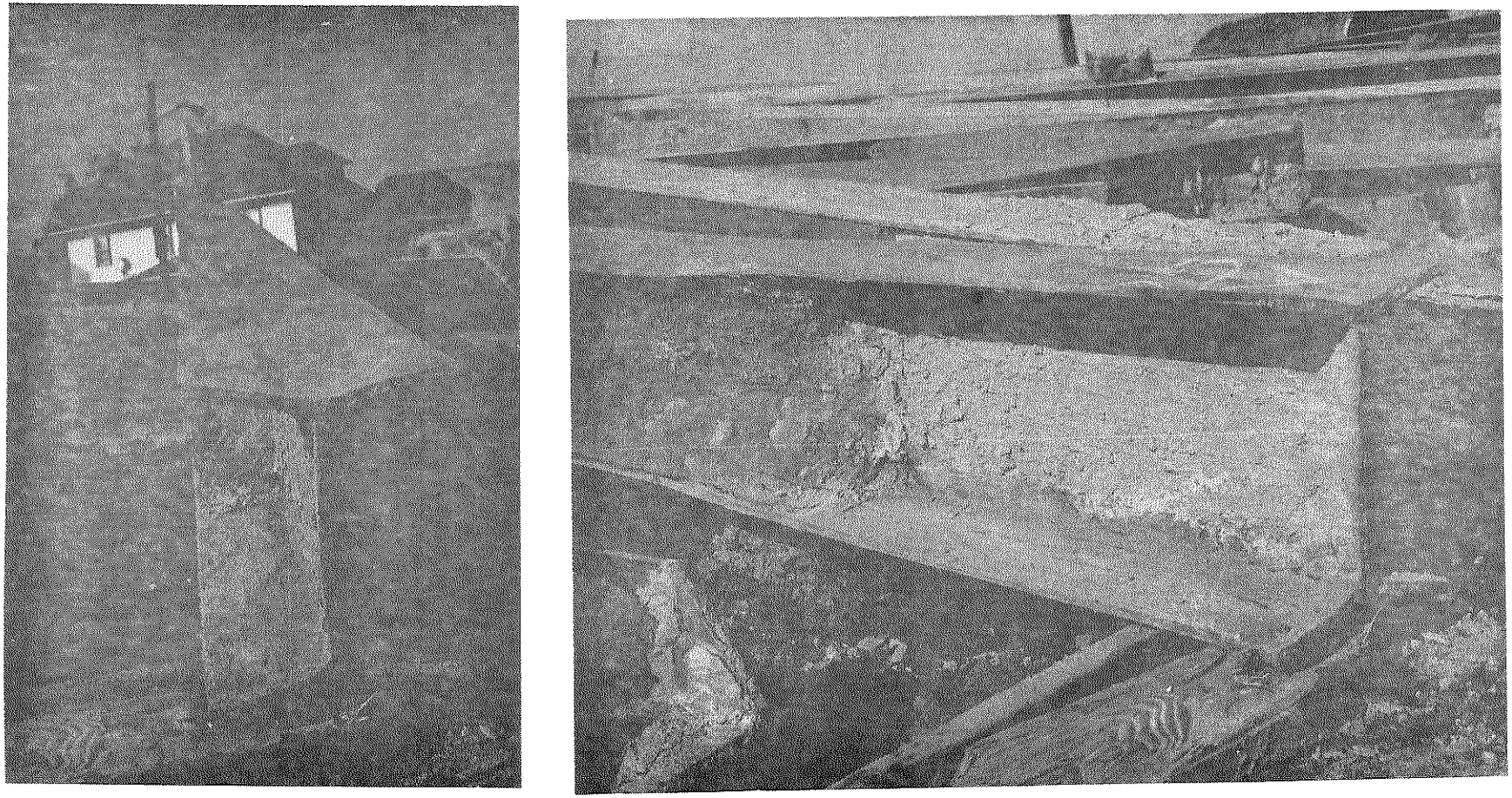

Figure 4.11: Tips for Piles Driven at W92 by the K25 Hammer

Depth	Blows/ Inch	VMax	DMax	EMax	FMax	P4	CD
13'	.8		.9				
14'	.8		1.1				
17'	.9		1.3				
18'	1.3		.9				
19'	1.4		.6				
20'	2.3		.9				
20'-6"	2.5		.7				
21'	3.7		.5				
21'-6"	3.3		.3				
21'-9"	3.3		.3				
22'	8.3		.3				
			.3				
			.4				
			.3				
			.3				
			.2				
			.2				
			.2				
22'-1"	70.		.3				
			.2				
			.2				
22'-2"	55.		.3				
22'-3"	55.		.2				
			.2				
22'-4"	75.		.2				

Table A1 : Sample dynamic results obtained by Case Method of Processing Sandusky 9B3V

Depth	Blows/ Inch	B.C.P.	VMax	DMax	EMax	FMax	P4	CD
19'-6"	1.2	8	4.0	.8	4.	77	71	64
					6.	87	76	68
					5.	89	82	73
					6.	93	85	77
20'	2.3	9	4.9	10.	6.	98	88	79
					6.	99	87	78
					7.	103	82	71
					6.	103	89	80
					6.	108	87	75
					6.	102	90	81
21'	2.2	10	4.9	.9	6.	104	91	82
					5.	102	92	83
					7.	109	86	73
21'-6"	1.0	10	4.8	.9	7.	113	93	81
					6.	114	91	78
					2.	136	106	89
					1.	132	123	115
			5.1	.4	5.	213	185	170
			7.4	.4	7.	312	264	249
			8.9	.4	7.	351	357	344
21'-11"	6		7.6	.4	6.	332	315	303
			9.7	.4	8.	375	360	348
			8.4	.4	7.	351	332	320
			7.0	.4	5.	310	290	279
			6.1	.3	4.	286	269	259
					4.	287	268	258
					5.	302	278	267
			8.1	.4	7.	354	331	320
			8.7	.4	6.	332	357	346
			6.1	.3	4.	282	264	254
					5.	292	271	261
					3.	248	221	212
			6.5	.3	5.	307	279	269
			8.4	.4	7.	368	344	333
			9.1	.4	8.	390	367	355
					8.	382	359	347
					7.	373	343	331
					7.	372	339	327
					7.	368	338	326
22'	20	19	8.3	.4	7.	363	343	331
					7.	366	340	328
					6.	347	328	316
					7.	346	321	309
					6.	348	325	313
					7.	357	330	318

Table A2: Sample dynamic results obtained by Case Method of Processing Sandusky LB520V

Depth	Blows/ Inch	B.C.P.	VMax	DMax	EMax	FMax	P4	CD
			8.3	.4	7.	362	334	322
					7.	368	332	320
					7.	356	335	323
					7.	364	334	321
					8.	378	347	334
					8.	379	342	329
					8.	379	345	332
					8.	383	347	334
					8.	389	358	345
			9.3	.5	8.	392	365	352
					8.	396	361	347
					8.	396	362	348
					8.	381	339	325
22'-1"	32	20	9.1	.4	8.	382	335	320
			9.5	.5	9.	396	356	341
					9.	390	349	334
22'-2"	18	21	9.4	.5	9.	391	346	329
					9.	393	349	333
					8.	378	340	324
22'-4"	9		8.7	.4	8.	346	307	291
23'-3"	8	20	9.8	.6	10.	342	289	269
23'-4"	5		9.2	.7	11.	296	248	227
			9.7	.6	10.	346	254	233
					11.	373	289	270
24'	12	21	9.9	.6	11.	372	291	271
			8.8	.6	10.	317	249	230
					8.	265	200	182
					8.	253	200	181
24'-3"	7	18	7.7	.6	9.	260	195	176
					10.	317	231	211
					10.	309	236	217
					10.	306	238	219
25'	10	21	9.3	.7	11.	308	243	223
			8.8	.6	10.	290	226	206
					11.	280	228	208
					10.	256	207	187
			8.0	.7	10.	237	200	180
					9.	217	184	164
25'-8"	5	17	7.1	.7	9.	201	168	148
					9.	202	158	139
			6.5	.8	9.	199	146	128
					8.	205	149	131
					9.	196	143	126
			5.8	.7	8.	188	139	124
26'-2"	4	15	6.9	.6	6.	163	144	126

Table A2: Sample dynamic results obtained by Case Method of Processing. (cont'd.) Sandusky LB520V

Depth	Blows/ Inch	B.C.P.	VMax	DMax	EMax	FMax	P4	CD
			5.2	1.6	6.	75	56	50
			5.0	1.1	5.	75	64	56
			4.6	.5	4.	194	165	160
			8.4	.4	8.	404	357	344
			9.2	.4	9.	448	380	366
21'-8"	20		8.8	.4	8.	449	423	409
			9.8	.4	9.	456	410	395
			8.7	.4	8.	437	404	391
			7.9	.3	6.	442	397	384
			8.7	.4	8.	421	393	381
			7.3	.3	6.	386	359	347
			7.2	.3	6.	365	322	308
			7.4	.3	6.	367	343	330
			7.0	.3	6.	361	329	316
21'-9"	26		8.6	.4	8.	418	392	380
			9.8	.5	10.	426	406	393
21'-10"	30	20	9.3	.4	8.	422	398	385
			9.2	.4	8.	426	397	384
			10.2	.5	10.	444	414	400
			10.0	.4	9.	444	421	408
21'-11"	24	22	9.8	.4	9.	446	406	394
			10.0	.4	9.	440	411	399
			9.7	.4	9.	464	423	410
22'	18	22	9.6	.4	9.	447	396	383

Table A3: Sample dynamic results obtained by Case Method of Processing Sandusky 520VP

Depth	Blows/ Inch	VMax	DMax	EMax	FMax	P4	CD
				3.	94	90	80
		4.7	.9	6.	121	98	88
				8.	118	100	88
		4.0	.6	6.	132	127	114
				7.	161	140	124
				9.	167	125	106
				9.	160	128	109
				7.	156	126	109
				9.	166	129	111
				8.	166	138	121
				8.	174	145	126
		5.6	.7	8.	187	157	137
				10.	187	153	132
				7.	177	152	135
				7.	182	150	132
				8.	194	166	147
		6.6	.6	8.	207	182	162
		8.4	.5	9.	325	266	248
22'-11"		9.6	.5	10.	372	336	319
		10.1	.5	11.	381	355	339
				10.	378	360	344
		10.1	.5	10.	389	368	353
				11.	410	382	366
				10.	411	385	370
				10.	410	385	370
				9.	379	346	334
		10.2	.5	11.	420	389	373
				11.	414	380	365
				10.	417	393	376
				10.	406	377	361
		10.0	.5	11.	435	401	383
				10.	425	391	375
				9.	417	417	395
				11.	425	383	368
				10.	417	385	371
23'	23	9.9	.5	10.	406	381	368
				10.	408	382	368
				10.	421	391	377
				10.	418	393	379
				10.	435	404	390
				10.	436	409	395
				10.	428	399	386
				11.	453	412	399
				11.	444	410	397
				10.	440	403	390
				10.	448	406	393
				11.	450	411	398
		10.0	.5	10.	451	412	398
				10.	442	405	392

Table A4: Sample dynamic results obtained by Case Method of Processing. Sandusky LB520B

Depth	Blows/ Inch	Vmax	Dmax	Emax	Fmax	P4	CD
				11.	452	416	402
				11.	452	409	396
		10.0	.4	11.	470	435	419
				11.	463	414	401
23'-1"	35	10.5	.5	11.	459	421	407
				11.	465	419	405
				11.	461	415	403
				12.	466	416	403
				10.	465	427	412
				11.	456	419	405
				11.	457	419	406
				10.	455	411	399
				10.	459	394	383
				10.	448	407	394
				10.	450	412	399
				10.	451	411	399
				10.	447	411	398
				10.	449	416	403
				10.	455	414	401
		10.4	.5	10.	457	412	399
				11.	454	408	395
				10.	450	406	393
				10.	451	407	394
23'-2"	50	10.4	.5	11.	451	408	394
				11.	449	403	388
				10.	438	394	379
		10.0	.5	10.	428	384	369
				10.	418	370	354
		9.7	.5	10.	408	361	344
				10.	396	347	329
		9.5	.5	10.	377	321	302
				10.	356	303	283
				11.	373	312	291
				12.	379	314	293
				12.	370	314	293
				13.	366	308	286
23'-6"	6	10.0	.6	12.	374	302	281
				12.	374	307	286
		10.2	.6	12.	398	325	305
				11.	424	341	322
		10.3	.6	12.	431	350	331
				12.	433	353	335
				12.	459	378	359
24'	10	10.5	.5	11.	462	381	363
				11.	448	372	355
				11.	448	372	355
				11.	450	371	354
		10.1	.5	11.	436	364	346
				10.	417	338	320
24'-3"	9	9.4	.5	10.	410	334	316

Table A4: (cont'd.) Sample dynamic results obtained by Case Method of Processing Sandusky LB520B

Depth	Blows/ Inch	VMax	DMax	EMax	FMax	P4	CD
		9.3	.5	10.	394	319	300
		9.0	.5	9.	365	295	275
24'-5"	7	8.5	.5	9.	351	276	257
				8.	346	276	256
				9.	342	270	250
				10.	331	261	240
		9.0	.6	10.	324	255	234
		8.4	.6	9.	310	240	219
				9.	301	226	204
		8.8	.6	10.	314	228	206
				9.	325	240	219
24'-8"	5	9.1	.6	11.	341	254	233
				11.	351	260	238
				11.	362	272	251
				11.	355	266	246
				11.	358	277	256
		9.5	.6	10.	364	278	257
				12.	371	286	265
		9.6	.6	11.	392	295	275
24'-11"	5	10.1	.5	11.	407	316	296

Table A4: Sample dynamic results obtained by Case Method of Processing (cont'd.) Sandusky LB520B

I	Depth (Ft)	Quake (In)	Res (Kips)	Sum Res (Kips)	J (K-S/Ft)	Weight (Lb)	Stiffness (K/in)	Max Spring Force
1	4.1	.100	1	369	.33	172	7800.	441.
2	8.1	.100	1	368	.33	172	7800.	443.
3	12.1	.100	1	367	.33	172	7800.	422.
4	16.3	.100	2	365	.66	172	7800.	413.
5	20.4	.100	2	363	.66	172	7800.	419.
6	24.4	.100	5	358	1.65	172	7800.	404.
7	28.5	.100	5	353	1.65	172	7800.	382.
8	28.5	.120	353	0	1.12			

Maximums

Measured Pile Top	Force	397
	Velocity	9.7
	Disp.	.49
Computed Pile Toe	Velocity	7.0
	Disp.	.25

Maximum Sum of Damping Forces Occurring Simultaneously 47 Kips

Sandusky LB 520V

I	Depth (Ft)	Quake (In)	Res (Kips)	Sum Res (Kips)	J (K-S/Ft)	Weight (Lb)	Stiffness (K/in)	Max Spring Force
1	4.1	.010	1	399	.56	172	7800.	365.
2	8.1	.010	1	398	.56	172	7800.	358.
3	12.2	.010	2	396	1.12	172	7800.	374.
4	16.3	.010	2	394	1.12	172	7800.	354.
5	20.4	.010	2	392	1.12	172	7800.	335.
6	24.4	.010	4	388	2.24	172	7800.	366.
7	28.5	.010	4	384	2.24	172	7800.	377.
8	28.5	.040	384	0	1.12			

Maximums

Measured Pile Top	Force	449
	Velocity	8.0
	Disp.	.27
Computed Pile Toe	Velocity	3.1
	Disp.	.04

Maximum Sum of Damping Forces Occurring Simultaneously 47.

Sandusky LB 520P

Table A5: CAPWAP Resistance Distribution Results for Piles 520V and 520P at Sandusky

Depth	Blows/ Inch	VMax	DMax	EMax	FMax	P4	CD
16'	.3	11.4	3.2	13.	261	76	31
		11.5	3.0	14.	266	80	35
				15.	267	86	41
				14.	266	90	46
17'	.3	11.3	2.7	14.	266	88	43
				14.	268	94	50
				15.	265	90	46
				16.	267	93	48
				15.	268	96	52
18'	.4	11.5	2.5	15.	267	95	51
				16.	268	98	54
				16.	268	99	55
				16.	270	103	60
				17.	271	103	59
19'	.4	11.4	2.7	17.	272	104	60
				16.	272	103	59
				16.	275	106	61
		11.6	2.3	15.	276	109	65
				16.	276	112	68
20'	.4	11.9	2.5	16.	273	112	69
				16.	276	114	70
				17.	276	118	75
20'-6"	.5	12.1	2.5	17.	276	115	71
				15.	277	120	76
				17.	277	121	77
21'	.5	12.1	2.5	17.	277	123	80
				16.	276	127	84
				18.	278	130	87
21'-6"	.5	11.9	2.3	17.	277	130	88
				17.	277	131	88
		11.5	2.0	16.	278	137	95
				17.	278	141	99
22'	.7	11.6	2.0	17.	278	141	99
		11.5	1.3	15.	278	148	107
		11.3	.7	15.	386	317	295
		10.9	.6	13.	428	400	386
		11.4	.6	15.	457	422	410
				13.	465	427	416
		11.0	.6	14.	480	432	421
		10.6	.5	13.	477	429	419
				13.	496	443	432
		11.3	.6	13.	496	443	432
		11.3	.6	13.	496	455	445
		11.2	.5	13.	496	444	434
				13.	496	443	434
		10.9	.5	13.	493	440	431
22'-2"	6.5	10.8	.5	12.	487	433	424

Table A6 : Sample dynamic results obtained by Case Method of Processing. Sandusky O8V

Depth	Blows/ Inch	VMax	DMax	EMax	FMax	P4	CD
12'		9.3	2.5	5.	225	23	
15'		10.4	3.3	8.	252	38	
18'		11.2	3.1	11.	260	48	
		11.5	3.1	15.	263	69	23
20'	.4	11.8	2.9	18.	270	87	41
21'	.4	11.7	2.5	18.	273	102	57
21'-6"	.5	11.8	2.4	19.	276	119	76
		11.3	.8	15.	388	269	242
		11.6	.7	15.	457	413	400
		11.4	.6	15.	499	436	426
		11.8	.6	15.	526	460	451
		11.5	.6	15.	525	451	443
		10.8	.6	14.	514	450	443
		10.4	.6	14.	504	421	414
		9.2	.6	13.	468	388	380
		8.8	.6	13.	419	360	353
22'	15.	8.5	.5	11.	406	353	346

Pile Top Damaged

Table A7

Sample dynamic results obtained by Case Method of Processing
Sandusky 08VP

Depth	Blows/ Inch	VMax	DMax	EMax	FMax	P4	CD
				6.	241	26	
				5.	242	31	
				6.	254	37	
		10.4	3.2	8.	257	42	
				9.	262	51	
				14.	270	96	
				16.	276	77	29
				17.	275	86	39
		11.4	2.7	17.	273	90	44
				12.	228	88	51
22'	.6	10.6	1.6	13.	264	119	77
				15.	263	116	74
22'-6"	.8	11.2	1.1	16.	269	151	112
		11.4	.8	16.	337	293	269
				14.	370	336	315
22'-11"	6	11.2	.7	15.	385	349	329
				17.	382	340	319
				16.	362	326	304
				14.	376	319	296
				14.	410	333	311
				15.	430	368	349
23'	6	10.8	.6	13.	462	381	365
		11.1	.6	13.	448	389	374
				16.	434	369	352
				14.	421	353	335
		10.9	.6	14.	410	340	320
				14.	397	330	309
		11.5	.8	16.	386	317	295
				14.	379	300	277
				15.	378	309	286
		11.3	.7	15.	375	299	274

Table A8: Sample dynamic results obtained by Case Method of Processing. Sandusky 08B

Depth	Blows/ Inch	VMax	DMax	EMax	FMax	P4	CD
				16.	376	295	270
				15.	392	304	280
		11.4	.7	15.	408	316	295
				16.	428	343	324
				17.	446	365	347
23'-6"	3	11.0	.6	15.	446	370	353
				17.	440	368	351
		11.6	.7	16.	416	336	314
				17.	385	310	285
				14.	382	297	271
				19.	390	303	277
24'	4	11.5	.8	15.	367	291	264
		11.6	.8	16.	346	278	250
24'-2"	3	11.7	.8	17.	380	296	271
				16.	395	305	279
				15.	400	311	287
24'-4"	3.5	11.5	.8	17.	401	299	274
		11.6	.8	17.	414	317	292
24'-6"	3.5	11.3	.8	16.	369	286	260
24'-8"	2	11.1	.8	15.	341	252	224
				16.	334	248	220
24'-10"	3	10.8	.8	15.	360	259	232
		10.7	.7	15.	393	272	246
25'	3.5	11.4	.9	16.	345	242	214
				17.	400	284	261
25'-2"	4.5	10.2	.8	16.	426	302	285
				14.	436	314	294
25'-4"	3.5	10.8	.7	15.	431	311	290
				15.	366	261	235
		10.5	.9	15.	313	233	205
25'-8"	3	10.7	.9	17.	361	273	253
				19.	361	260	233
25'-10"	3	10.3	.8	13.	306	231	203
		11.1	1.0	16.	305	221	191
			.9	16.	377	251	224
26'	4	11.5	.9	17.	394	250	222
			.9	16.	373	237	209
26'-2"	3.5	11.5	1.0	19.	362	237	209
			.9	18.	352	232	202
		11.9	1.1	19.	341	226	196
			1.1	19.	332	226	196
			1.2	20.	323	216	185
26'-4"	2.5	11.4	1.1	18.	313	212	181
			1.0	16.	305	212	181
		10.8	.9	15.	297	205	173

Table A8: Sample dynamic results obtained by Case Method of Processing (cont'd.)
Sandusky 08B

I	Depth (Ft)	Quake (In)	Res (Kips)	Sum Res (Kips)	J (K-S/Ft)	Weight (Lb)	Stiffness (K/in)	Max Spring Force
1	4.1	.100	0	450	0.00	172	7800.	511.
2	8.1	.100	0	450	0.00	172	7800.	512.
3	12.2	.100	0	450	0.00	172	7800.	509.
4	16.3	.100	2	448	1.50	172	7800.	505.
5	20.4	.100	2	446	1.50	172	7800.	499.
6	24.4	.100	4	442	2.99	172	7800.	494.
7	28.5	.100	4	438	2.99	172	7800.	472.
8	28.5	.150	438	0	1.12			

Maximums

Measured Pile Top	Force	497.
	Velocity	10.9
	Disp.	.55
Computed Pile Toe	Velocity	5.4
	Disp.	.24

Maximum Sum of Damping Forces Occurring Simultaneously 70.

Sandusky 08V

I	Depth (Ft)	Quake (In)	Res (Kips)	Sum Res (Kips)	J (K-S/Ft)	Weight (Lb)	Stiffness (K/in)	Max Spring Force
1	4.1	.150	0	501	0.00	172	7800.	549.
2	8.1	.150	0	501	0.00	172	7800.	545.
3	12.1	.150	1	500	.64	172	7800.	537.
4	16.3	.150	1	499	.64	172	7800.	531.
5	20.4	.150	1	498	.64	172	7800.	537.
6	24.4	.150	2	496	1.28	172	7800.	533.
7	28.5	.150	2	494	1.28	172	7800.	516.
8	28.5	.150	494	0	1.12			

Maximums

Measured Pile Top	Force	533.
	Velocity	11.2
	Disp.	.59
Computed Pile Toe	Velocity	6.9
	Disp.	.25

Maximum Sum of Damping Forces Occurring Simultaneously 46.

Sandusky 08VP

Table A9 : CAPWAP Resistance distribution results for Piles 08V and 08VP at Sandusky

Depth	Blows/ Inch	Stroke	VMax	DMax	EMax	FMax	P4	CD
			5.7	1.2	7.	148	77	55
			6.7	.7	7.	167	133	112
			7.3	.5	7.	200	190	172
			7.6	.5	7.	230	228	211
19'-8"	2.5	7.1	7.5	.5	7.	221	250	234
			7.7	.5	7.	208	225	206
			7.5	.6	5.	193	186	166
20'	2.5	6.5	4.1	.2	2.	134	141	134
			4.2	.3	4.	166	133	121
			6.5	.4	5.	178	176	158
20'-4"	2.5	7.0	7.5	.5	8.	223	195	174
			7.2	.6	8.	200	165	141
20'-8"	2.5	6.7	7.3	.6	8.	200	174	151
21'	2.5	6.3	7.4	.7	8.	200	164	140
21'-4"	3	6.8	7.3	.6	8.	204	164	140
			7.7	.6	8.	222	180	157
21'-8"	5	7.0	7.9	.6	7.	221	192	170
			8.3	.6	8.	231	219	197
21'-11"	8	7.4	8.3	.5	8.	237	236	214
22'	7	7.0	8.3	.5	8.	216	223	202
			8.0	.5	8.	215	208	185
			8.3	.7	9.	213	179	154
22'-5"	1.5	5.9	7.1	.8	8.	188	125	100
			7.6	.7	8.	216	149	125
			8.2	.5	8.	259	217	196
			8.9	.5	8.	268	288	271
22'-8"	9	7.4	8.7	.5	7.	274	277	259
			8.6	.4	7.	256	283	265
23'	18	7.7	8.9	.4	8.	263	290	271
			9.3	.5	8.	265	297	279
			8.8	.4	7.	253	284	265
23'-1"	13	7.4	9.2	.5	8.	243	272	253
			8.9	.5	8.	252	286	267
			9.4	.5	8.	264	301	283
			9.3	.5	8.	261	290	271
			9.4	.5	8.	248	291	272
23'-3"	20	7.6	9.5	.5	8.	272	315	297
			8.9	.4	7.	241	289	270
			8.6	.5	7.	234	254	232
23'-6"	12	7.3	9.0	.5	8.	241	266	245
23'-9"	9	7.1	9.0	.5	8.	237	237	213
			8.9	.6	8.	236	222	197
24'	5	6.7	8.5	.5	8.	233	210	184
			8.6	.6	8.	231	193	166
24'-3"	3	6.6	8.1	.6	8.	221	179	152
			7.8	.7	8.	217	163	136
24'-6"	3	6.6	8.0	.8	9.	215	157	129

Table A10:Sample dynamic results obtained by Case Method of Processing Sandusky K13V

Depth	Blows/ Inch	Stroke	VMax	DMax	EMax	FMax	P4	CD
10'	.2		4.9	1.1	6.	148	65	42
11'	.2	4.5	5.1	1.0	6.	150	73	50
15'	.3	4.5	5.4	1.0	6.	158	79	55
17'	.4		5.8	.9	6.	169	89	64
18'	.5	5.3	5.9	.9	6.	174	94	68
19'-6"	.7	5.9	6.2	.8	7.	181	106	80
20'	1.0	6.1	6.5	.9	7.	184	105	79
20'-6"	1.0	6.4	6.7	.9	7.	188	108	81
21'	1.0	7.0	6.6	.7	6.	193	115	88
21'-3"	1.3	7.5	8.4	.4	6.	332	298	282
20'-6"	1.3	7.5	8.5	.4	6.	344	339	329
20'-8"	3.	7.6	9.3	.3	6.	410	390	381
			9.5	.4	7.	424	410	401
			9.7	.4	7.	441	416	406
20'8$\frac{3}{4}$"	32.	7.9	9.5	.4	7.	440	407	398
			9.7	.4	7.	436	412	402
20'-9"	120.	8.0	10.2	.4	8.	446	422	411
			10.1	.4	7.	442	413	402
			9.9	.3	7.	447	426	416
			10.0	.4	7.	445	415	405
			10.0	.4	7.	425	414	404
			10.0	.4	7.	445	414	404
20'9$\frac{1}{4}$"	120	8.0	9.9	.3	7.	437	412	401
			10.2	.4	7.	434	419	408
			9.9	.3	7.	434	424	413
			10.0	.4	7.	444	408	397
20'9$\frac{3}{8}$"	160	8.0	10.1	.4	8.	444	416	405

Table A11: Sample dynamic results obtained by Case Method of Processing Sandusky K13VP

Depth	Blows/ Inch	Stroke	VMax	DMax	EMax	FMax	P4	CD
			5.6	1.4	7.	156	81	58
			6.3	1.1	8.	166	98	74
			6.9	.8	7.	182	124	99
			6.9	.7	7.	191	141	116
20'	.3	4.5	6.8	.6	7.	195	149	125
			7.1	.6	7.	202	171	147
20'-6"	.5	4.9	7.2	.5	6.	203	189	167
			7.4	.4	6.	230	209	188
			7.8	.4	6.	273	252	233
21'	.7	5.4	8.2	.4	7.	302	283	266
			8.2	.4	7.	318	288	272
21'-6"	1.0	5.6	8.2	.4	7.	325	288	271
21'-10"	1.2		8.2	.4	7.	332	289	272
22'	2	6.4	8.5	.4	7.	335	294	278
			8.4	.4	7.	341	304	288
22'-6"	2.5		8.6	.4	7.	339	299	283
22'-8"	16	7.4	8.5	.4	7.	357	321	307
22'-9"	31	7.8	8.6	.4	7.	363	323	310
			8.5	.4	7.	369	334	320
			8.9	.4	7.	368	346	333
		8.2	9.2	.4	7.	369	342	329
			9.2	.5	8.	380	337	323
22'-10"	70	8.0	8.9	.4	7.	368	346	333

Table A12: Sample dynamic results obtained by Case Method of Processing Sandusky K13B

I	Depth (Ft)	Quake (In)	Res (Kips)	Sum Res (Kips)	J (K-S/Ft)	Weight (Lb)	Stiffness (K/in)	Max Spring Force
1	4.1	.100	0	255	0.00	172	7800.	310.
2	8.1	.100	0	255	0.00	172	7800.	320.
3	12.2	.100	2	253	.80	172	7800.	326.
4	16.3	.100	2	251	.80	172	7800.	316.
5	20.4	.100	2	249	.80	172	7800.	310.
6	24.4	.100	4	245	1.60	172	7800.	300.
7	28.5	.100	4	241	1.60	172	7800.	273.
8	28.5	.150	241	0	1.12			

Maximums

Measured Pile Top	Force	288.
	Velocity	8.6
	Disp.	.46
Computed Pile Toe	Velocity	7.6
	Disp.	.31

Maximum Sum of Damping Forces Occurring Simultaneously 53.

Sandusky K13V

I	Depth (Ft)	Quake (In)	Res (Kips)	Sum Res (Kips)	J (K-S/Ft)	Weight (Lb)	Stiffness (K/in)	Max Spring Force
1	3.9	.100	1	429	.56	165	8100.	420.
2	7.8	.100	1	428	.56	165	8100.	424.
3	11.8	.100	1	427	.56	165	8100.	422.
4	15.7	.100	3	424	1.67	165	8100.	409.
5	19.6	.100	3	421	1.67	165	8100.	399.
6	23.5	.100	3	418	1.67	165	8100.	411.
7	23.5	.100	418	0	1.11			

Maximums

Measured Pile Top	Force	442.
	Velocity	9.6
	Disp.	.34
Computed Pile Toe	Velocity	5.4
	Disp.	.10

Maximum Sum of Damping Forces Occurring Simultaneously 51.

Sandusky K13VP

Table A13: CAPWAP Resistance Distribution Results for Piles K13V and K13VP at Sandusky

Depth	Blows/ Inch	Stroke	VMax	DMax	EMax	FMax	P4	CD
15'	.1		4.6	1.2	3.	64	35	33
			4.5	1.2	4.	97	46	43
17'	.5		5.4	1.9	9.	127	62	43
			6.4	2.0	12.	148	82	60
18'	.8		7.3	2.0	14.	168	91	66
			7.4	2.2	16.	175	99	74
			7.7	1.8	14.	188	112	85
19'	.6	4.2	8.3	1.3	15.	219	160	132
			9.7	1.2	17.	247	197	167
			10.0	1.3	17.	247	193	163
20'-6"	.7		8.0	.6	10.	250	210	181
21'	1.2	6.4	10.6	1.0	16.	267	240	211
			10.0	.8	14.	268	242	212
22'	1.7	6.7	10.2	.9	15.	267	257	230
			11.1	.7	14.	314	301	276
22'-4"	4.	7.5	11.7	.6	14.	342	349	324
		8.0	13.3	.8	18.	349	344	317
22'-8"	3.	7.3	11.9	.7	14.	344	322	297
			11.0	.6	13.	308	314	288
			11.6	.9	17.	277	283	256
			9.9	.7	12.	262	251	224
23'-2"	1.	6.4	9.7	.7	12.	257	240	213
			11.8	1.1	17.	266	269	242
			12.9	.9	17.	294	333	308
23'-6"	2.	7.5	12.4	.7	16.	361	372	347
			12.9	.6	15.	395	394	370
			13.7	.7	17.	427	409	386
23'-10"	4.5	8.8	14.0	.7	17.	433	414	391
			13.2	.7	16.	422	399	374
			13.8	.8	18.	398	372	345
24'-3"	2.	7.8	13.7	.9	18.	364	349	321
			11.6	.7	13.	317	302	273
			12.8	1.1	19.	302	270	236
			11.2	.9	16.	286	240	207
			11.0	1.0	16.	281	216	181
			10.6	1.3	17.	252	162	128
25'	1.5	6.1	10.2	1.2	15.	236	155	123
			9.6	1.1	15.	250	168	135
			9.0	.6	8.	234	162	131

Table A14: Sample dynamic results obtained by Case Method of Processing Sandusky K25V

Depth	Blows/ Inch	Stroke	VMax	DMax	EMax	FMax	P4	CD
22'	.5	5.7	6.0	1.5	10.	176	90	63
22'-6"	.5		6.9	1.4	13.	195	118	91
			7.7	1.1	12.	212	148	120
22'-9"	1.6	6.3	8.6	.9	13.	232	188	160
			8.4	.6	10.	260	235	212
			10.1	.6	13.	311	308	287
			10.6	.6	12.	343	338	317
22'-10"	4.	8.0	11.4	.6	14.	383	368	349
22'-11"	5.	8.0	10.9	.6	13.	376	366	347
23'	5.	8.3	11.7	.6	13.	430	390	372
			11.9	.6	14.	452	415	399
			12.4	.6	14.	463	431	416
23'-1"	7.		11.7	.6	13.	462	422	407
			11.5	.5	12.	442	401	384
			12.1	.6	14.	432	393	373
			12.0	.7	15.	407	364	343
23'-3"	5.		12.0	.7	15.	377	349	326
			11.6	.7	14.	355	323	299
23'-6"	3.		11.2	.8	15.	314	289	263
			12.0	.7	14.	389	344	322
23'-10"	4.5		12.1	.6	14.	421	384	364
			12.7	.6	14.	446	412	393
24'	7.		13.0	.7	15.	442	401	381
			12.3	.6	14.	414	367	345
24'-2"	4.		11.3	.7	15.	340	308	283
24'-4"	2.		10.4	.8	14.	299	259	232
			11.3	.7	14.	375	321	298
			12.1	.6	13.	436	384	363
			12.4	.6	14.	445	400	380
24'-8"	5.		12.6	.6	14.	427	385	363
			13.0	.7	15.	426	384	360
			12.7	.7	15.	410	364	340
25'	5.	8.0	12.2	.7	14.	374	353	328
25'-2"	2.5	8.1	11.4	.7	14.	326	301	275
			12.0	.9	16.	308	282	252
25'-8"	2.	7.4	11.1	.8	15.	305	264	234
			12.2	.8	16.	361	311	284
			11.9	.7	14.	370	336	311

Table A15: Sample dynamic results obtained by Case Method of Processing Sandusky K25B

Depth	Blows/ Inch	Stroke	VMax	DMax	EMax	FMax	P4	CD
			5.5	3.0	9.	125	33	11
20'-6"	.5	4.0	6.0	1.9	7.	86	54	47
21'	.8	4.0	5.1	1.8	10.	150	71	48
21'-6"	.5	4.2	5.6	1.6	10.	149	80	58
22'	.7	4.4	6.4	1.9	14.	168	92	67
		4.5	6.3	1.4	11.	177	101	76
			5.7	.6	8.	268	113	89
		5.5	7.7	.5	8.	374	309	298
		7.0	10.8	.6	13.	474	435	420 *
		8.0	11.9	.6	14.	549	495	481
		8.4	12.0	.6	14.	571	506	493
22'-1"	10.	8.7	12.4	.5	15.	655	535	522
		9.2	12.8	.6	17.	730	539	527
		8.5	11.5	.5	14.	723	494	482
		8.6	12.2	.6	16.	828	534	523
		8.8	12.1	.5	15.	737	552	541
22'1$\frac{3}{4}$"	16.	8.1	11.6	.6	12.	278	365	346

Sample dynamic results obtained by Case Method of Processing
Sandusky K25VP

TableA16

*Values too high due to excess strain from yielding of steel.

Depth	Blows/ Inch	VMax	DMax	EMax	FMax	P4	CD
		6.7	4.1	10.	153	33	5
		7.0	4.3	12.	158	38	10
		7.3	4.4	17.	170	50	20
		5.2	.3	4.	274	222	210
		9.1	.4	9.	409	374	361
		11.7	.5	12.	425	410	391
19'-6"	3	11.6	.5	11.	485	462	449

Sample dynamic results obtained by Case Method of Processing
Sandusky K25VE

TableA17

I	Depth (Ft)	Quake (In)	Res (Kips)	Sum Res (Kips)	J (K-S/Ft)	Weight (Lb)	Stiffness (K/in)	Max Spring Force
1	4.1	.100	0	400	0.00	172	7800.	435.
2	8.1	.100	0	400	0.00	172	7800.	446.
3	12.2	.100	2	398	.78	172	7800.	451.
4	16.3	.100	4	394	1.55	172	7800.	443.
5	20.4	.100	4	390	1.55	172	7800.	423.
6	24.4	.100	8	382	3.11	172	7800.	409.
7	28.5	.100	8	374	3.11	172	7800.	400.
8	28.5	.400	374	0	2.24			

Maximums

Measured Pile Top	Force	431
	Velocity	12.8
	Disp.	.71
Computed Pile Toe	Velocity	12.1
	Disp.	.44

Maximum Sum of Damping Forces Occurring Simultaneously 148.

Sandusky K25V

I	Depth (Ft)	Quake (In)	Res (Kips)	Sum Res* (Kips)	J (K-S/Ft)	Weight (Lb)	Stiffness (K/in)	Max Spring Force
1	4.1	.100	0	550	0.00	172	7800.	595.
2	8.1	.100	0	550	0.00	172	7800.	597.
3	12.2	.100	0	550	0.00	172	7800.	590.
4	16.3	.100	2	548	1.12	172	7800.	579.
5	20.4	.100	2	546	1.12	172	7800.	575.
6	24.4	.100	4	542	2.24	172	7800.	583.
7	28.5	.100	4	538	2.24	172	7800.	572.
8	28.5	.100	538	0	1.12			

Maximums

Measured Pile Top	Force	828.*	*Values too high due to excess strain from yielding of steel.
	Velocity	12.1*	
	Disp.	.56	
Computed Pile Toe	Velocity	5.1	
	Disp.	.17	

Maximum Sum of Damping Forces Occurring Simultaneously 58.

Sandusky K25VP

Table A18: CAPWAP Resistance Distribution Results for Piles K25V and K25VP at Sandusky

I	Depth (Ft)	Quake (In)	Res (Kips)	Sum Res (Kips)	J (K-S/Ft)	Weight (Lb)	Stiffness (K/in)	Max Spring Force
1	3.9	.100	1	464	.52	165	8100.	491.
2	7.8	.100	1	463	.52	165	8100.	499.
3	11.8	.100	1	462	.52	165	8100.	500.
4	15.7	.100	4	458	2.08	165	8100.	498.
5	19.6	.100	4	454	2.08	165	8100.	482.
6	23.5	.100	4	450	2.08	165	8100.	452.
7	23.5	.150	450	0	1.11			

Maximums

Measured Pile Top	Force	486.
	Velocity	11.4
	Disp.	.43
Computed Pile Toe	Velocity	7.5
	Disp.	.17

Maximum Sum of Damping Forces Occurring Simultaneously 76.

Sandusky K25VE

Table A19: CAPWAP Resistance Distribution Results for Pile K25VE at Sandusky

Depth	Blows/ Inch	VMax	DMax	EMax	FMax	Flmp	P4	CD
5'	1.7	10.3	.5	3.	218	218	70	
6'	2.4	10.1	.4	3.	218	218	81	
7'	2.0	10.0	.4	3.	217	217	91	
8'	2.8	9.5	.4	3.	221	221	84	
		10.1	.3	3.	214	214	109	
9'	3.3	10.7	.4	3.	226	226	119	18
		10.8	.3	3.	231	231	126	24
10'	3.6	10.2	.3	3.	232	232	129	27
		10.9	.4	3.	228	228	132	35
11'	3.8	10.7	.3	3.	232	232	140	42
12'	4.2	10.3	.3	3.	231	231	139	43
		10.4	.3	3.	227	227	135	39
13'	4.1	11.7	.4	4.	241	241	150	50
		10.8	.2	3.	235	235	172	82
14'	4.2	11.5	.3	3.	234	234	180	93
		10.7	.3	3.	242	242	172	79
		10.4	.2	3.	244	244	182	90
15'	4.4	10.9	.3	3.	247	247	179	84
		10.8	.3	4.	243	243	178	85
		9.4	.2	3.	248	248	202	113
15'-7"	6.9	11.2	.3	3.	224	224	223	155
15'-9"	8.0	9.4	.2	3.	215	215	195	125
		10.8	.2	3.	210	210	210	146
16'	12.0	11.2	.4	5.	217	217	193	120
16'-2"	7.0	11.8	4.3	6.	211	211	190	120
		10.5	3.0	3.	207	207	193	126
16'-4"	9.0	8.8	.1	2.	216	216	218	153
16-51/4	20/1/2	10.0	.2	3.	213	213	198	152

Table A20: Sample dynamic results obtained by Case Method of Processing W92 9B3V

Depth	Blows/ Inch	VMax	DMax	EMax	FMax	F1	P4	CD
2'	.3	8.7	.9	2.	206	206	28	
4'	.6	9.8	1.1	3.	206	206	27	
5'	.8	8.0	.9	2.	201	201	63	
6'	1.0	7.5	.9	2.	143	143	55	
7'	1.5	6.7	.9	2.	151	151	73	
8'	1.7	8.4	.6	2.	197	197	54	
9'	1.7	9.0	.8	3.	193	193	48	
10'	2.0	9.1	.7	3.	190	190	59	
		9.5	.4	2.	197	197	78	
		9.2	.6	2.	217	217	104	
11'	2.0	9.7	.3	2.	217	217	112	
		9.1	.4	2.	219	219	104	
12'	2.5	9.2	.3	2.	218	218	130	
13'	2.8	7.8	.2	2.	212	212	140	61
14'	3.2	9.2	.3	2.	218	213	140	55
		8.5	.2	2.	206	206	148	69
		8.5	.1	2.	219	219	174	94
15'	5.6	8.3	.1	2.	233	233	193	112
15'-2"	5.0	8.4	.2	2.	215	215	183	114
15'-4"	6.0	8.9	.1	2.	217	217	199	133
15'-6"	5.0	8.2	.1	2.	227	227	178	95
15'-8"	5.0	7.3	.1	1.	237	237	179	90
15'-10"	6.0	9.2	.2	2.	236	236	209	129
16'	6.0	8.3	.1	2.	224	224	210	140
16'-2"	8.0	8.3	.1	2.	226	226	204	131
16'-4"	13.0	8.5	.1	2.	226	226	223	156
16'-6"	20.0	8.4	.4	2.	220	220	199	126

Table A21

Sample dynamic results obtained by Case Method of Processing
W92 9B3P

I	Depth (Ft)	Quake (In)	Res (Kips)	Sum Res (Kips)	J (K-S/Ft)	Weight (Lb)	Stiffness (K/in)	Max Spring Force
1	3.3	.100	0	151	0.00	139	9400.	212.
2	6.6	.100	0	151	0.00	139	9400.	208.
3	9.9	.100	7	144	.39	139	9400.	224.
4	13.1	.100	20	124	1.11	139	9400.	238.
5	16.4	.100	31	93	1.73	139	9400.	233.
6	19.7	.100	31	62	1.73	139	9400.	201.
7	23.0	.100	31	31	1.73	139	9400.	151.
8	23.0	.150	31	0	3.34			

Maximums

Measured Pile Top	Force	208
	Velocity	10.1
	Disp.	.22
Computed Pile Toe	Velocity	12.4
	Disp.	.16

Maximum Sum of Damping Forces Occurring Simultaneously 96.

W92 9B3-V

I	Depth (Ft)	Quake (In)	Res (Kips)	Sum Res (Kips)	J (K-S/Ft)	Weight (Lb)	Stiffness (K/in)	Max Spring Force
1	3.3	.070	0	170	0.00	139	9400.	229.
2	6.6	.070	0	170	0.00	139	9400.	227.
3	9.9	.070	5	165	.32	139	9400.	238.
4	13.1	.070	25	140	1.59	139	9400.	250.
5	16.4	.070	40	100	2.54	139	9400.	243.
6	19.7	.070	40	60	2.54	139	9400.	204.
7	23.0	.070	30	30	1.91	139	9400.	141.
8	23.0	.120	30	0	3.34			

Maximums

Measured Pile Top	Force	229
	Velocity	10.1
	Disp.	.17
Computed Pile Toe	Velocity	8.6
	Disp.	.12

Maximum Sum of Damping Forces Occurring Simultaneously 98.

W92 9B3-P

Table A22: CAPWAP Resistance Distribution Results For Piles 9B3V and 9B3P at W92

Depth	Blows/ Inch	VMax	DMax	EMax	FMax	F1	P4	CD
3'	1.0	5.4	1.5	2.	91	91	16	
4'	1.7	5.6	1.0	3.	108	108	29	
5'	2.0	5.6	.7	2.	109	109	37	
6'	3.0	5.3	.5	2.	108	108	47	
		5.6	.5	2.	118	118	52	
7'	4.0	6.0	.5	2.	117	117	56	
8'	4.3	6.0	.4	2.	123	123	66	11
9'	4.8	6.2	.5	2.	127	127	66	9
10'	4.8	6.3	.6	2.	121	121	64	10
11'	5.6	6.2	.4	2.	129	129	75	19
12'	5.2	5.8	.4	2.	123	123	75	23
13'	5.6	5.7	.3	2.	126	216	79	27
14'	6.2	6.0	.3	2.	128	128	84	31
		5.9	.2	1.	129	129	102	54
15'	8.8	6.4	.2	2.	134	134	119	74
15'-3"	13.	6.3	.2	2.	138	138	122	75
15'-6"	11.	6.2	.2	2.	136	136	122	76
15'-9"	13.	6.6	.2	2.	145	145	127	78
16'	12.	6.8	.2	2.	142	142	132	86
		6.4	.2	2.	138	138	134	91
16'-2"	14	6.8	.2	2.	145	145	144	100
		6.7	.2	2.	149	149	152	107
16'-4"	17	7.2	.2	2.	150	150	161	118
		6.9	.2	2.	148	148	165	125
16'-5"	20	6.9	.2	2.	153	153	173	132

Table A23: Sample dynamic results obtained by Case Method of Processing W92 D5V

Depth	Blows/ Inch	VMax	DMax	EMax	FMax	F1	P4	CD
4'	1.0	5.3	1.4	3.	96	96	13	
5'	1.2	5.9	1.6	3.	106	106	17	
6'	1.5	5.0	1.4	2.	94	94	18	
7'	1.8	5.3	1.0	2.	103	103	27	
8'	2.0	5.1	.7	2.	111	111	37	
9'	2.0	5.4	.6	2.	115	115	42	
11'	2.3	5.6	.5	2.	121	121	55	
12'	2.6	5.9	.6	3.	124	124	61	
13'	3.0	6.0	.5	2.	125	125	63	
14'	3.7	6.0	.4	2.	130	130	80	25
15'	5.8	6.3	.5	3.	129	129	87	36
		6.7	.4	3.	143	143	103	48
15'-2"	9.0	6.5	.3	2.	143	143	111	58
15'-6"	8.0	6.3	.3	2.	137	137	108	58
15'-8"	9.0	6.1	.3	2.	138	138	110	60
15'-10"	9.0	6.7	.3	2.	138	138	113	63
16'	10.0	6.4	.2	2.	145	145	125	75
		6.7	.2	2.	147	147	138	91
16'-1"	12.0	6.8	.2	2.	148	148	142	95
		7.1	.3	2.	152	152	147	100
16'-2"	20.0	7.1	.2	2.	147	147	154	111

Table A24

Sample dynamic results obtained by Case Method of Processing
W92 D5P

Depth	Blows/ Inch	VMax	DMax	EMax	FMax	F1	P4	CD
3'	1.4	5.1	1.1	3.	100	100	21	
4'	2.5	5.4	1.0	2.	101	101	24	
5'	3.0	5.3	.7	2.	102	102	34	
		5.1	.6	2.	107	107	38	
6'	4.5	5.2	.5	2.	112	112	50	
7'	3.2	5.3	.5	2.	106	106	52	3
8'	6.1	6.1	.6	2.	104	104	51	3
		5.4	.4	2.	109	109	65	18
9'	7.2	5.7	.4	2.	116	116	67	17
		5.5	.4	2.	116	116	69	19
10'	6.7	5.3	.3	2.	116	116	70	21
11'	6.3	5.2	.3	2.	112	112	70	24
12'	7.4	5.0	.3	1.	112	112	76	31
13'	9.1	5.4	.3	2.	120	120	81	33
14'	11.2	4.8	.3	1.	104	104	78	38
14'-2"	12	5.0	.3	1.	111	111	83	40
14'-4"	11	5.0	.3	1.	110	110	83	41
		4.4	.2	1.	101	101	82	46
		5.2	.2	1.	112	112	80	36
14'-8"	14	4.3	.2	1.	98	98	81	46
		5.0	.3	1.	112	112	85	43
		5.1	.3	1.	114	114	85	43
15'	16	5.0	.3	1.	108	108	86	46
		4.6	.2	1.	101	101	85	49
		4.5	.2	1.	108	108	89	50
		5.2	.2	1.	118	118	95	52
		4.9	.2	1.	109	109	92	54
15'-4"	17	5.6	.3	2.	121	121	99	55
		4.7	.2	1.	103	103	93	58
		5.1	.2	1.	118	118	99	57
		5.9	.2	1.	117	117	101	60
		5.5	.2	1.	123	123	105	62
		5.1	.2	1.	114	114	103	65
		5.3	.2	1.	117	117	105	66
15'-8"	17	5.5	.2	1.	122	122	108	66
		5.0	.2	1.	112	112	104	67
		5.0	.2	1.	114	114	106	69
15'-10"	20	4.7	.2	1.	110	110	105	69

Table A25

Sample dynamic results obtained by Case Method of Processing
W92 D5B

I	Depth (Ft)	Quake (In)	Res (Kips)	Sum Res (Kips)	J (K-S/Ft)	Weight (Lb)	Stiffness (K/in)	Max Spring Force
1	3.3	.060	0	130	0.00	139	9400.	148.
2	6.6	.060	0	130	0.00	139	9400.	153.
3	9.9	.060	10	120	.65	139	9400.	164.
4	13.1	.060	24	96	1.55	139	9400.	162.
5	16.4	.060	28	68	1.81	139	9400.	139.
6	19.7	.060	28	40	1.81	139	9400.	106.
7	23.0	.060	20	20	1.30	139	9400.	65.
8	23.0	.120	20	0	4.01			

Maximums

Measured Pile Top	Force	152.
	Velocity	6.5
	Disp.	.17
Computed Pile Toe	Velocity	6.1
	Disp.	.12

Maximum Sum of Damping Forces Occurring Simultaneously 63.

W92 D5V

I	Depth (Ft)	Quake (In)	Res (Kips)	Sum Res (Kips)	J (K-S/Ft)	Weight (Lb)	Stiffness (K/in)	Max Spring Force
1	3.3	.100	0	117	0.00	139	9400.	152.
2	6.6	.100	0	117	0.00	139	9400.	153.
3	9.9	.100	7	110	.49	139	9400.	160.
4	13.1	.100	21	89	1.46	139	9400.	162.
5	16.4	.100	26	63	1.81	139	9400.	145.
6	19.7	.100	21	42	1.46	139	9400.	118.
7	23.0	.100	21	21	1.46	139	9400.	81.
8	23.0	.100	21	0	4.45			

Maximums

Measured Pile Top	Force	147.
	Velocity	6.8
	Disp.	.21
Computed Pile Toe	Velocity	7.4
	Disp.	.16

Maximum Sum of Damping Forces Occurring Simultaneously 74.

W92 D5P

Table A26: CAPWAP Resistance Distribution Results for Piles D5V and D5P at W92

Depth	Blows/ Inch	VMax	DMax	EMax	FMax	F1	P4	CD
7'	.6	3.0	.4	3.	99	70	87	73
8'	1.1	4.0	.6	5.	113	100	104	83
		4.3	.8	7.	134	130	110	78
		4.7	.6	6.	152	140	134	101
10'	1.1	5.0	.6	7.	168	150	145	110
11'	1.1	4.9	.5	6.	168	150	152	120
		5.4		6.	174	160	159	123
		5.8		7.	181	170	164	105
13'	1.2	6.1	.5	6.	187	180	176	120
14'	1.3	7.7	.4	7.	250	210	236	179
		7.8		7.	254	210	241	184
15'	1.4	8.3	.4	7.	270	220	256	199
		9.3	.4	7.	260	230	287	231
		7.2		6.	288	210	262	214
16'	2.5	9.3	.5	8.	307	230	290	234
		7.7		8.	291	210	271	223
		8.8	.5	8.	294	220	280	228
		8.1		7.	295	210	277	229
16'-10"	4.2	8.2	.5	8.	294	210	274	227
		8.0		8.	298	220	280	231
		8.2	.5	8.	297	210	280	232
17'	12.	7.2	.5	8.	290	200	259	215
		8.2	.4	7.	298	210	283	236
17'-1"	19	8.4	.4	8.	313	230	297	247
17'-2"	15	7.2	.4	7.	303	200	268	227
		9.2	.5	8.	317	230	305	252
		8.0		8.	307	220	300	255
17'-3"	18	9.4	.4	8.	323	240	317	263
		8.0	.5	9.	311	220	305	262
		8.9	.4	8.	322	230	308	259
17'-4"	20	9.4	.4	8.	313	240	321	270

Sample dynamic results obtained by Case Method of Processing
W92 520V

Table A27

Depth	Blows/ Inch	VMax	DMax	EMax	FMax	F1	P4	CD
10'	.8	4.5	1.4	5.	65	50	51	40
11'	1.0	5.4	1.5	8.	83	60	65	51
12'	1.0	4.4	1.1	6.	81	60	69	55
		5.3		10.	120	100	102	78
13'	1.2	5.1	1.2	9.	113	90	96	77
14'	1.3	5.0	1.2	8.	110	80	92	74
		4.6		8.	112	100	97	76
		4.8	1.0	8.	125	110	111	86
15'	1.8	3.8	.7	7.	166	160	131	90
		4.8	.6	8.	200	190	162	115
		4.6		7.	202	200	168	120
16'	2.6	5.4	.6	8.	216	210	182	132
16'-2"	6.5	5.5	.5	8.	229	220	191	138
16'-4"	10	7.0	.5	8.	281	250	259	220
		6.8		8.	308	250	276	228
16'-6"	10	7.7	.5	9.	315	260	288	238
		7.7		9.	321	270	294	243
		8.3		11.	331	280	306	255
16'-7"	11	8.0	.5	10.	321	270	300	251
		8.2		10.	332	280	311	260
		7.6		9.	323	270	304	257
		8.4		11.	336	270	312	263
		7.6		9.	331	270	314	266
16'-9"	15	8.0	.5	10.	335	270	314	265
		8.3		10.	340	270	322	274
		8.0		10.	336	270	324	276
		8.7		11.	347	280	330	282
		8.1		10.	340	270	324	278
		8.2		10.	347	280	331	285
16'-11"	16	8.4	.5	10.	352	270	333	287
		8.5		10.	359	280	336	290
		8.2		10.	358	270	336	291
		8.5	.5	10.	359	280	343	297
17'	16	8.7	.5	11.	365	290	352	304
17'-3"	20/$\frac{3}{4}$"	Remainder of Data is not of good quality						

Sample dynamic results obtained by Case Method of Processing
W92 520P

Table A28

Depth	Blows/ Inch	VMax	DMax	EMax	FMax	F1	P4	CD
9'	1.4	4.2	1.1	5.	74	60	67	54
		4.7	1.3	7.	86	70	75	60
		4.8		8.	102	90	90	71
11'	1.3	3.8	.8	6.	102	90	93	74
12'	1.2	4.5	1.0	8.	118	100	106	84
		4.5		7.	120	100	104	82
13'	1.4	4.8	1.1	8.	117	100	102	80
		4.6		8.	113	100	99	77
14'	1.6	4.9	1.2	9.	119	100	107	84
		4.4		8.	122	100	106	83
15'	1.7	4.5	.9	8.	131	110	112	89
		4.1	.8	7.	137	110	122	99
		3.9	.8	8.	158	150	143	108
16'	2.3	4.7	.7	8.	202	190	178	136
		5.1	.7	9.	218	200	190	145
		5.3		8.	230	220	202	154
		5.4	.6	8.	235	220	206	158
		5.5		8.	240	220	216	169
17'	3.3	5.9	.6	9.	257	230	229	180
		6.2	.5	8.	278	240	262	216
		6.9		.9	289	250	275	228
		7.1	.5	10.	302	250	286	239
		6.9		9.	314	250	290	246
17'-4"	6.8	7.3	.5	9.	321	260	304	259
		6.4		8.	320	250	295	253
		6.8		8.	321	250	300	257
17'-5"	13	6.7	.4	8.	327	250	300	259
		7.2		9.	336	260	315	272
17'-6"	12	7.3	.5	9.	344	260	318	275
		7.1		9.	343	260	315	272
		7.4		9.	340	260	320	277
17'-7"	14	7.2	.5	9.	341	260	316	274
		6.8		8.	339	250	314	273
		7.3		9.	348	260	321	280
17'-8"	16	7.2	.4	8.	349	260	325	284
		7.4		9.	358	260	329	287
		7.3	.4	9.	361	250	331	291
		7.6	.5	9.	366	270	339	298
17'-9"	19	7.6	.5	9.	364	260	333	293
17-10"	$20/\frac{7}{8}$	7.5	.5	9.	359	260	334	295

Sample dynamic results obtained by Case Method of Processing
W92 520B

Table A29

I	Depth (Ft)	Quake (In)	Res (Kips)	Sum Res (Kips)	J (K-S/Ft)	Weight (Lb)	Stiffness (K/in)	Max Spring Force
1	4.0	.100	0	280	0.00	169	7700.	325.
2	8.0	.100	0	280	0.00	169	7700.	327.
3	12.0	.100	2	278	.08	169	7700.	322.
4	16.0	.100	3	275	.12	169	7700.	316.
5	20.0	.100	10	265	.41	169	7700.	319.
6	24.0	.100	30	235	1.24	169	7700.	307.
7	28.0	.100	90	145	3.73	169	7700.	263.
8	28.0	.160	145	0	2.24			

Maximums

Measured Pile Top	Force	287.
	Velocity	8.8
	Disp.	.45
Computed Pile Toe	Velocity	6.9
	Disp.	.27

Maximum Sum of Damping Forces Occurring Simultaneously 55.

W92 520V

Table A30 : CAPWAP Resistance Distribution Results for Pile 520V at W92

Depth	Blows/ Inch	VMax	DMax	EMax	FMax	F1	P4	CD
		6.9	.2	3.	218	170	239	218
		6.8	.2	3.	215	170	240	218
		7.0	.3	4.	213	160	234	213
		7.8	.3	4.	231	180	262	239
		7.5	.3	4.	225	170	254	233
		6.8	.2	3.	222	170	252	230
		7.1	.2	4.	227	180	251	228
		7.5	.3	4.	215	170	244	224
		7.9	.4	4.	210	160	233	212
		6.7	.2	3.	219	170	240	219
		7.0	.2	3.	222	180	251	229
		7.2	.3	4.	219	170	244	222
		6.8	.2	3.	222	170	250	228
		7.5	.3	4.	221	170	247	225
		7.1	.2	4.	221	180	253	231
		7.6	.3	4.	222	170	249	228
		7.4	.3	4.	218	170	249	227
		7.4	.3	4.	218	170	250	229
		7.1	.2	3.	220	180	255	233
		7.7	.3	4.	228	180	253	21
		7.4	.3	4.	234	180	261	238
		7.4	.3	4.	234	180	266	245
		7.1	.2	4.	237	190	266	242
		7.8	.3	4.	243	190	273	249
		7.2	.2	4.	249	190	277	254
		7.5	.2	4.	250	200	281	257
		7.6	.3	4.	235	180	266	244
		7.6	.3	4.	242	190	277	254
		8.0	.3	5.	239	190	272	248
		7.4	.2	4.	242	190	279	255
		7.6	.3	4.	245	190	271	247
		7.1	.2	4.	249	190	273	250
		7.8	.3	4.	232	180	266	243
		8.0	.3	5.	230	180	261	238
		7.5	.3	4.	234	180	262	239
		7.4	.3	4.	234	180	266	243
		7.4	.3	4.	235	190	269	246
		7.2	.2	4.	232	180	265	242
		7.2	.3	4.	229	170	250	230
		6.9	.2	3.	225	180	252	230
		6.6	.2	3.	228	180	252	229
		7.2	.2	3.	211	190	264	239

Sample dynamic results obtained by Case Method of Processing
W92 520V/440

Table A31

I	Depth (Ft)	Quake (In)	Res (Kips)	Sum Res (Kips)	J (K-S/Ft)	Weight (Lb)	Stiffness (K/in)	Max Spring Force
1	3.3	.060	0	190	0.00	139	9400.	190.
2	6.6	.060	0	190	0.00	139	9400.	199.
3	9.9	.060	5	185	.31	139	9400.	207.
4	13.1	.060	15	170	.92	139	9400.	207.
5	16.4	.060	40	130	2.46	139	9400.	193.
6	19.7	.060	55	75	3.38	139	9400.	151.
7	23.0	.060	48	27	2.95	139	9400.	93.
8	23.0	.110	27	0	4.45			

Maximums

Measured Pile Top Force		215
	Velocity	6.7
	Disp.	.22
Computed Pile Toe Velocity		4.8
		.13

Maximum Sum of Damping Forces Occurring Simultaneously 68.

W92 520V/440E (Early Blow)

I	Depth (Ft)	Quake (In)	Res (Kips)	Sum Res (Kips)	J (K-S/Ft)	Weight (Lb)	Stiffness (K/in)	Max Spring Force
1	3.3	.045	0	239	0.00	139	9400.	214.
2	6.6	.045	0	239	0.00	139	9400.	228.
3	9.9	.045	5	234	.23	139	9400.	232.
4	13.1	.045	15	219	.68	139	9400.	235.
5	16.4	.045	41	178	1.87	139	9400.	224.
6	19.7	.045	58	120	2.64	139	9400.	184.
7	23.0	.045	62	58	2.82	139	9400.	127.
8	23.0	.120	58	0	4.90			

Maximums

Measured Pile Top Force		231.
	Velocity	7.4
	Disp.	.24
Computed Pile Toe Velocity		4.2
	Disp.	.12

Maximum Sum of Damping Forces Occurring Simultaneously 58.

W92 520V/440L (Later Blow)

Table A32: CAPWAP Resistance Distribution Results for Piles 520V/440R and 520V/440L at W92

Depth	Blows/ Inch	VMax	DMax	EMax	FMax	F1	P4	CD
6'	.5	10.8	2.3	15.	248	240	78	
		10.7		14.	247	240	87	5
9'	.5	11.4	2.3	17.	268	260	99	12
10'	.7	10.9	1.9	15.	260	250	95	10
13'	.8	11.6	1.4	16.	297	290	153	64
14'	.9	11.4	1.3	16.	301	300	164	76
15'	1.0	11.3	1.3	16.	304	300	163	74
		11.4	1.1	16.	305	300	201	119
16'	1.4	11.5	1.0	16.	315	300	231	154
		11.6	.8	17.	318	310	297	231
16'-10"	2.5	10.7	.6	13.	336	280	346	300
17'	5	11.1	.7	16.	352	300	365	315
		11.0		15.	369	290	376	331
		8.9		13.	360	290	372	327
17'-2"	7	11.0	.6	14.	387	300	387	343
		10.9		14.	390	300	389	346
		11.3	.6	15.	409	310	408	363
17'-4"		11.8	.6	16.	425	300	419	379
		11.4	.6	16.	425	300	417	377
		10.2		15.	421	300	409	369
		10.8	.5	14.	427	300	416	377
		11.5	.6	16.	432	300	422	383
17'-6"	12	11.1	.6	15.	428	290	415	378
		10.3		16.	420	270	396	365
		9.8		14.	422	280	400	364
		10.0		14.	430	290	413	377
17'-7"	20	10.7	.6	14.	439	300	422	386

Table A33 : Sample dynamic results obtained by Case Method of Processing W92 08V

Depth	Blows/ Inch	VMax	DMax	EMax	FMax	F1	P4	CD
7'	.2	11.1	2.5	8.	236	220	37	
10'	.3	11.7	3.0	11.	243	230	40	
12'	.5	11.8	2.8	12.	249	240	52	
13'	.6	11.8	2.7	16.	257	250	77	
14'	.6	11.7	2.5	17.	271	270	92	
15'	.8	11.0	1.5	15.	277	270	123	36
16'	1.3	10.9	1.3	14.	282	270	150	69
		10.2	1.0	13.	287	270	177	100
		10.5	.9	15.	303	290	218	143
		11.0	.7	15.	334	290	324	270
		11.1		14.	347	280	330	282
17'	4.3	10.9	.6	14.	372	280	359	314
		11.2		15.	370	290	363	319
		9.8		13.	390	290	379	336
17'-3"	9	10.1	.6	14.	397	270	372	336
		10.6		13.	402	280	389	352
		9.6		13.	385	250	356	324
17'-7"	6	11.2	.7	15.	382	270	371	333
		10.8		13.	388	290	380	338
17'-9"	8	10.9	.6	14.	388	270	373	335
		10.6	.6	14.	395	290	384	343
		11.1		15.	394	290	383	342
18'	6	10.5	.6	14.	401	290	391	350
		10.5		14.	417	290	395	356
		11.0	.6	15.	429	290	410	374
		11.4		16.	448	300	426	389
18'-2"	12	11.2	.6	16.	458	290	431	398
		8.9		12.	453	270	409	380
		8.9	15	11.	439	310	438	400
18'-3"	25	9.5	.5	12.	449	300	438	403

Table A34

Sample dynamic results obtained by Case Method of Processing
W92 08P

Depth	Blows/ Inch	VMax	DMax	EMax	FMax	F1	P4	CD
6'	.5	11.9	2.4	16.	248	240	94	13
7'	.6	12.3	2.6	19.	253	250	99	17
		11.8		17.	260	260	104	20
10'	.6	10.9	1.2	12.	260	250	138	62
11'	.8	11.0	1.2	12.	268	260	144	65
12'	.8	11.8	1.5	14.	264	260	142	64
13'	.8	10.9	1.1	13.	277	270	164	85
14'	.9	10.8	1.0	12.	271	270	160	83
15'	1.2	10.9	1.0	13.	269	260	184	113
		10.5	.9	13.	283	270	209	140
16'	1.3	10.3	.8	13.	291	270	229	163
		9.7	.6	12.	292	270	300	248
		10.8	.6	13.	366	270	359	320
17'	2.1	10.9	.6	14.	371	280	371	331
17'-4"	6	9.3	.5	12.	391	280	374	336
		10.1		15.	403	270	381	345
17'-6"	10	10.4	.6	15.	410	280	390	355
		10.5		14.	410	270	389	356
		9.5		12.	417	280	397	361
17'-8"	10	9.4	.5	13.	416	280	394	359
		7.9		11.	399	250	351	319
		9.6	.5	13.	417	290	406	369
		8.6		12.	390	270	369	334
		8.9	.5	13.	408	280	389	352
		8.2	.5	12.	392	260	368	335
		8.5		12.	409	250	369	339
17'-10"	12	8.6	.5	11.	404	230	337	310
		9.1		12.	409	250	356	326
		9.0		12.	404	240	349	319
		7.0		10.	397	180	280	260
18'-1"	24/1/2	7.8	.6	11.	392	170	274	260

Table A35

Sample dynamic results obtained by Case Method of Processing
W92 08B

I	Depth (Ft)	Quake (In)	Res (Kips)	Sum Res (Kips)	J (K-S/Ft)	Weight (Lb)	Stiffness (K/in)	Max Spring Force
1	4.0	.100	0	405	0.00	169	7700.	436.
2	8.0	.100	0	405	0.00	169	7700.	445.
3	12.0	.100	10	395	.29	169	7700.	453.
4	16.0	.100	20	375	.58	169	7700.	446.
5	20.0	.100	45	330	1.31	169	7700.	424.
6	24.0	.100	70	260	2.04	169	7700.	369.
7	28.0	.100	85	175	2.48	169	7700.	286.
8	28.0	.300	175	0	3.36			

Maximums

Measured Pile Top	Force	409.
	Velocity	11.4
	Disp.	.63
Computed Pile Toe	Velocity	7.4
	Disp.	.37

Maximum Sum of Damping Forces Occurring Simultaneously 75.

W92 08V

Table A36: CAPWAP Resistance Distribution Results for Pile 08V at W92

Depth	Blows/ Inch	VMax	DMax	EMax	FMax	F1	P4	CD
		6.6	.2	3.	219	170	240	219
		6.7	.2	3.	224	170	246	224
		6.7	.2	3.	221	180	250	227
		7.5	.2	4.	239	190	270	246
		7.5	.3	4.	233	190	269	245
		8.0	.3	5.	236	190	267	242
		7.1	.2	4.	227	180	260	237
		8.1	.3	4.	240	190	278	254
		8.1	.3	4.	251	200	285	260

Sample dynamic results obtained by Case Method of Processing
W92 08V/440

Table A37

I	Depth (Ft)	Quake (In)	Res (Kips)	Sum Res (Kips)	J (K-S/Ft)	Weight (Lb)	Stiffness (K/in)	Max Spring Force
1	3.3	.060	0	230	0.00	139	9400.	220.
2	6.6	.060	0	230	0.00	139	9400.	229.
3	9.9	.060	5	225	.19	139	9400.	237.
4	13.1	.060	26	199	.99	139	9400.	237.
5	16.4	.060	58	141	2.22	139	9400.	214.
6	19.7	.060	78	63	2.98	139	9400.	157.
7	23.0	.060	37	26	1.41	139	9400.	76.
8	23.0	.100	26	0	2.23			

Maximums

Measured Pile Top	Force	220.
	Velocity	7.4
	Disp.	.24
Computed Pile Toe	Velocity	5.5
	Disp.	.14

Maximum Sum of Damping Forces Occurring Simultaneously 52.

W92 08V/440R (Early Blow)

Table A38: CAPWAP Resistance Distribution Results for Pile 08V/440R at W92

Depth	Blows/ Inch	VMax	DMax	EMax	FMax	F1	P4	CD
4'	.6	7.7	1.8	8.	177	170	48	
5'	.8	8.5	1.6	8.	186	180	57	
7'	1.2	8.5	1.0	7.	201	200	88	25
9'	1.3	9.0	1.1	9.	212	210	99	33
14'	1.5	9.7	1.0	8.	212	210	127	67
15'	2.0	9.9	.7	7.	226	220	150	89
16'	3.8	9.5	.5	6.	213	210	170	118
16'-11"	14	11.0	.1	3.	291	260	371	339
17'-1"	14	12.8	.3	7.	291	260	351	316
17'-3"	25	13.3	.6	7.	309	300	371	323

Sample dynamic results obtained by Case Method of Processing
W92 D15V

Depth	Blows/ Inch	VMax	DMax	EMax	FMax	F1	P4	CD
17'-8"	11	14.8	.6	11.	326	310	381	330
		13.1	.4	10.	328	300	387	343
17'-10"	12	15.8	.6	10.	329	310	409	364
		15.0	.6	11.	344	300	412	371
		15.7	.6	10.	337	320	417	371
18'	13	13.9	.4	8.	325	300	408	367
		12.5	.4	8.	322	310	386	338
18'-2"	9	11.2	.2	5.	309	280	390	355
		12.3	.3	7.	323	310	392	343
		13.4	.6	9.	321	280	395	359
18'-5"	14	12.8	.5	9.	319	310	392	345

Sample dynamic results obtained by Case Method of Processing
W92 D15P

Table A39

I	Depth (Ft)	Quake (In)	Res (Kips)	Sum Res (Kips)	J (K-S/Ft)	Weight (Lb)	Stiffness (K/in)
1	3.3	.100	0	290	0.00	139	9400.
2	6.6	.100	0	290	0.00	139	9400.
3	9.9	.100	10	280	.26	139	9400.
4	13.1	.100	23	257	.61	139	9400.
5	16.4	.100	33	224	.87	139	9400.
6	19.7	.100	42	182	1.11	139	9400.
7	23.0	.100	61	121	1.61	139	9400.
8	23.0	.120	121	0	2.23		

Maximums

Measured Pile Top	Force	290.
	Velocity	12.5
	Disp.	.33
Computed Pile Toe	Velocity	11.7
	Disp.	.18

Maximum Sum of Damping Forces Occurring Simultaneously 74.

W92 D15V

I	Depth (Ft)	Quake (In)	Res (Kips)	Sum Res (Kips)	J (K-S/Ft)	Weight (Lb)	Stiffness (K/in)	Max Spring Force
1	3.3	.100	0	351	0.00	139	9400.	317.
2	6.6	.100	6	345	.12	139	9400.	331.
3	9.9	.100	13	332	.25	139	9400.	351.
4	13.1	.100	26	306	.51	139	9400.	357.
5	16.4	.100	44	262	.86	139	9400.	348.
6	19.7	.100	61	201	1.20	139	9400.	301.
7	23.0	.100	77	124	1.51	139	9400.	221.
8	23.0	.200	124	0	4.45			

Maximums

Measured Pile Top	Force	324.
	Velocity	13.6
	Disp.	.40
Computed Pile Toe	Velocity	11.2
	Disp.	.22

Maximum Sum of Damping Forces Occurring Simultaneously 98.

W92 D15P

Table A40: CAPWAP Resistance Distributions Results for Piles D15V and D15P at W92

Depth	Blows/ Inch	VMax	DMax	EMax	FMax	F1	P4	CD
12'	.8	8.3	1.7	14.	204	200	106	45
13'	.9	10.5	2.3	18.	199	190	110	52
14'	4.5	9.4	1.9	16.	206	200	121	64
15'	5	10.0	1.4	15.	226	210	142	82
16'-6"	7	9.6	.9	14.	272	240	207	149
		11.5	1.4	17.	293	270	279	223
17'-3"	6	13.6	1.1	20.	356	320	371	316
17'-9"	9	13.7	.7	17.	413	330	444	399
17'-8"	11	14.0	.6	17.	442	340	474	430
		14.8	.7	19.	445	350	493	449
17'-10"	13	13.9	.5	15.	464	360	508	464
18'	13	14.7	.6	20.	482	380	523	473
18'-6"	14	14.7	.7	19.	484	360	529	487
18'-7"	12	14.1	.5	17.	489	360	534	493
		14.3	.6	16.	495	360	543	504
18'-8"	14	15.2	.7	19.	491	380	550	507
		16.0	.8	20.	466	360	536	496
18'-9"	13	13.8	.6	15.	415	340	509	472

Pile Top Damaged

Sample dynamic results obtained by Case Method of Processing
W92 K25V

Depth	Blows/ Inch	VMax	DMax	EMax	FMax	F1	P4	CD
17'-5"	2	12.5	.7	16.	348	320	347	286
17'-8"	3	12.8	.7	16.	349	320	344	283
17'-10"	3	12.9	.7	16.	354	330	358	296
18'-2"	3	12.9	.7	16.	358	330	380	320
18'-6"	6	13.7	.6	18.	406	360	431	372
		13.6	.6	16.	412	360	453	399
		13.8	.6	17.	436	350	466	415
18'-8"	8	14.3	.6	17.	446	360	481	432
		14.7	.6	18.	449	360	487	437
		14.7	.6	18.	464	370	507	457
18'-10"	9	14.9	.6	19.	471	370	509	460
		14.8	.6	18.	480	370	521	473
19'	9	15.7	.7	21.	489	380	531	482

Pile Top Damaged

Sample dynamic results obtained by Case Method of Processing
W92 K25P

Table A41: Dynamic Parameters and Case Method Capacity Predictions for Piles K25V and K25P at W92

I	Depth (Ft)	Quake (In)	Res (Kips)	Sum Res (Kips)	J (K-S/Ft)	Weight (Lb)	Stiffness (K/in)	Max Spring Force
1	4.0	.120	0	450	0.00	169	7700.	467.
2	8.0	.120	3	447	.10	169	7700.	476.
3	12.0	.120	7	440	.22	169	7700.	480.
4	16.0	.120	20	420	.64	169	7700.	475.
5	20.0	.120	65	355	2.08	169	7700.	452.
6	24.0	.120	85	270	2.72	169	7700.	398.
7	28.0	.120	100	170	3.20	169	7700.	311.
8	28.0	.170	170	0	4.48			

Maximums

Measured Pile Top	Force	481.
	Velocity	15.1
	Disp.	.64
Computed Pile Toe	Velocity	7.5
	Disp.	.34

Maximum Sum of Damping Forces Occurring Simultaneously 115.

W92 K25V

Table A42 : CAPWAP Resistance Distribution Results for Pile K25V at W92

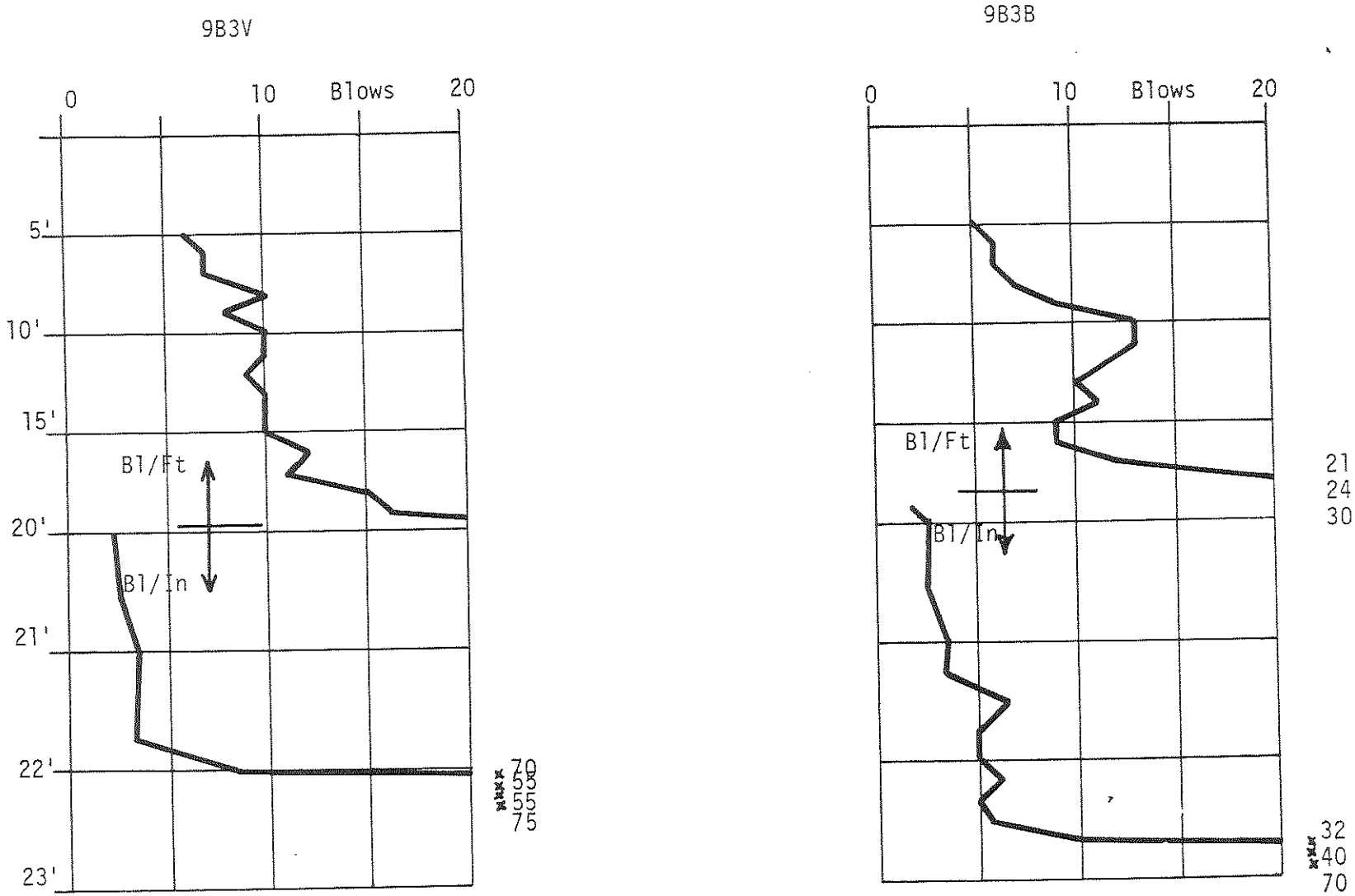

SANDUSKY

Figure A1: Blow Count Records for Piles Driven by the 9B3 Hammer

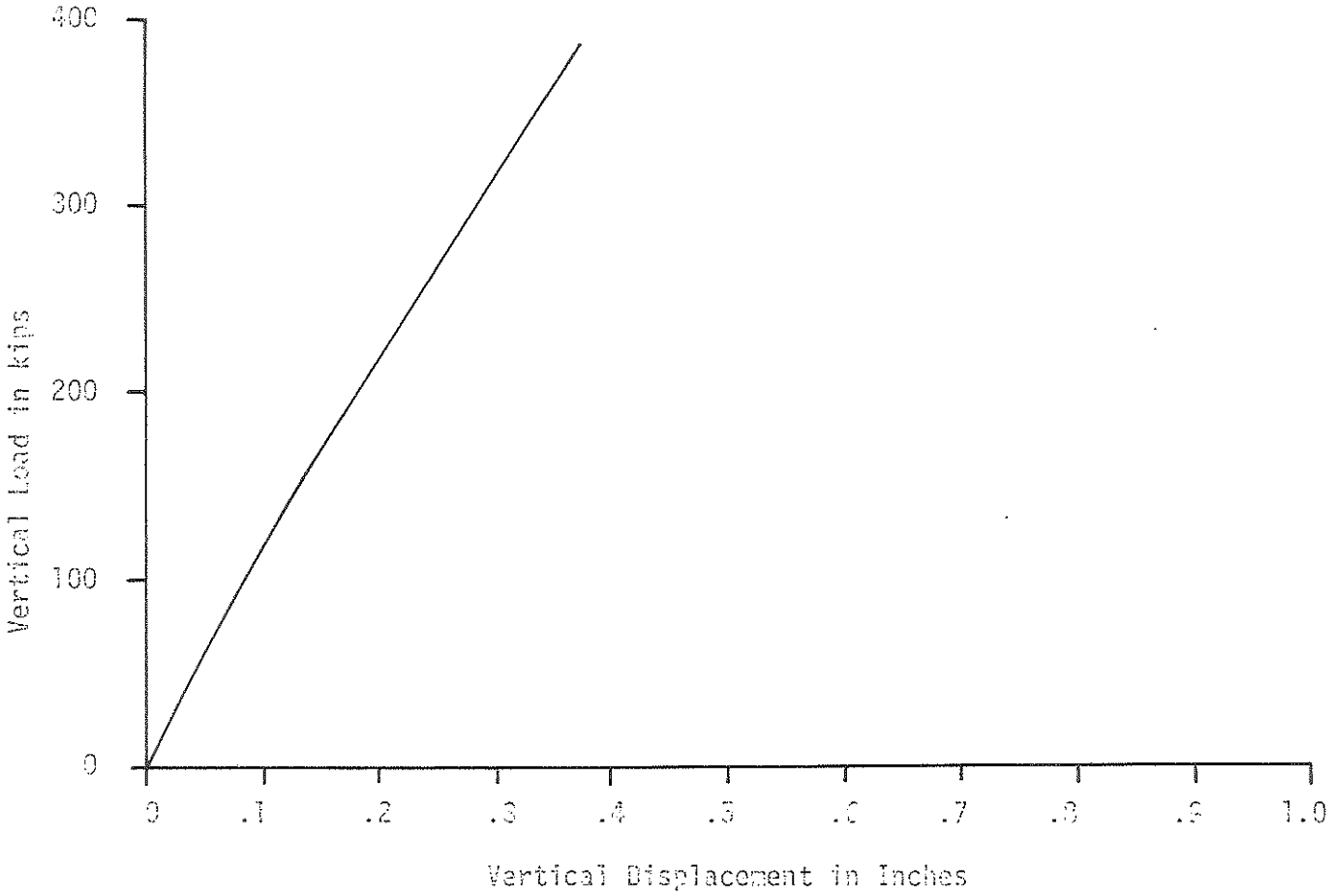

Figure A2: Static Load Test Curve Sandusky Pile No. 9B3V

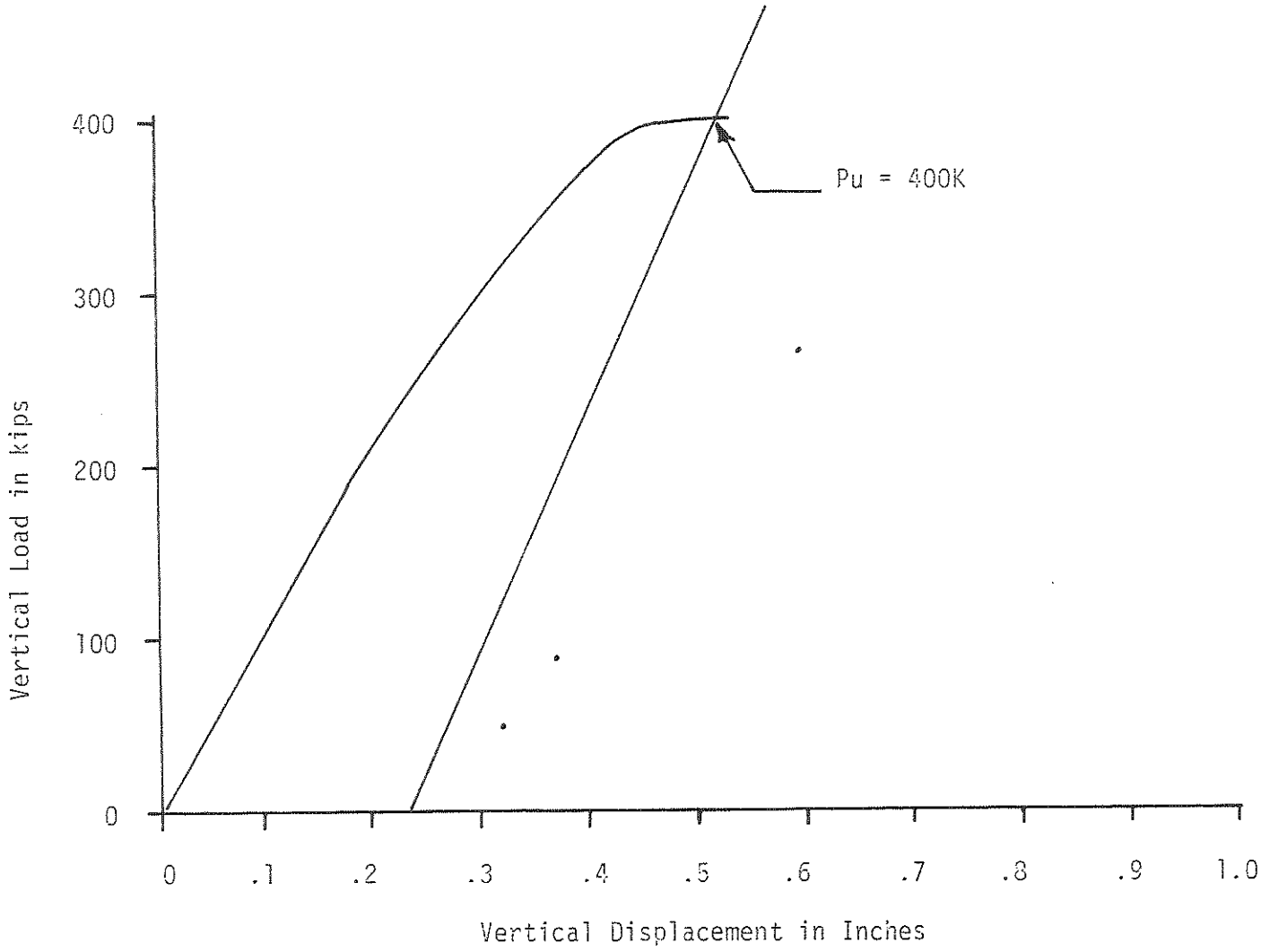

Figure A3: Static Load Test Curve Sandusky Pile No. 9B3B

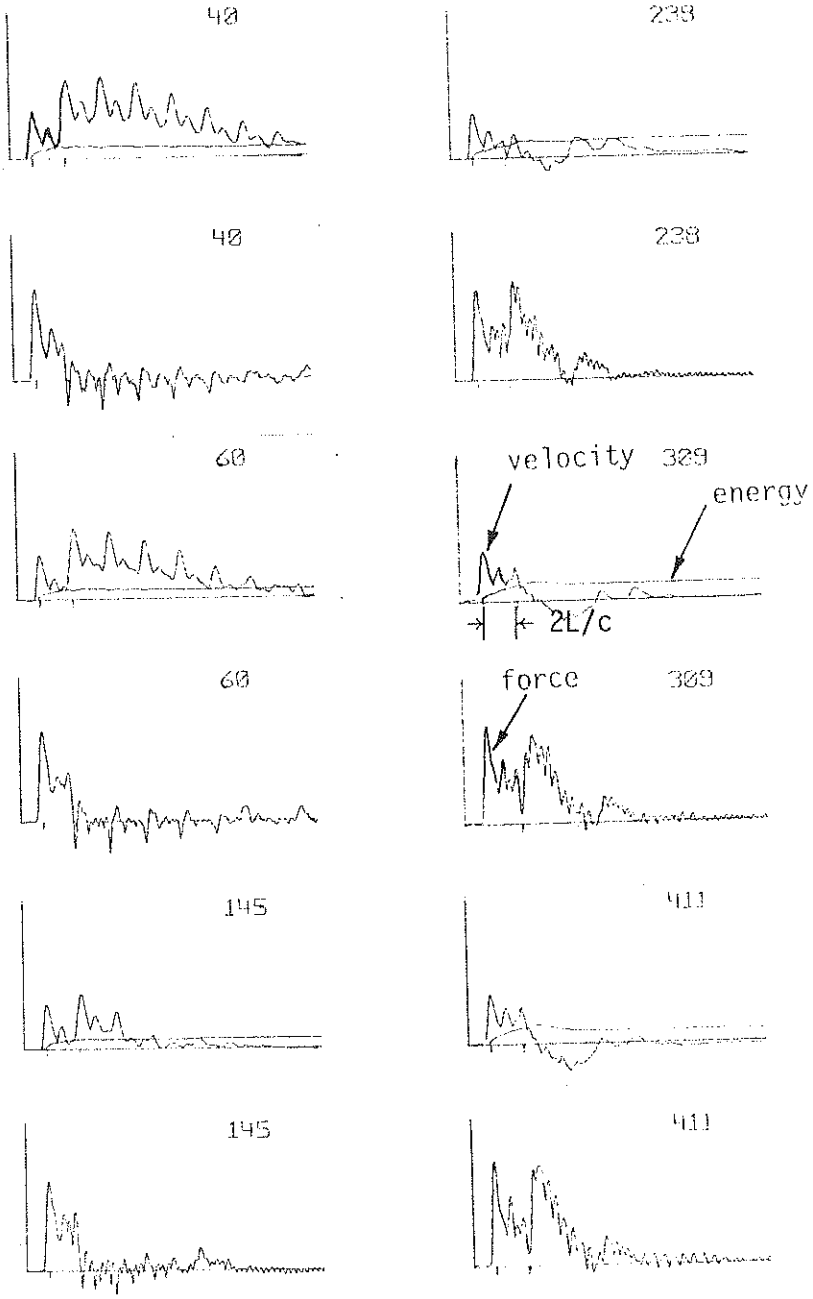

Figure A4: Sample records of force, energy and velocity plotted by Case Method of Processing. Sandusky 9B3V

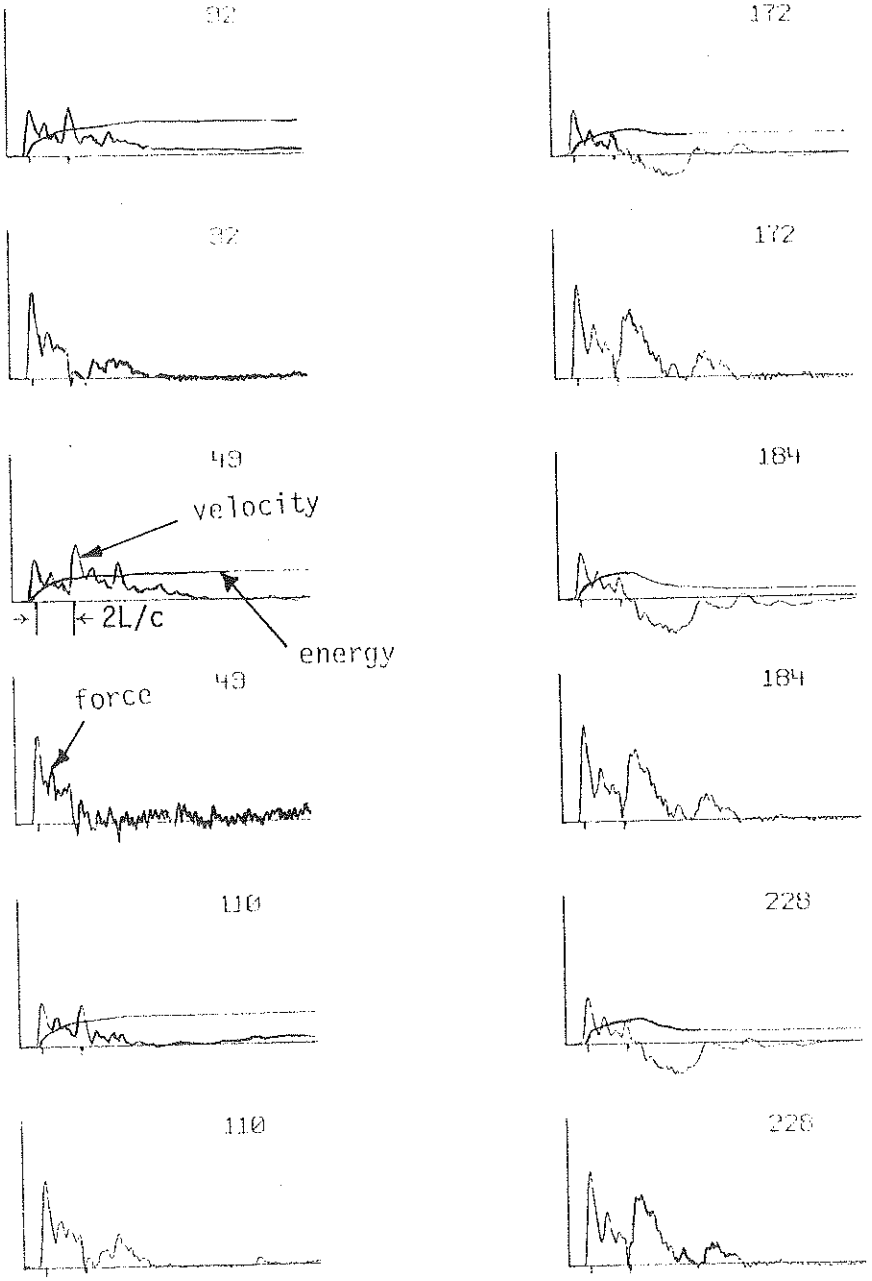

Figure A5 : Sample records of force, energy and velocity plotted by Case Method of Processing. Sandusky 9B3B

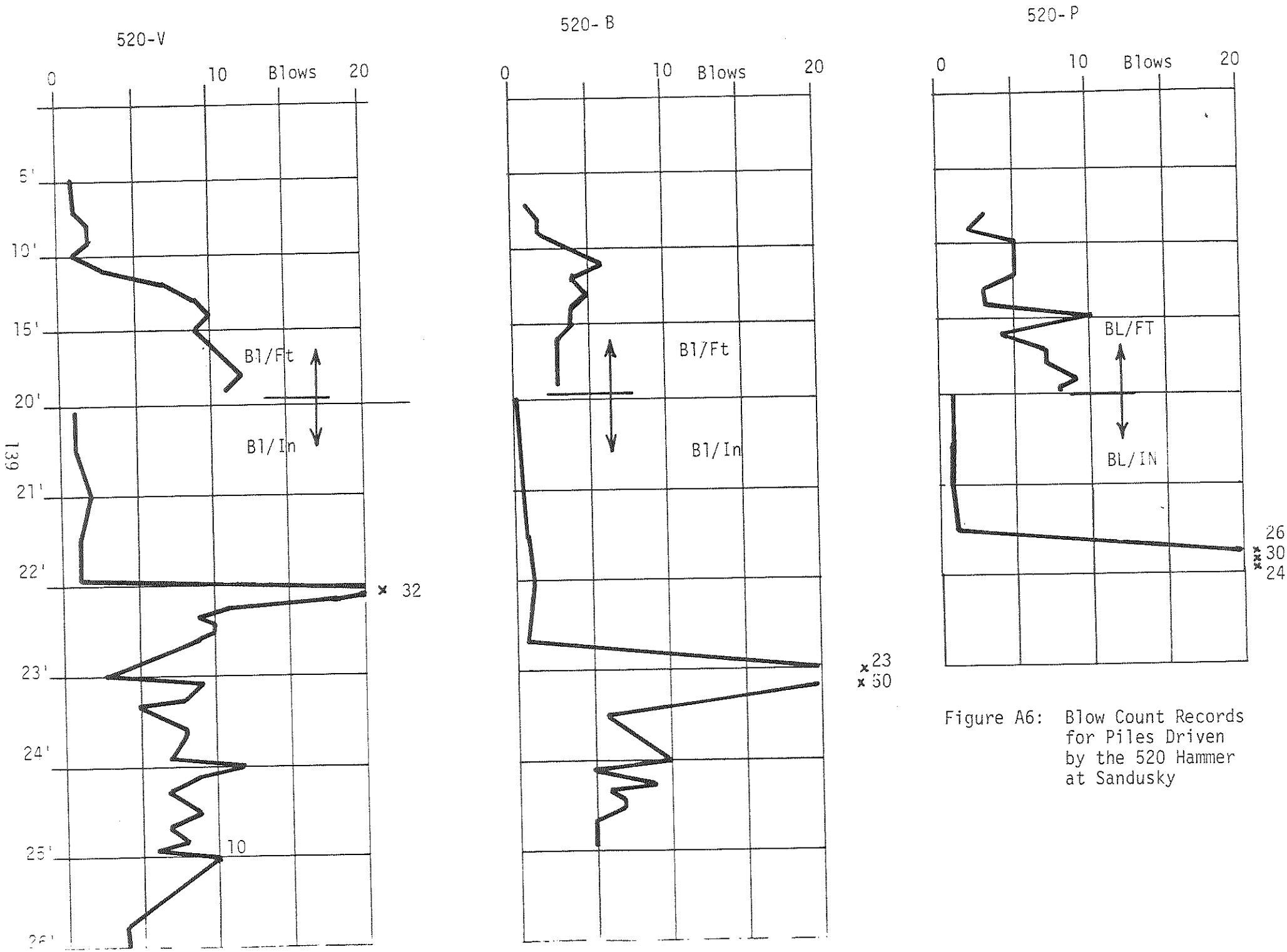

Figure A6: Blow Count Records for Piles Driven by the 520 Hammer at Sandusky

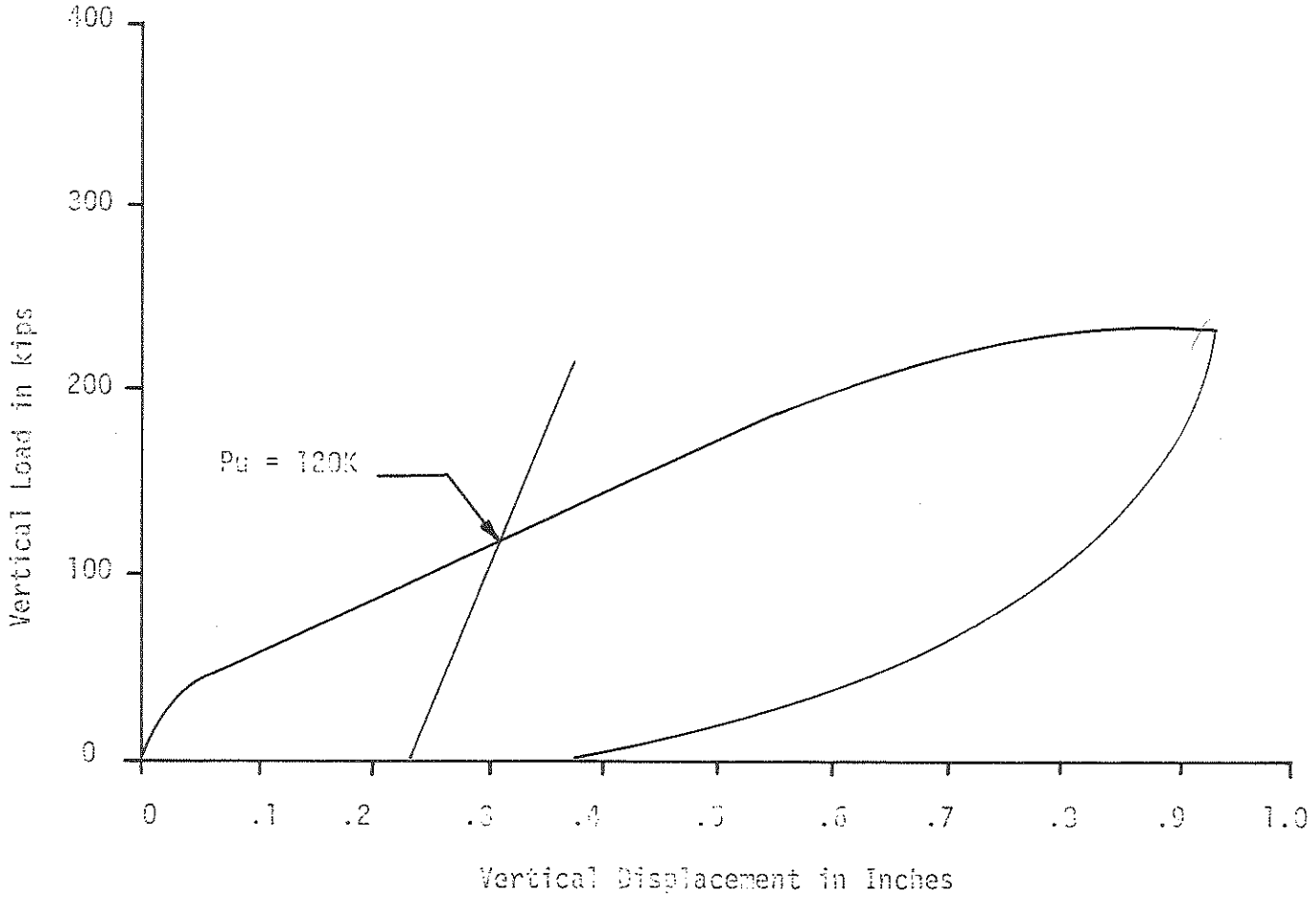

Figure A7: Static Load Test Curve Sandusky Pile No. LDS20V

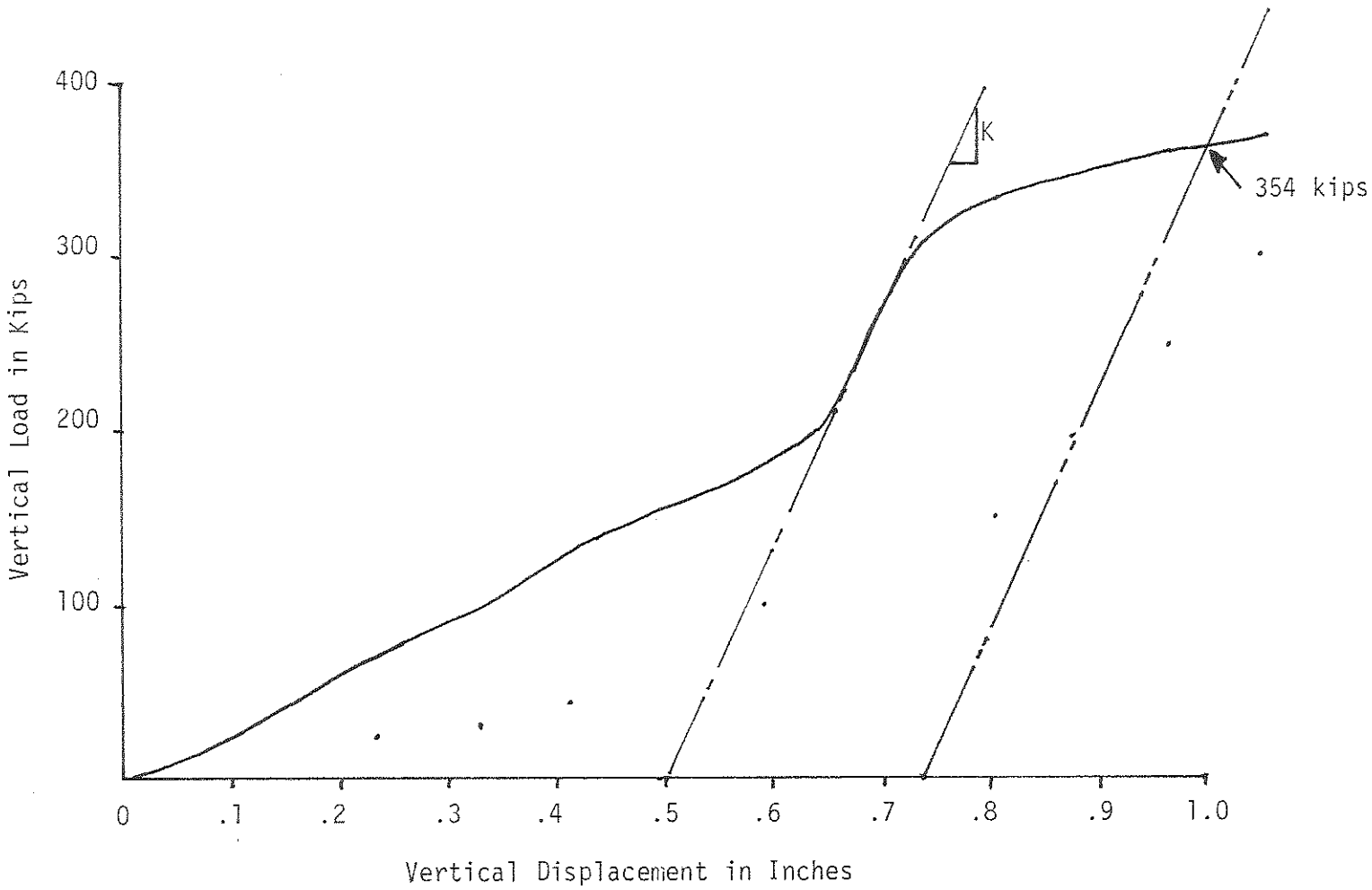

Figure A8: Static Load Test Curve Sandusky Pile No. 520B

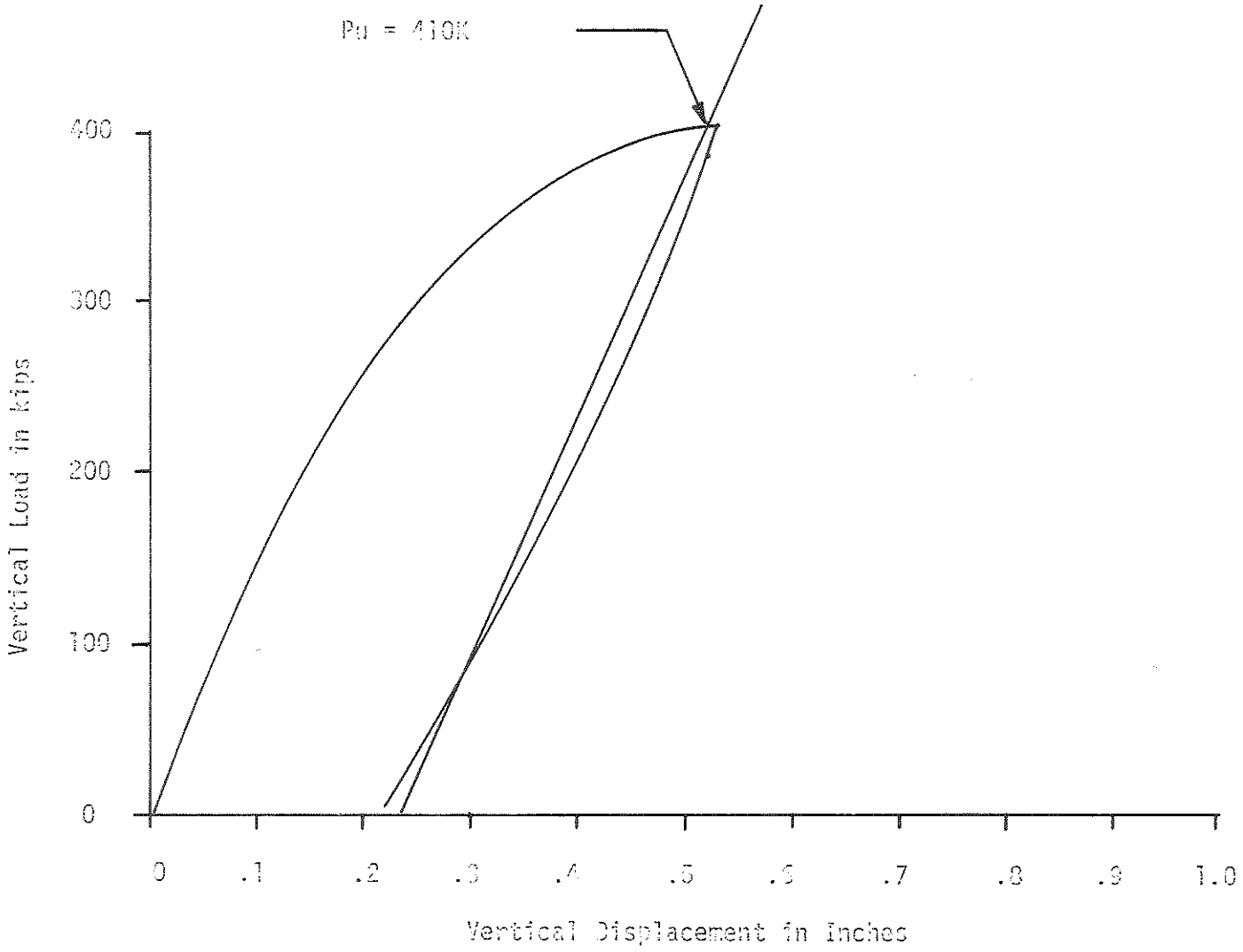

Figure A9: Static Load Test Curve Sandusky Pile No. L3520V-P

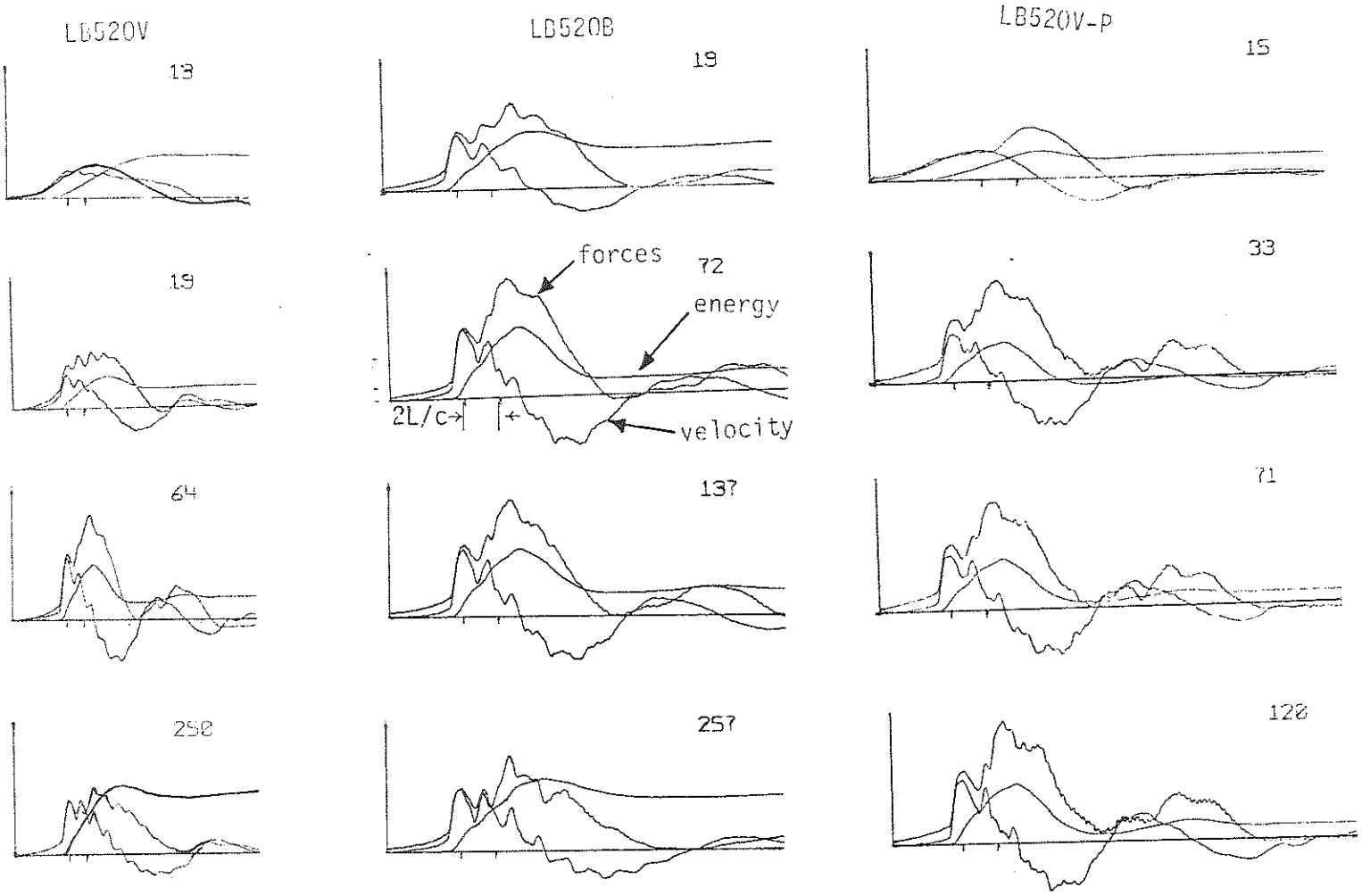

Figure A10: Sample records of force, energy and velocity plotted automatically by Case Method of Processing. Sandusky LB520V LB520B LB520V-P

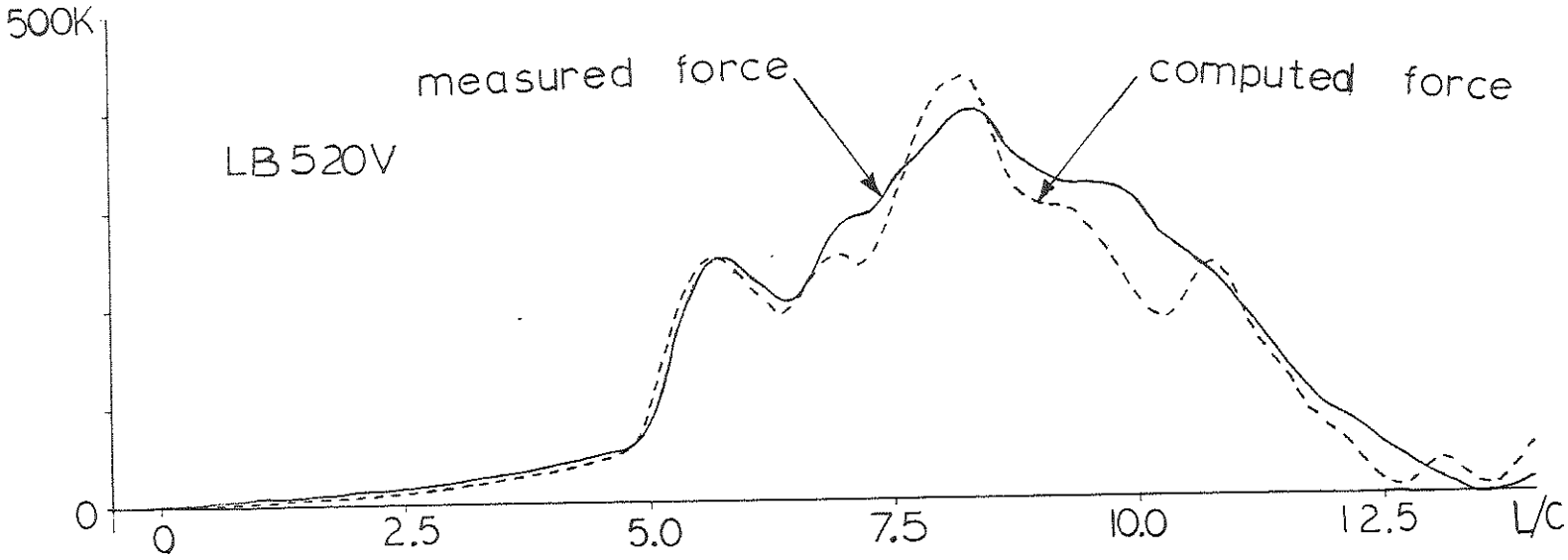

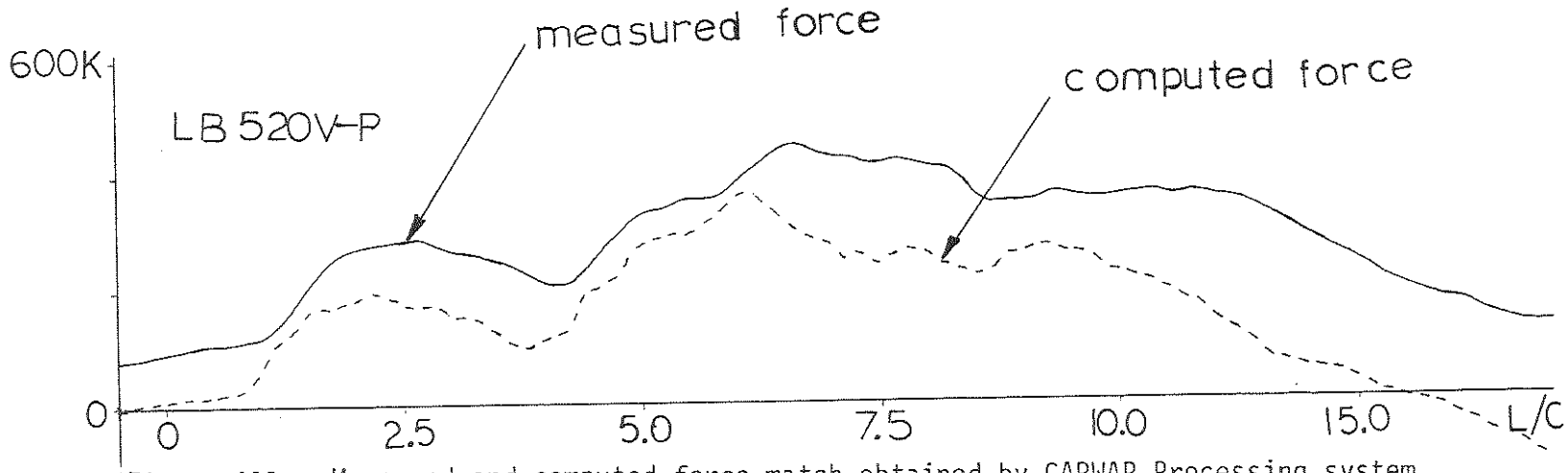

Figure A11: Measured and computed force match obtained by CAPWAP Processing system
Sandusky LB520V LB520V-P

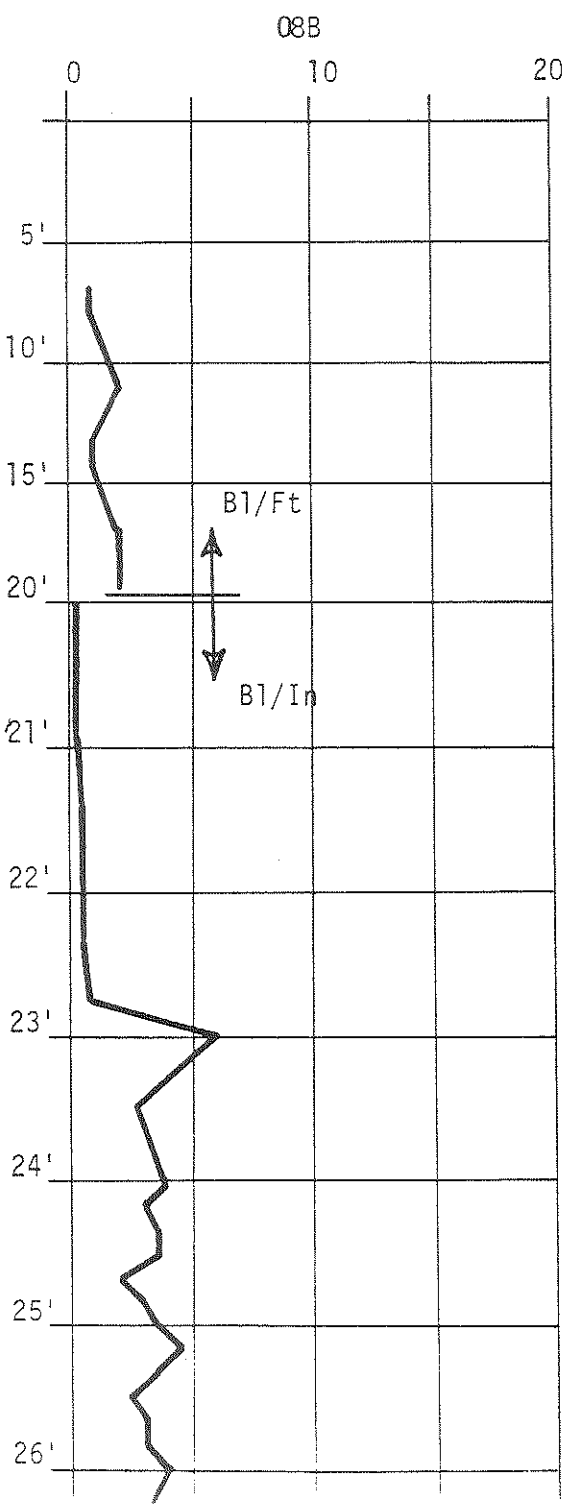

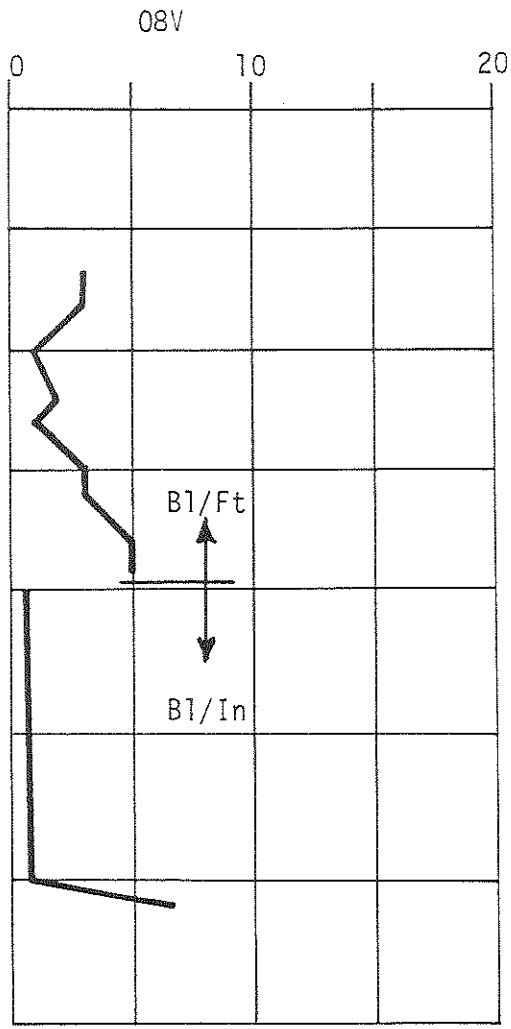

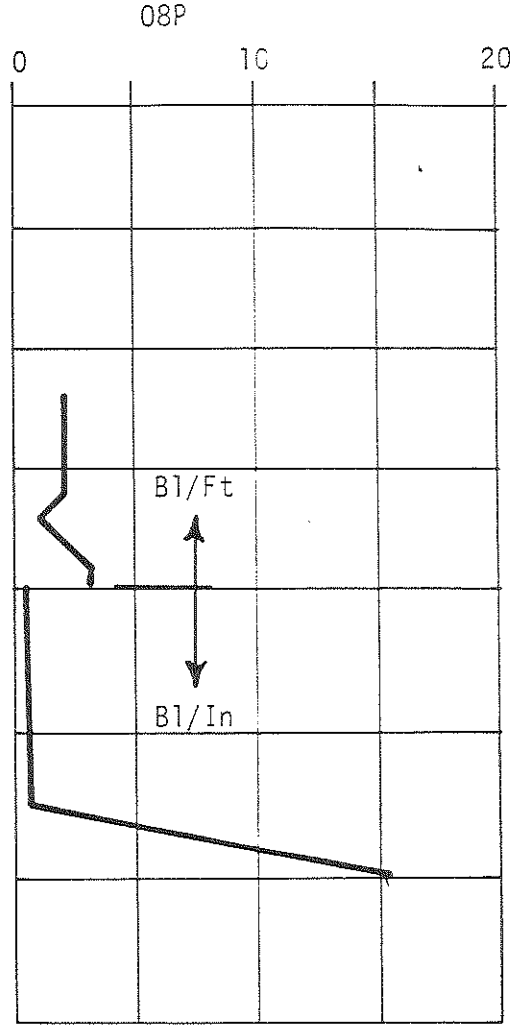

SANDUSKY

Figure A12: Blow Count Records for Piles Driven by the 08 Hammer at Sandusky

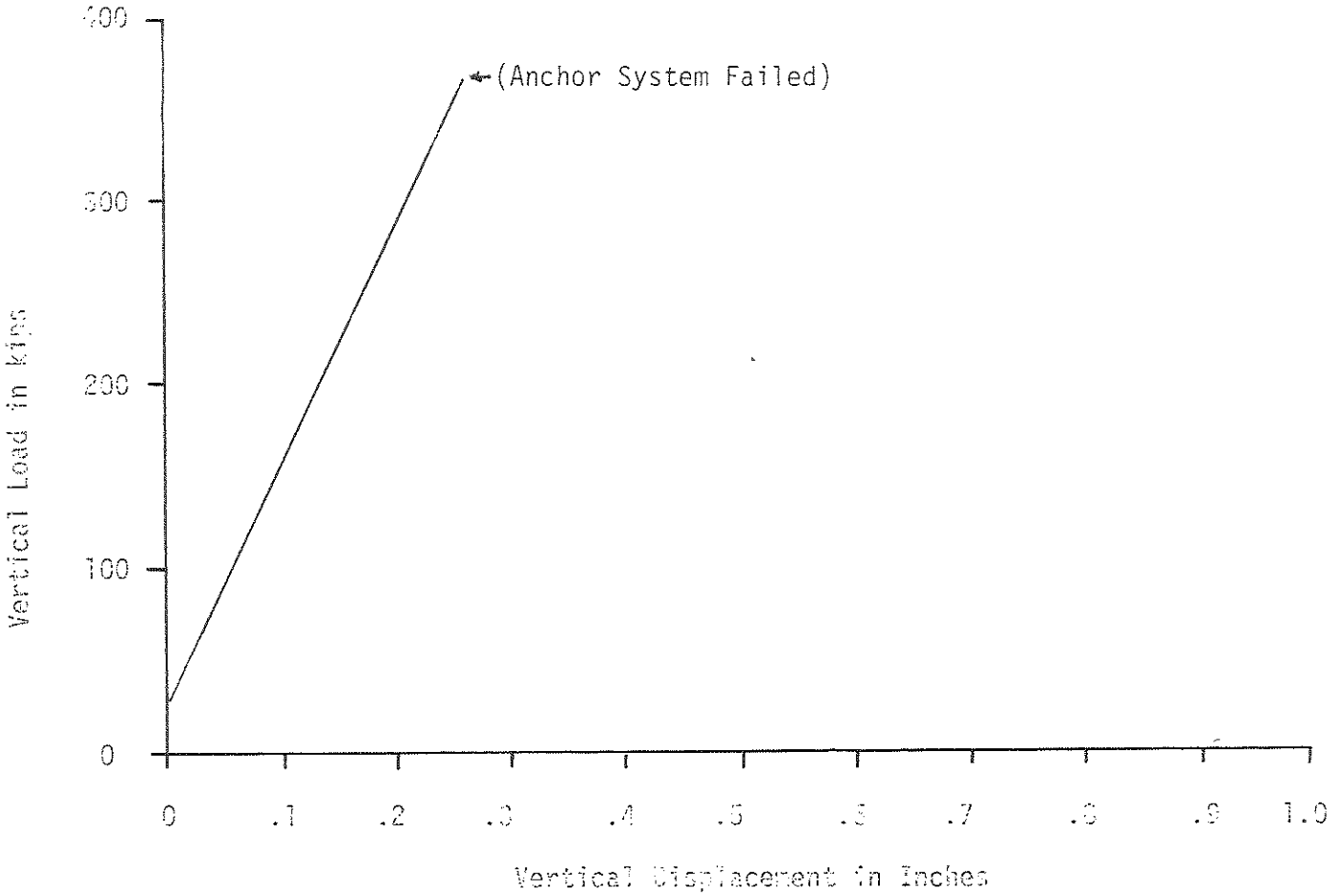

Figure A.13: Static Load Test Curve Sandusky Pile No. 03V

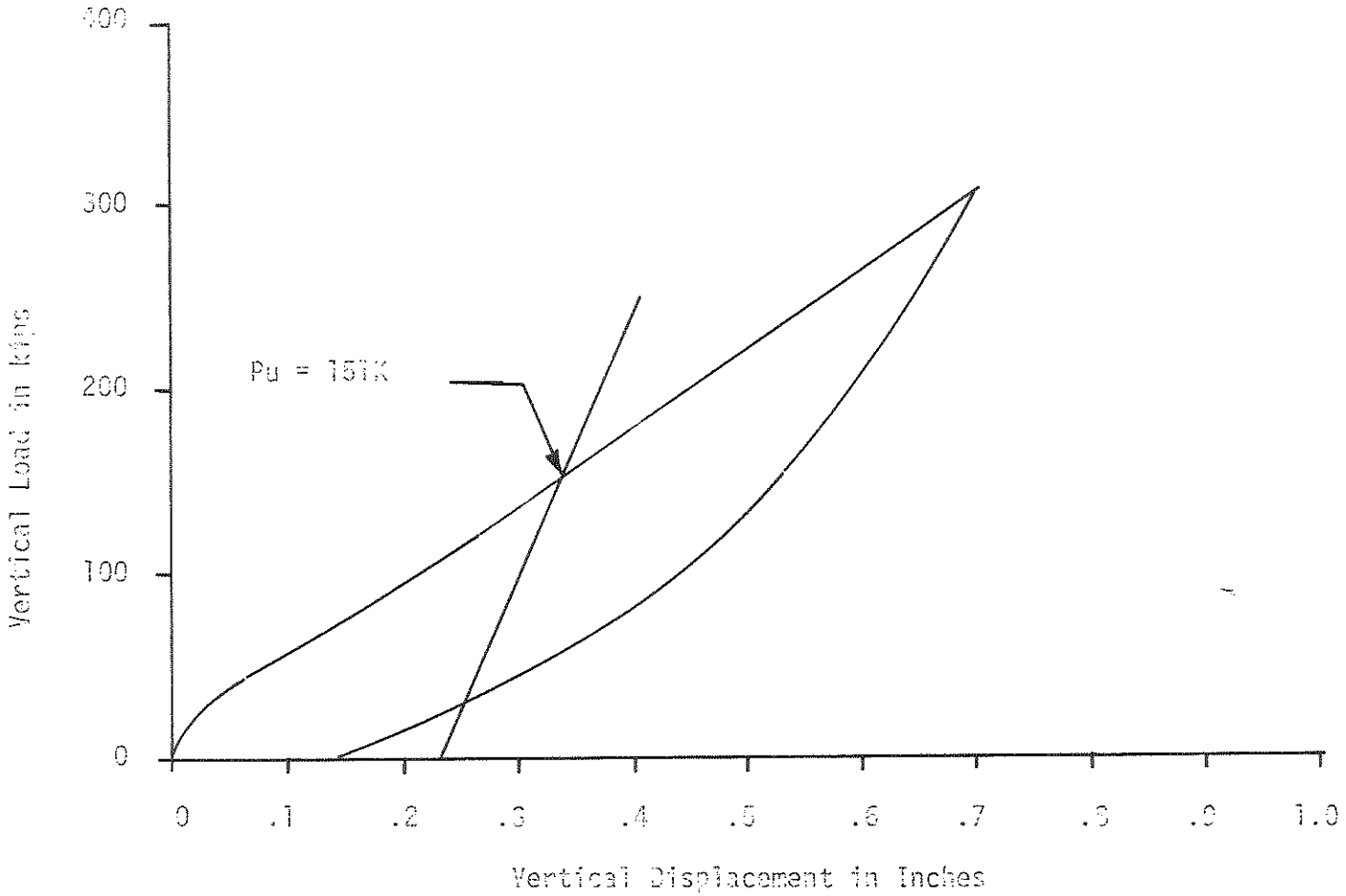

Figure A14. Static Load Test Curve Sandusky Pile No. 033

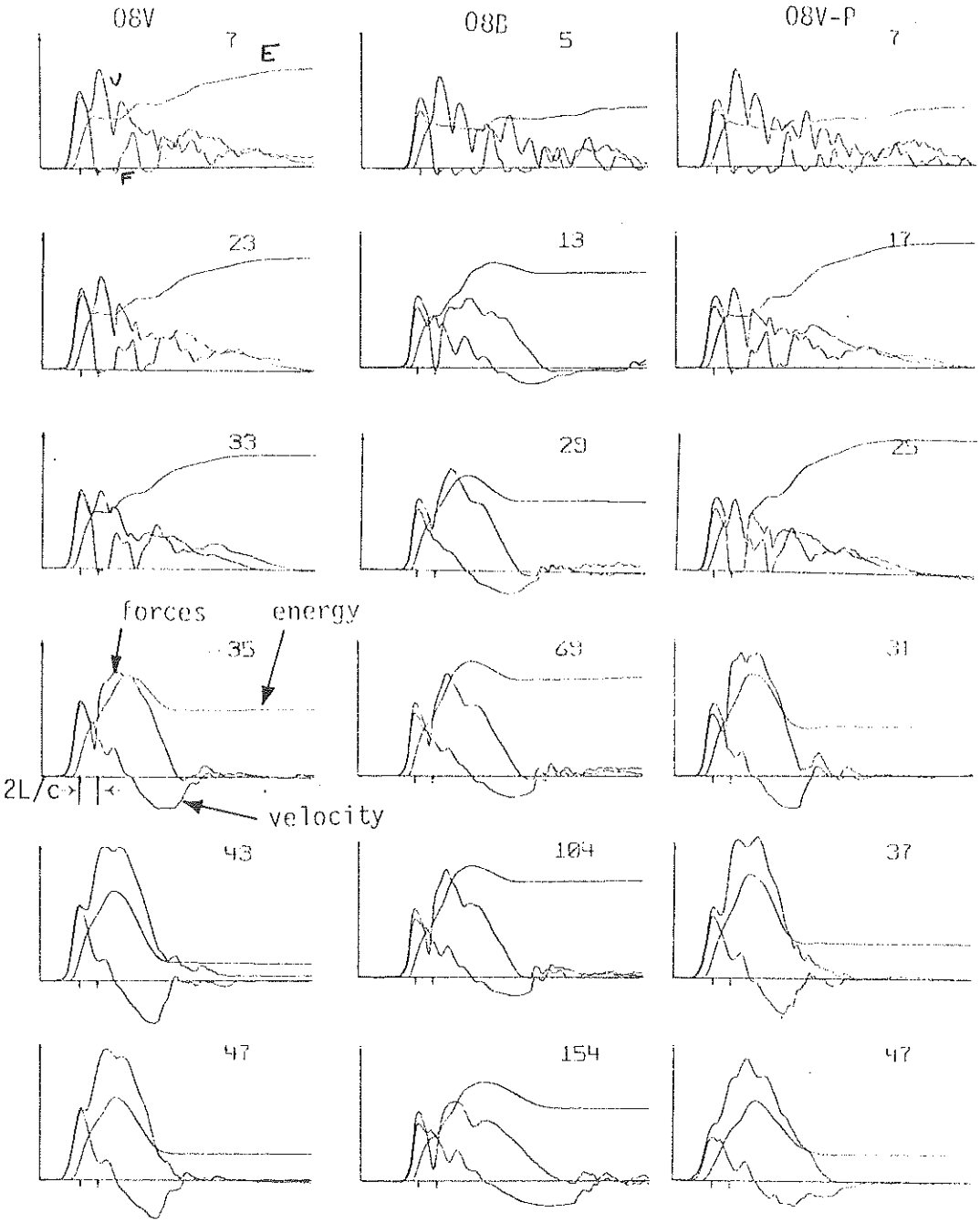

Figure A15: Sample records of force, energy and velocity plotted by Case Method of Processing. Sandusky 08V 08D 08V-P

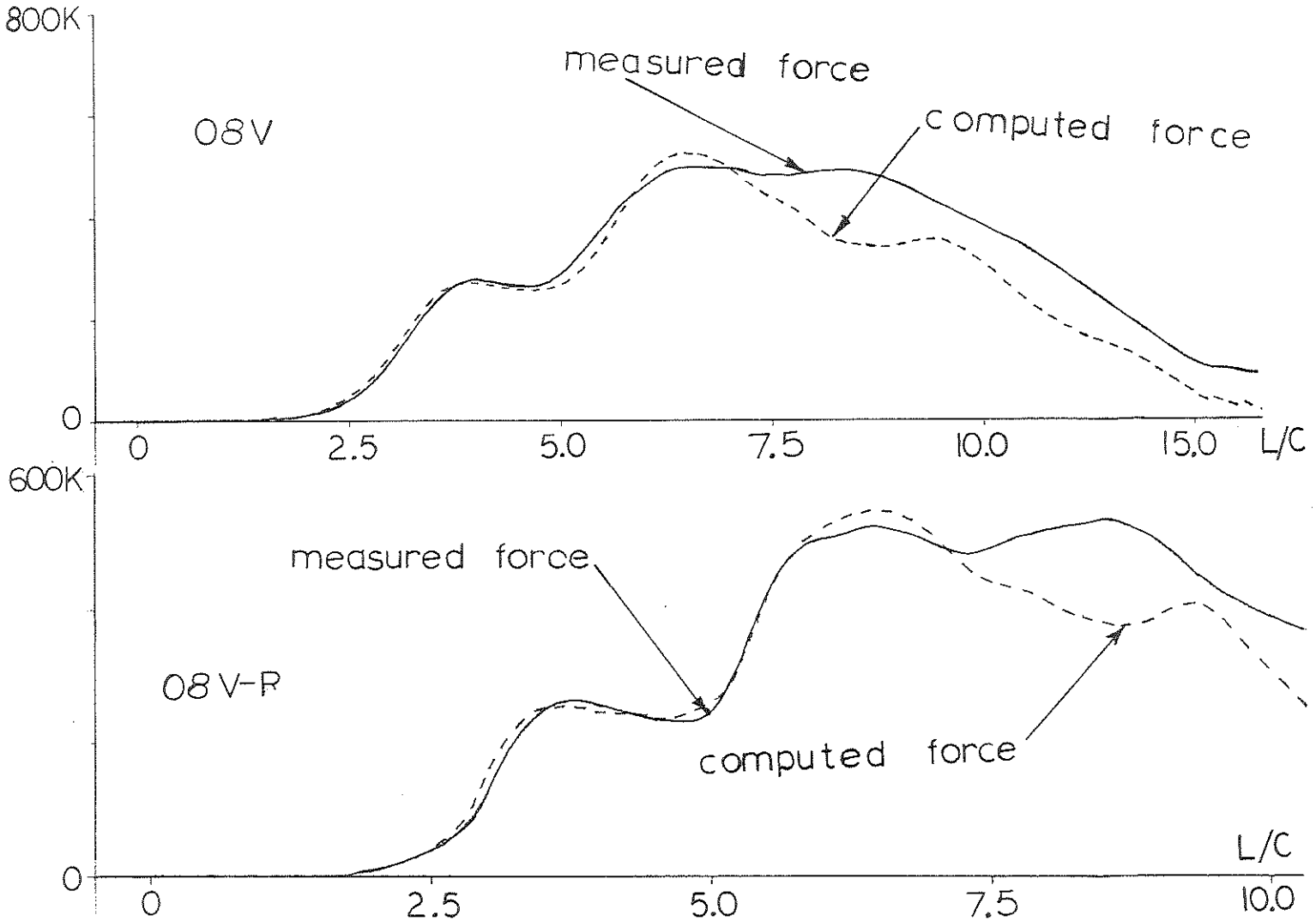

Figure A16 : Measured and computed force match obtained by CAPWAP Processing system
Sandusky 08V 08V-P

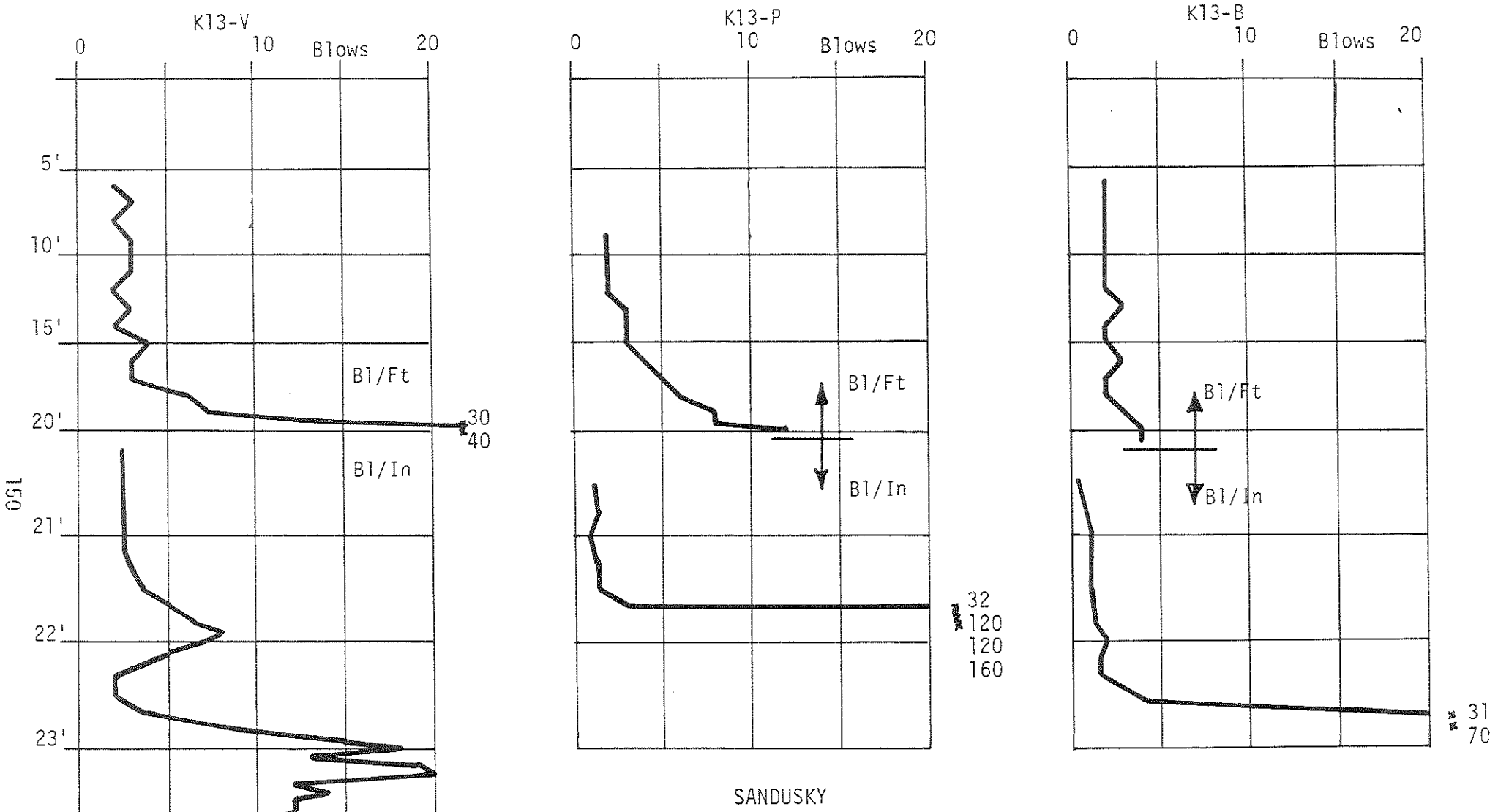

Figure A17: Blow Count Records for Piles Driven by the K13 Hammer at Sandusky

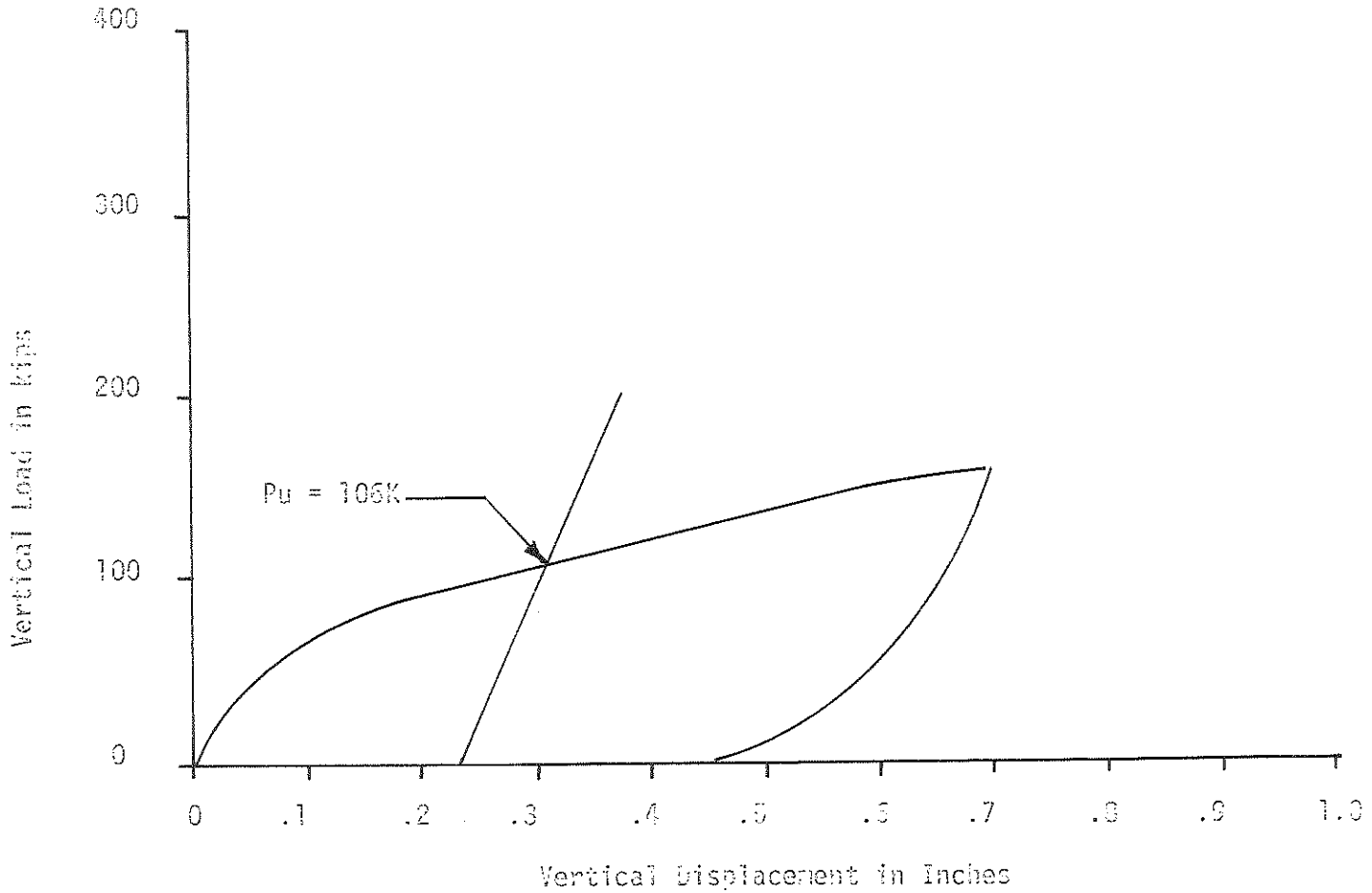

Figure A18: Static Load Test Curve Sandusky Pile No. KTCV

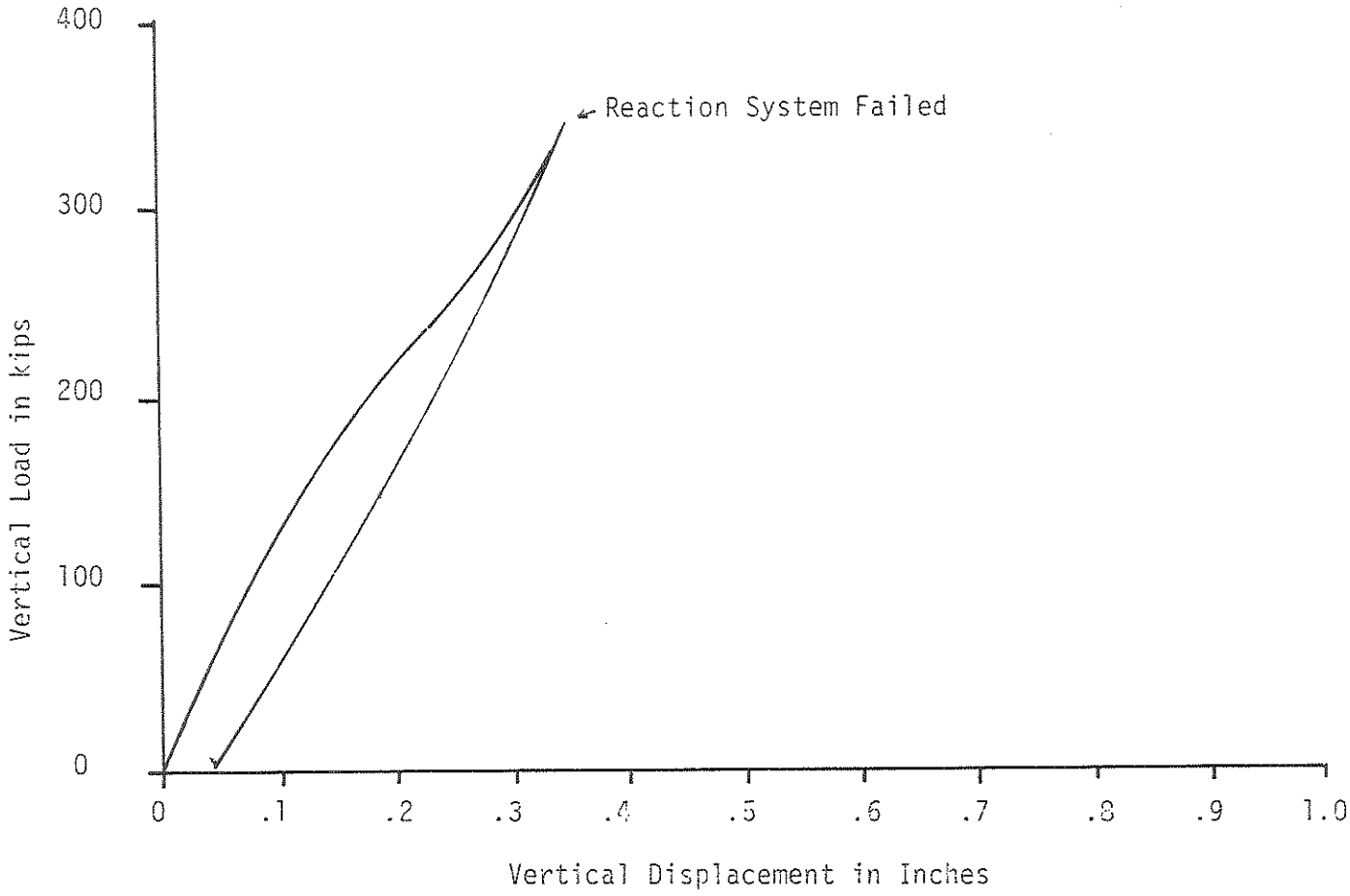

Figure A19: Static Load Test Curve Sandusky Pile No. K13B

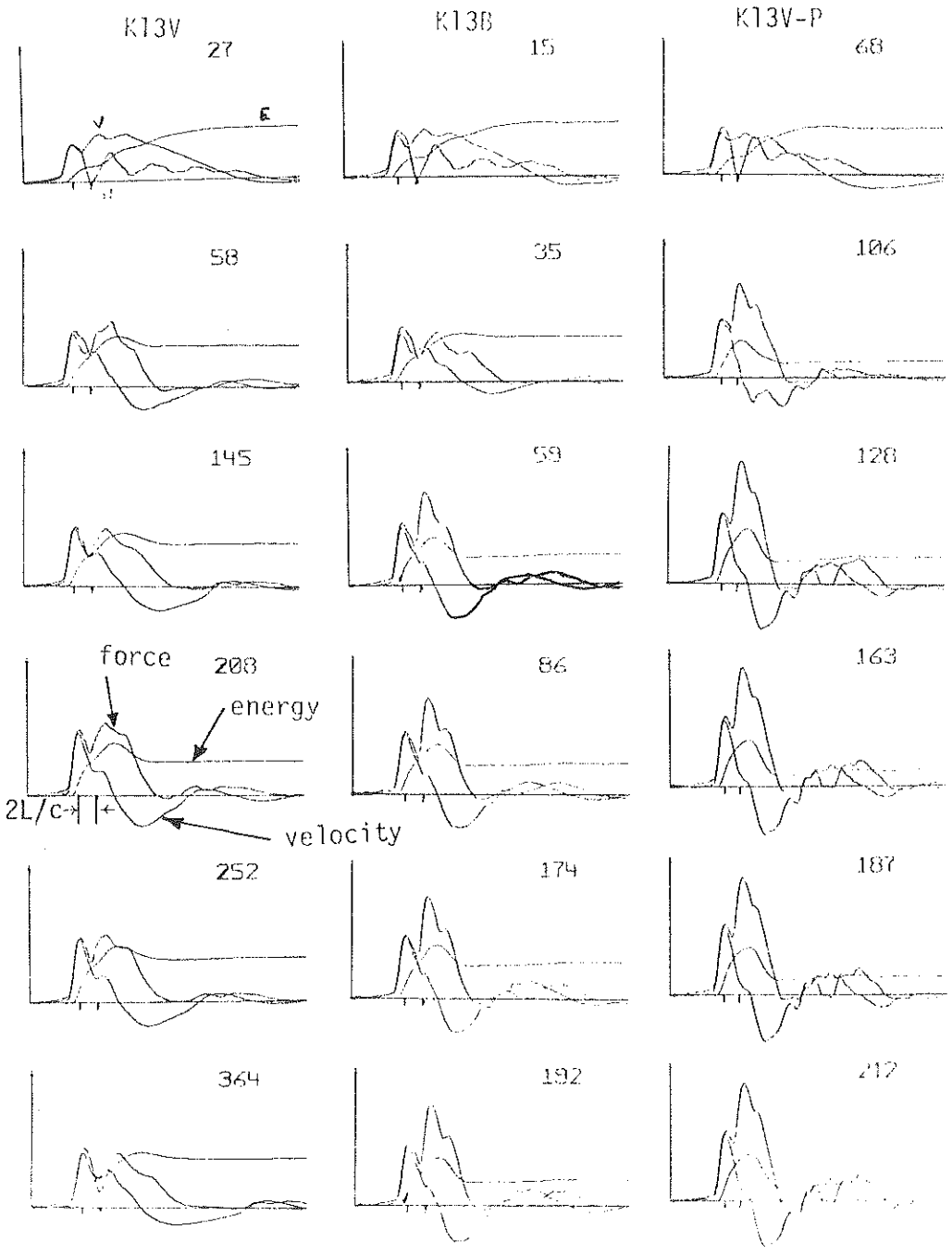

Figure A20 : Sample records of force, energy and velocity plotted by Case Method of Processing. Sandusky K13V K13B K13V-P

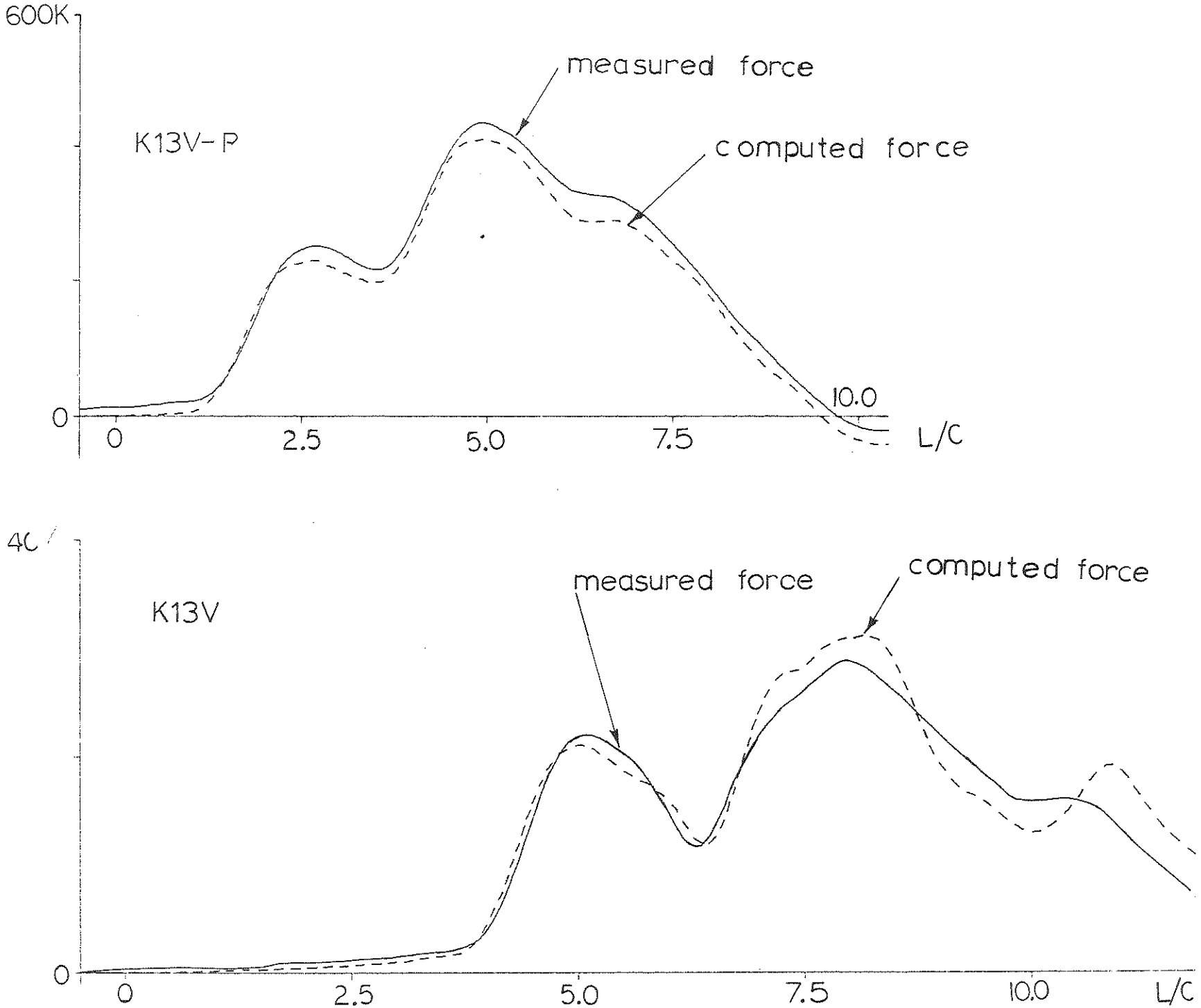

Figure A21: Measured and computed force match obtained by CAPWAP Processing system

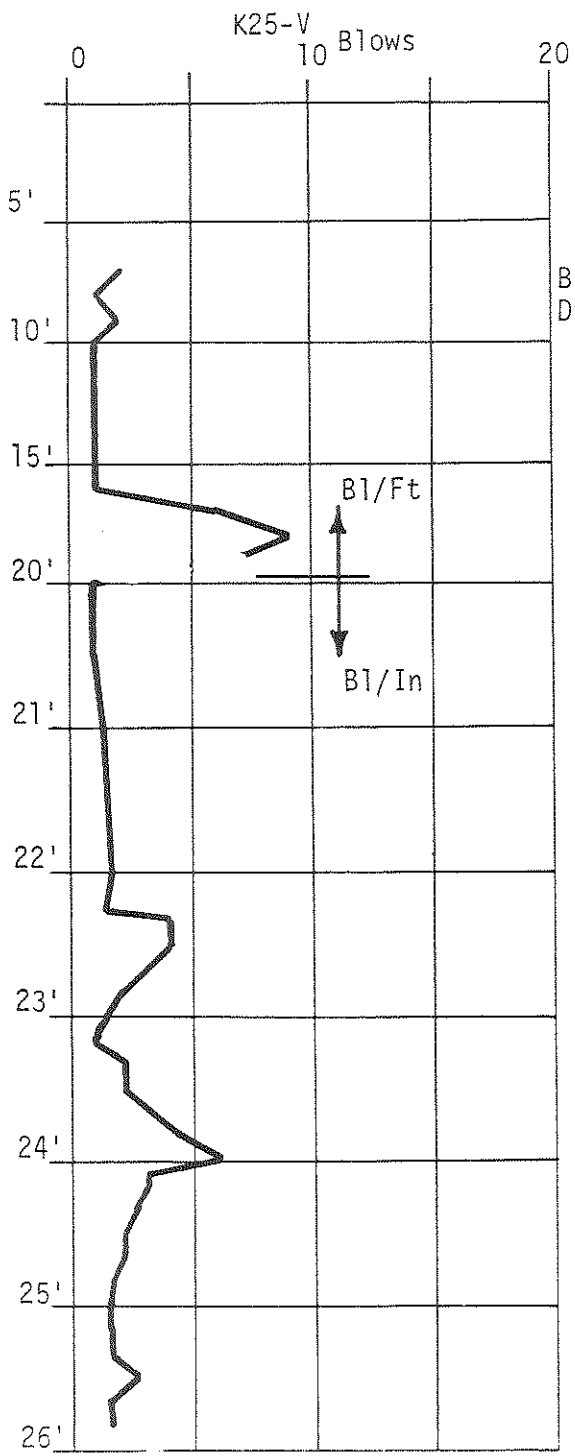

Figure A22:
Blow Count Records for Piles Driven by the K25 Hammer at Sandusky

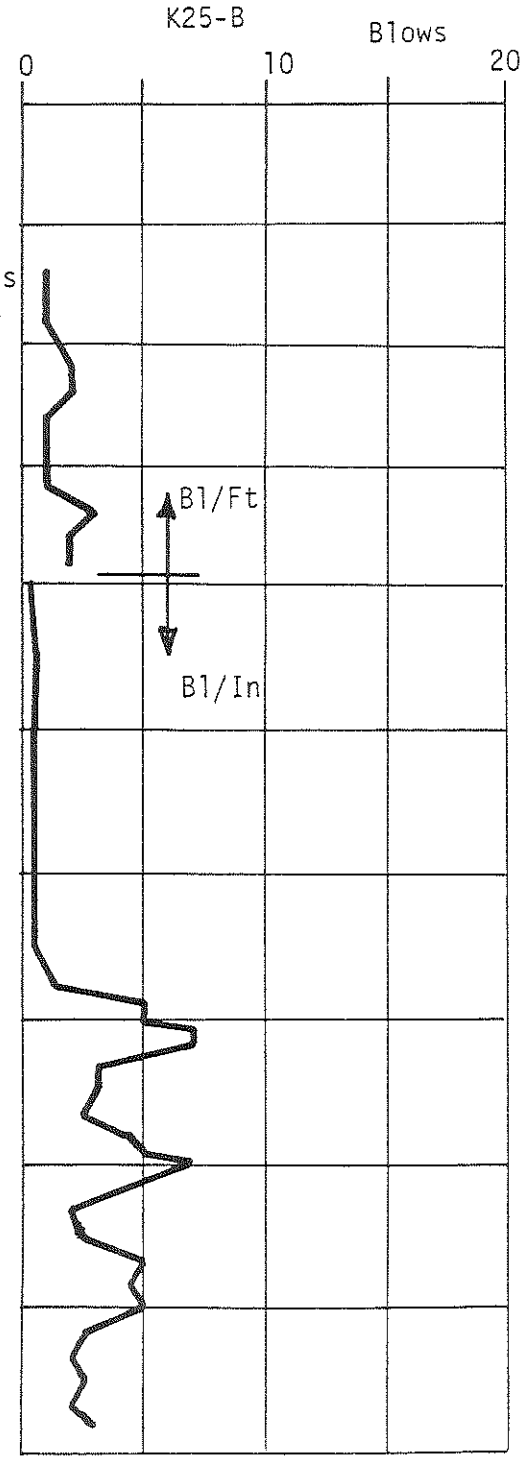

SANDUSKY

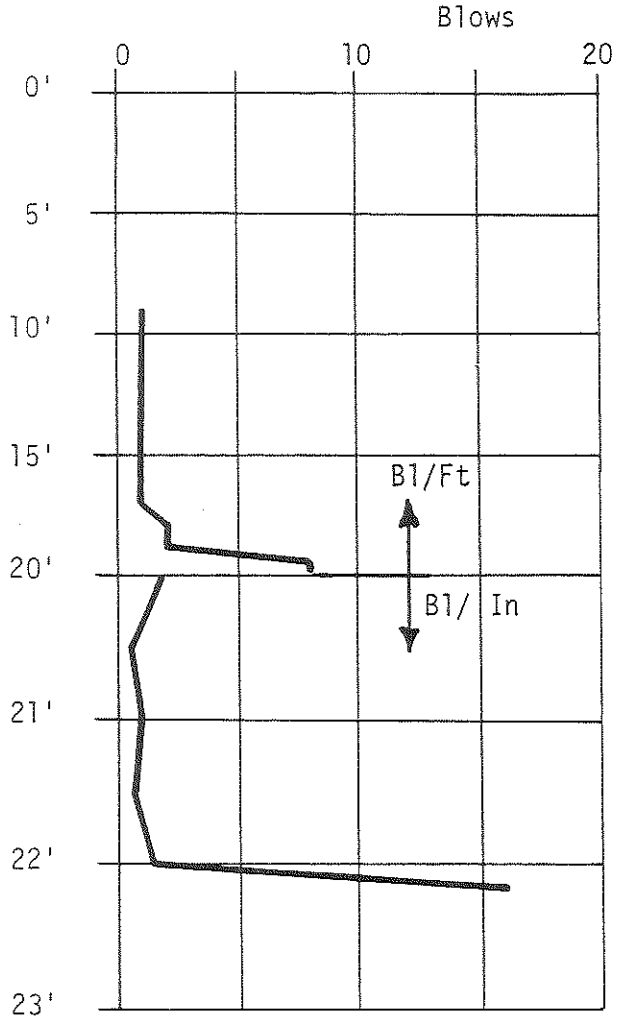

K25P

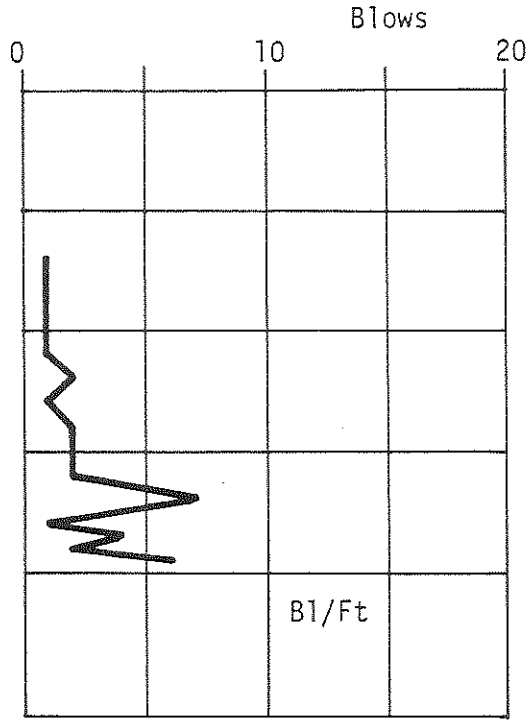

K25V-E

SANDUSKY

Figure A23: Blow Count Records for Piles Driven by the K 25 Hammer at Sandusky

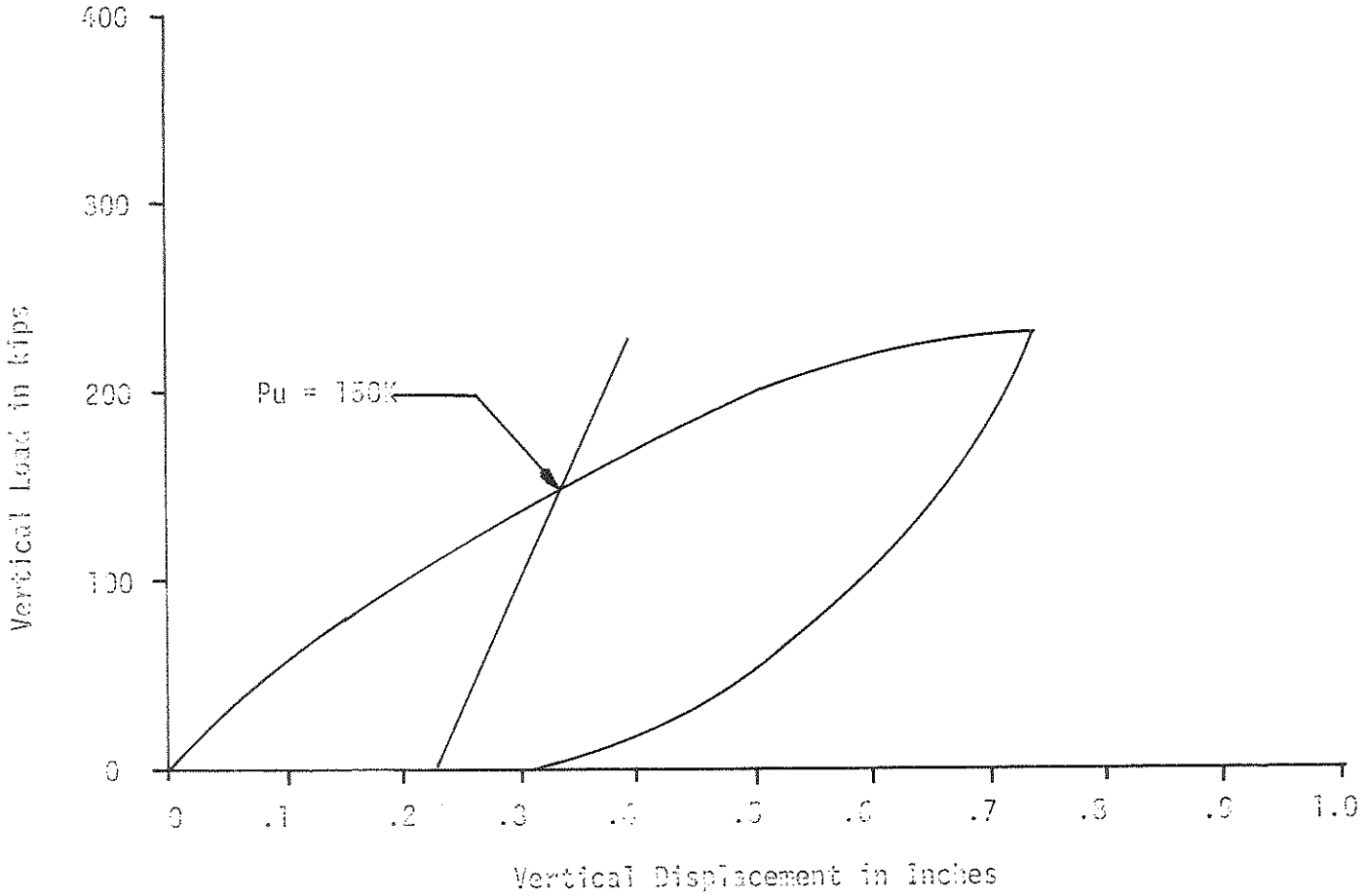

Figure A24: Static Load Test Curve Sandusky Pile No. K25V

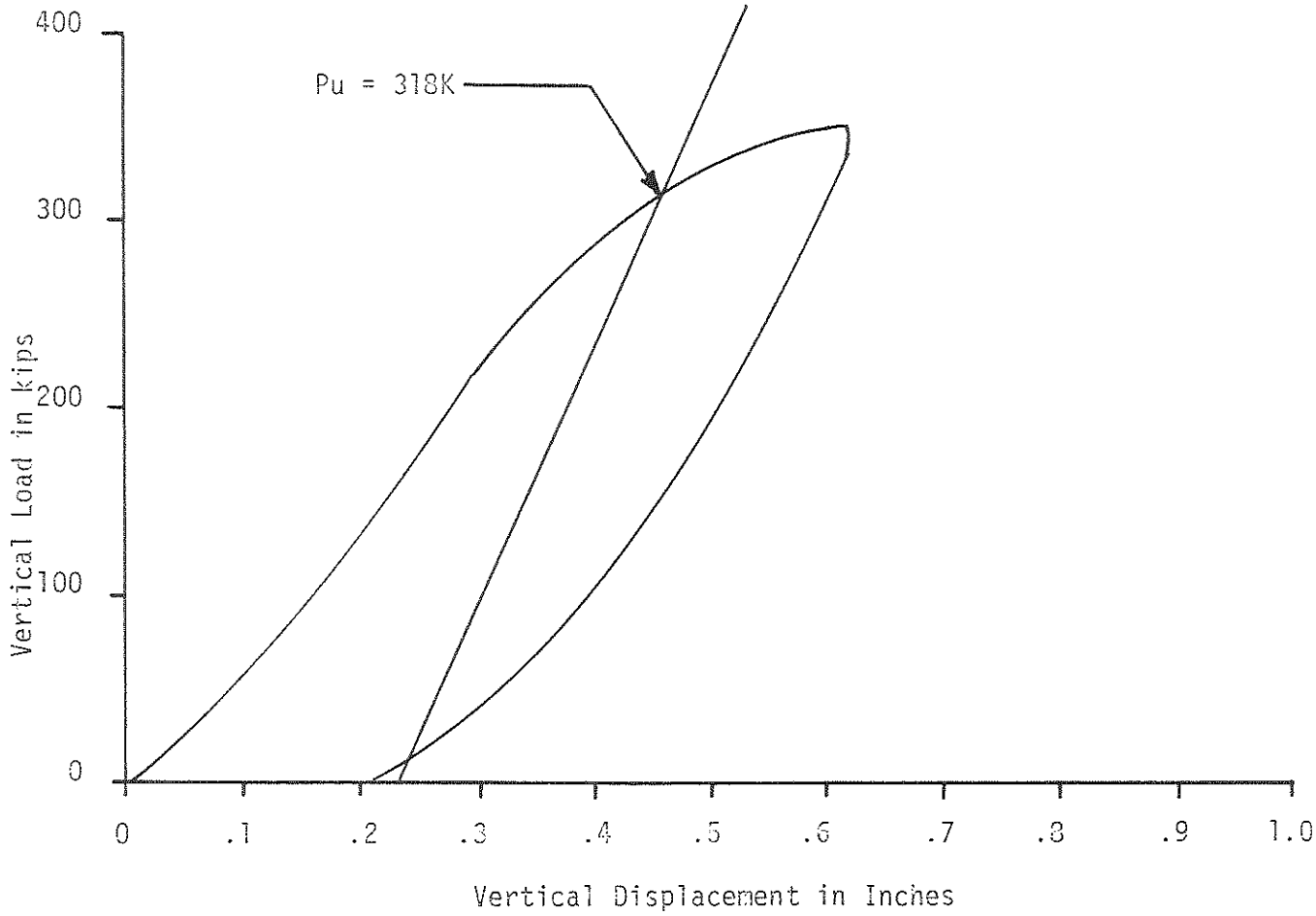

Figure A25: Static Load Test Curve Sandusky Pile No. K25B

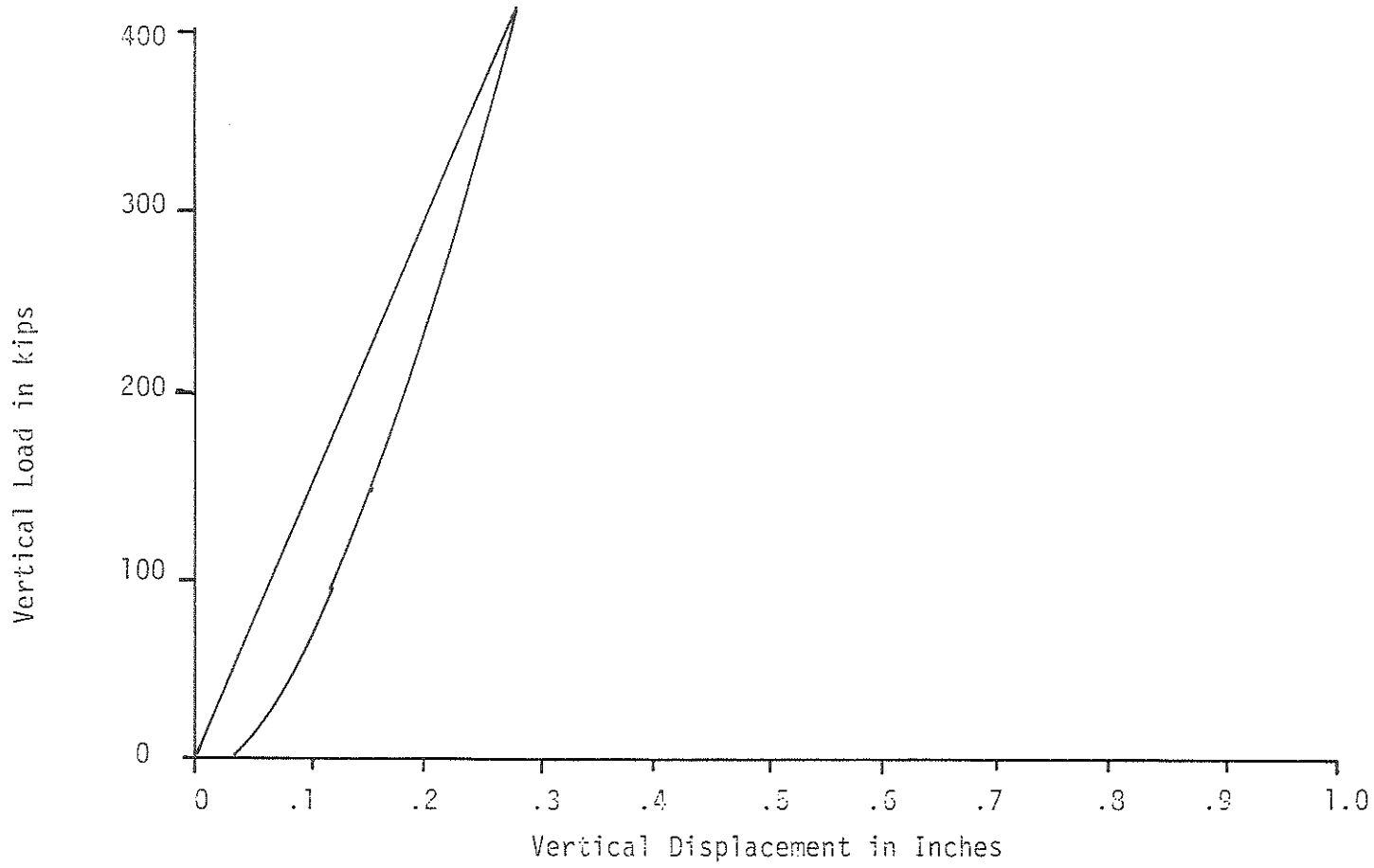

Figure A26: Static Load Test Curve Sandusky Pile No. K25V-E

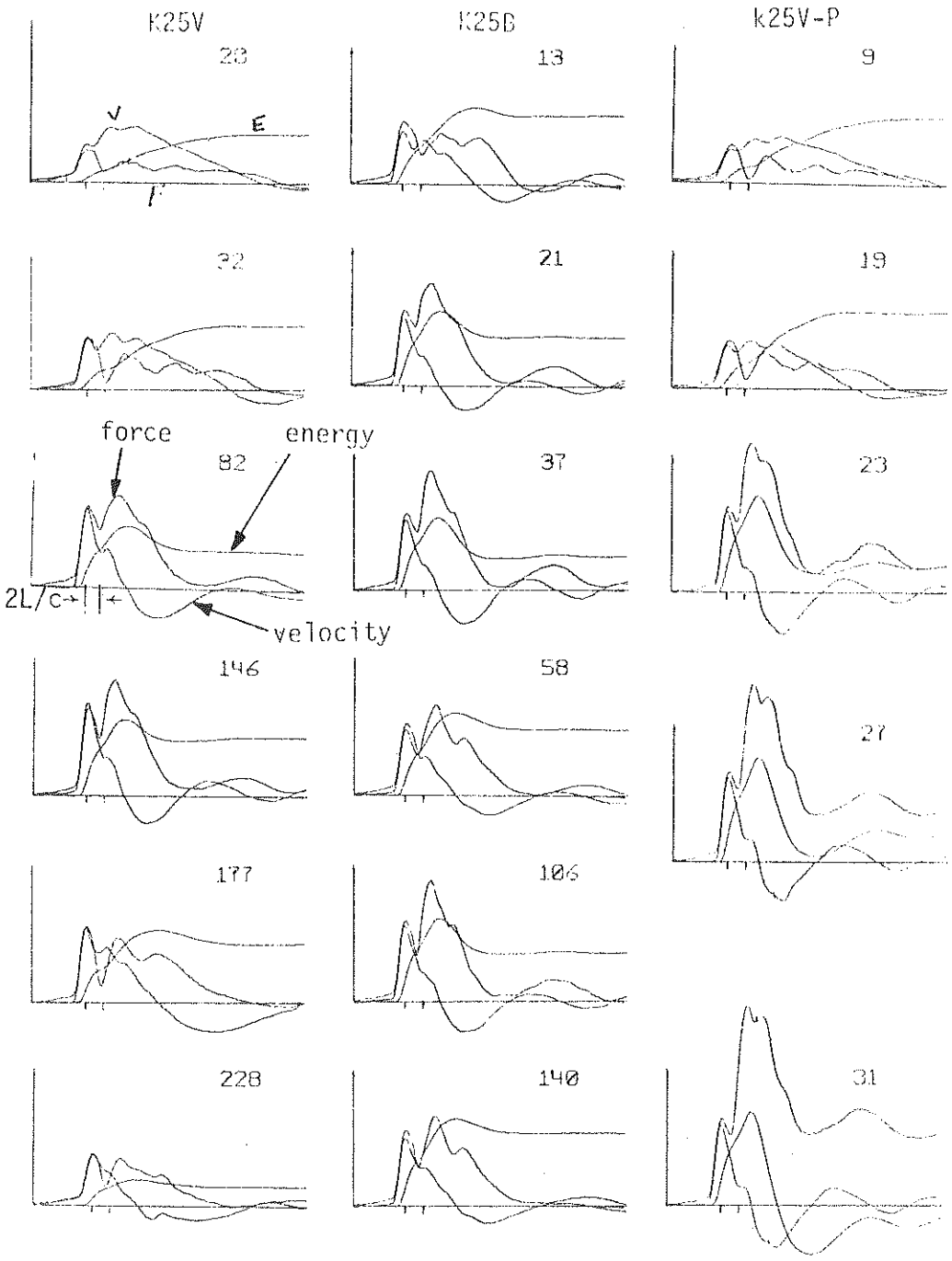

Figure A27: Sample records of force, energy and velocity plotted by Case Method of Processing. Sandusky K25V K25B k25V-P

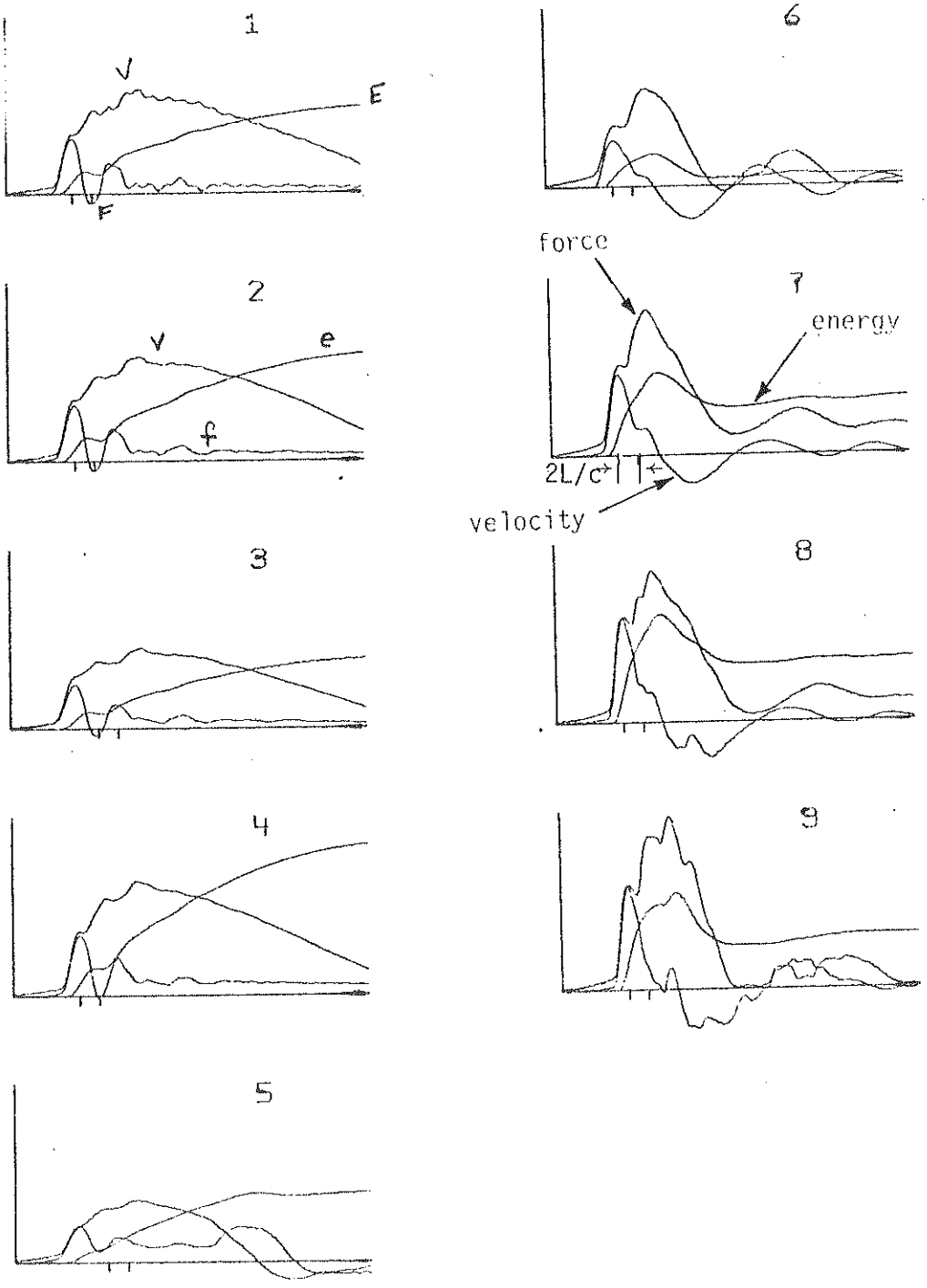

Figure A28 : Sample records of force, energy and velocity plotted by Case Method of Processing. Sandusky V25V-E

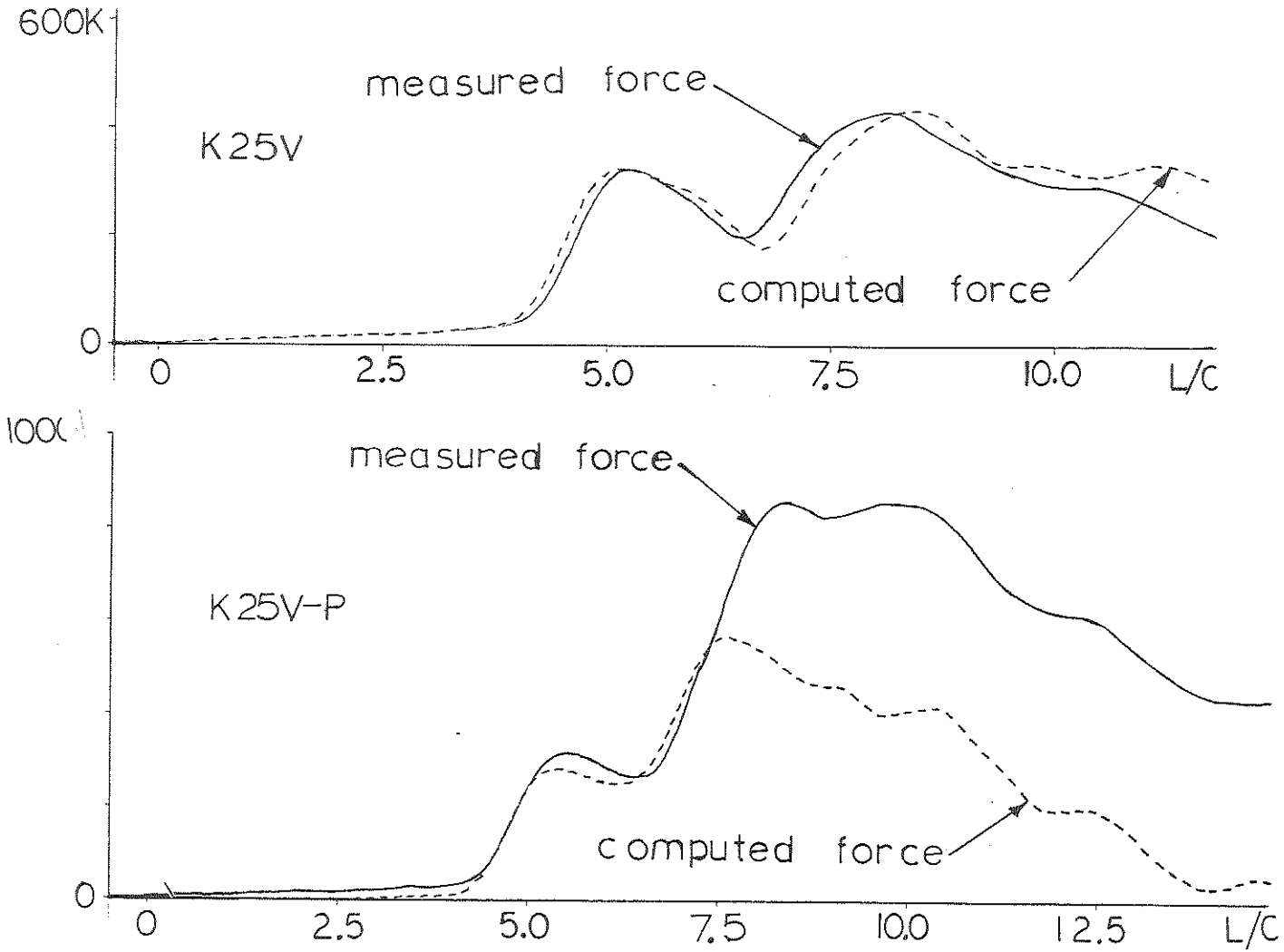

Figure A29: Measured and computed force match obtained by CAPWAP Processing system
Sandusky K25V k25V-P

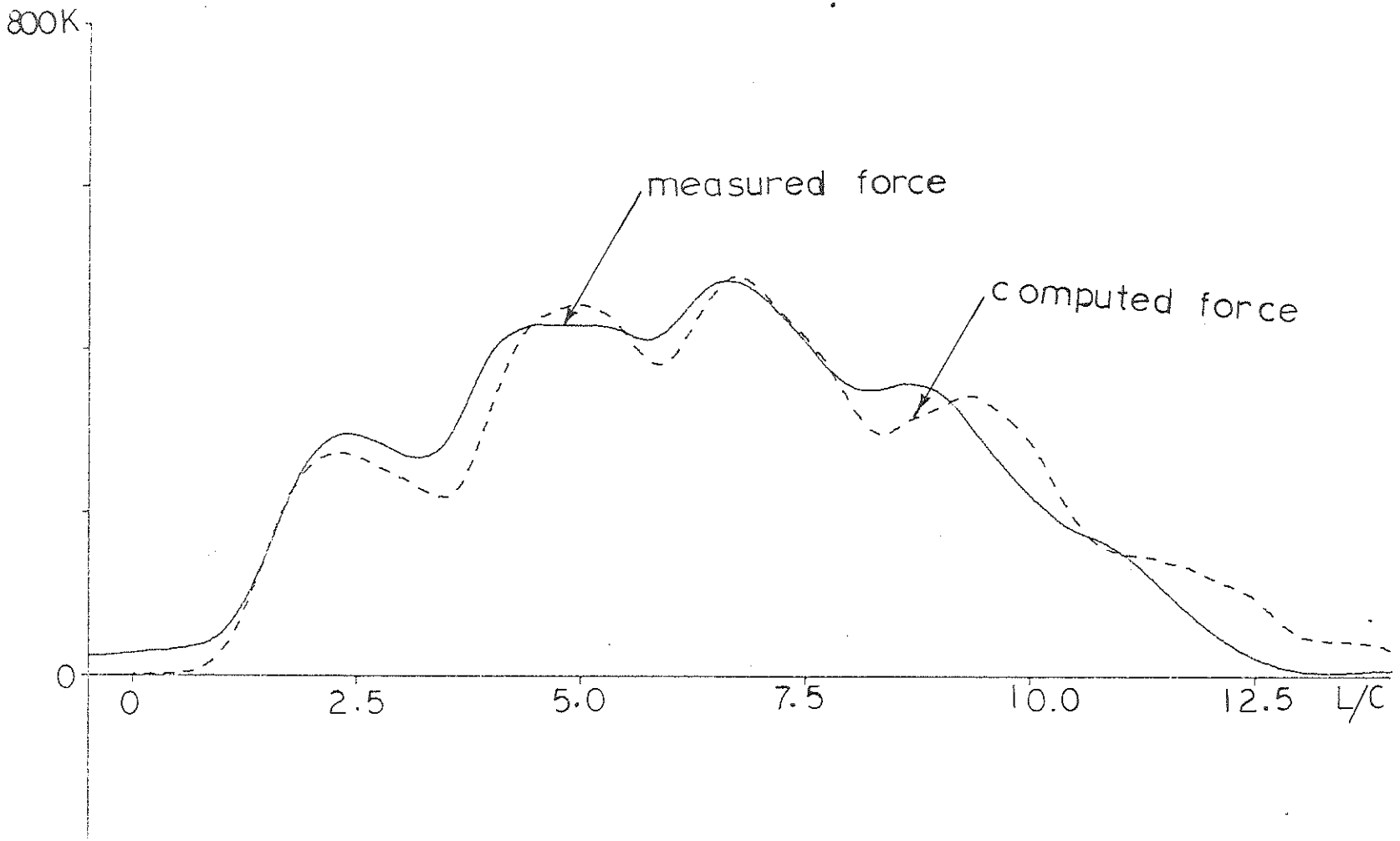

Figure A30: Measured and computed force match obtained by CAPWAP Processing system
Sandusky K25V-E

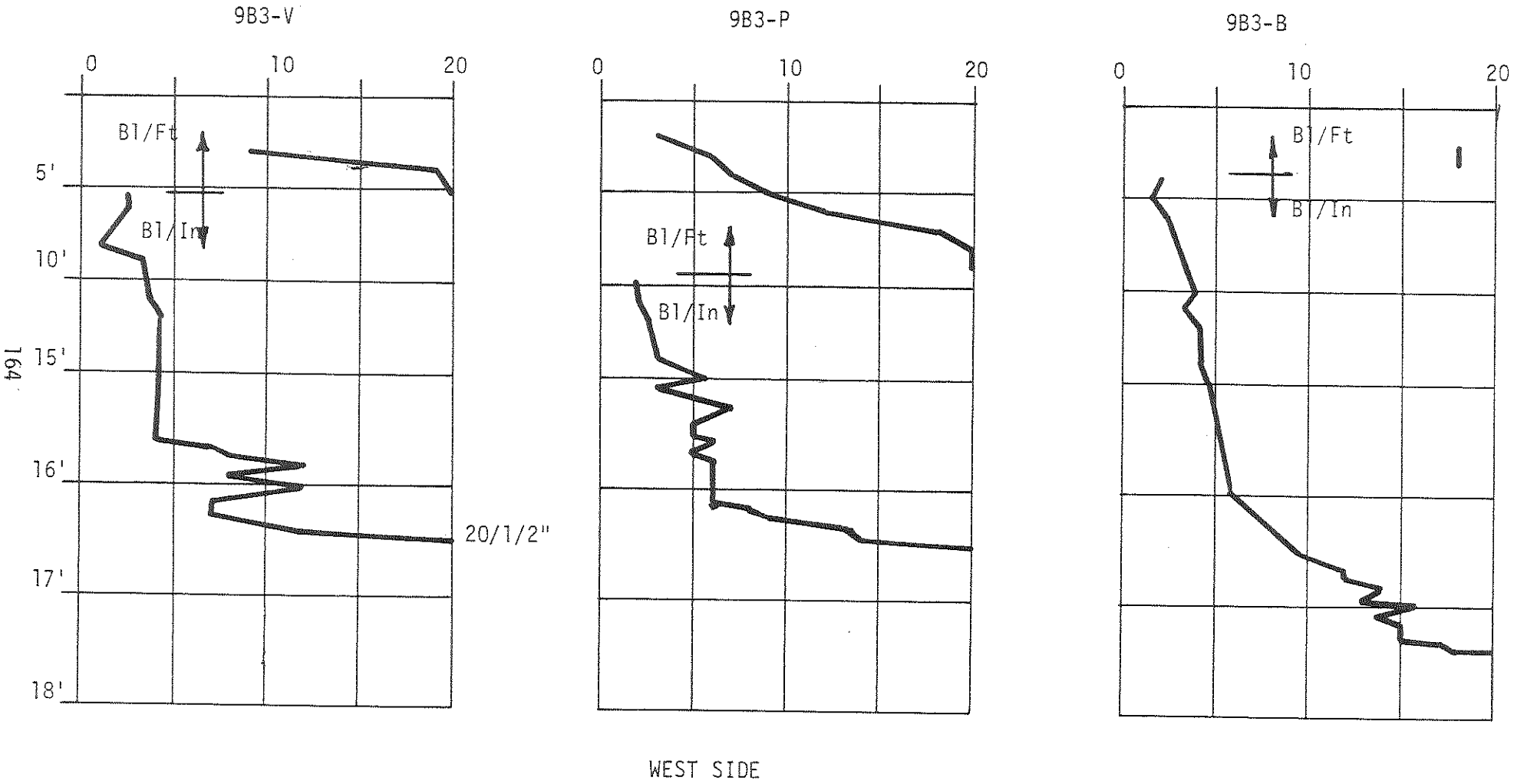

Figure A31: Blow Count Records for Piles Driven by the 9B3 Hammer at W92

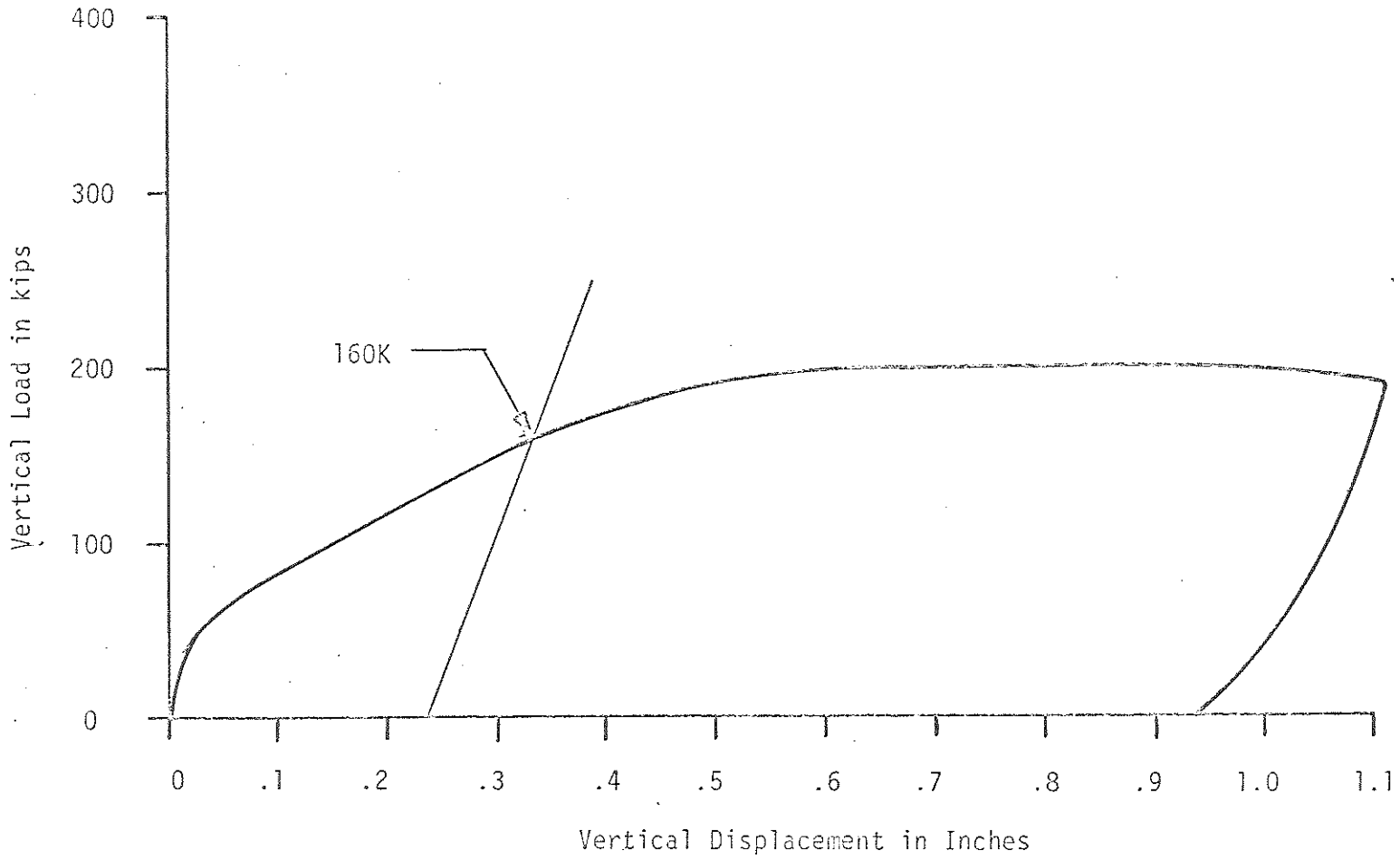

Figure A32: Static Load Test Curve W92 Pile No. 9B3-V

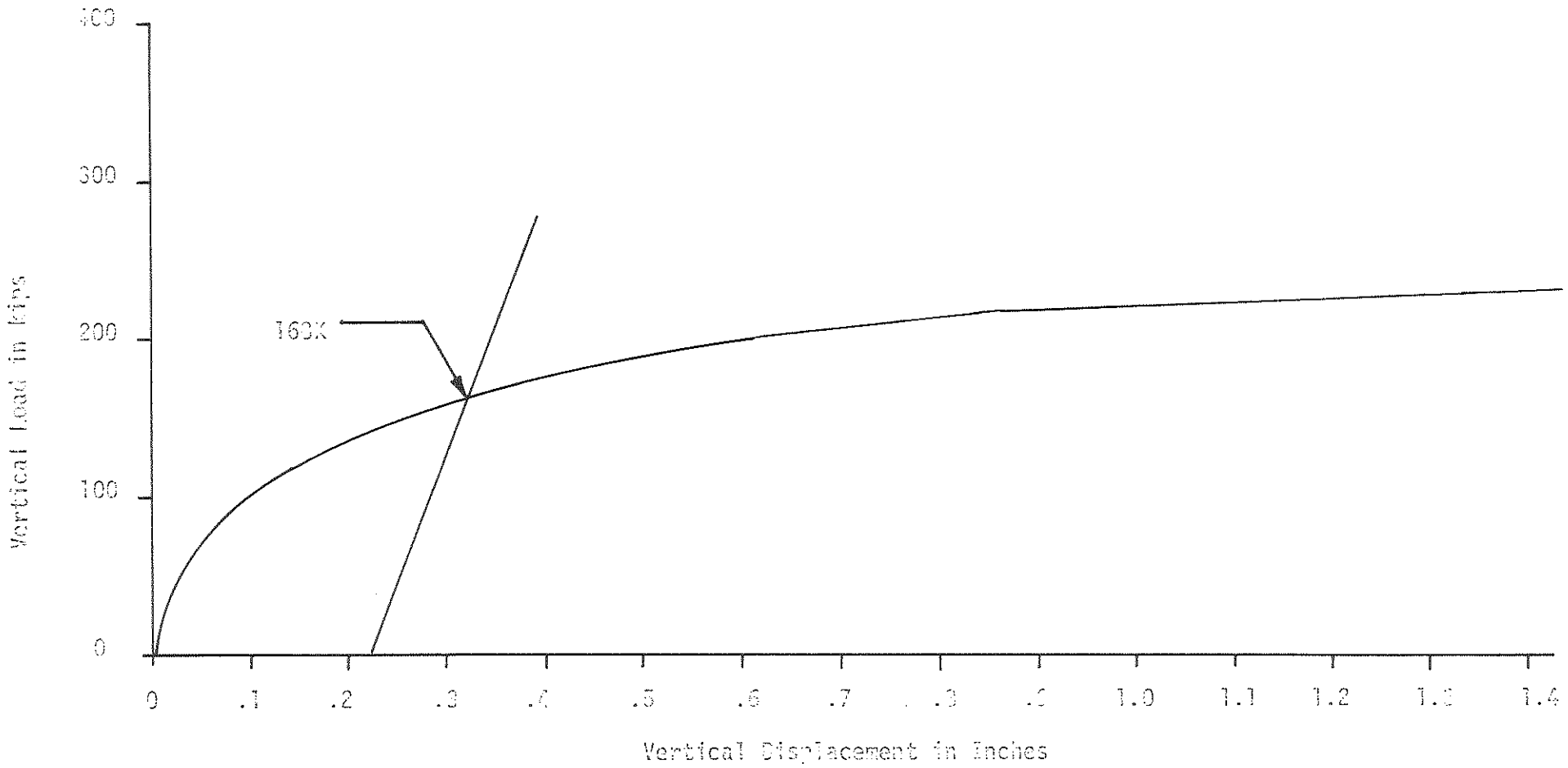

Figure A33: Static Load Test Curve [illegible] Pile No. 9B3-P

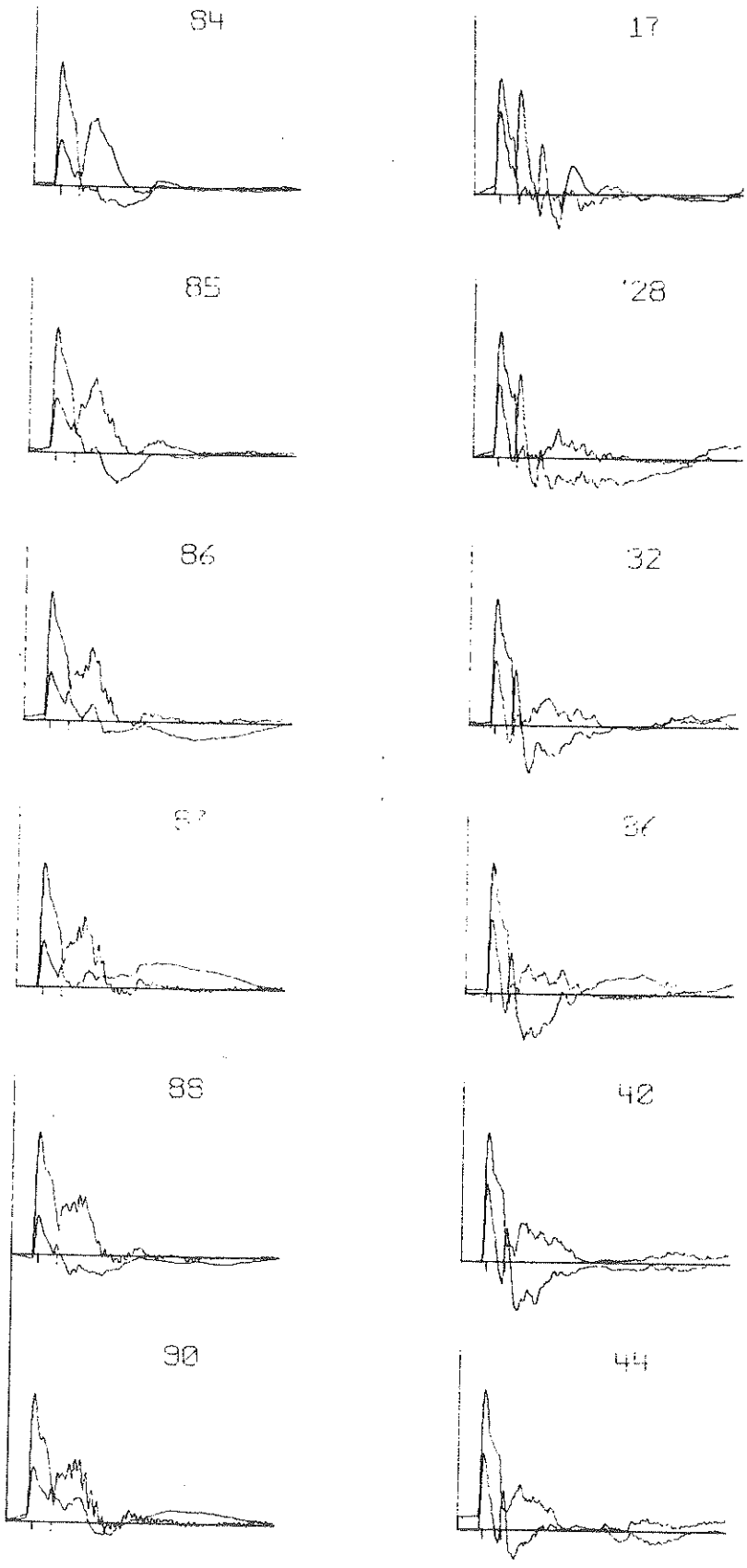

Sample records of force and velocity plotted by Case Method of Processing for W92

Figure A34

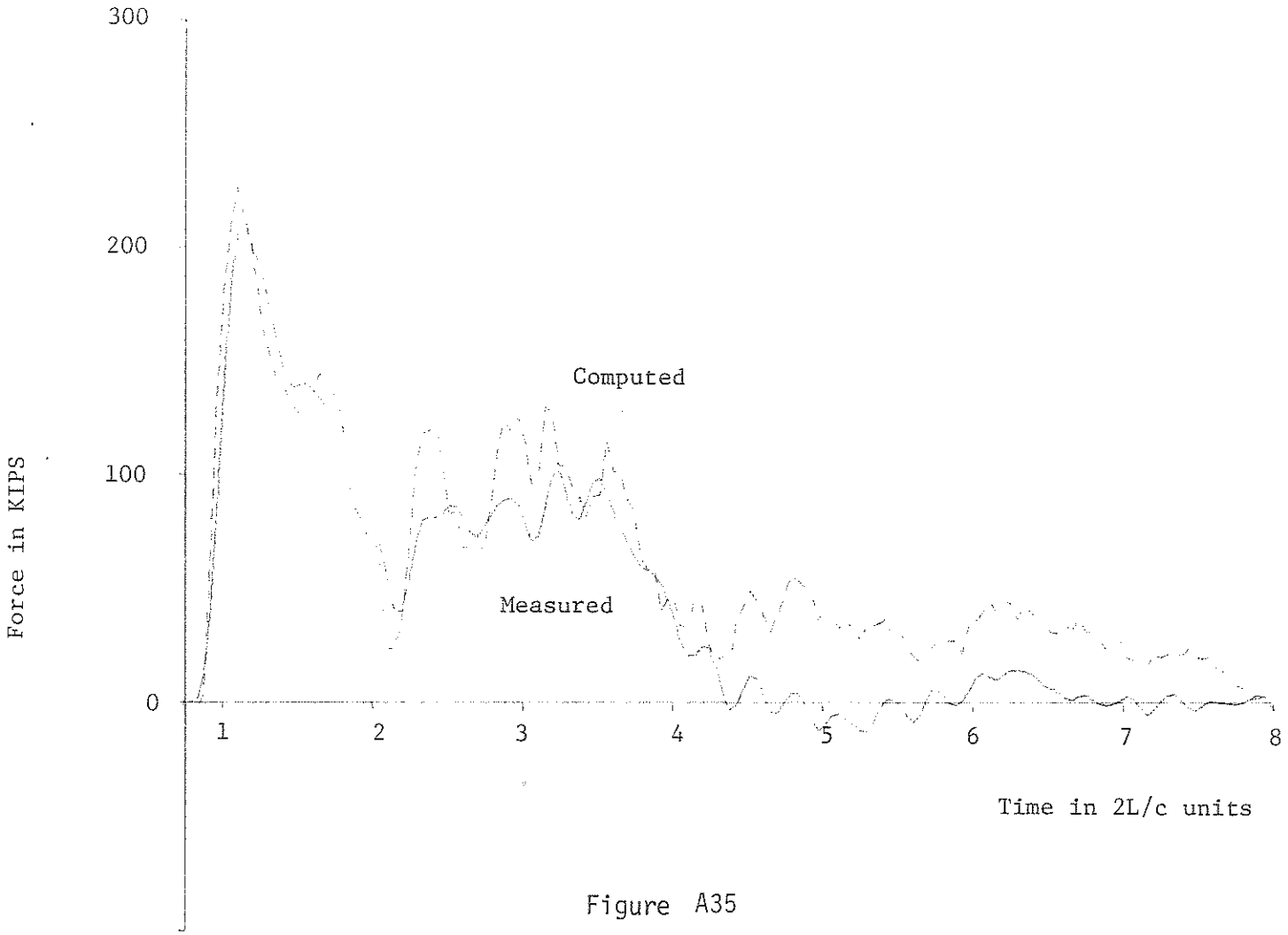

Figure A35

Computed and measured force curves from CAPWAP for 9B3V at W92

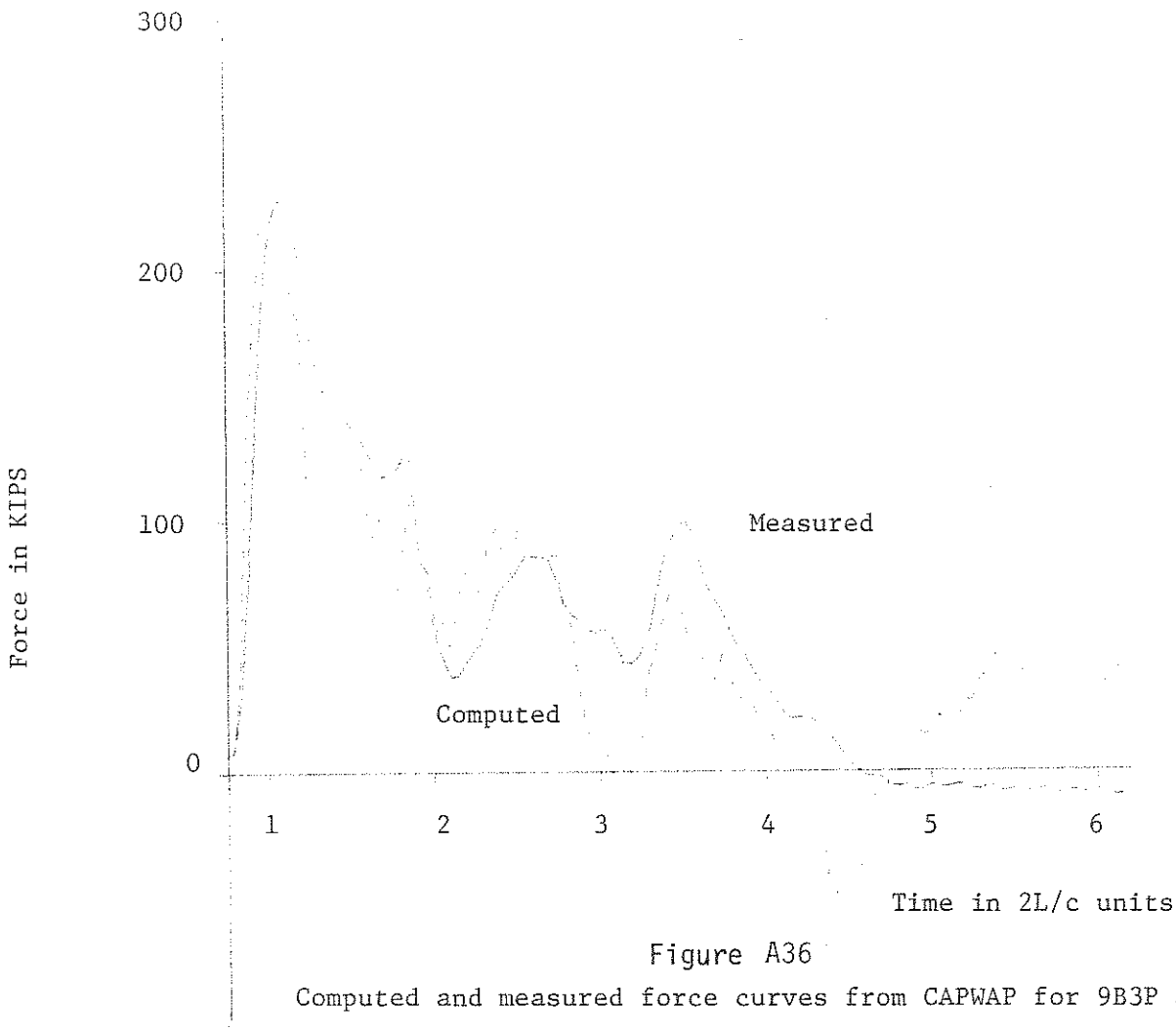

Figure A36

Computed and measured force curves from CAPWAP for 9B3P at W 92

Figure A37: Blow Count Records for Piles Driven by the D5 Hammer at W92

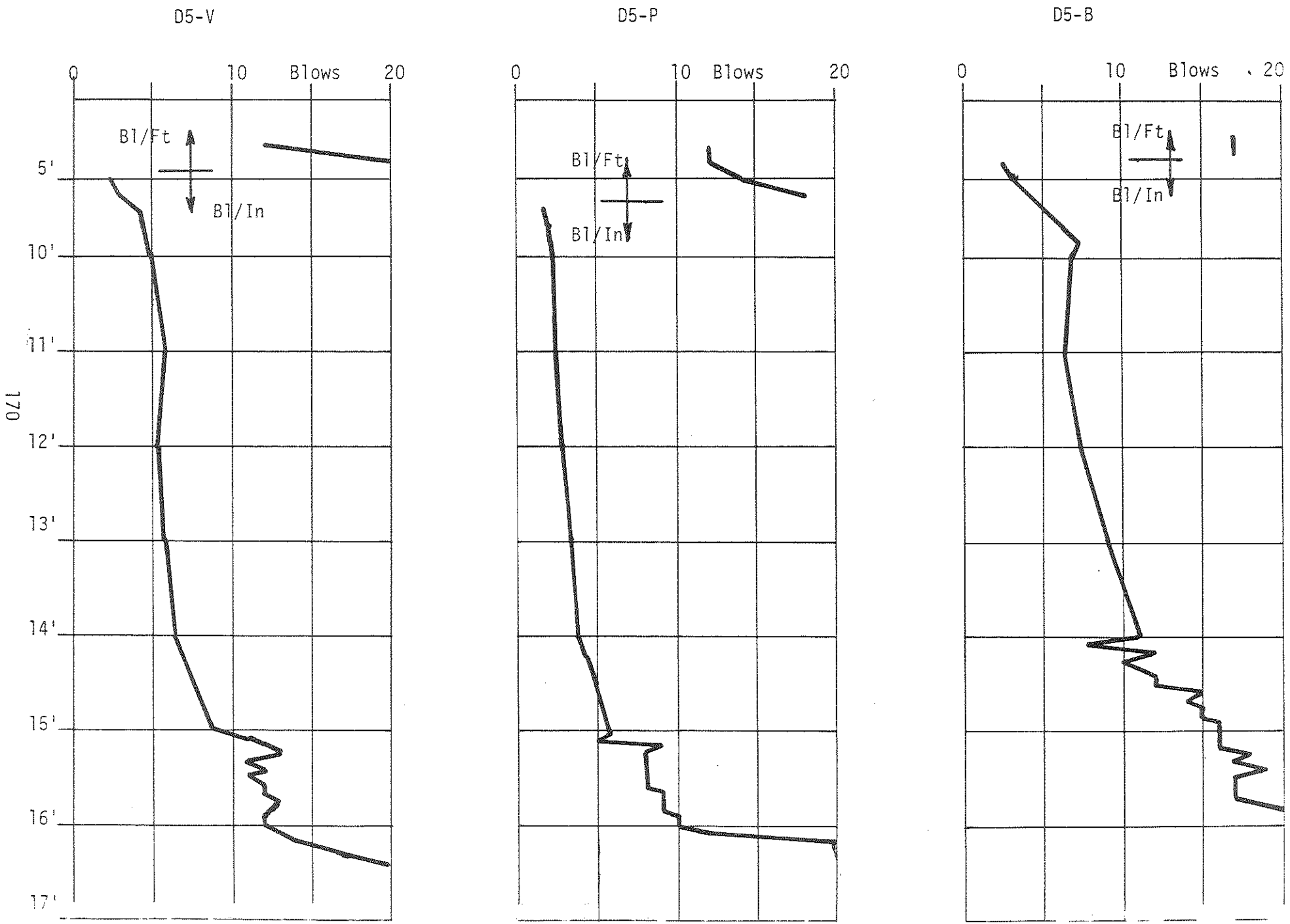

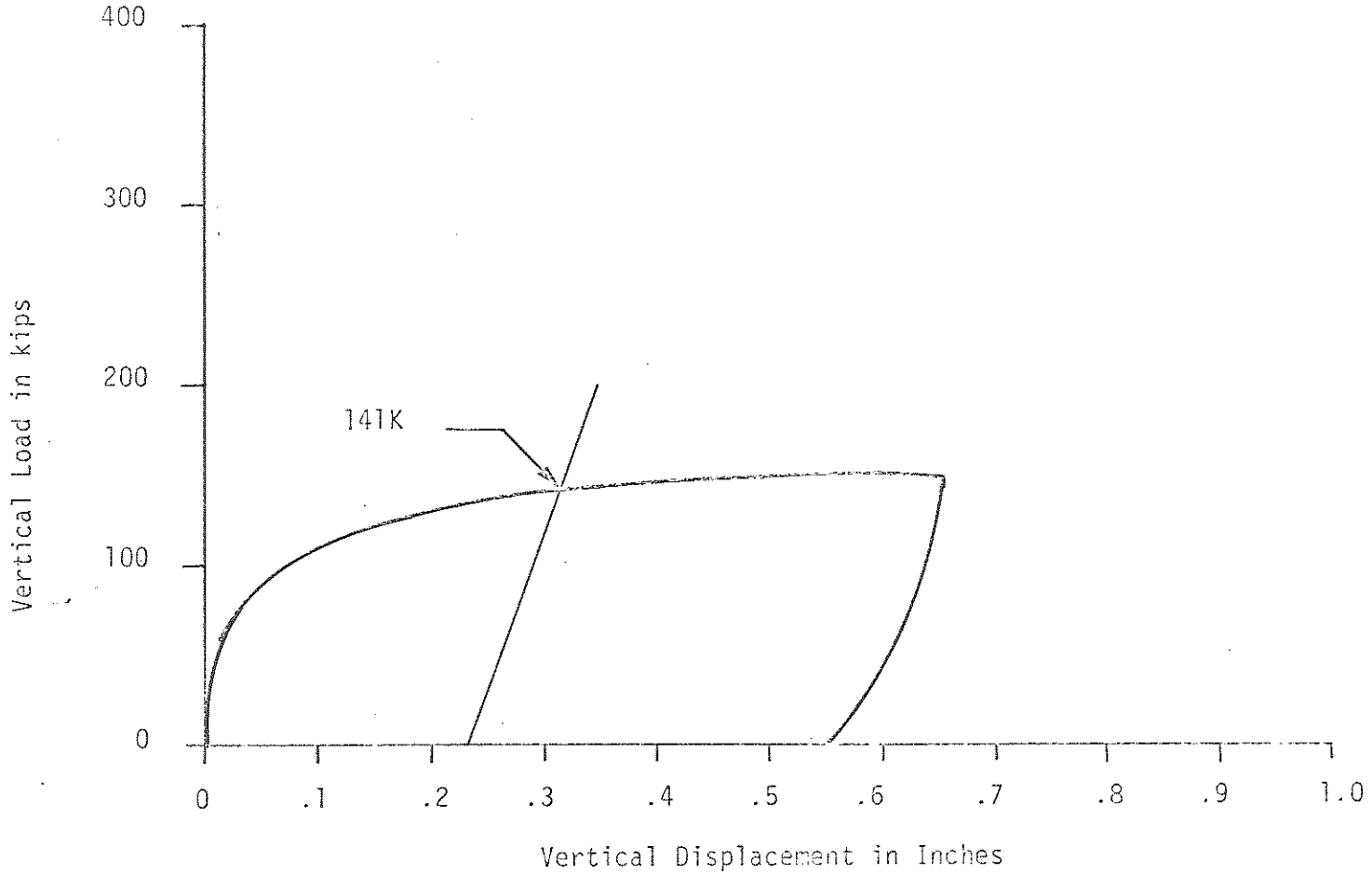

FigureA33 : Static Load Test Curve W92 Pile No. D5V

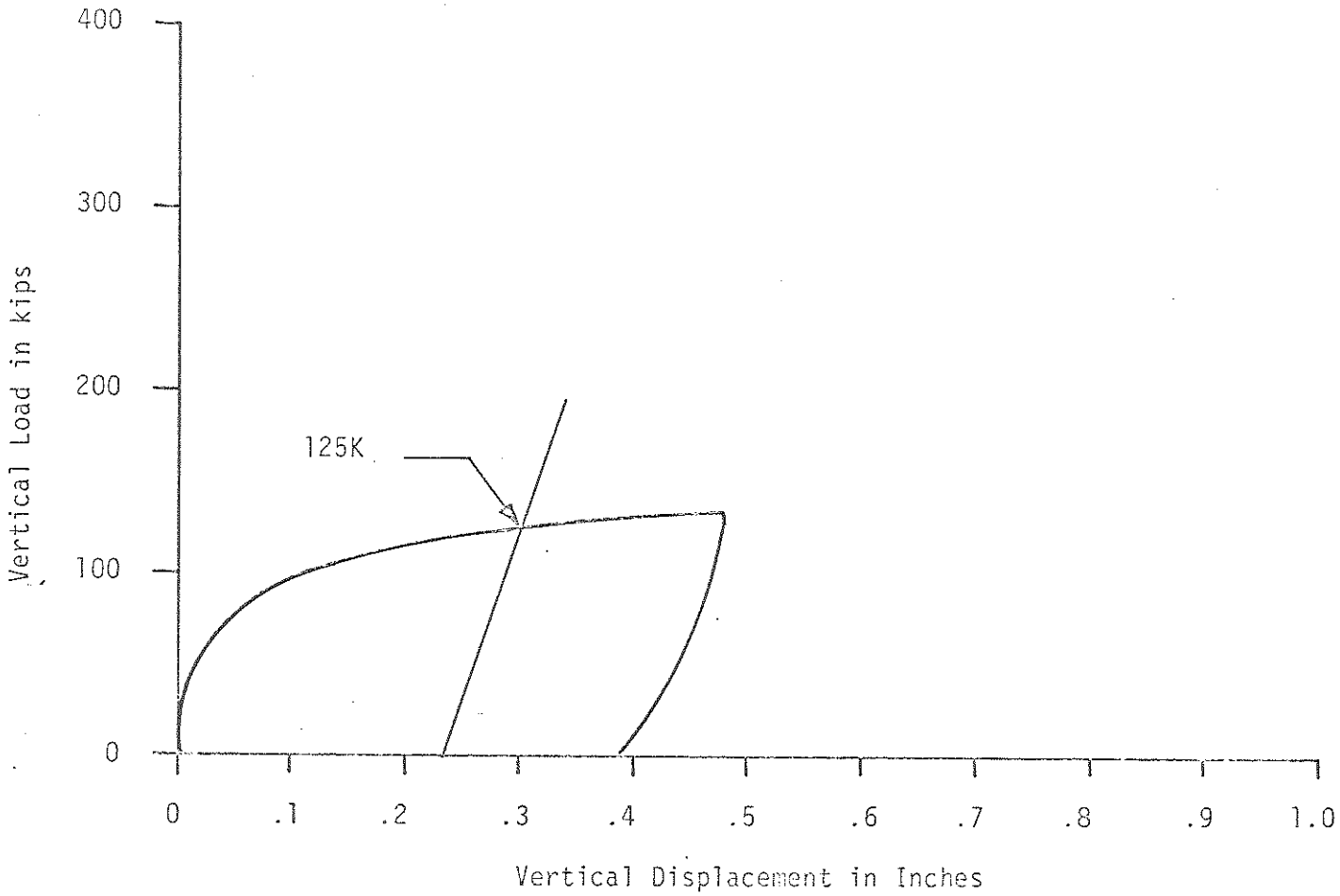

Figure A39: Static Load Test Curve M92 Pile No. D5-P

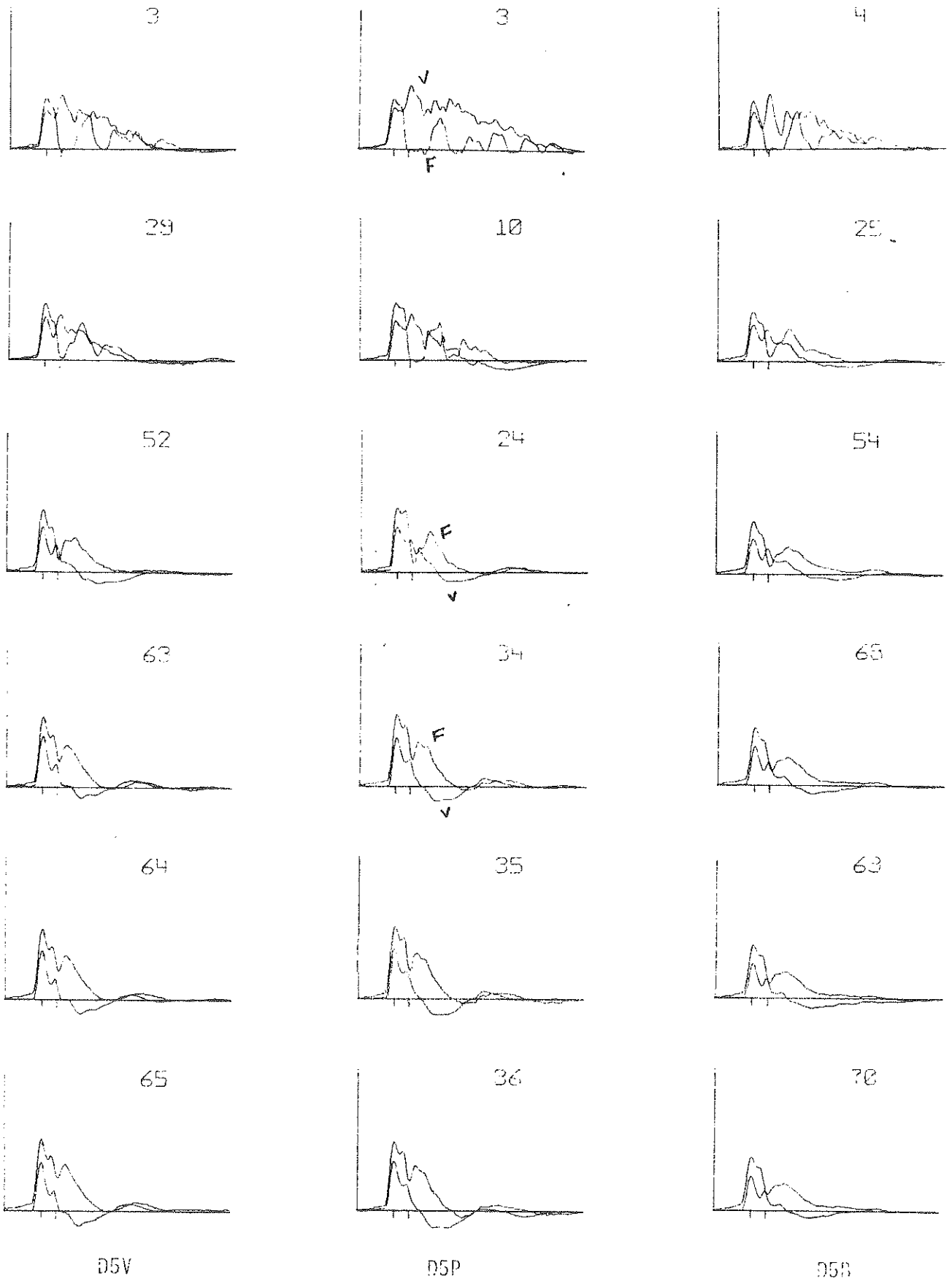

Sample records of force and velocity plotted by Case Method of Processing for W92

Figure A40

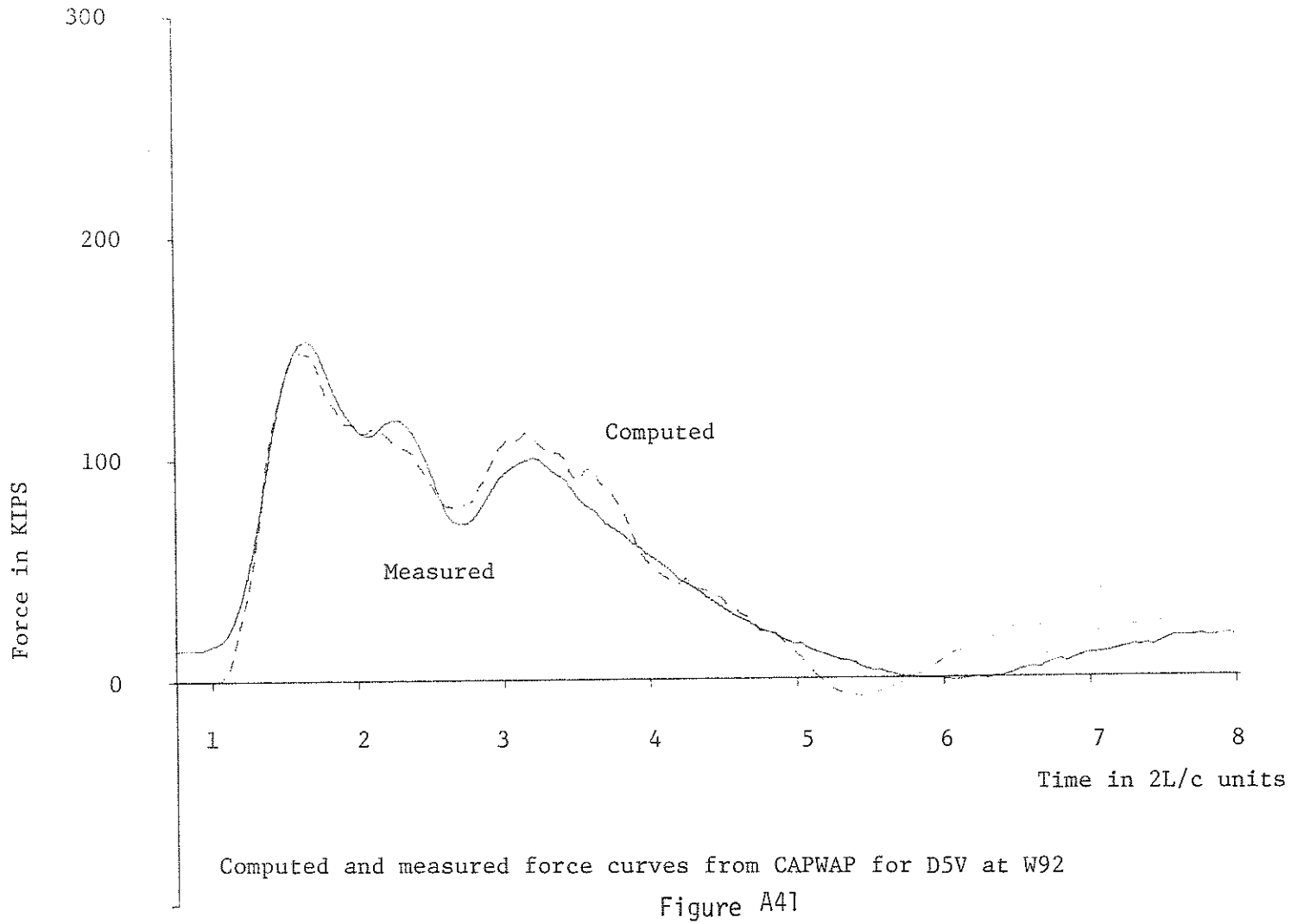

Computed and measured force curves from CAPWAP for D5V at W92

Figure A41

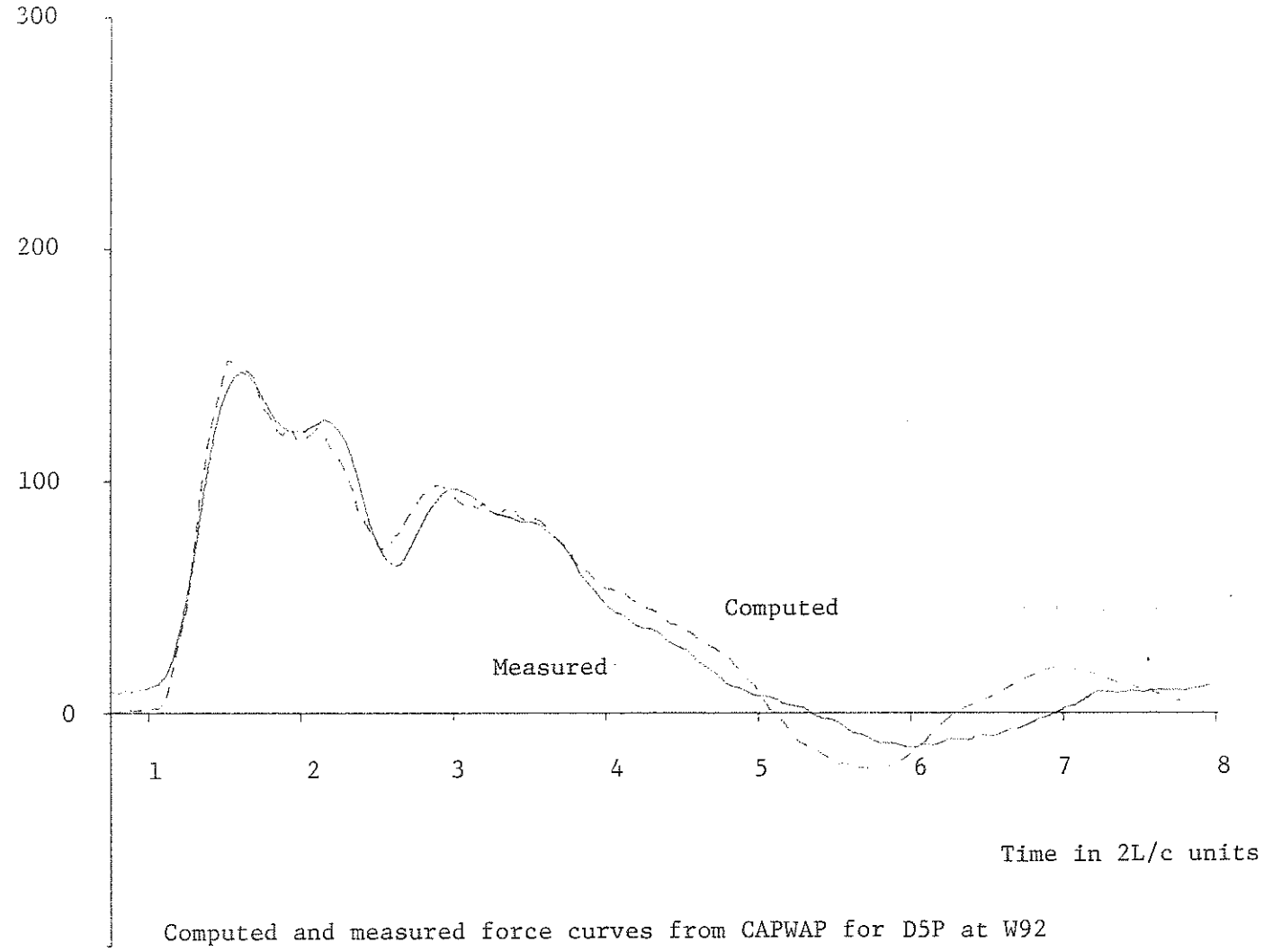

Computed and measured force curves from CAPWAP for D5P at W92

Figure A42

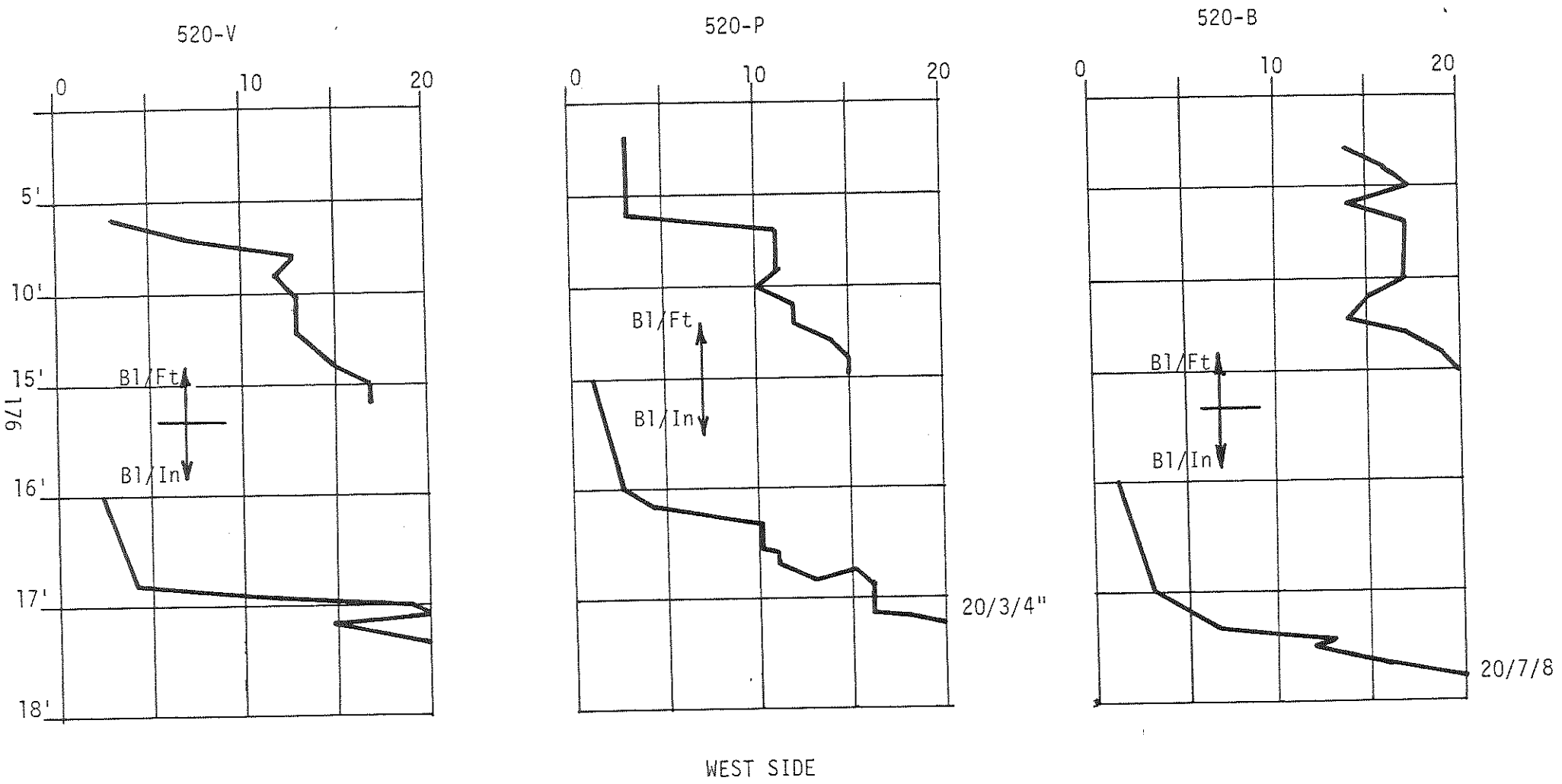

Figure A43 : Blow Count Records for Piles Driven by the 520 Hammer at W92

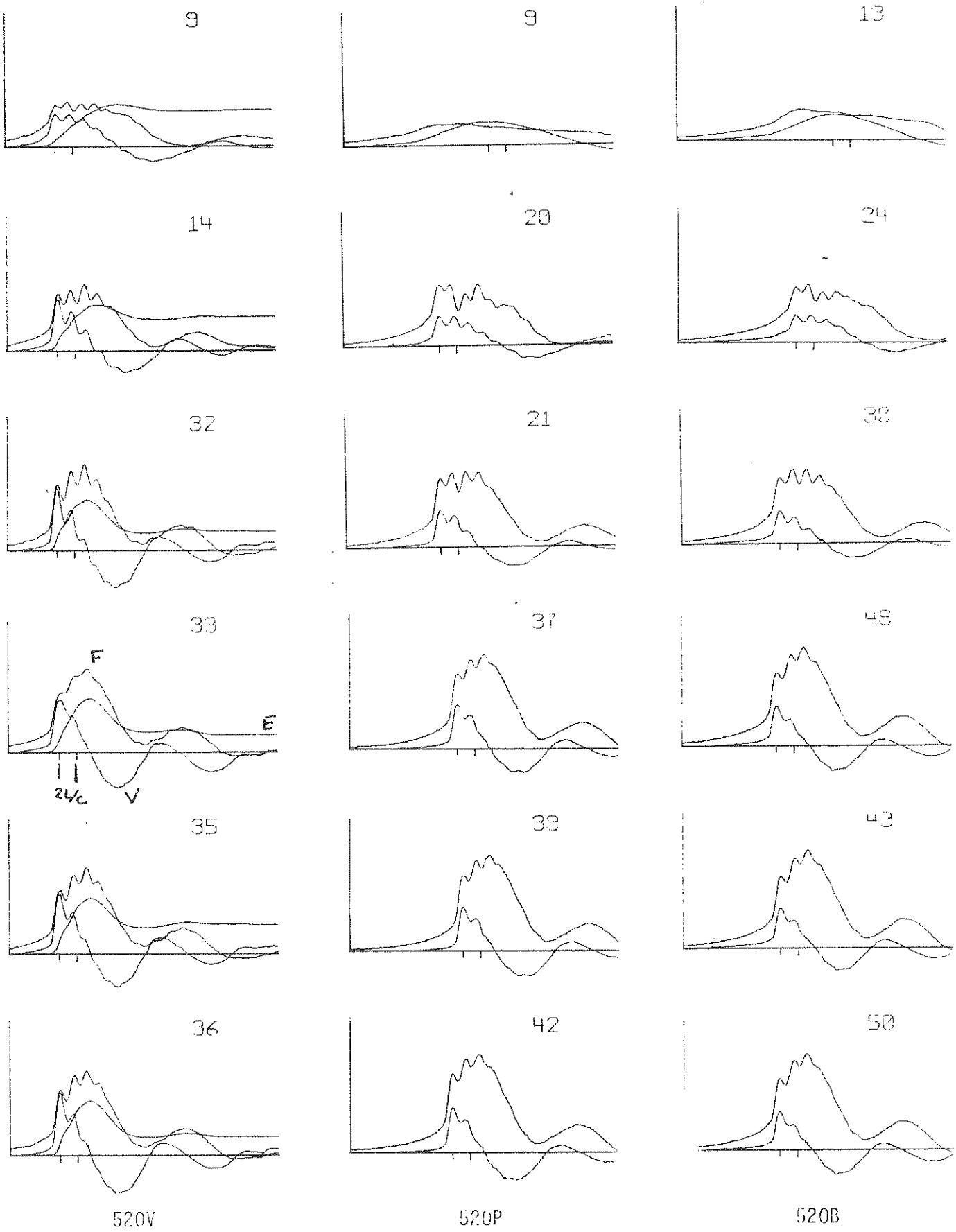

Sample records of force and velocity plotted by Case Method of Processing for W92

Figure A44

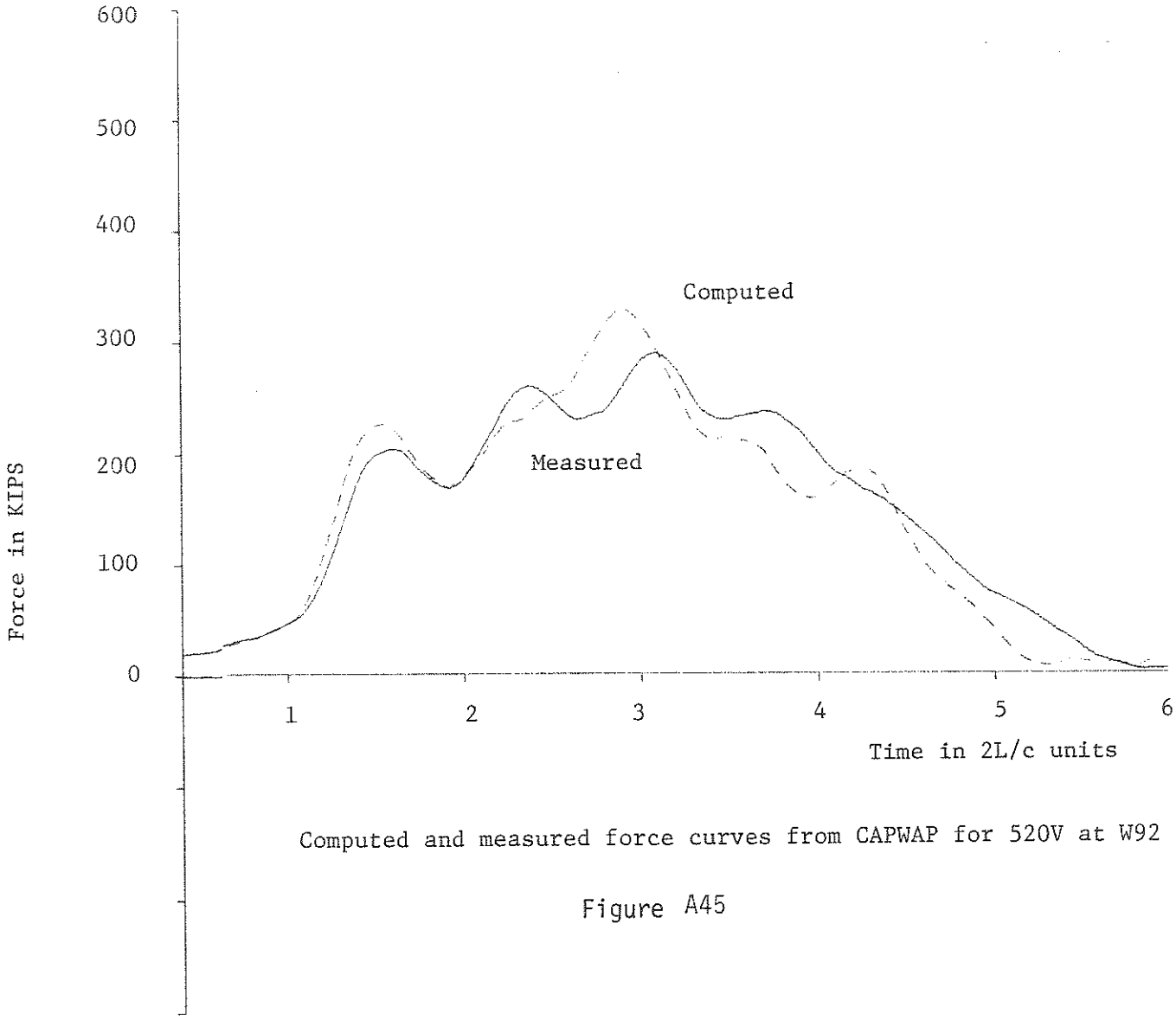

Computed and measured force curves from CAPWAP for 520V at W92

Figure A45

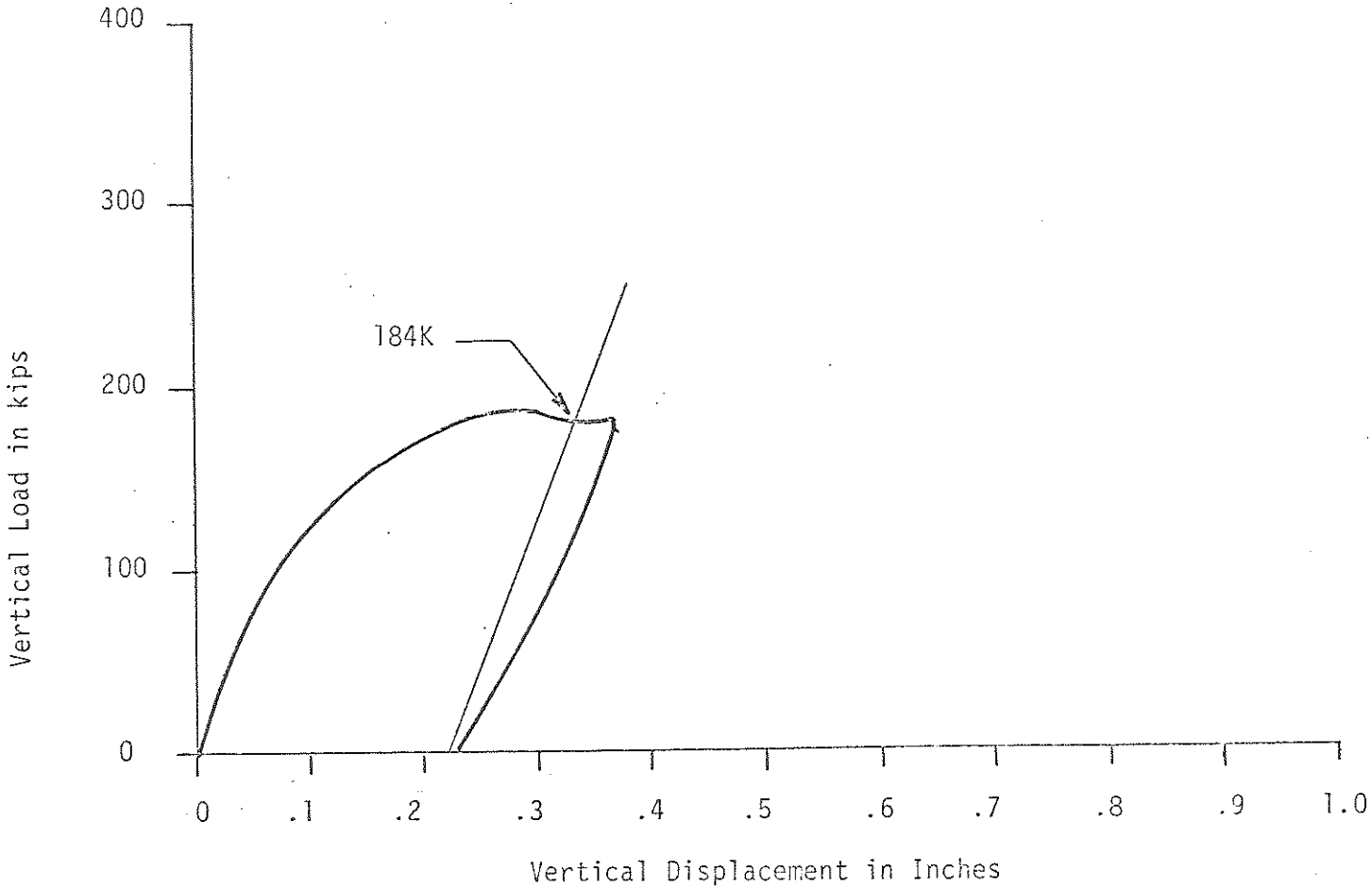

Figure A46 : Static Load Test Curve W92 Pile No. LB520-V

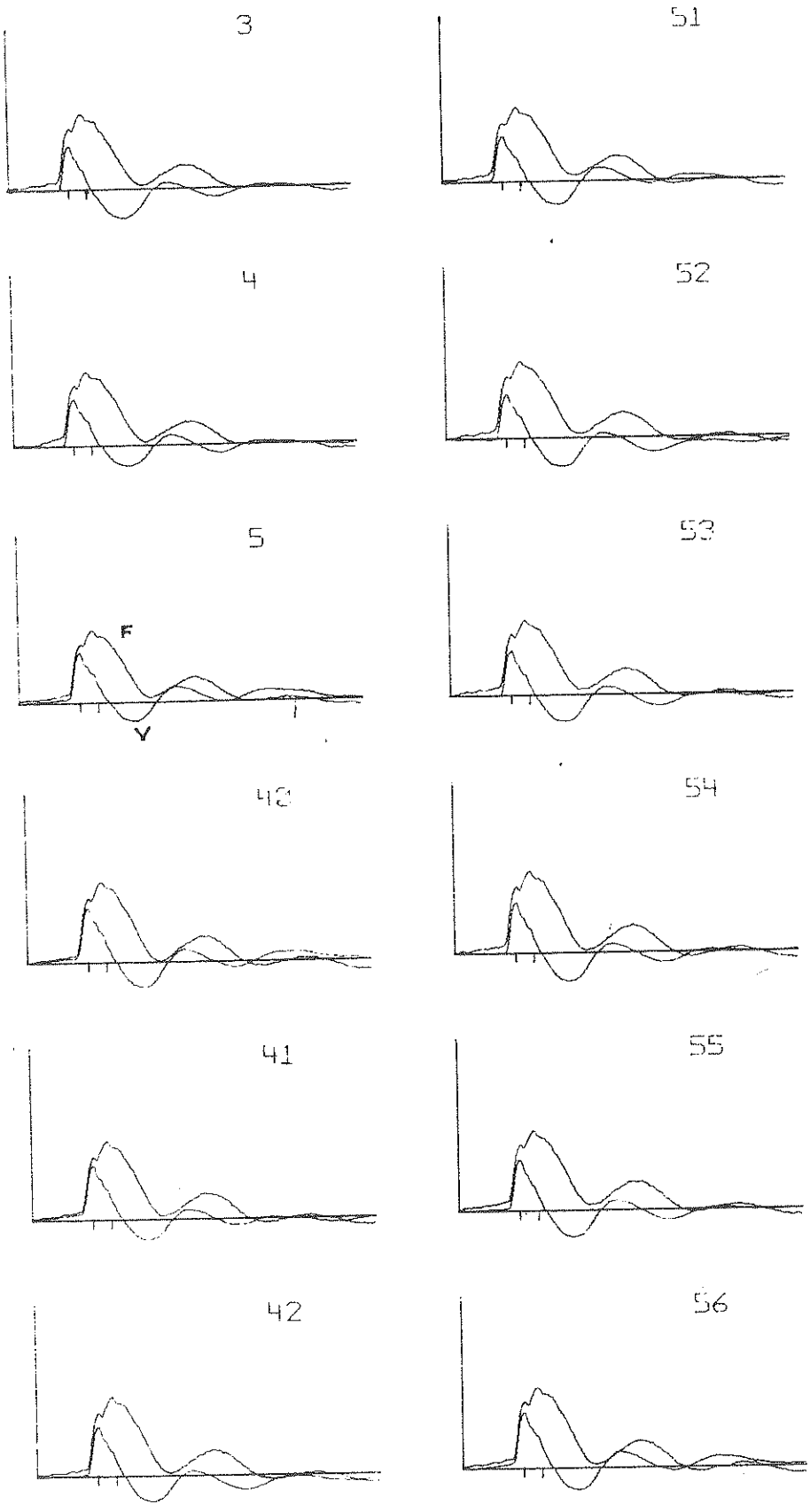

520V/440R 08V/440R

Sample records of force and velocity plotted by Case Method of Processir for W92

Figure A47

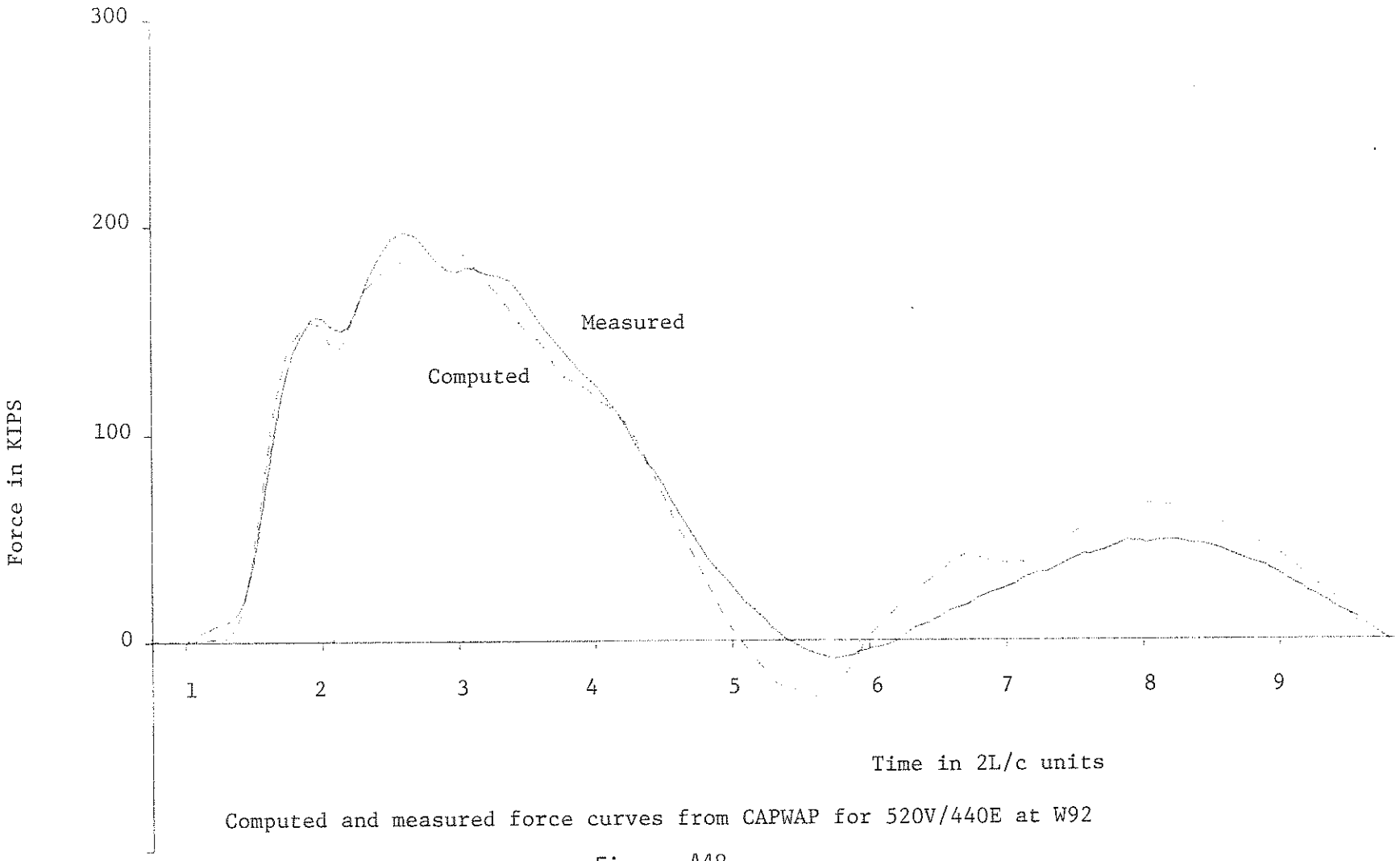

Computed and measured force curves from CAPWAP for 520V/440E at W92

Figure A48

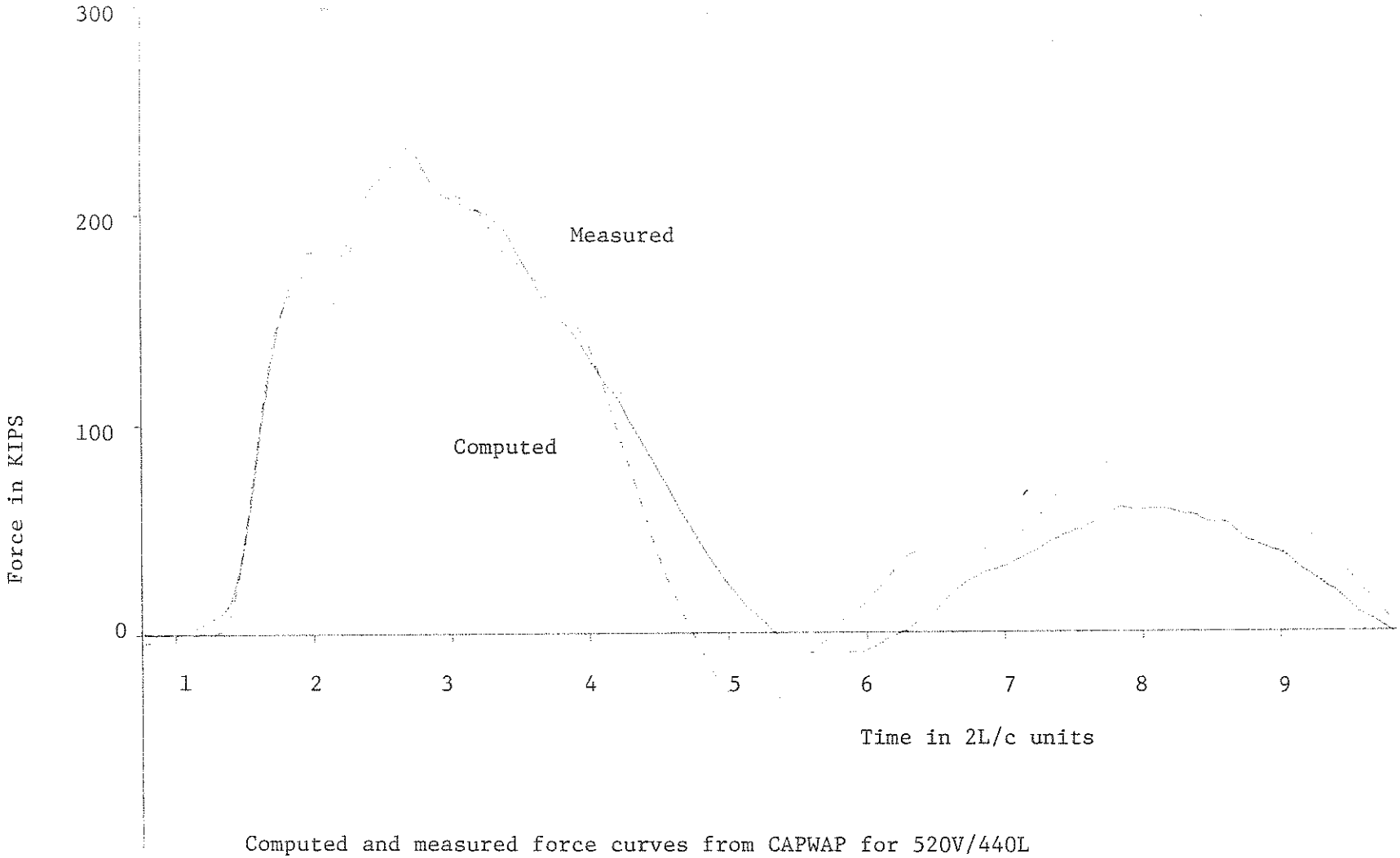

Computed and measured force curves from CAPWAP for 520V/440L

Figure A49

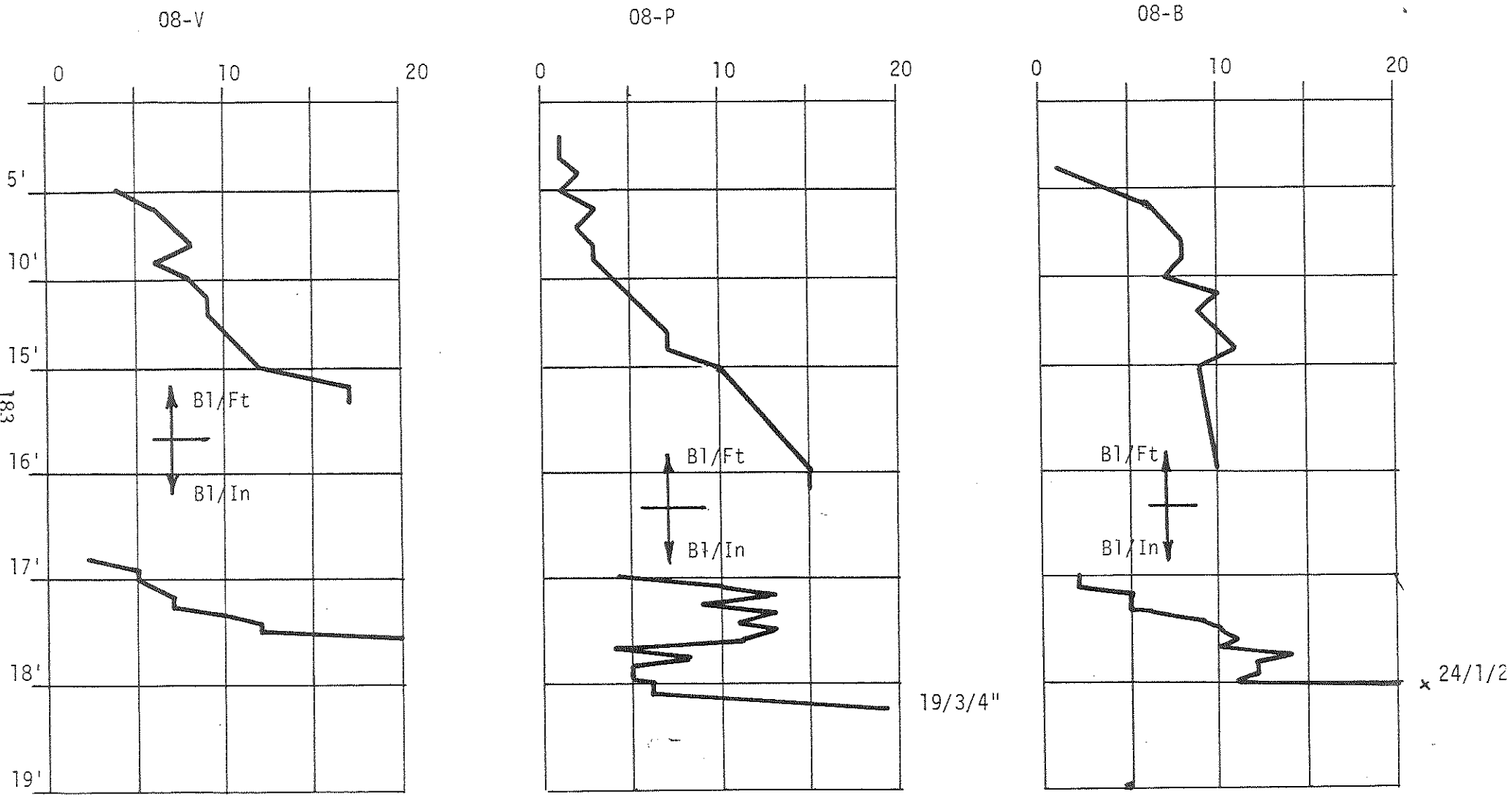

Figure A50 : Blow Count Records for Piles Driven by the 08 Hammer at W92

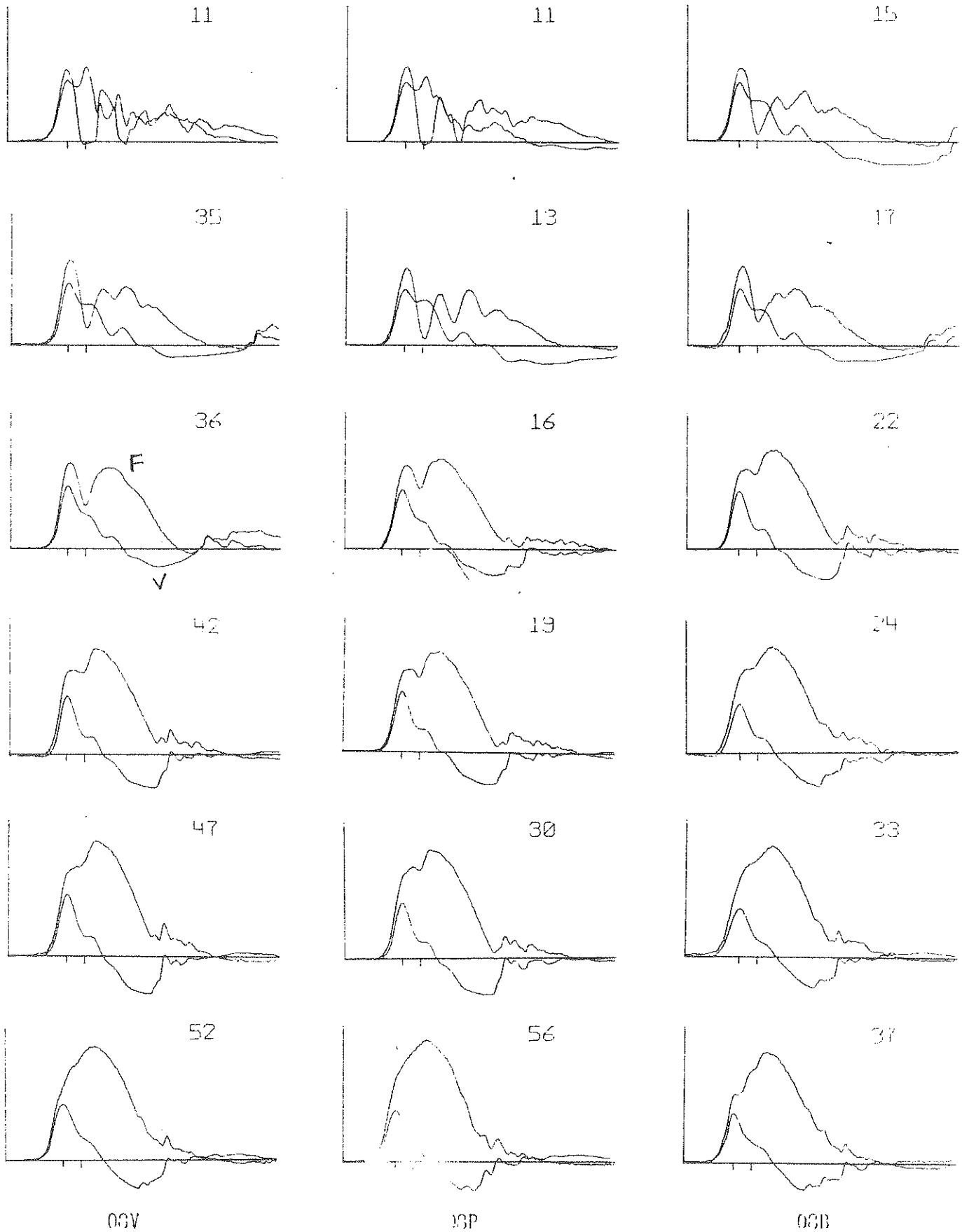

Sample records of force and velocity plotted by Case Method of Processing for W92

Figure A51

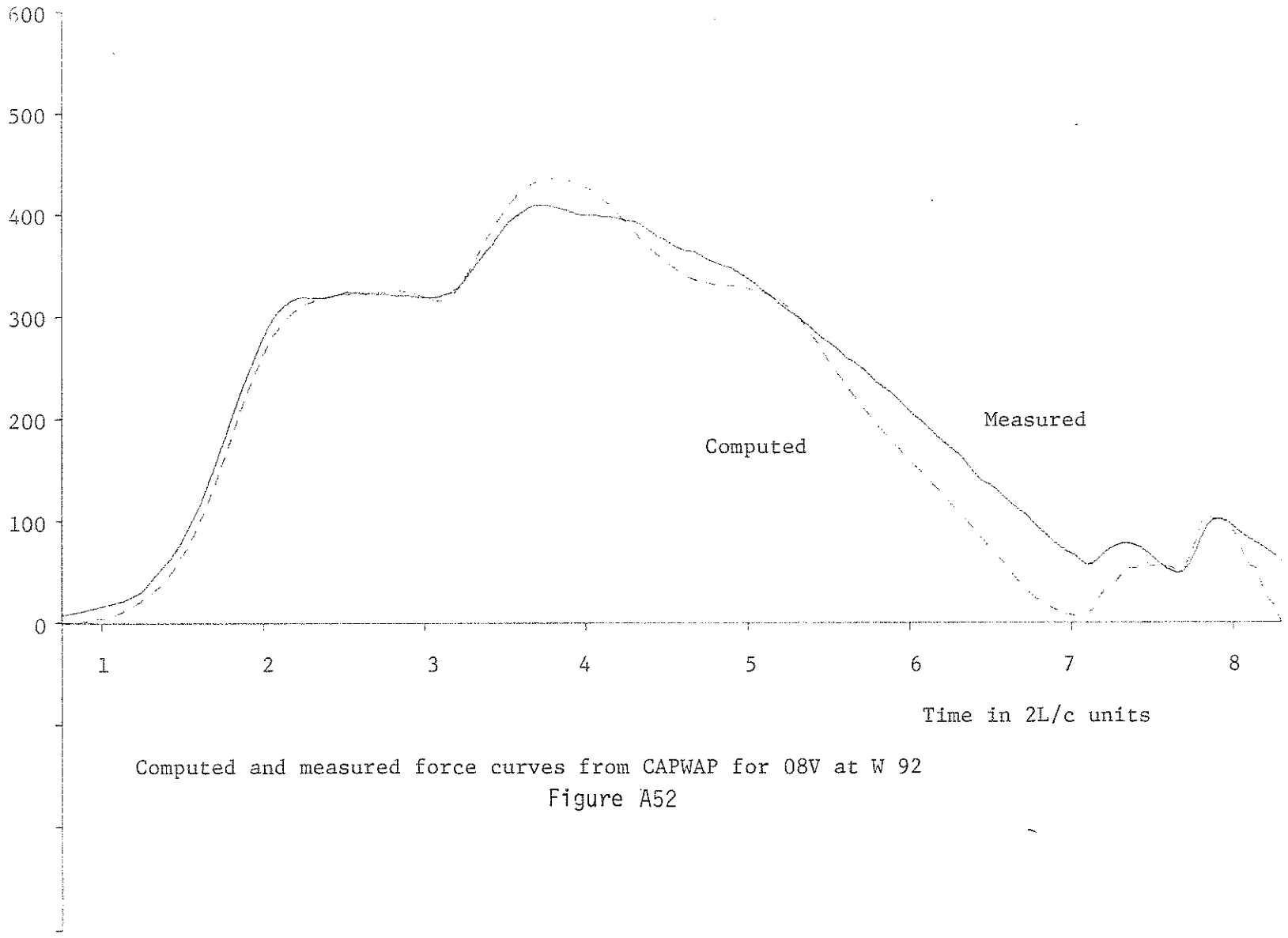

Computed and measured force curves from CAPWAP for 08V at W 92

Figure A52

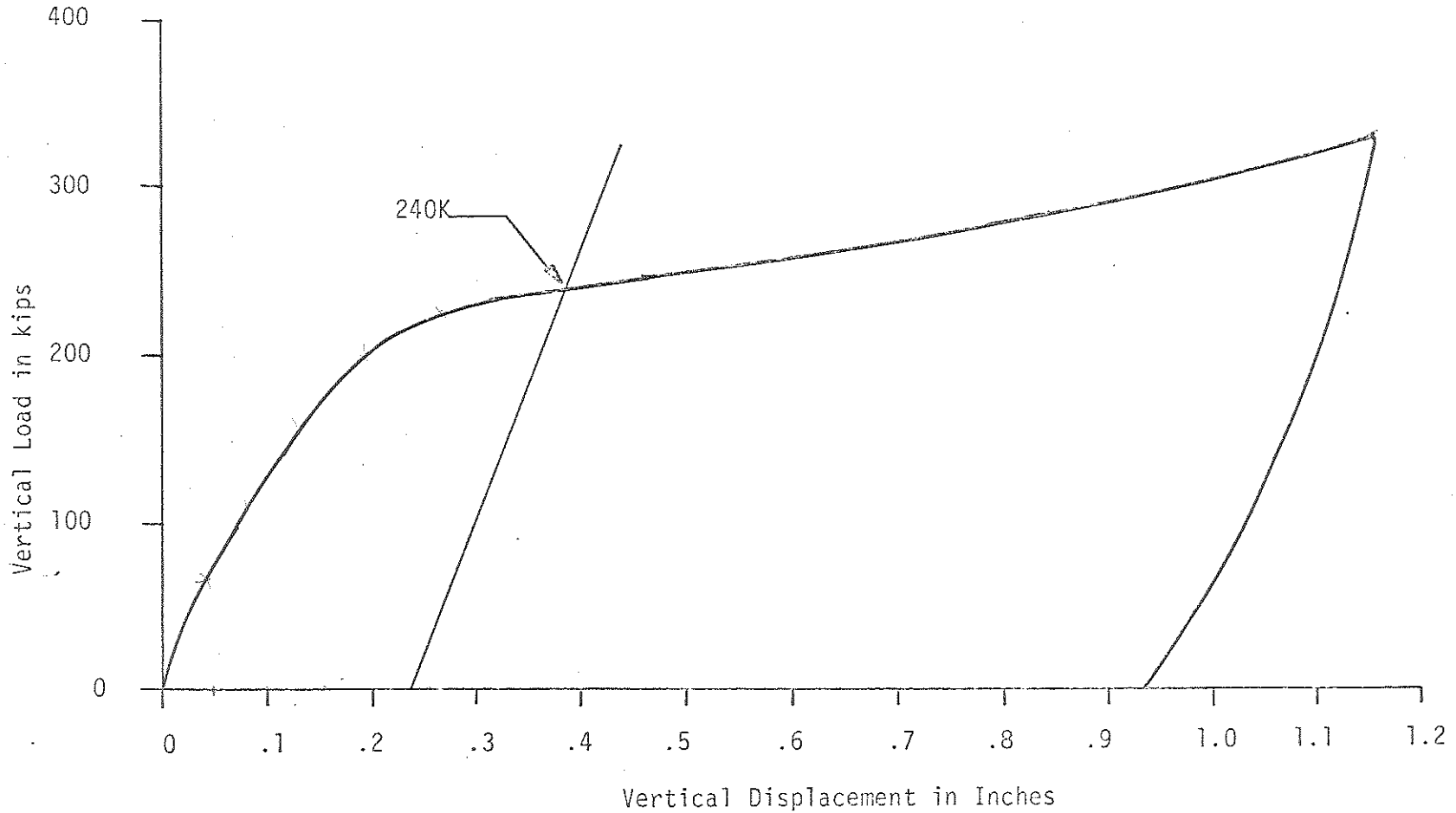

Figure A53 : Static Load Test Curve W92 Pile No. 08-V

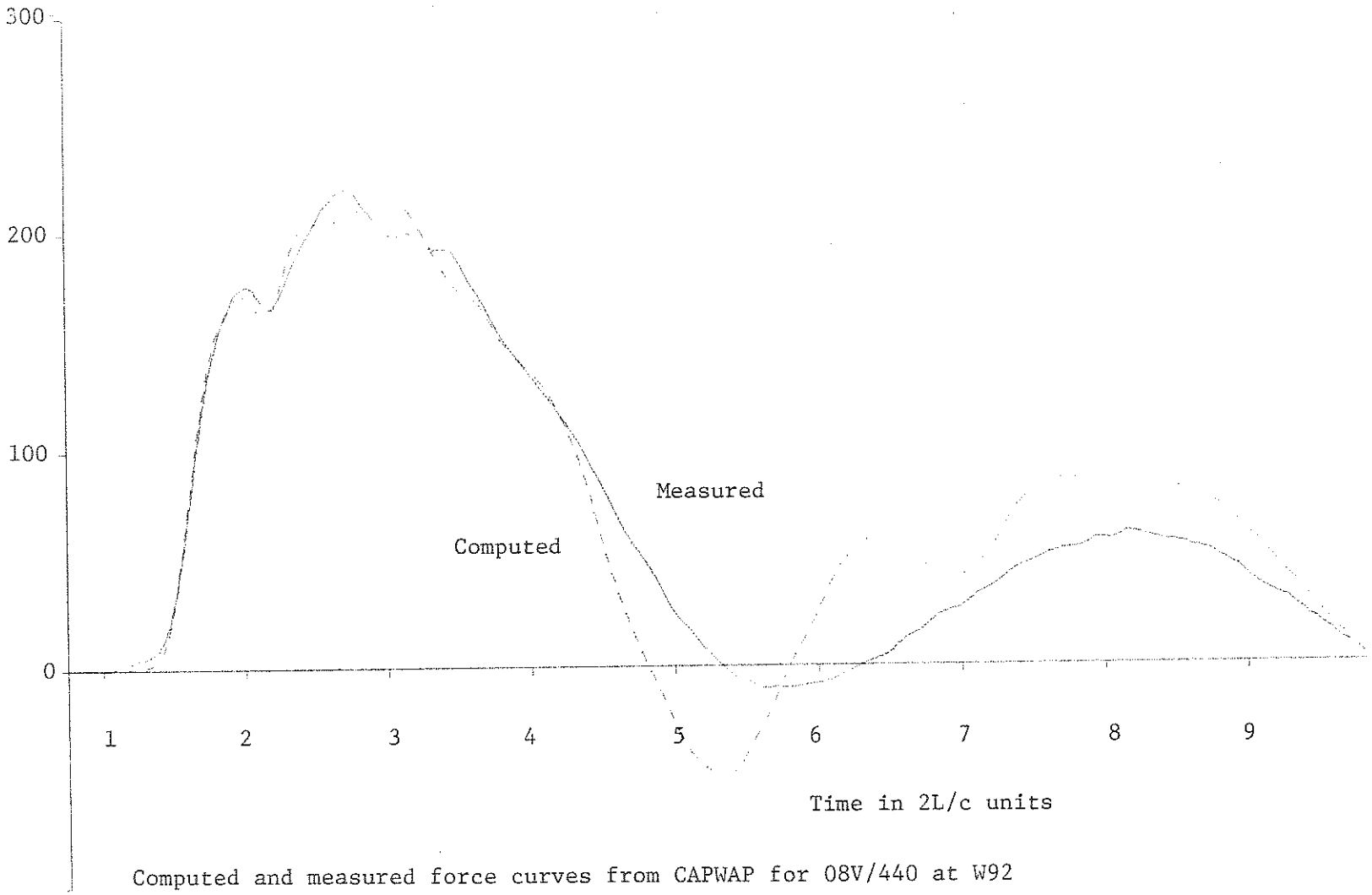

Computed and measured force curves from CAPWAP for 08V/440 at W92

Figure A54

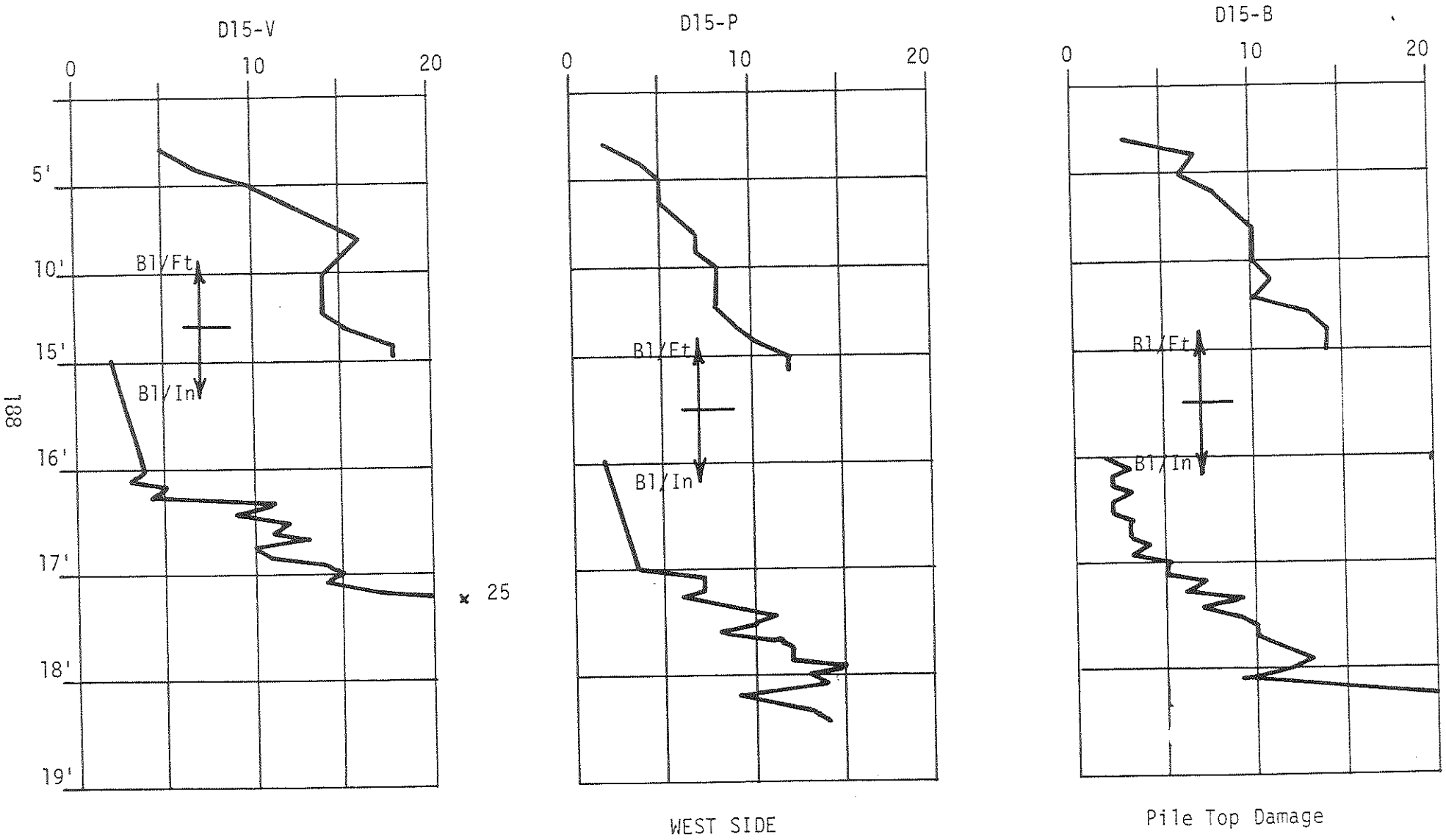

Figure A55 : Blow Count Records for Piles Driven by the D15 Hammer at W92

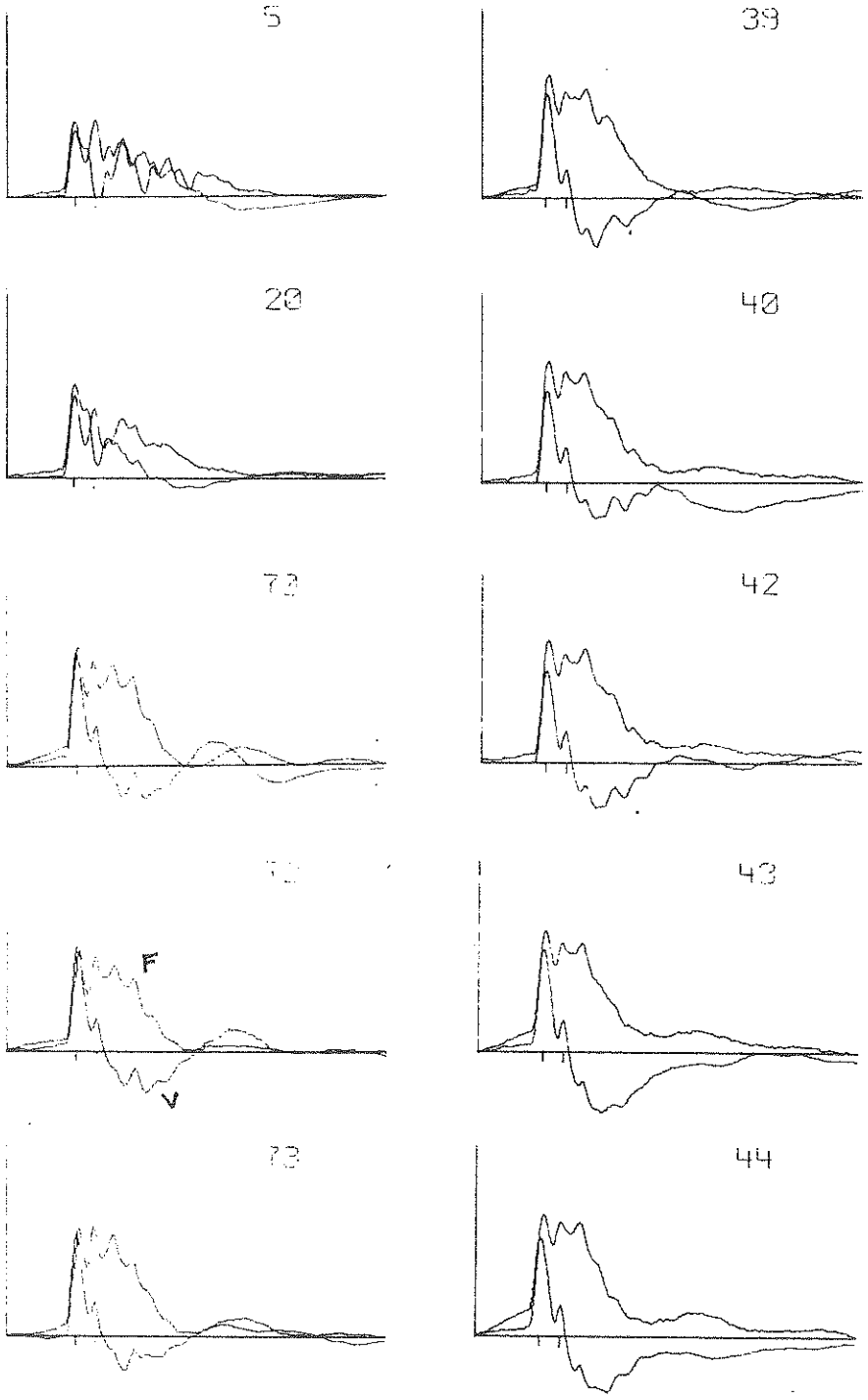

D15V D15P

Sample records of force and velocity plotted by Case Method of Processing for W32

Figure A56

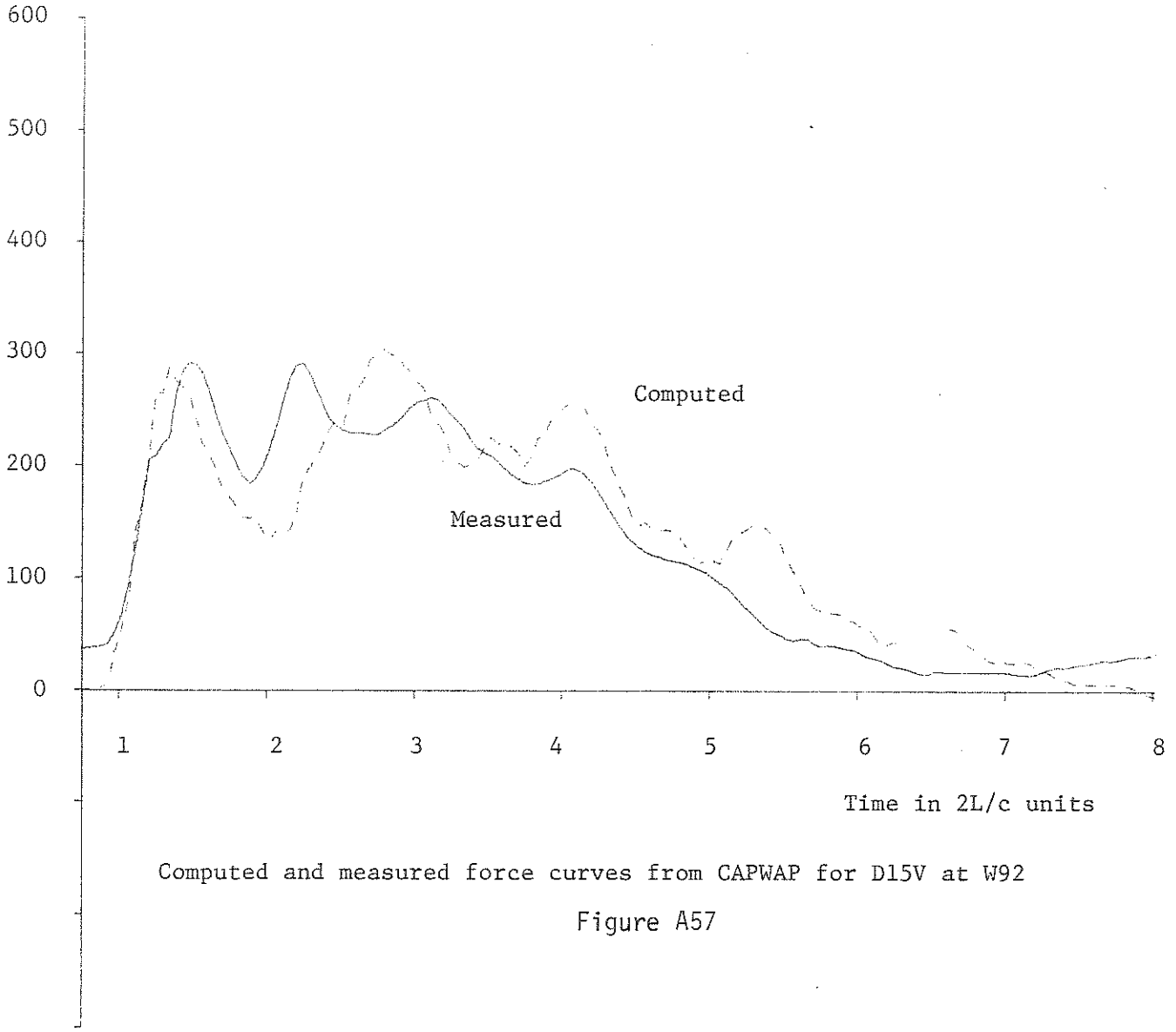

Computed and measured force curves from CAPWAP for D15V at W92

Figure A57

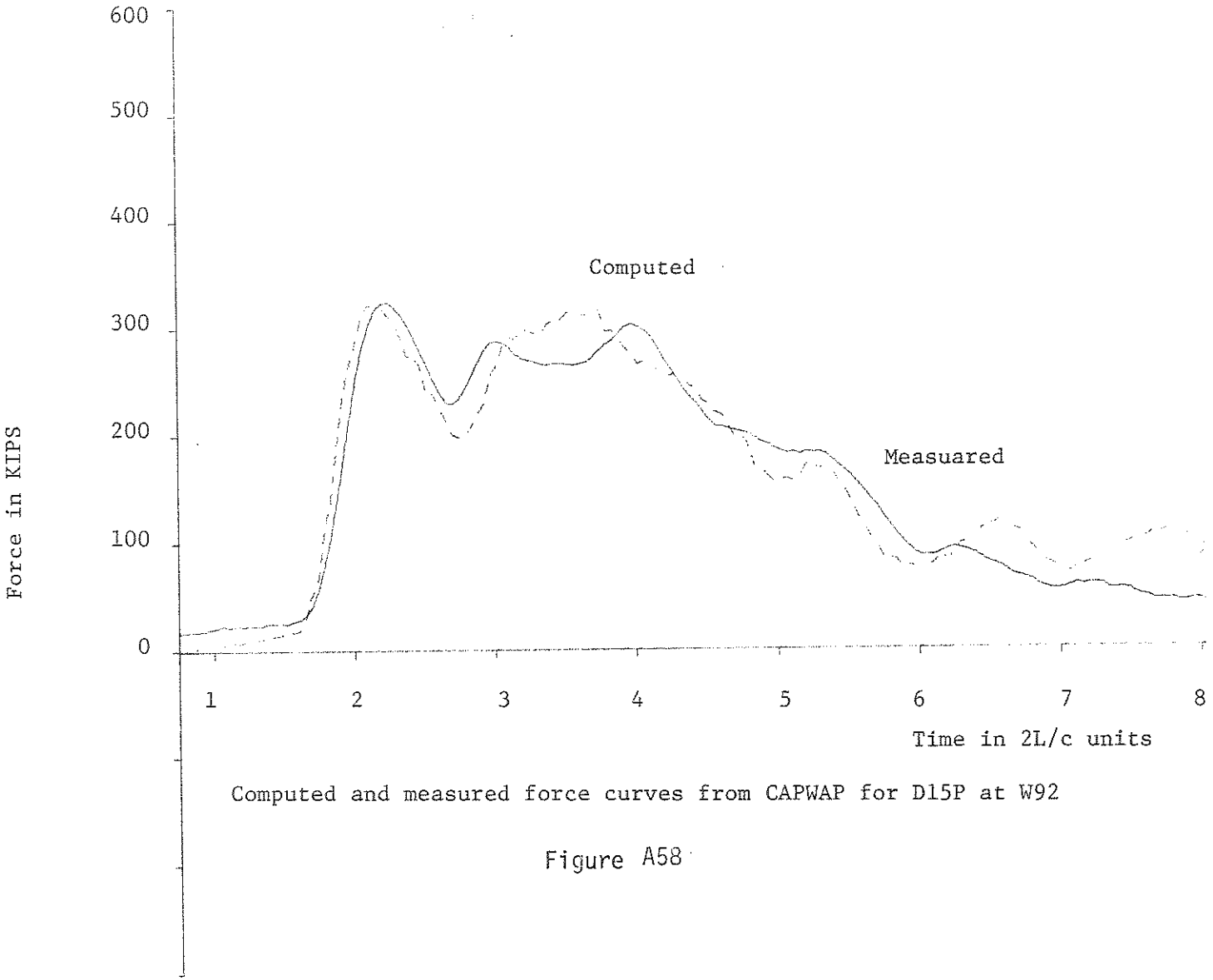

Computed and measured force curves from CAPWAP for D15P at W92

Figure A58

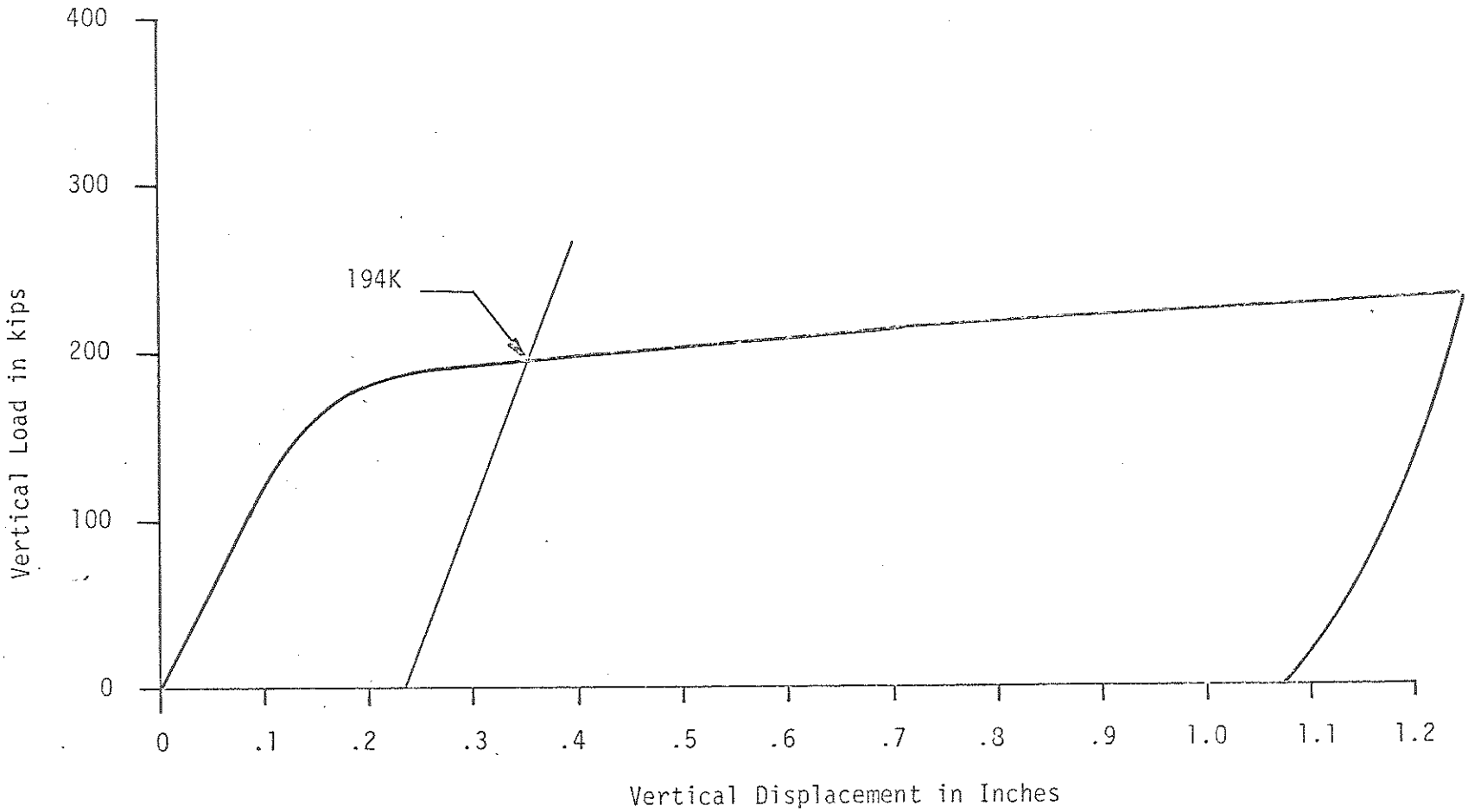

Figure A59 : Static Load Test Curve W92 Pile No. D15-V

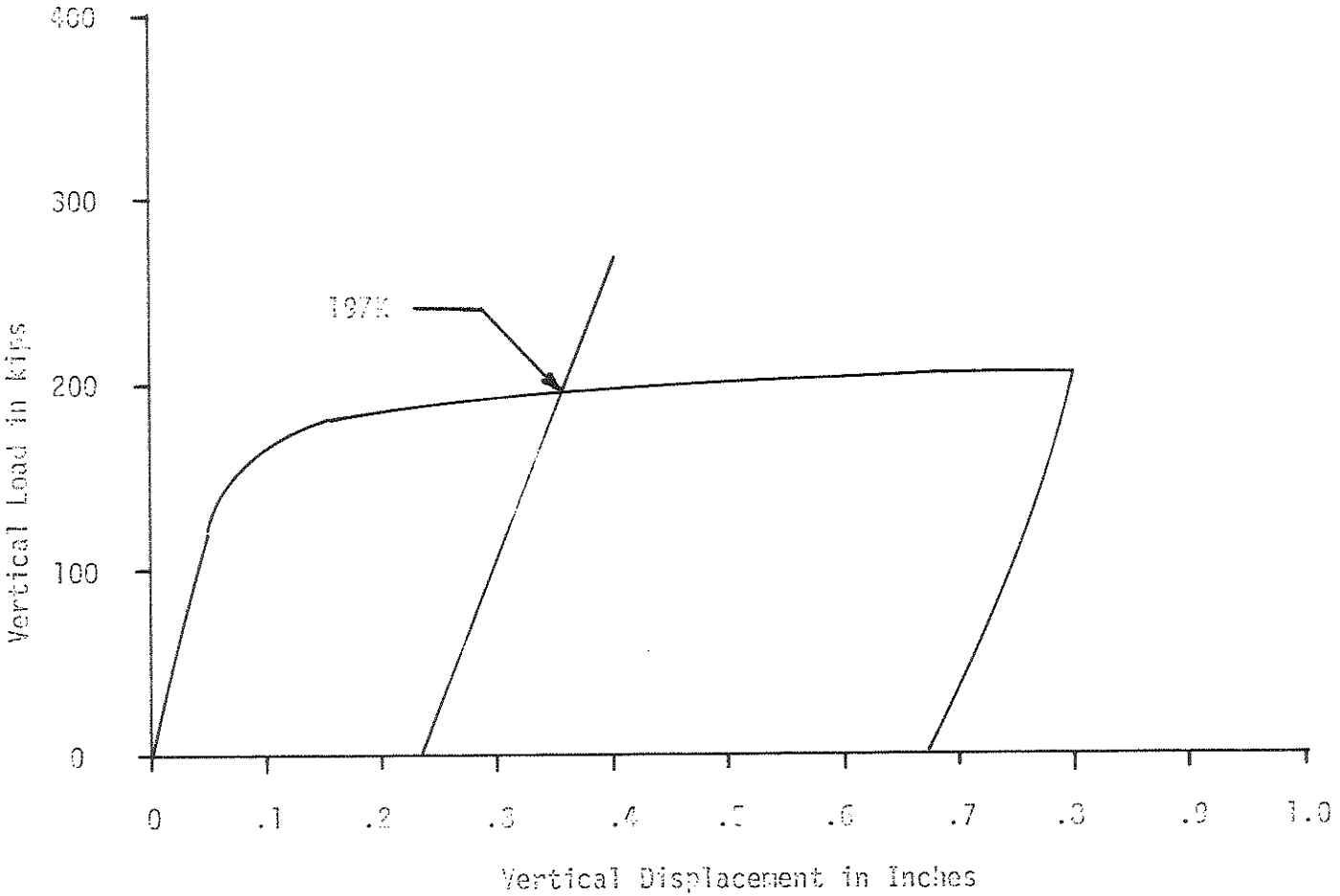

Figure A60: Static Load Test Curve M32 Pile No. D15-P

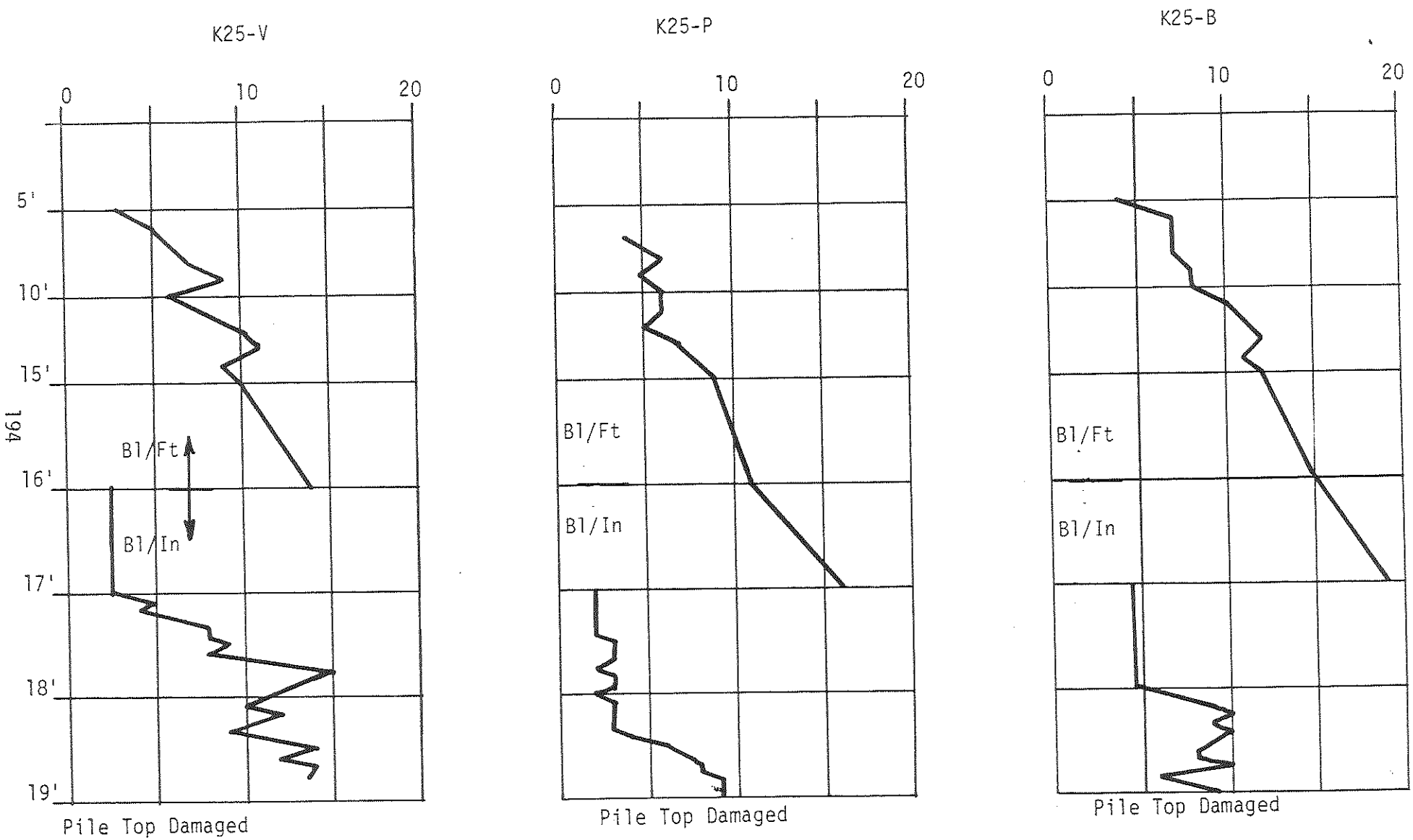

WEST SIDE

Figure A61: Blow Count Records for Piles Driven by the K25 Hammer at W92

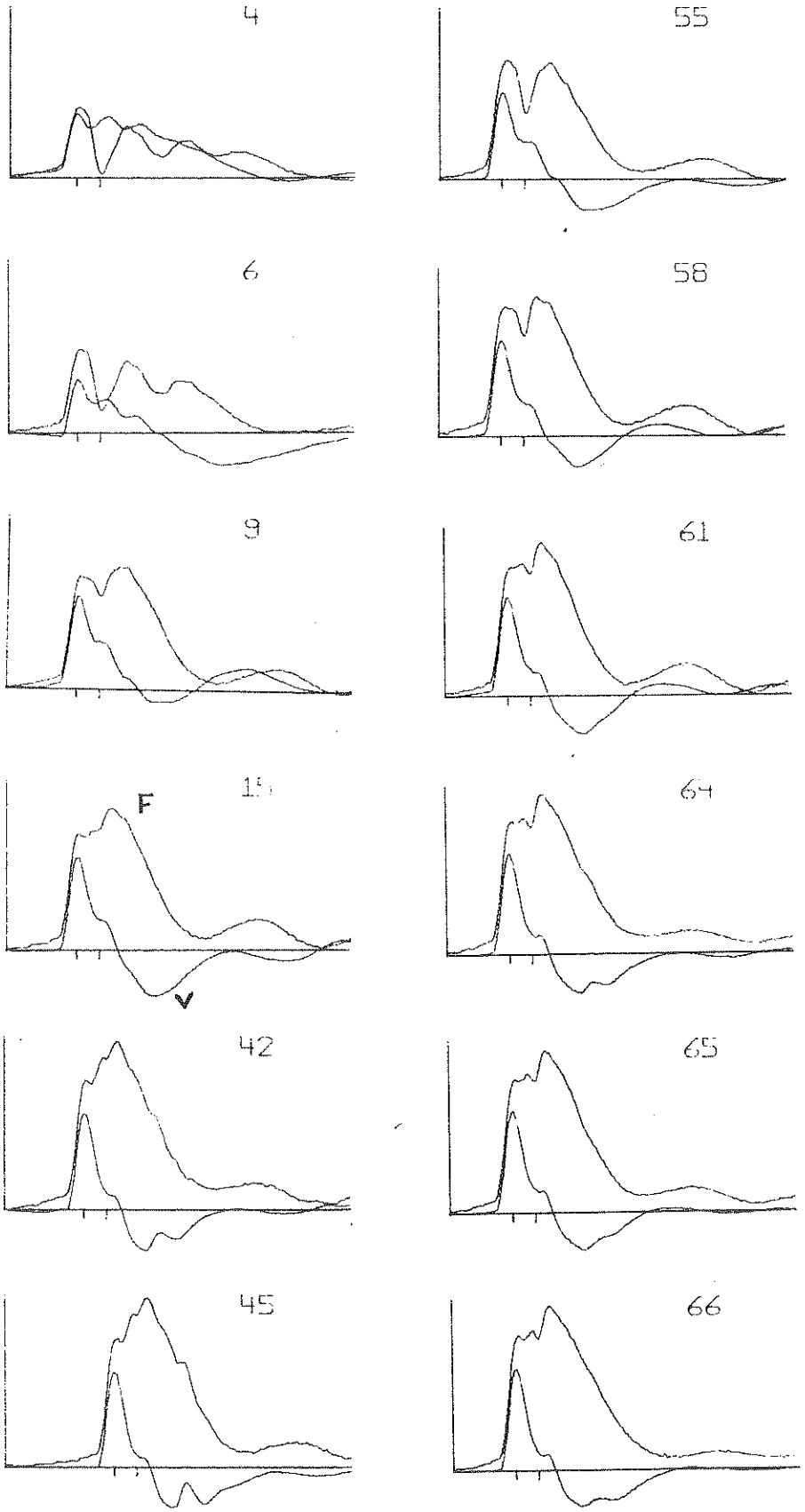

K25V K25P

Sample records of force and velocity plotted by Case Method of Processing for W92

Figure A62

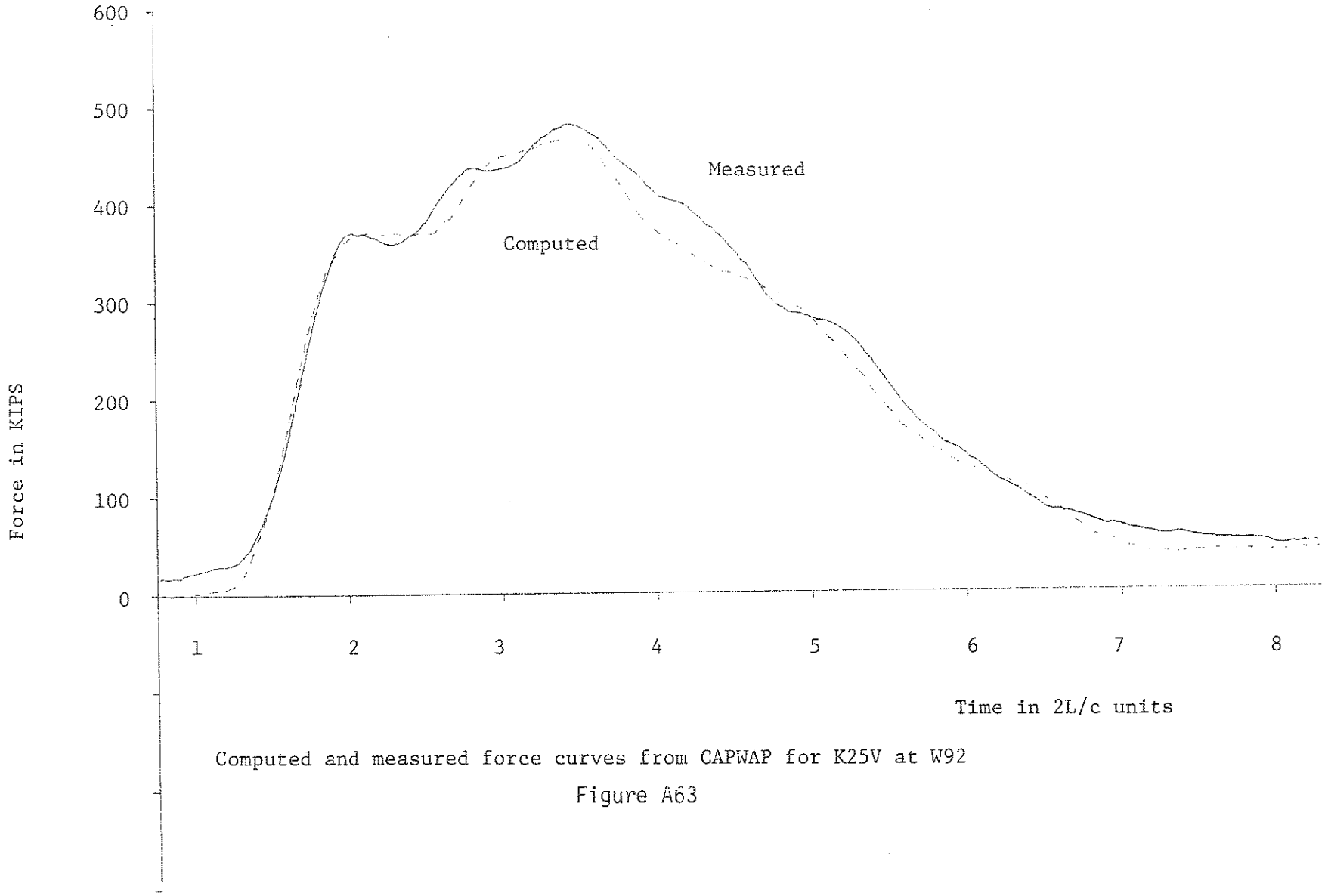

Computed and measured force curves from CAPWAP for K25V at W92

Figure A63

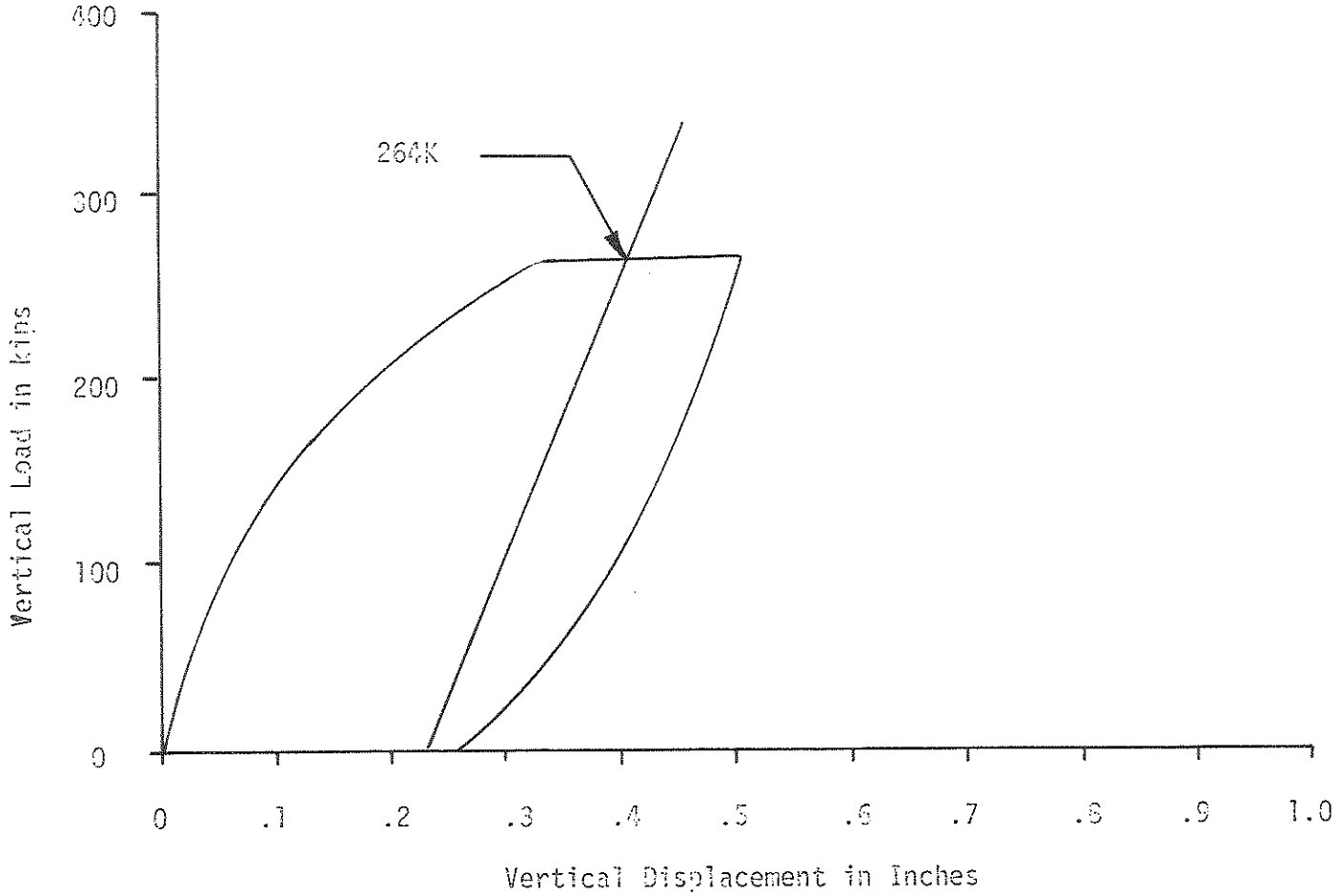

Figure A64: Static Load Test Curve M92 Pile No. K25-V

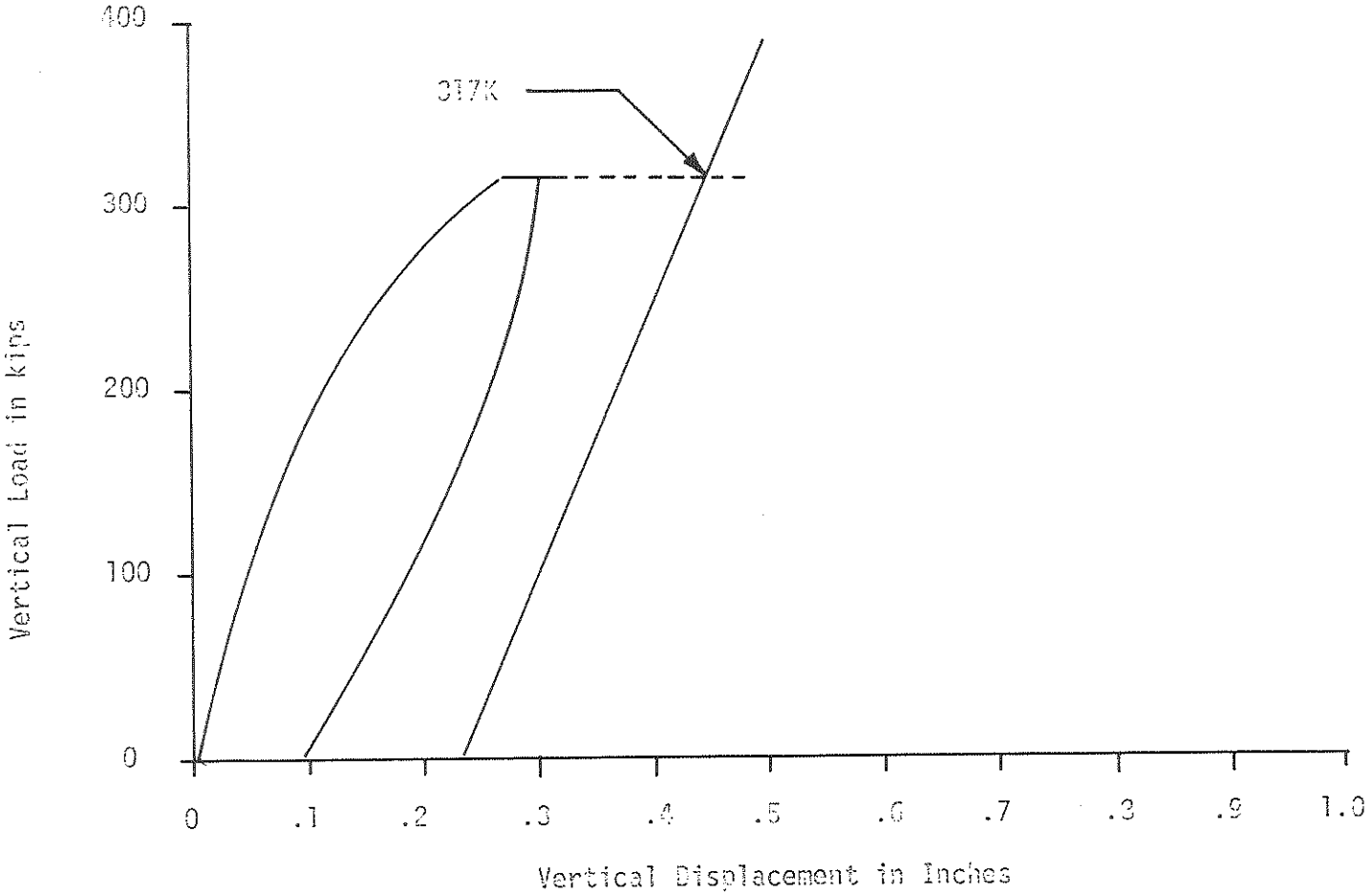

Figure A65: Static Load Test Curve M32 Pile No. K25-B

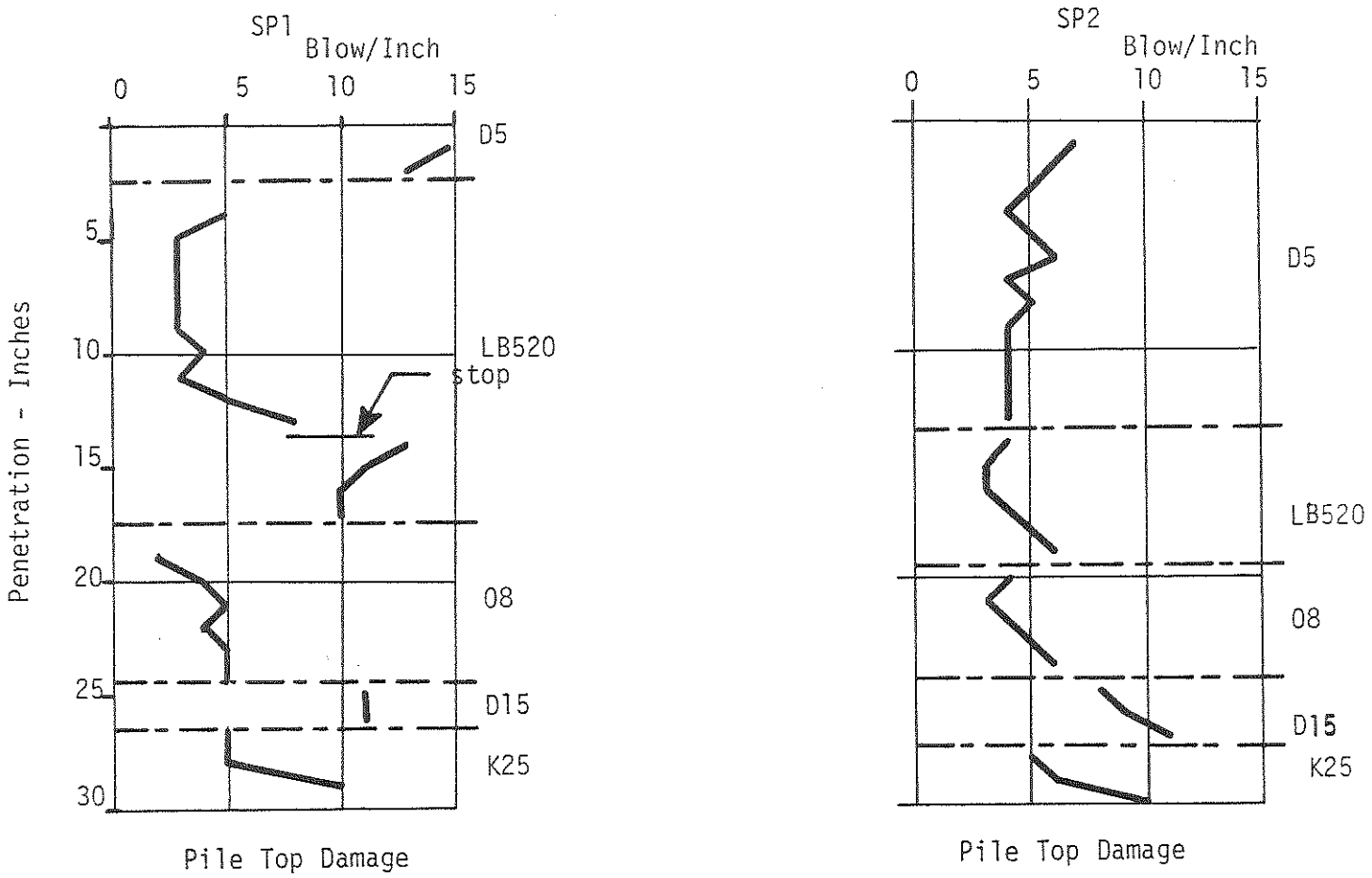

Figure A66: Blow Count Records for Piles Driven by the SP1 and SP2 Hammers at W92

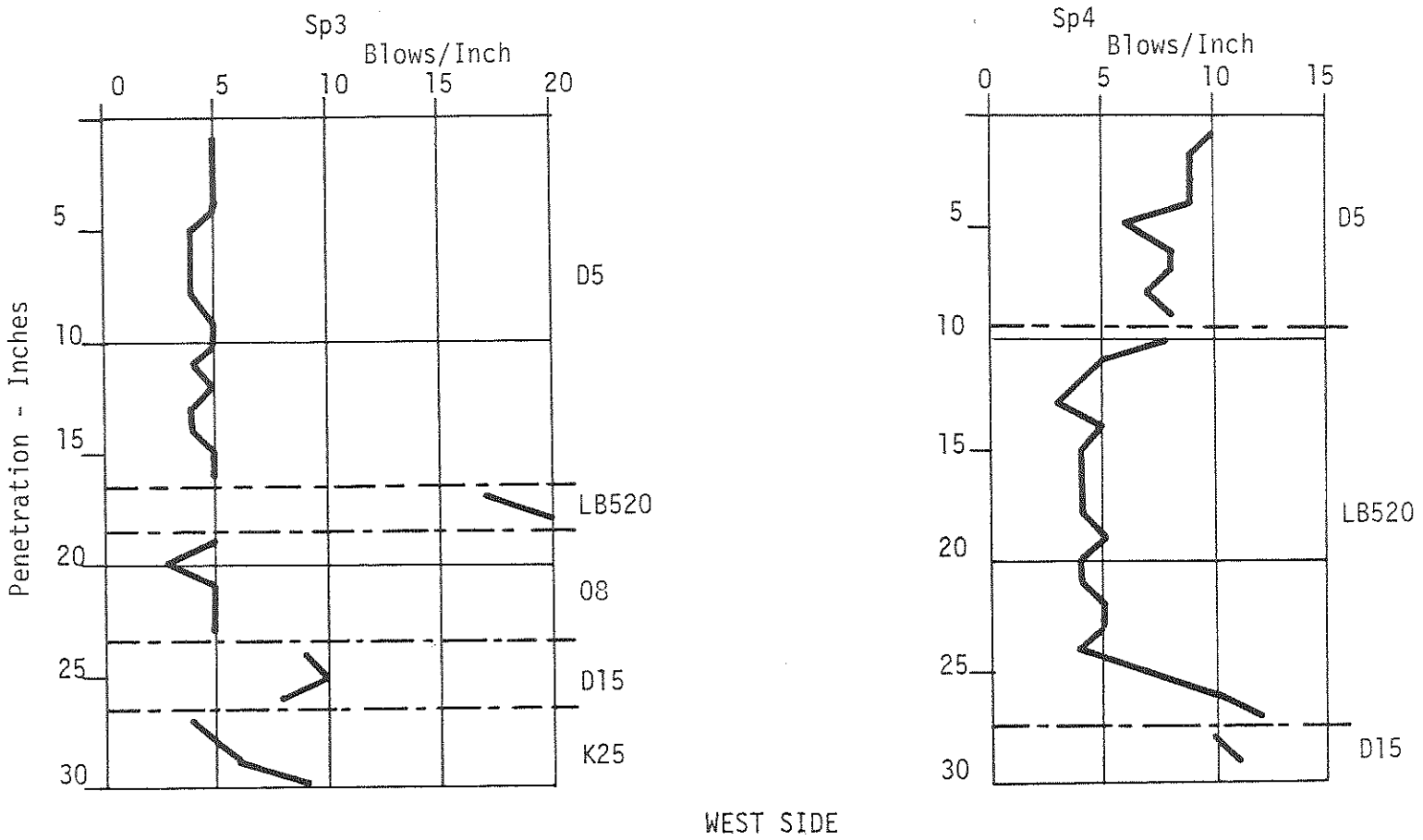

Figure A67 : Blow Count Records for Piles Driven by the SP3 and SP4 Hammers at W92